THE UNIVERSITY *of* EDINBURGH

Role of macrophage 11β-HSD1 in inflammation mediated angiogenesis, arthritis and obesity

Zhenguang Zhang

Ph.D – The University of Edinburgh – 2014

Abstract

11β-hydroxysteroid dehydrogenase type 1 (11β-HSD1, encoded by *Hsd11b1*) is an enzyme that predominantly converts inactive glucocorticoids (cortisone in human and most mammals, 11dehydro-corticosterone in mice and rats) into their active forms (cortisol and corticosterone, respectively). Thus 11β-HSD1 amplifies intra-cellular levels of glucocorticoids. Studies in globally 11β-HSD1 deficient mice have revealed changes in glucocorticoid-regulated physiological and pathological processes, including metabolism, aging, arthritis and angiogenesis. The function of macrophages, which play an important role in inflammation, is also altered. For example, 11β-HSD1 deficiency in macrophages causes a delay in their acquisition of phagocytic capacity. To dissect the role of macrophage 11β-HSD1 in angiogenesis, arthritis and obesity, both in *vitro* macrophage stimulation and in *vivo* functional assays in macrophage-specific 11β-HSD1 knockout mice, were conducted.

Thioglycollate-elicited peritoneal macrophages from globally 11β-HSD1 deficient and control C57BL/6 mice were used for *in vitro* studies. In M1/M2 macrophage polarisation experiments, 11β-HSD1 deficient macrophages showed increased expression of mRNAs encoding pro-inflammatory factors upon lipopolysaccharide and interferon-ϒ treatment and decreased expression of pro-resolution genes with interleukin-4 stimulation. However, at cytokine or protein levels, there was little difference between the genotypes except for decrease IL12 p40 levels in 11β-HSD1 deficient macrophages. Hypoxic stress failed to show differences between genotypes in hypoxia-regulated gene expression. These data do not support a strong role for macrophage 11β-HSD1 in inflammation regulation, nor in response to hypoxia, at least when measured *in vitro*. The discrepancy between transcriptional and translational responses is currently unexplained, but may reflect altered post-transcriptional activity.

To investigate the role of macrophage 11β-HSD1 *in vivo*, macrophage-specific *Hsd11b1* knockout mice, *LysM-Cre Hsd11b1*$^{flox/flox}$ (MKO) mice and *Hsd11b1*$^{flox/flox}$

littermate controls were generated. In MKO mice, 11β-HSD1 protein levels and enzyme activity were reduced by >80% in resident peritoneal macrophages. However, 11β-HSD1 protein and enzyme activity levels were unchanged or only modestly reduced in thioglycocollate-elicited peritoneal neutrophils, monocytes/macrophages, or in bone marrow-derived macrophages, despite >80% decrease in *Hsd11b1* mRNA levels in these cells. A relatively long half-life of 11β-HSD1 protein compared to that of circulating myeloid cells may underlie this mismatch between transcriptional and translational expression. Furthermore, following 12 days of inflammatory arthritis induced by K/BxN serum transfer, the reduction in 11β-HSD1 protein levels in circulating neutrophils of MKO mice is consistently around 50%, which corroborates the above explanation.

MKO mice and littermate controls were subjected to inflammatory models which may involve resident macrophages. First, to address the role of 11β-HSD1 in macrophages in angiogenesis, sponge implants were inserted subcutaneously into the flanks of adult male mice and harvested after 21 days. Chalkley counting on hematoxylin and eosin stained sponge sections showed significantly increased angiogenesis in MKO mice (scores: 5.2 ±1.0 versus 4.3 ±0.7; $p<0.05$, n=9-11). *Cdh5* expression (encoding VE-cadherin, a marker of endothelial cells) was higher in sponges from MKO mice (relative expression: 1.5 ±0.9 versus 0.8 ±0.6; $p<0.05$), as was *Il1b* (encoding IL-1 beta, a marker of inflammation, relative expression: 6.5 ±6.4 versus 1.5 ±0.9; $p<0.05$). *Vegfa* mRNA (encoding vascular endothelial growth factor alpha) was unchanged, with a trend for higher *Angpt1* (encoding angiopoietin 1, $p=0.09$) expression levels in the MKO group. These results suggest that lack of 11β-HSD1 in resident macrophages increases their pro-angiogenic activity, independently of VEGF-α.

The K/BxN serum transfer model of arthritis was used to investigate the role of macrophage 11β-HSD1 in arthritis. Adult male MKO and control mice received a single i.p. injection of 125µl K/BxN serum per mouse, followed by 21 days of clinical scoring to assess joint inflammation. The onset of inflammation (d1-8) was similar between MKO and control mice, but MKO mice exhibited greater clinical

inflammation scores in the resolution phase of arthritis (d13-21; area-under-the-curve: 86.6 ±14.7 versus 60.1 ±13.4; $p<0.005$), indistinguishable from globally 11β-HSD1-deficient mice. Hematoxylin and eosin staining revealed pronounced fibroplasia predominantly in the supporting mesenchyme associated with the tenosynovium, with new bone and blood vessel formation. These results suggest that macrophage 11β-HSD1 deficiency is fully accountable for the worse arthritis resolution phenotype in the globally 11β-HSD1 deficient mice, but not the earlier onset of inflammation with global 11β-HSD1 deficiency.

Macrophage activation states are closely linked with adipose insulin sensitivity. Globally 11β-HSD1 deficient mice are protected from high fat diet induced insulin resistance and adipose tissue hypoxia and fibrosis. To study the effect of macrophage 11β-HSD1 deficiency on insulin sensitivity, adult male MKO and control mice were given a 14 week high fat diet, which typically causes insulin resistance in control but not globally 11β-HSD1 KO mice. The level of fibrosis in subcutaneous adipose tissues was reduced as indicated by quantification of picrosirius red staining of collagen, though GTT data so far does not support protection from insulin resistance in MKO mice.

In summary, in *vitro* macrophage polarisation experiments do not support a strong role of 11β-HSD in M1/M2 macrophage polarisations or response to hypoxia. However, MKO mice reveal, for the first time, an important *in vivo* role of macrophage 11β-HSD1 to promote angiogenesis and facilitate resolution of K/BxN serum transfer induced arthritis. Modulation of fibrosis is context dependent. Reduced adipose fibrosis may be one of the mechanisms that improve insulin sensitivity. Meanwhile, these findings suggest caution regarding the potential side effects of 11β-HSD1 inhibitors in treating metabolic disease in patients with inflammation-related co-morbidities, such as rheumatoid arthritis.

Dedication

To my grandmother, whose love and kindness from simple Buddhism belief, has expelled fear and hunger in my childhood life in the small village of Shilou and filled my heart with light, hope and love.

Acknowledgements

First, i would like to take this opportunity to express my gratitude to my first supervisor Professor Karen Chapman. Without her kindness to train junior students, I may not have had the chance to take the postgraduate study here in Edinburgh. Without her patience in instruction, my study would have been much more difficult. Her passion, optimistic and organised way of life offer valuable wisdom to my growth. I enjoy lots of benefits of Dr. Agnes Coutinho's pioneer work during my Ph.D. Without her hard work to collaborate and introduce different inflammation models into an endocrinology lab, I couldn't imagine my Ph.D study finished on time. Dr. Tiina Kipari's broad knowledge and strong interest in immunology leads me into immune research. Dr. Patrick Hadoke helps a lot in organising the thesis committee meeting and more importantly, he led me into the way of angiogenesis study. My supervisor Professor Jonathan Seckl's kind support and valuable vision shapes the Ph.D project.

I owe lots of gratitude to lots of people in the lab, for their patience to teach me different techniques and share their experiences. Ms Tak Yung Man, as my first lab mentor, patiently taught me a lot both in work and in life, including the Chinese cooking recipes! Without her, I would be really very lonely in the UK. I enjoy a lot of the friendly, cheerful atmosphere with people in the department. People in the Office C.01a, both in the past and present, you make my life colourful and very warm in the cold Scotland! I've learned how nice it is to have so many good buddies together. What's more, the nice cakes make my body more adapted to survive the cold weather!

I would like to thank other teachers here as well, for the study discussion, Dr. Yuri Kotelevtsev, Gillian Gray, Chris Kenyon, Nik Morton and Margarete Heck. Thanks for Larraine, Lee in the animal unit to take care of the mice. Thanks for Spike and Gary for the animal surgical help and Ailiang Zhang, Meng Cai for generous help.

Thanks for all my friends in Edinburgh outside the lab, for all the time accompanying me and having fun together.

Last, but not the least, I would like to thank my family members for their encouragements and delicate care and Ms Jingli Yang for the understanding and support.

Declaration

I, Zhenguang Zhang, declare that this thesis and the data presented in it are the results of my own efforts with technical help from the following individuals: Dr. Sophie Turban who performed the serum glucose and insulin measurement and Mr Olive Brown who analysed the picrosirius red staining and measured the adipocyte size. This work has not been submitted for any other professional qualification or degree.

_____

Zhenguang Zhang

Edinburgh, 2014

Table of contents

Contents

Index of Figures

Index of abbreviations

11β-HSD	11β-Hydroxysteroid dehydrogenase
11-DHC/A	11-Dehydrocorticosterone
ACTH	Adrenocorticotrophic hormone
ANOVA	Analysis of variance
AP-1	Activator protein-1
B	Corticosterone
BMDM	Bone marrow derived macrophages
bp	Base pairs
BSA	Bovine serum albumin
CBG	Corticosteroid binding globulin
CD	Cluster of differentiation
COX-2	Cyclooxygenase 2
CRH	Corticotrophin releasing hormone
DI H_2O	Deionized water
DEPC	Diethylpyrocarbonate
DMEM	Dulbeco's modification of Eagle's medium

DNA	Deoxyribo nucleic acid
dNTP	Deoxyribonucleotide triphosphate
DTT	Dithiothreitol
EDTA	Ethylene diamine tetraacetic acid
FBS/FCS	Fetal bovine/calf serum
FITC	Fluorescein isothiocyanate
GM-CSF	Granulocyte macrophages colony stimulating factor
GC	Glucocorticoid
GR	Glucocorticoid receptor
GRE	Glucocorticoid response element
H6PDH	Hexose-6-phosphate dehydrogenase
H&E	Hematoxylin and eosin
h	Hour
Hh	Hedgehog
HPA axis	Hypothalamic-pituitary-adrenal axis
HPLC	High pressure liquid chromatography
HSP	Heat shock protein
HRP	Horseradish peroxidase
IFN-γ	Inteferon gamma
Ig	Immunoglobulin

IL	Interleukin
i.p.	Intra-peritoneal
LPS	Lipopolysaccharide
Min	Minute
MCP-1	Monocyte chemoattractant protein l
MR	Mineralocorticoid receptor
mRNA	Messenger RNA
NAD	Nicotinamide adenine dinucleotide
NADP	Nicotinamide adenine dinucleotide phosphate
NFκB	Nuclear factor-kappa B
PBS	Phosphate buffered saline
PCR	Polymerase chain reaction
PE	Phycoerythrin
RNA	Ribo-nucleic acid
RT	Room temperature
s	Second
TAE	Tris EDTA acetate
TG	Thioglycollate
TGF-β	Transforming growth factor beta
TLC	Thin Layer Chromatography

TNF-α	Tumor necrosis factor alpha
VEGF	Vascular endothelial growth factor

Chapter 1: Introduction

Cortisone, a natural but intrinsically inert glucocorticoid was discovered in the middle of the 20th century and is one of the most useful drugs to suppress inflammation. However, its efficacy was subsequently revealed to be dependent on an enzyme called 11β-hydroxysteroid dehydrogenase type 1,which converts the inert cortisone into active cortisol (reviewed by (Chapman, Holmes et al. 2013)). More than half a century later, glucocorticoids remain one of the most widely prescribed anti-inflammatory drugs and efforts to elucidate the anti-inflammatory mechanisms continues, including studies on the role of endogenous glucocorticoids. The theme of this thesis is to dissect the role of reactivation of endogenous glucocorticoids by 11β-hydroxysteroid dehydrogenase type 1 in macrophages, in modulating inflammation development.

1.1 Inflammation and tissue homeostasis

1.1.1 Inflammation and immune cells

Inflammation was described by Cornelius Celsus in as early as the 1st century AD in his treatise *De medicina*. The four cardinal signs of inflammation were described as: *rubor et tumor cum calore et dolore* (redness and swelling with heat and pain; reviewed by (Medzhitov 2010)). In the 19th century, with only a microscope to study inflammatory tissues, Julius Cohnheim observed vasodilation, leakage of plasma, and migration of leukocytes out of blood vessels and into the surrounding tissues (reviewed by (Majno 2004)). *Functio laesa* (disturbance of function), was added as the fifth cardinal sign by Rudolph Virchow in 1858 (reviewed by (Majno 1975)). According to the duration of the symptoms, inflammation can be classified into acute and chronic forms. Acute inflammation usually resolves within days to weeks, with restoration of normal tissue function, while chronic inflammation, such as rheumatoid arthritis, causes long lasting damage to tissues (reviewed by (Ryan and Majno 1977; Medzhitov 2010)).

The modern study of inflammatory mechanisms began in the late 19th century; Robert Koch and Louis Pasteur introduced the germ theory of diseases to explain a major cause of inflammation. Later, Elie Metchnikoff discovered that some blood cells, macrophages and microphages (neutrophils) are able to phagocytose micro-organisms, a beneficial aspect of inflammation (reviewed by (Tauber 2003)). Phagocytes are found in both plants and vertebrates as the 'first line' cells of host defence and are appreciated as innate immune cells. Emil von Behring and Shibasaburo Kitasato discovered serum therapy against diphtheria and tetanus toxins in 1890, which led to early development of the humoral immunity theory (reviewed by (Medzhitov 2010)). Serum antibodies were found to be produced by B cells with the help of T cells in the middle of the 20th century. B and T cells are adaptive immune cells, found only in vertebrates.

Humoral immunity explained the long lasting immunity against some infections. But the puzzle of how innate immune cells were linked with adaptive immune cells was not solved until the 1990s. Bruce A. Beutler and Jules A. Hoffmann discovered toll-like receptors (TLRs) and uncovered their roles in the recognition of micro-organism components. At a similar time, Ralph M. Steinman discovered the ability of dendritic cells to present antigens to T cells. Their works was honoured by the 2011 Nobel Prize in Physiology or Medicine (2011). The hemogenesis of immune cells is depicted in Figure 1-1.

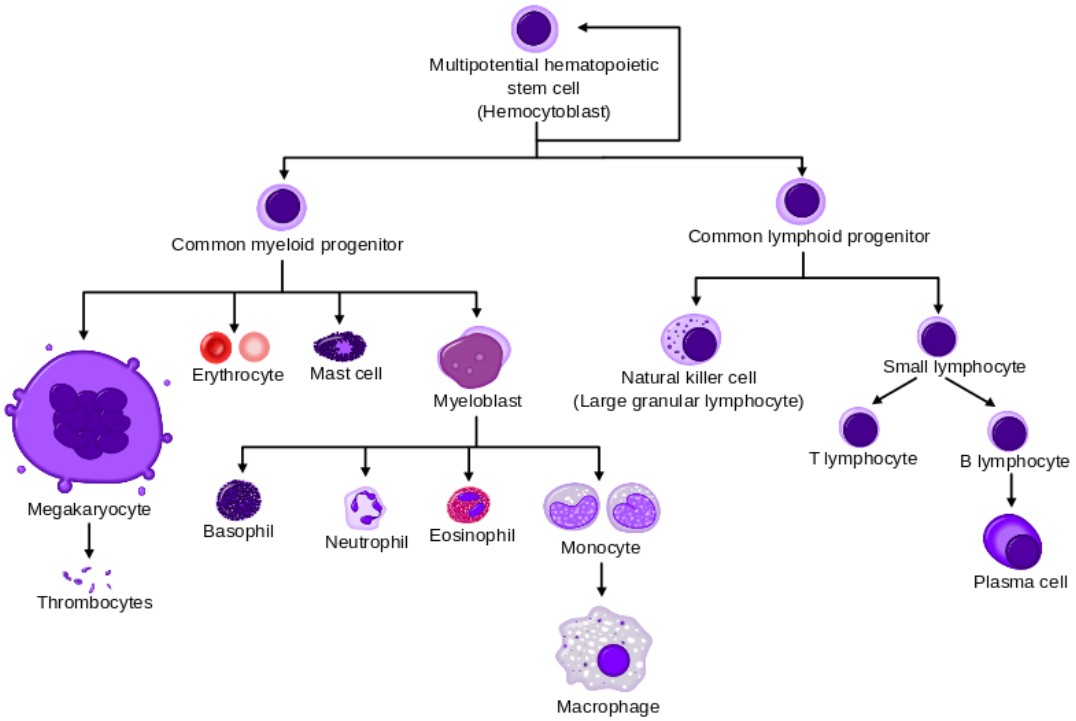

Figure 1-1 Hemogenesis of bone marrow derived immune cells.

'White blood cells' are immune cells, which are generated along the myeloid and lymphoid lineages in the bone marrow. Macrophages and neutrophils are the main innate myeloid cells and T and B cells are the main adaptive lymphoid cells. Image Hematopoiesis_(human)_diagram.png by A. Rad was obtained from Wikimedia Commons under GNU Free Documentation License.

1.1.2 Different types of inflammatory response

Ruslan Medzhitov proposed that inflammation comprises four components: inflammatory inducers, sensors in immune cells, the inflammatory mediators produced by immune cells and the affected target tissues (Medzhitov 2010) (inflammation resolution was not included). Different inflammatory inducers trigger different inflammatory responses. Bacterial products such as lipopolysaccharide (LPS) are sensed by TLR4 on macrophages, which then produce inflammatory cytokines, such as tumour necrosis factor (TNF) alpha, interleukin (IL) -1, IL-6 and chemokines. These products can directly induce blood vasodilation and elicit neutrophils, as well as induce liver production of acute phase reaction proteins, such as C-reactive protein. Viral infection induces production of type-I interferons (IFN-α, IFN-β) in infected cells, whereas parasitic worms induce mast cells and basophils to produce histamine, IL-4, IL-5, and IL-13.

The signalling in sterile inflammation, such as tissue injury, is less understood. Dead cell products, such as ATP, high-mobility group box 1 (HMGB1), DNA, heat shock proteins, etc., may be the inflammatory inducer (reviewed by (Chen and Nunez 2010; Medzhitov 2010; Shen, Kreisel et al. 2013)). Inflammasome activation to generate Il-1β revealed by genetic studies in humans is one of the most intensively studied pathological signalling pathways and it plays an important role in lots of clinical autoinflammatory diseases, such as familial cold autoinflammatory syndrome, Muckle-Wells syndrome, neonatal-onset multisystem inflammatory disease (reviewed by (Masters, Simon et al. 2009)).

According to the patterns of lymphokine production, two types of murine helper T cell clones were reported in 1986 (Mosmann, Cherwinski et al. 1986). The different populations of helper T cells were later found during *in vivo* studies. In viral infection, Th1 cells are induced to exert cellular cytolytic activity by production of inflammatory cytokines, like TNF-α and IFN. In parasitic infection, Th2 cells produce IL-4, 5, and 13, to stimulate B cell generation of immunoglobulin (Ig) G and IgE. Th2 responses are linked to the allergy response (reviewed by (Constant and Bottomly 1997)). Similar to Th1/Th2, there is the M1/M2 macrophage nomenclature

based on *in vitro* experiments, though macrophages *in vivo* are highly heterogeneous and frequently do not confine to the M1/M2 classifications (detailed description in Section 1.2.2).

Like the sterile inflammation mentioned above, the inflammatory inducers are not always clear for *in vivo* inflammatory models. Models used in the studies described in this thesis will be briefly discussed below. Thioglycollate induced sterile peritonitis is often used to elicit large quantities of myeloid cells, especially macrophages. The sensor for thioglycollate remains elusive. In this model, neutrophils are first recruited and their number peaks between 4-24h, followed by accumulation of macrophages peaking on day 3 or 4 (Van Furth, Diesselhoff-den Dulk et al. 1973). The macrophage peak accumulation is dissociated from the peak production of inflammatory mediators on day 1 (Lam, Harris et al. 2013).

High fat or high cholesterol diet feeding is usually conceived to be associated with development of low-grade inflammation. Again, there is no clear pathway that describes how lipid or cholesterol induces immune cell activation and whether the inflammation is dominated by hepatocytes and adipocytes or the infiltrating immune cells needs further clarification. Microarray of cholesterol loaded macrophages (foam cells) surprisingly showed decreased inflammatory gene expression profiles (Spann, Garmire et al. 2012). The primary inflammatory response to lipid may come from adipocytes, which could recognize lipid by TLR4 and secrete inflammatory cytokines in response (Pal, Dasgupta et al. 2012).

In the K/BxN serum transfer model of inflammatory arthritis, the serum anti-glucose-6-phosphate isomerase (anti-G6PI) antibody forms immune complexes when injected into naïve mice and the immune complexes are sensed by FcϒIIIR receptor in myeloid cells (Binstadt, Patel et al. 2006). A subsequent lipid-cytokine-chemokine cascade leads to accumulation of neutrophils, and the arthritis resolution is likely to be dependent on macrophage clearance of apoptotic neutrophils (Elliott, Van Ziffle et al. 2011; Sadik and Luster 2012).

1.1.3 Inflammation resolution, angiogenesis and fibrosis in the tissue repair process

The beneficial side of inflammation to clear debris and infection was first appreciated by Metchnikoff in his discovery of macrophage (Metchnikoff 1892). However, in the other side of the inflammation 'coin', tissue damage usually happens as a 'trade-off'. For example, reactive oxygen species generated by neutrophils can induce DNA damage (van Berlo, Wessels et al. 2010). Chronic low-grade inflammation without a clear (but possibly persistent) stimulus accompanies a large number of diseases, including atherosclerosis, obesity, type 2 diabetes mellitus and Alzheimer's disease (reviewed by (Nathan and Ding 2010; Aguzzi, Barres et al. 2013; Odegaard and Chawla 2013; Swirski and Nahrendorf 2013; Tabas and Glass 2013)). To restore normal tissue homeostasis, effective inflammation resolution is required, the mechanism of which is still poorly understood. Cytokines IL-4, IL-10, transforming growth factor beta (TGF-β), endogenous glucocorticoids and lipoxins are able to suppress inflammation (reviewed by (McMahon and Godson 2004; Medzhitov 2010)). Accumulating evidence suggests that apoptotic cells induce an anti-inflammatory response (Fadok, Bratton et al. 1998; Ren, Xie et al. 2008; Miles, Heaney et al. 2012).

Angiogenesis and fibrosis are usually induced by inflammatory tissue damage, which may further perpetuate inflammation development. Both angiogenesis and fibrosis occur in response to hypoxic conditions in tissue injury, under control of the transcription factors, hypoxia induced factors (HIFs). To facilitate tissue repair, HIFs upregulate expression of metabolic proteins (GLUT-1), soluble growth factors (TGF-β and vascular endothelial growth factor (VEGF)) and extracellular matrix components (type I collagen and fibronectin) (reviewed by (Walshe and D'Amore 2008; Lokmic, Musyoka et al. 2012)).

Angiogenesis is a process of new capillary formation from pre-existing vessels. In this process, inflammatory cells secrete pro-angiogenic factors such as vascular endothelial growth factor (VEGF), basic fibroblast growth factor, angiopoietins, TNF-α, nitrogen oxide (NO) and IL-1β, to stimulate endothelial cell mitosis and migration (Costa, Incio et al. 2007). It can be beneficial to restore tissue

homoeostasis, for example providing oxygen and nutrition by re-vascularisation in ischemic areas. However, it is deleterious and facilitates inflammation development in other situations, such as promotion of synovitis in rheumatoid arthritis (Szekanecz, Besenyei et al. 2010).

To repair the injury caused by inflammation and maintain tissue integrity, cytokines such as TGF-β activate fibroblasts and transform them into smooth muscle actin positive (SMA+) myofibroblasts, which then secret collagens to maintain tissue intactness (Lee and Kalluri 2010). After tissue repair, these myofibroblasts usually become apoptotic (Wynn and Ramalingam 2012). Persistence of myofibroblasts in tissues can lead to fibrosis. In addition, activated fibroblasts were shown to play an important role in supporting inflammation development, by secreting inflammatory cytokines, like IL-6 and IFNs (reviewed by (Flavell, Hou et al. 2008). The source of myofibroblasts remains unclear and has been mainly attributed to bone marrow derived fibrocytes and endothelial-mesenchymal transition (Hinz and Gabbiani 2010). However, a number of fate mapping studies have suggested that local vessel pericytes are likely to be the main source (reviewed by (Hutchison, Fligny et al. 2013)).

1.2 Macrophages

1.2.1 Macrophage origin and differentiation

As the first discovered immune cells, macrophages have been extensively studied for over 100 years. They can be broadly divided into tissue-resident macrophages and infiltrating inflammatory macrophages. The former group includes liver Kupffer cells, brain microglia, lung alveolar macrophages, peritoneal macrophages, splenic red pulp macrophages and bone marrow resident macrophages. Tissue resident macrophages are conceived to be sentinels for tissue patrolling to clear cell debris and sense tissue injury (Soehnlein and Lindbom 2010). Infiltrating macrophages arise in pathological situations. They differentiate from blood monocytes, and accumulated evidence has shown that classical monocytes (also known as "inflammatory" or Ly6C^{hi} monocytes) are the source of infiltrating macrophages found in pathological settings, such as in cancer, atherosclerosis, and metabolic diseases (reviewed by (Hashimoto, Chow et al. 2013)).

The origin of tissue resident macrophages has been debated. Until recently, it was though that they originated from bone marrow derived Ly6C^{low} 'patrolling' monocytes, amid suggestions of a different origin. For example, resident peritoneal macrophage density is normal in mice lacking C-C chemokine receptor type 2 (CCR2, the receptor for the monocyte chemo-attractant protein (MCP)1), despite defects in monocyte infiltration of these mice (Kuziel, Morgan et al. 1997). Tissue resident macrophages in mice have recently been revealed to derive from the yolk sac during embryo development, and they are maintained independently of hematopoietic stem cells (Schulz, Perdiguero et al. 2012). Tissue resident macrophages can divide in response to Th2 inflammation (Jenkins, Ruckerl et al. 2011), in contradiction to the paradigm that macrophages are terminally differentiated cells that cannot divide. Gene array analysis of tissue resident macrophages shows heterogeneous gene expression signatures in different population of tissue resident macrophages (Gautier, Shay et al. 2012).

1.2.2 Classic and alternative macrophage polarizations

Similar to the Th1/Th2 nomenclature, classically activated macrophages (M1) and alternatively activated macrophages (M2) were defined by Siamon Gordon during *in vitro* experiments with bone marrow derived macrophages (reviewed by (Mantovani, Sica et al. 2005)). M1 macrophages, usually activated by IFN-γ and/or LPS, are mainly microbicidal, characterized by high production of inflammatory cytokines and chemokines (such as IL-1, IL-6, TNF-α, IFN-ϒ and CCL2), as well as reactive oxygen species and NO. M2 macrophages, in contrast, are induced by Th2 cell products like IL-4, IL-13, IL-10 or apoptotic cells or glucocorticoids, with high expression levels of YM1, FIZZ1 and arginase 1 (reviewed by (Varin and Gordon 2009)). They are associated with resolution of inflammation, angiogenesis and fibrosis (reviewed by (Gordon and Martinez 2010)). The M1/M2 polarisation scheme is summarized in Figure 1-2.

Based on *in vitro* experiments, M2 macrophages can be sub-divided into 3 categories: IL-4/13-stimulated M2a cells, IL-1R+TLR-stimulated M2b cells and glucocorticoid-activated M2c cells (reviewed by (Mantovani, Sica et al. 2004)). Different to M2a and M2c, there is also a high inflammatory response in M2b cells, in addition to the common anti-inflammatory features of M2 macrophages (Mantovani, Sica et al. 2004). Actually, monocyte-derived macrophages are very plastic to stimuli during *in vitro* experiments and exhibit high differentiation heterogeneity. It is further proposed that macrophage polarisation state is best described as in a full spectrum (Mosser and Edwards 2008; Geissmann, Gordon et al. 2010; Gordon 2012).

It should be noted that the M1/M2 macrophage nomenclature does not correspond to the classifications of recruited and tissue resident macrophages. Macrophage polarisation experiments are usually carried out in monocyte derived macrophages, while tissue resident macrophages are generally shown to be important for inflammation resolution. For example, 12/15 lipoxygenase which is enriched in peritoneal resident, but not recruited macrophages, generates pro-resolution lipoxins that mediate phagocytosis of apoptotic neutrophils (Uderhardt, Herrmann et al.

2012). Even for bone marrow derived macrophages, so far, there is no direct *in vivo* evidence to separate the two distinct populations of macrophages which regulate different physiological processes. Heterogeneous macrophage gene expression profiles (a mixture of both M1 and M2) are found during either wound repair or tissue fibrosis (Duffield, Forbes et al. 2005; Daley, Brancato et al. 2010; Novak and Koh 2013).

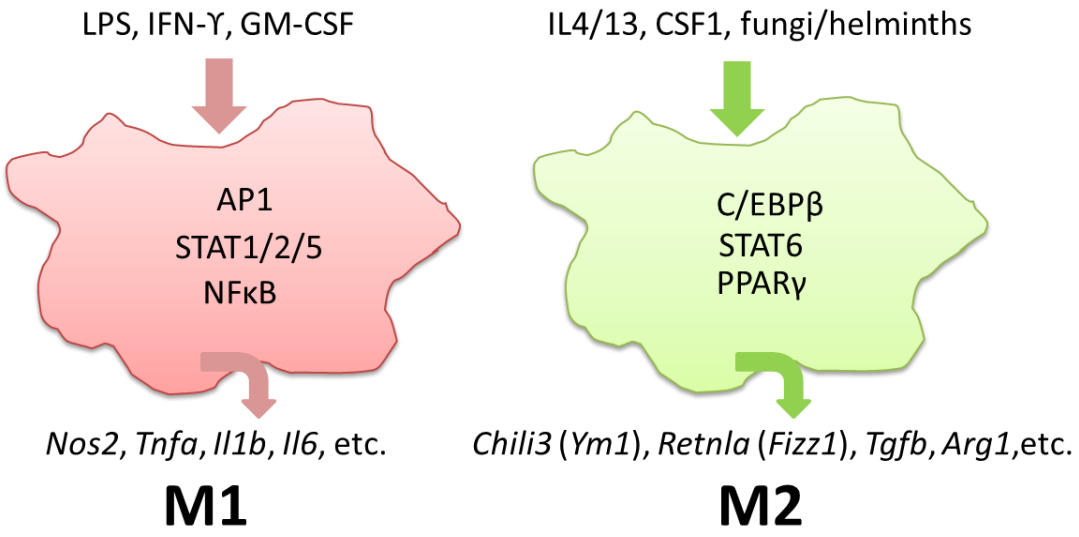

Figure 1-2 Classical (M1) and alternative (M2) Macrophage polarisation.

The respective stimuli to induce M1/M2 polarisations are shown at the top of the picture, with related transcription factors in the middle, and characteristic products/markers at the bottom of the picture. Adapted from (Lawrence and Natoli 2011).

1.2.3 Macrophages in tissue repair

Inflammation is accompanied by tissue remodelling, such as angiogenesis and fibrosis, as introduced in section 1.1.3. So far, of all the immune cells, macrophages are considered the main regulators of tissue remodelling. In physiological situations, macrophages are essential to many tissue developmental processes, such as bone morphogenesis, ductal branching, neuronal patterning and vascular patterning (reviewed by (Pollard 2009; Wynn, Chawla et al. 2013)). Macrophages are also extensively and actively involved in pathological situations as introduced below.

The interest of macrophages in situations of pathological angiogenesis probably stems from observations of tumour associated macrophages in supporting tumour growth and metastasis (Sunderkotter, Steinbrink et al. 1994; Lin, Li et al. 2006). These observations led to the discovery of a subset of $TIE2^{+}NRP1^{+}$macrophages that promote angiogenesis (De Palma, Venneri et al. 2005). TIE2 is the angiopoietin receptor and NRP1 is a receptor for specific class 3 semaphorins and VEGF isoforms (Kawamura, Li et al. 2008). The presence of this subset of macrophages was later described in healthy mouse blood and developing embryos (Pucci, Venneri et al. 2009). Their role is to stimulate fusion of activated endothelial tip cells to form new circuits from existing blood vessel networks (Fantin, Vieira et al. 2010). Apart from tumour angiogenesis, they are also important for angiogenesis in ischaemic situations (Patel, Smith et al. 2013). In an *in vitro* angiogenesis model of aortic ring assay, macrophages play a non-redundant role, as they are 'rich sources' of pro-angiogenic factors such as TNF-α, IL-6, IL-1, VEGFα and angiopoiten 1. (Ligresti, Aplin et al. 2011). But macrophages are also able to suppress angiogenesis, mediated through the Wnt-Flt1 pathway to inhibit VEGF signalling (Stefater, Lewkowich et al. 2011).

The important role of macrophages in fibrosis during tissue repair was recognised as early as the 1970s. Depletion of monocytes/macrophages, with combined systemic glucocorticoid and local anti-macrophage serum treatment, impaired wounding healing with delayed fibroblast recruitment and activation (Leibovich and Ross 1975). From separate studies of liver fibrosis and wound healing in CD11b-DTR and LysM-Cre/iDTR mice, where macrophages can be specifically depleted by

administration of diphtheria toxin, macrophages were shown to promote fibrosis development and wound healing (Duffield, Forbes et al. 2005; Goren, Allmann et al. 2009; Lucas, Waisman et al. 2010). The functions of macrophages in fibrosis include phagocytosis of cell debris, secretion of TGF-β and platelet derived growth factor (PDGF) to activate mesenchymal stem cells, expression of arginase activity to generate proline for collagen synthesis, as well as production of matrix metalloproteinase (MMPs) to degrade extracellular matrix in tissue remodelling (Wynn and Barron 2010).

It is of note that there are also suggestions that lack of resident macrophages and recruiting neutrophils doesn't impair wound healing, with normal wound healing in myeloid cell deficient *PU.1*$^{-/-}$ mice on antibiotics (Martin, D'Souza et al. 2003). Thus, the exact role of myeloid cells in tissue remodelling awaits further investigation.

1.3 Glucocorticoids

1.3.1 History of glucocorticoid discovery

In the 1930s, Dr Tadeus Reichstein in Switzerland first isolated 25 steroid compounds from the adrenal cortex and shared the results with Dr Edward Kendall at the Mayo Clinic in the United States. After chromatographic separation of the steroids, Dr. Kendall decided to characterise 5 of the compounds named A-E, the chemical structures of which were published simultaneously and independently by him and Drs. Reichstein and Pfiffner (Mason, Myers et al. 1936; Reichstein 1936; Wintersteiner and Pfiffner 1936). These compounds were later revealed as the following chemicals: Kendall's compound A, 11-dehydrocorticosterone; Kendall's compound B (Reichstein's substance H), corticosterone; Kendall's compound C (Reichstein's substance C), 5α-pregnane-3α,11β,17α,21-tetrol-20-one; Kendall's compound D (Reichstein's substance A), 5α-pregnane-3β,11β,17α,20β,21-pentol; Kendall's compound E (Reichstein's substance F), cortisone, and Kendall's compound F (Reichstein's substance M) is cortisol.

Dr. Philip Hench at the Mayo Clinic, who had been long interested in the observation of an adrenal hormone 'X', likely to relieve rheumatoid arthritis (RA), pioneered the use of the newly discovered 'E' (cortisone) in RA patients. The first patient, Mrs Gardner, a 29 year old woman with severe RA, was injected with compound E on 21st of September 1948 and showed a 'miraculous' cure (Hench, Slocumb et al. 1950; Slocumb, Polley et al. 1950). Dr Philip Hench received the Nobel Prize in 1950 for this clinical application, together with Dr. Tadeus Reichstein and Edward Kendall.

Since then, a variety of synthetic glucocorticoids (GCs), have gained widespread use in the treatment of various inflammatory diseases, including hydrocortisone (cortisol, a natural GC) (Peterson and Murray 1952), prednisone (Oliveto 1959), prednisolone (Arthur 1958), methylprednisolone (Sebek and Spero 1959), triamcinolone (Seymour and Allen 1957), betamethasone (David, Wendler et al. 1962), dexamethasone (Georges, Roland et al. 1961), fluodrocortisone (Spero, Magerlein et al. 1958), fluticasone (H, M et al. 1982) and budesonide (Brattsand, Af Ekenstam et al. 1975)

including RA, asthma and autoimmune diseases such as systemic lupus erythematosus (reviewed by (Joanny 2011)).

1.3.2 Physiological regulation of endogenous glucocorticoids

Endogenous GCs are synthesised and secreted from the zona fasciculata-reticularis of the adrenal cortex, under the control of hypothalamic-pituitary-adrenocortical (HPA) axis activity. Integration of numerous neural and humoral signals by the hypothalamus leads to release of corticotrophin-releasing hormone (CRH) and arginine vasopressin (AVP) from the hypothalamic paraventicular nucleus (PVN) into the portal vessels, to reach the anterior pituitary gland. This triggers ACTH release and production of its precursor pro-opiomelanocortin (POMC). Following release of ACTH into the circulation, it reaches the adrenal cortex and binds with melanocortin receptor type 2 to stimulate GC synthesis (reviewed by (McEwen, Biron et al. 1997)). The HPA axis is negatively regulated by circulating GC, which reduces CRH and ACTH secretion from the hypothalamus and anterior pituitary gland, respectively (reviewed by (Gomez, De Kloet et al. 1998)).

There is a circadian rhythm in the secretion of GCs, with a peak in the morning and nadir in the evening in humans, opposite to that in nocturnally active mammals, such as mice (reviewed by (Dickmeis 2009)). GCs are secreted in a pulsatile manner, and this is determined to be in an hourly pattern in rats, with alternating phases of activation and inhibition, accompanied by shuttle of glucocorticoid receptor (GR) between nucleus and cytoplasm (Lightman, Wiles et al. 2008).

In the circulation, in addition to weak binding to albumin, more than 90% cortisol/corticosterone is bound to corticosteroid binding globulin (CBG), which is a glycoprotein secreted by the liver with poor affinity for inert forms of GCs and aldosterone (Funder, Feldman et al. 1973). CBG is a substrate of the elastase released from inflammatory neutrophils and after cleavage, CBG releases more than 80% of the bound GC (Hammond, Smith et al. 1990) and this may act as GC ‘local’ delivery mechanism by inflammatory neutrophils. CBG binding with GC is an

important control of GC availability, as only free GC can diffuse through the lipid membrane of cells. In CBG deficient mice, total corticosterone levels were reduced by 50% but with a 10-fold increase in the free fraction of the hormone (Petersen, Andreassen et al. 2006). However, GCs are also subject to trafficking by cell membrane GC transporters such as multidrug resistance protein 1 (MDR1, ABCB1) and ABCG1, which can export GCs out of cells and may actively regulate intracellular levels of GC (Webster and Carlstedt-Duke 2002; Nieuwenhuis, Luth et al. 2009).

1.3.3 GCs in inflammation

Synthetic GCs have been widely used to treat inflammatory diseases since their initial success in RA patients, but the role of endogenous GCs in inflammation has been less studied. Early evidence supporting a role for endogenous GCs to suppress inflammation includes the higher mortality rate in adrenalectomised mice or mice treated with the glucocorticoid receptor (GR) antagonist RU486, upon challenge with endotoxin treatment or infection (Bertini, Bianchi et al. 1988; Hawes, Rock et al. 1992). Higher lethality was also observed in macrophage-specific GR knockout mice in response to LPS stimulation (Bhattacharyya, Brown et al. 2007) and in T cell specific GR knockout mice in response to parasite infection (Kugler, Mittelstadt et al. 2013).

In contrast, the effects of synthetic GCs have been well documented. They have many effects on immune cells during inflammation. Generally, GCs modulate immune cell functions by decreasing activation and promoting differentiation of pro-resolution phenotypes (summarized in Figure 1-3). GCs promote neutrophilia by increasing neutrophil mobilization from the bone marrow and reducing neutrophil extravasation from blood vessels by down-regulating adherence molecule expression on endothelial cells (Mishler and Emerson 1977; Jilma, Voltmann et al. 1997; Jilma, Stohlawetz et al. 1998). GCs also delay neutrophil apoptosis, in contrast to the apoptosis-inducing effects in most other immune cells such as eosinophils, mast cells and T lymphocytes (Cox 1995; Meagher, Cousin et al. 1996; Saffar, Ashdown et al.

2011). GCs suppress pro-inflammatory gene expression in macrophages, induce an anti-inflammatory M2 polarization of blood monocytes (Ehrchen, Steinmuller et al. 2007) and increase the phagocytosic ability of macrophages (Giles, Ross et al. 2001). Mast cell degranulation is decreased by GCs, which is linked to the anti-allergic effect of GCs (Zhou, Liu et al. 2008). GCs also suppress dendritic cell functions, such as migration, differentiation and antigen presentation (Moser, De Smedt et al. 1995). In terms of the effect of GCs on adaptive immune cells, GCs decrease Th1 and promote Th2 development (Ashwell, Lu et al. 2000). Decreased IgG production from B cells by GC treatment was reported, but this is still debated (Baschant, Lane et al. 2012).

To dissect the main effective immune cells for the anti-inflammatory effects of GCs, tissue specific GR knockout mice have been used in inflammatory models. This has revealed that the effective immune cell populations for inflammation suppression by GC are context dependent. While T cell GR is found to be important for GC in experimental autoimmune encephalomyelitis and collagen induced arthritis, myeloid cell GR is important for GC suppression of inflammation in a contact skin allergy model (Tuckermann, Kleiman et al. 2007; Wust, van den Brandt et al. 2008; Baschant, Frappart et al. 2011). Pharmacological targeting of GC to myeloid cells showed strong anti-inflammatory effects compared to systemic orally administrated GC, which confirmed the importance of GC action in myeloid cells (Metselaar, van den Berg et al. 2004; Ulmansky, Turjeman et al. 2012). Because inflammation models used in this thesis predominantly involve myeloid cells, more information about GCs and macrophages is introduced below.

Although the effects of GCs are generally known to be anti-inflammatory, it is reported that low dose GC (0.1nM corticosterone) can increase inflammatory responses in macrophages ((Lim, Muller et al. 2007)). Anti-inflammatory effect of GCs on macrophages during TLR4 mediated inflammatory response is specifically dependent on inhibition of p38 MAPK, but not PI3K/Akt, ERK, or JNK (Bhattacharyya, Brown et al. 2007). Another function of GC related to inflammation resolution is augmentation of macrophage phagocytosis, associated with high levels of active Rac and partially mediated through an IL-10–dependent induction of the

Gas6/MerTK pathway (Giles, Ross et al. 2001; Zizzo, Hilliard et al. 2012). Macrophage migration inhibitory factor is an endogenous factor counteracting anti-inflammatory effects of GC, inhibition of which may potentate anti-inflammatory actions of GC (reviewed (Flaster, Bernhagen et al. 2007)).

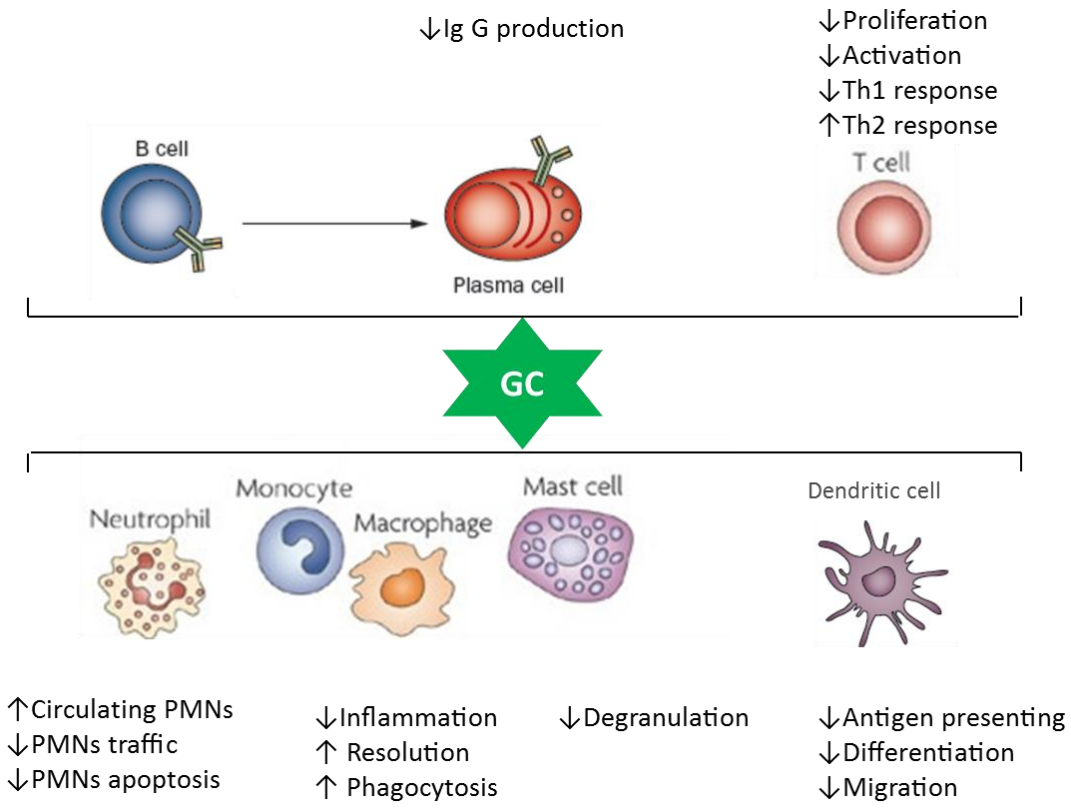

Figure 1-3 Effects of GCs on immune cells.

GCs modulate both innate and adaptive immune cell activity, usually shifting them from activated to pro-resolution states to restore homeostasis. Please refer to the above text for detailed description. Adapted from 2 publications (Perretti and D'Acquisto 2009; Baschant, Lane et al. 2012).

1.3.4 GCs in metabolism

As suggested by the name glucocorticoid (glucose-corticoid), GCs are important in energy metabolism. Although GCs can stimulate insulin secretion from pancreas during feeding, their main function is to counteract the anabolic effect of insulin. Insulin stimulates fast uptake and non-oxidative metabolism of glucose in liver, muscle and adipose tissue, and simultaneously inhibits glycogenolysis and gluconeogenesis during feeding. In contrast, in stress, such as pro-longed fasting or exercise, GCs increase lipolysis in skeletal muscle and adipose tissue, reduce glucose uptake in muscle and fat and increase gluconeogenesis in the liver to increase blood glucose levels (reviewed by (Vegiopoulos and Herzig 2007)).

The importance of GC in metabolism is evident in conditions of either GC deficiency or excess: Addison's disease and Cushing's syndrome, respectively. In Addison's disease (caused by autoimmunity against the adrenal cortex, inherited GC synthesis deficiency or pituitary disease), impaired GC action leads to chronic fatigue, weight loss and hypoglycemia. In Cushing's syndrome (caused by pituitary adenomas, ectopic ACTH-producing tumours or long term administration of synthetic GCs), excess GC action causes central obesity, reduced skeletal muscle mass, hyperglycemia, dyslipidemia, hypertension, hepatic steatosis and insulin resistance (reviewed by (Rose, Vegiopoulos et al. 2010)).

In the liver, during stress situations, GCs increase expression of key enzymes in gluconeogenesis such as phosphoenolpyruvate carboxykinase (PEPCK) (Friedman, Yun et al. 1993). Mice specifically deficient of hepatocyte GR exhibit profound hypoglycemia after prolonged fasting (Opherk, Tronche et al. 2004). GCs also increase serum VLDL-triglyceride (TG) levels and hepatic lipid accumulation, probably due to down-regulation of genes involved in hepatic TG lipolysis and β-oxidation of fatty acids, as well as an up-regulation of fatty acid uptake and storage (reviewed by (Macfarlane, Forbes et al. 2008)).

GCs are suggested to play different roles in white adipose tissue from different depots. This is reflected in the fat redistribution characterisation of Cushing's syndrome, with about a 2- and 5-fold increase in abdominal subcutaneous and

visceral fat, respectively but with reduced limb subcutaneous adipose tissue (Mayosmith, Hayes et al. 1989). During *in vitro* experiments, it was shown that GCs cause lipolysis in subcutaneous adipose tissues by inducing hormone-sensitive lipase and reducing lipoprotein lipase activity, whereas in visceral adipose tissue, GCs promote pre-adipocyte differentiation and induce lipogenic gene expression (Gaillard, Wabitsch et al. 1991; Slavin, Ong et al. 1994).

In muscle and adipose tissue, GCs blunt insulin-stimulated glucose uptake, insulin signalling, GLUT4 translocation and glycogen synthase activation (Buren, Lai et al. 2008). In the muscle, GCs are implicated in muscle protein degradation by induction of the muscle-specific ubiquitin E3 ligase, Murf1, and inhibition of protein synthesis by inducing an mTORC1 inhibitor protein REDD1 (reviewed by (Rose, Vegiopoulos et al. 2010).

1.3.5 Receptors for glucocorticoids, GR and MR

Soon after the success in treating RA with cortisone in 1950s, it was found that there are 2 receptors for endogenous GCs, now known as glucocorticoid receptor (GR, the type II GC receptor) and mineralocorticoid receptor (MR, the type I GC receptor). MR is ancestral to GR (Bridgham, Carroll et al. 2006). GR and MR show 90% identity in their DNA binding domains and 56% identity in the ligand binding domains (Arriza, Weinberger et al. 1987). In terms of ligand binding, MR has about 10-fold higher affinity than GR for GCs (Reul, Gesing et al. 2000). MR expression is confined to classical aldosterone target tissues, such as the kidney, colon, and salivary glands, and is modestly expressed in vascular tissues, adipocytes and specific immune cell populations including macrophages. In contrast, GR expression occurs at higher levels and in a wider range of tissues (reviewed by (Chapman, Holmes et al. 2013)). Activated GR and MR exert different functions. For example, GR and MR mediate opposing actions on the survival of hippocampal granule cells, partly explained by opposite changes in the ratios of pro- and anti-apoptotic gene expression (Almeida, Conde et al. 2000). In macrophages, while activation of GR

induces anti-inflammatory M2c macrophages, activation of MR promotes inflammatory M1 macrophage polarization (Usher, Duan et al. 2010).

Like MR (NR3C2), GR (NR3C1) belongs to the nuclear receptor superfamily. In humans, the *GR* gene is on chromosome 5 (Gehring et al., 1985) and comprises 9 exons, spread over ~124kb. The protein structure can be divided into an N-terminal transactivation domain (containing activation function 1, AF1, similar to all nuclear receptors), a DNA binding domain, a hinge region and a C-terminal ligand binding domain (containing AF2, similar to all nuclear receptors). There are a number of GR mRNA splice variants (GR-α, β, ϒ) arising from alternative splicing and there are different translational start sites of GR α. Thus, there is a complex group of GR proteins (summarized in Figure 1-4).

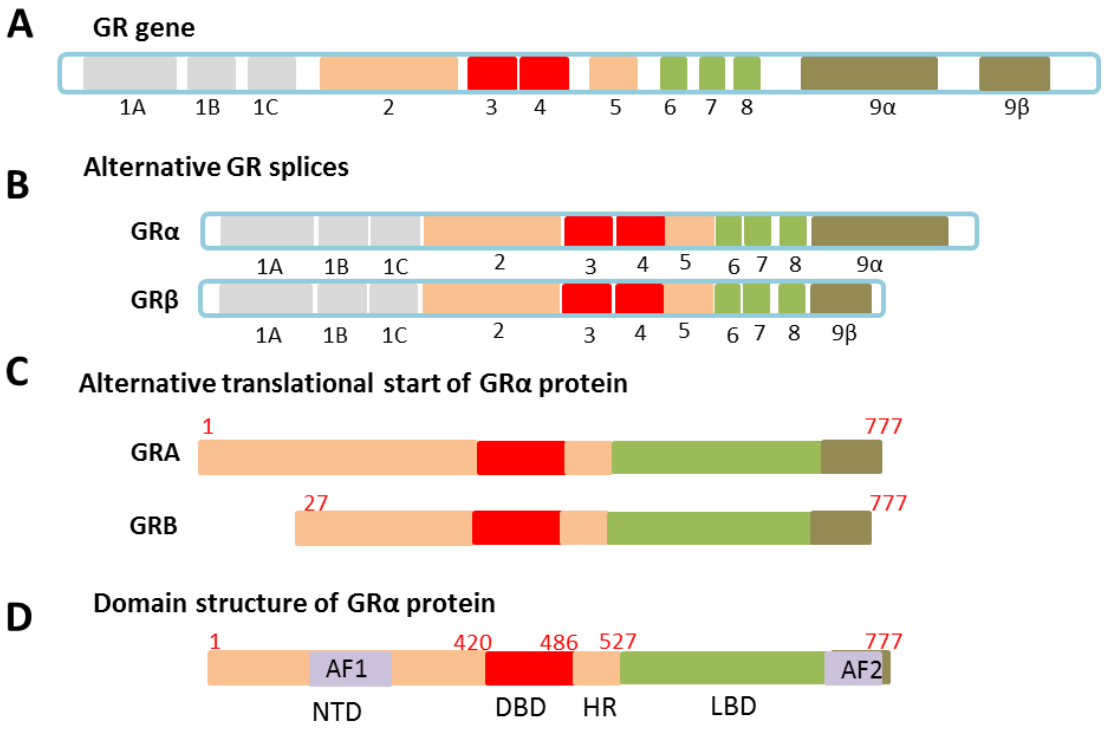

Figure 1-4 Schematic representation of the human GR gene structure, GR mRNA and GR protein structure.

(A) There are 9 exons in the GR gene. (B) Transcriptional splice variance in exon 9 generates GRα and GRβ (GRϒ not depicted in the figure). (C) From different translational start sites, GRα is translated into GRA and GRB (translational forms GRC1-3 and GRD1-3 (Revollo and Cidlowski 2009) not depicted in the figure). (D) Full length GR protein can be divided into 4 domains: N-terminal transactivation region (NTD), a pair of zinc-finger motifs comprising the DNA binding domains (DBD), the hinge region (HR) and the C-terminal ligand binding domain (LBD). AF1 and AF2 are in the NTD and LBD respectively. Numbers above the protein structure represent amino acid residue numbers.

1.3.6 Genetic regulation by GR

GC action can be divided into genomic effects (requiring binding of GR to DNA, resulting in changes of gene transcription) and non-genomic effects (occurring at the cell membrane, within minutes of GC administration, too rapidly to be attributed to effects on gene transcription). The underlying mechanism of the latter is still poorly understood, with a plausible role for GR (Perretti and D'Acquisto 2009). It is reported that around 2% of the genome is transcriptionally controlled by GCs (Reddy, Pauli et al. 2009).

In the absence of ligand, GR is normally retained in an inactive state by a complex containing chaperone proteins, including heat shock protein (HSP) -70 and HSP-90 (reviewed by (Muzumdar, Tasic et al. 2007)). Following binding of GC, the ligand-receptor complex dissociates from the HSP complex and translocates into the nucleus. The outcome is transactivation or transrepression, with the mechanism of the latter still under debate as described below.

It has been generally conceived that the anti-inflammatory effects of GCs are dependent on transrepression while the adverse metabolic effects of GCs arise from transactivation of metabolic genes. However, recent evidence has shown that there are a number of GC activated genes encoding anti-inflammatory factors, such as IL-10, β-adrenergic receptor, IL-1-receptor antagonist, tristetraprolin, dual-specificity protein phosphatase 1 (DUSP1) and annexin A1 (reviewed by (Clark 2007; Vandevyver, Dejager et al. 2013)). Tristetraprolin can reduce inflammatory signalling post-transcriptionally by aiding degradation of inflammatory mRNAs with adenosine and uridine rich elements in the 3’ UTR region. These elements are also found in many genes repressed by GCs (Carrick, Lai et al. 2004; Ishmael, Fang et al. 2008). DUSP1, also known as mitogen-activated protein kinase (MAKP) phosphatase 1, dephosphorylates and inactivates MAPKs (such as LPS activated p38, JNK and ERK), which negatively controls inflammation. DUSP1 induction by GC (Tchen, Martins et al. 2010) controls a subset of inflammatory gene expression, evidenced by impaired anti-inflammatory effect of GCs, worse experimental arthritis

in DUSP1 knockout mice (Abraham, Lawrence et al. 2006; Vattakuzhi, Abraham et al. 2012).

Similar to other nuclear receptors, the AF1 and AF2 regions of GR, where phosphorylation and recruitment of other co-factors such as p160, CBP/p300, RNA Pol II, SRC1, SRA RNA occur, are important to control GR activity (Freedman 1999; Leo and Chen 2000). More and more co-factors are revealed to cross-talk with GR including histone H3 lysine-9 methyltransferase G9a and the mediator component MED14 (Bittencourt, Wu et al. 2012; Bolt, Stossi et al. 2013). More specifically to GR, dimerization of the DBD has been extensively studied and suggested to be crucial for GR function, supporting stable GR-DNA complex formation as described below. Mutation of AF1, AF2 or the GR dimerization interface in the DBD all affects GR-DNA binding, but the binding affinity is not found to be linked to control of gene regulation (Meijsing, Pufall et al. 2009).

It used to be thought that transactivation and transrepression can be dissociated by mutation of the GR dimerization interface in the DBD. In this theory, transactivation was through homodimers of GR binding to glucocorticoid response elements (GRE, consensus: 5-GGT ACA NNN TGT TCT-3) in the *cis*-regulatory regions of target genes, while transrepression was mediated by direct GR and DNA interaction at negative GRE or composite GRE sites, or by indirect GR and DNA interaction via tethering with other transcriptional factors, such as AP-1, NF-κB (Diamond, Miner et al. 1990; Dahlman-Wright, Wright et al. 1991). The DBD intersubunit contact was thought to be crucial for functional stable GR homodimer binding with DNA. By changing one amino acid in the DBD region of GR (GR^{dim}), this intersubunit contact can be abolished. In this way, from both *in vitro* and *in vivo* studies, it was argued that that ablation of GR homodimer formation abolished the transactivation while maintaining the transrepression function (Heck, Kullmann et al. 1994; Reichardt, Kaestner et al. 1998).

This theory has met with a number of challenges recently. First, the GR^{dim} mutant can still bind with GRE DNA probes and transactivation of some genes is intact in mice homozygous for a 'knock-in' GR^{dim} mutation (e.g. *PNMT*). From this, it is

reasoned that GR dimerization is necessary for transactivation of genes containing a simple inverted repeat GRE, such as TAT or MMTV, but is not necessary for genes containing different arrangement of GRE half sites such as *PNMT* (Liu, Wang et al. 1996; Adams, Meijer et al. 2003). It has been reasoned that a higher order of GR complex for transactivation may form between possible links over the N-terminus or C-terminus of GR, in addition to the well-established dimerization interface in the DBDs. Although most evidence suggests $GR^{dim/dim}$ mice are less protected from inflammation by GC treatment, there are also studies showing a normal immunosuppressive response to GCs in them, for example in a model of irritative skin inflammation (reviewed by (Vandevyver, Dejager et al. 2013). Second, in a large scale genomic GR binding chip-sequencing and gene array experiment, most of GR binding sites were devoid of GRE sequences resembling the consensus GRE motif. In fact, GRE motif is present in only ~20% of both GC up-regulated and down-regulated genes in LPS treated macrophages (Uhlenhaut, Barish et al. 2013). GR is found to exclusively occupy accessible chromatin in dexamethasone treated hepatocytes, most of which are 'pre-programmed sites' occupied by liver enriched transcription factor, CCAAT/enhancer binding protein (C/EBP) β (Grontved, John et al. 2013). This suggests selective targeting of GR in other tissues is likely mediated by the combined action of cell-specific priming proteins and chromatin remodellers Third, tethering is not always associated with transrepression, according to the observation of the frequent proximity of GR binding sites with sites of AP-1, NF-kB, and/or GRIP1 binding at both induced and repressed inflammatory enhancers (Uhlenhaut, Barish et al. 2013). A simplified updated GR transactivation and transrepression model is depicted in the figure below (Figure 1-5). Other models explaining transrepression via prevention of transcription factor binding to DNA include competitive GR binding to the DNA, sequestration of GR and competitive GR binding to co-factor (reviewed by (Vandevyver, Dejager et al. 2013)).

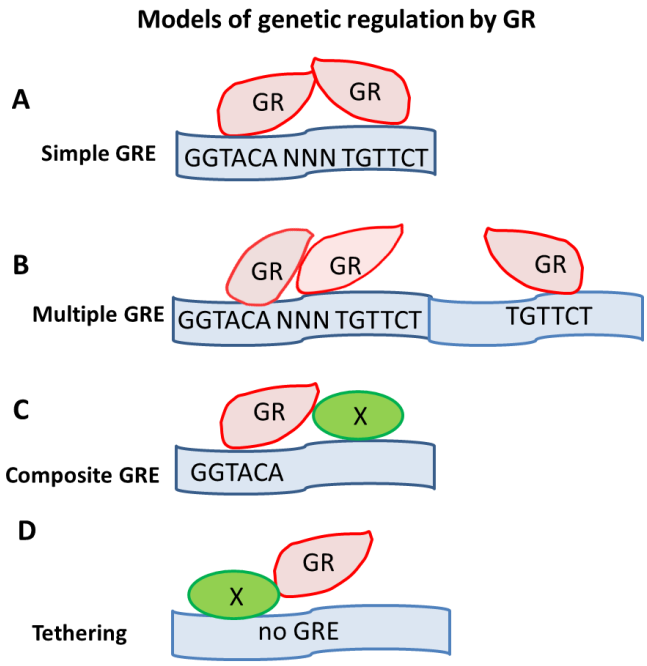

Figure 1-5 Different models of transcriptional gene control by GR.

(A) At a 'simple' GRE site, the GR homodimer binds to an inverted repeat of 2 GRE half-sites to activate gene expression. GR homodimer can bind with negative GRE to mediate transrepression (not depicted here). (B) In genes with multiple GRE or half GRE sites, GR monomer or multimers bind to an array of GRE half-sites to activate gene expression. (C) In genes with composite GRE sites, GR together with other transcriptional factors bind DNA to activate or repress gene expression. (D) In genes without GRE or half GRE sites, GR can also indirectly control gene expression by tethering with other transcriptional factors to activate or repress gene expression. 'X' represents other proteins different to GR.

1.3.7 Interaction between hedgehog signalling and glucocorticoid

Hedgehog signalling was first discovered in *Drosophila* embryonic development, in which mutation of *Hh* gene causes the short and "spiked" phenotype of the cuticle of Drosophila larvae (Nusslein-Volhard and Wieschaus 1980). Genes in this pathway were gradually discovered and *Hh* ortholog genes were found in the vertebrates as well, expanding to *Desert Hedgehog (Dhh)*, *Indian Hedgehog (Ihh)*, and *Sonic Hedgehog (Shh)* groups (Echelard, Epstein et al. 1993). Hedgehog signalling plays lots of functions in cell growth, survival and fate decision (reviewed by (Varjosalo and Taipale 2008)). One of them is to control tissue patterning in development, such as lung branching (Pepicelli, Lewis et al. 1998), chondrocyte differentiation (Kobayashi, Soegiarto et al. 2005) and neural development (reviewed by (Dessaud, McMahon et al. 2008)). It is also involved in lots of pathological changes, such as fibrosis (Philips, Chan et al. 2011; Horn, Palumbo et al. 2012), Warburg effect (Teperino, Amann et al. 2012)and heterotopic ossification (Ruiz-Heiland, Horn et al. 2012; Regard, Malhotra et al. 2013).

A schematic picture describing the signalling pathway is shown in Figure 1-6. Basically, when there are no hedgehog ligands, the Gli transcriptional factors are sequestered in the tips of primary cilium and processed for degradation. Upon binding of hedgehog ligands with the receptor Patched in receiving cells, Smoothened (SMO) translocates into the tip of primary cilium. Subsequently, Gli transcriptional factors are released and translocate into the nucleus to drive gene expressions, such as *Cyclin D*, *Cyclin E* and *Myc*. For detailed information, please refer to some review papers (Wilson and Chuang 2010; Hui and Angers 2011; Ingham, Nakano et al. 2011).

In recent years, evidence showing interaction between glucocorticoid and hedgehog signalling emerges. Glucocorticoid may bind with Smo. Initially, it is discovered that select glucocorticoid compounds activate hedgehog pathway, beneficial for neural repair (Wang, Lu et al. 2010; Wang, Barak et al. 2011). However, a large scale screen shows that the effects of glucocorticoid compounds on hedgehog signalling

varies; some lead to hypersensitivity while others cause inhibition of hedgehog signalling (Wang, Davidow et al. 2012).

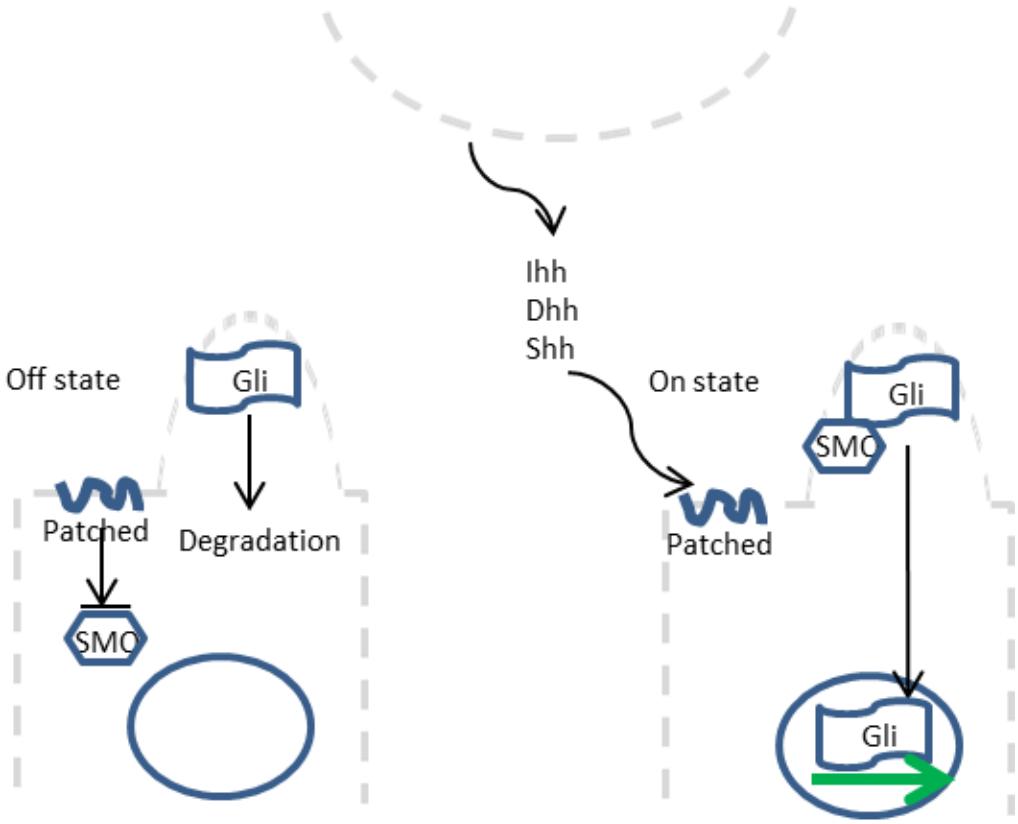

Figure 1-6 Schematic hedgehog signalling pathway.

When there are no hedgehog ligands, cells are on the off-state, with Gli transcriptional factors sequestered in the tips of primary cilium and processed for degradation. In the on state, upon binding of hedgehog ligands with the receptor Patched in receiving cells, Smoothened (SMO) translocates into the tip of primary cilium. Subsequently, Gli transcriptional factors are released and translocate into the nucleus to regulate gene expressions.

1.4 11β-HSD1

1.4.1 11β-hydroxysteroid dehydrogenases

Cortisol is the main form of GC in humans and most vertebrates, with about 5% of total circulating GCs being corticosterone, whose biological significance in humans is still under debate (Peterson 1957; Nishida, Matsumura et al. 1977; Raubenheimer, Young et al. 2006). The inert 11-keto derivates of cortisol and corticosterone, cortisone and 11dehydro-corticosterone respectively, are also present in the circulation. In mice and rats, there are only corticosterone and 11-dehydrocorticosterone, which is due to the absence of 17 alpha-hydroxylase in the adrenal gland.

Co-existence of these active and inactive GCs results from interconversion by 11β-hydroxysteroid dehydrogenase enzymes (11β-HSDs), of which there are 2 isozymes: 11β-HSD1 and 11β-HSD2 (reviewed by (Seckl and Chapman 1997; Chapman, Holmes et al. 2013)). *In vivo* and in intact cells, 11β-HSD1 mainly acts as a reductase catalysing the conversion of the 11-keto form of inactive GCs into the active 11-hydroxyl form, while 11β-HSD2 catalyses the opposite reaction as a dehydrogenase. Therefore, 11β-HSD1 amplifies intracellular GC action whilst 11β-HSD2 diminishes intracellular GC action (Figure 1-7).

11β-HSD1 is expressed in many tissues, including liver, kidney, brain, lung, adipose tissue, placenta, ovary and immune cells, whereas 11β-HSD2 is more restricted, with expression largely limited to aldosterone target tissues (eg. kidney, colon) as well as the developing embryo and placenta (reviewed by (Chapman, Holmes et al. 2013)). By inactivating intracellular GCs, 11β-HSD2 confers specificity of aldosterone binding to MR (Stewart, Wallace et al. 1987; Funder, Pearce et al. 1988; van Uum, Hermus et al. 1998). Because the adrenal glands produce little cortisone or 11-dehydrocortocosterone (11β-HSD1 substrates), 11β-HSD1 activity is dependent on 11β-HSD2 to generate its substrates. In the circulation, although data on the ratio of active and inactive GCs in large population studies are scarce, the ratio is reported in some studies to be about 5.4 : 1 (F:E) in humans (Vogeser, Groetzner et al. 2003) and

10.6:1 (B:A) in rats (Usa, Singh et al. 2007). A study in mice showed that the ratio is dependent on both stress and the time of the day (Harris, Kotelevtsev et al. 2001).

This thesis is focused on 11β-HSD1, with more information provided below. 11β-HSD1 is a 34kDa transmembrane glycosylated protein located inside the endoplasmic reticulum, in close association with hexose-6-phosphate dehydrogenase (H6PDH), which supplies the co-factor, NADP(H), to drive the reductase direction of 11β-HSD1 activity. In tissue homogenates and liver microsomes, without NADPH generation, 11β-HSD1 exhibits dehydrogenase activity in the presence of NADP (reviewed by (Tomlinson, Walker et al. 2004)). Apart from GCs, 7-ketocholesterol and 7-oxo-lithocholic acid are also substrates for 11β-HSD1 (Nashev, Chandsawangbhuwana et al. 2007; Odermatt, Da Cunha et al. 2011; Penno, Morgan et al. 2013)

There are 3 promoters in the *HSD11B1* gene, P1, P2 and P3 (reviewed by (Chapman, Holmes et al. 2013)), with the main one being P2. The P2 promoter contains several binding sites for C/EBP transcription factors. Transcription from P3 encodes a protein without 11β-HSD1 activity. In hepatocytes, basal expression of 11β-HSD1 is under the control of C/EBPα (Williams, Lyons et al. 2000). C/EBPβ and LAP:LIP (different translational forms of CEBPβ) ratio directly control the transcriptional regulation of *Hsd11b1* in adipocytes and lung epithelial cells in response to pro-inflammatory cytokines, GCs, diet, and other regulators (Williams, Lyons et al. 2000; Sai, Esteves et al. 2008; Ignatova, Kostadinova et al. 2009; Esteves, Kelly et al. 2012). In mesenchyme stromal fibroblasts (which use the P2 promoter, in contrast to freshly isolated lung fibroblast using P1 promoter (Yang 2010)), during inflammatory stimulations, 11β-HSD1 expression is positively regulated via NFκB (p65) binding to the *Hsd11b1* promoter, with a synergistic effect of GCs to further increase *Hsd11b1* expression through inhibition of MAPK p38 (Ahasan, Hardy et al. 2012).

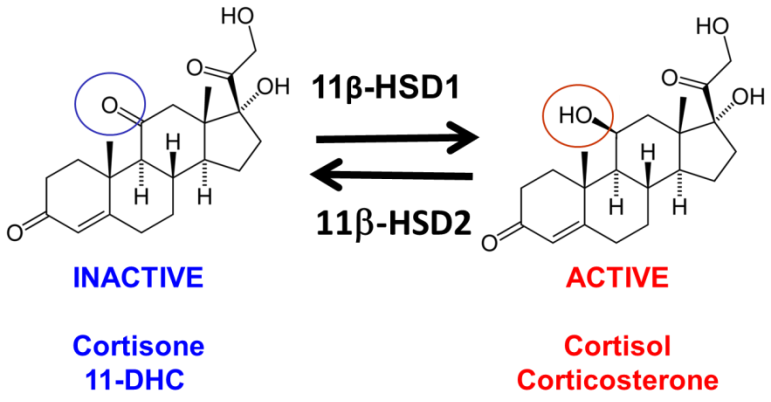

Figure 1-7 11β-HSDs mediate interconversion of 11-keto forms (cortisone, 11-dehydrocorticosterone) and 11-hydroxyl forms (cortisol, corticosterone) of GCs.

The circle indicates the hydroxyl/keto group at the 11 position. Arrows indicate the reaction direction in *vivo*, but 11β-HSD1 can work as a dehydrogenase in cell free conditions.11-DHC, 11-dehydrocorticosterone.

1.4.2 11β-HSD1 in metabolism

Chronic GC excess, exemplified by Cushing's syndrome in association with a low-grade inflammation, causes metabolic disturbances (discussed in section 1.3.4), despite the well-known anti-inflammatory effect of GCs. 11β-HSD1 increases intracellular GC levels without an increase in circulating GC levels. Increased 11β-HSD1 enzyme activity has emerged as a possible link to human obesity, diabetes and metabolic syndrome (Draper, Echwald et al. 2002; Walker 2006; Smit, Dekker et al. 2007; Miyamoto, Morisaki et al. 2009; Munoz, Carvajal et al. 2009; Gambineri, Tomassoni et al. 2011; Moon, Lee et al. 2011; Dujic, Bego et al. 2012; Olza, Gil-Campos et al. 2012).

Globally 11β-HSD1 deficient mice are protected against the adverse effects of diet-induced obesity (Kotelevtsev, Holmes et al. 1997; Morton, Paterson et al. 2004; Wamil, Battle et al. 2011), development of atherosclerosis in the *Apoe*$^{-/-}$ genetic background (Garcia, Search et al. 2013; Kipari, Hadoke et al. 2013) and the normal cognitive loss and skin thinning associated with aging (Sandeep, Yau et al. 2004; Yau, Noble et al. 2011; Tiganescu, Tahrani et al. 2013).

The following mechanisms of metabolic protection conferred by 11β-HSD1 deficiency in mice with high fat diet induced obesity: a Microarray study of white adipose tissue from 11β-HSD1 deficient mice showed a profile consistent with higher lipid oxidation and reduced inflammatory gene expression in subcutaneous and mesenteric depots, respectively. This was accompanied by decreased macrophage and T cell infiltration in the mesenteric adipose tissue (Wamil, Battle et al. 2011). There is also increased angiogenesis and less fibrosis in adipose tissue of 11β-HSD1 deficient mice after 12 weeks of high fat diet, suggesting more efficient adipose tissue remodeling (Michailidou, Turban et al. 2012). Inhibition of 11β-HSD1 was shown to promote brown adipocyte differentiation (Liu, Kong et al. 2013), which suggests a negative role of 11β-HSD1 in brown adipocyte development.

Conversely, tissue-specific overexpression of 11β-HSD1 in transgenic mice causes detrimental effects. Mice overexpressing 11β-HSD1 in adipose tissue (using the adipocyte *Fab4* promoter) developed visceral obesity and exhibited pronounced

insulin-resistant diabetes, hyperlipidemia and hypertension, hyperphagia despite hyperleptinemia (Masuzaki, Paterson et al. 2001; Masuzaki, Yamamoto et al. 2003). Mice overexpressing 11β-HSD1 in liver (using the *Apoe* promoter/enhancer) showed fatty liver and dyslipidemia, impaired hepatic lipid clearance and transgene-dose-associated hypertension paralleled by increased liver angiotensinogen expression (Paterson, Morton et al. 2004). Another line of mice overexpressing 11β-HSD1 in forebrain (using the CamIIKα promoter) exhibited premature age-associated cognitive decline (Holmes, Carter et al. 2010).

Several different selective 11β-HSD1 inhibitors in mice have shown protection against metabolic dysfunction, particularly insulin resistance induced by high fat diet feeding and atherosclerosis (Hermanowski-Vosatka, Balkovec et al. 2005; Feng, Huang et al. 2010; Park, Rhee et al. 2012; Wang, Liu et al. 2012; Luo, Thieringer et al. 2013). Clinical trials of 11β-HSD1 inhibitors showed improvements of insulin sensitivity in type 2 diabetes (reviewed by (Gathercole, Lavery et al. 2013; Hardy, Seibel et al. 2013). One of the concerns of long term 11β-HSD1 inhibitor administration is the possible effects on the HPA axis (reviewed by (Harno and White 2010)).

1.4.3 11β-HSD1 in the cardiovascular system and wound repair

Globally 11β-HSD1 deficient mice showed increased angiogenesis in an *in vivo* assay using s.c. sponge implantation and in an *in vitro* aortic ring assay (Small, Hadoke et al. 2005). These mice also showed better recovery after myocardial infarction with increased angiogenesis in the infarcted area of heart accompanied by earlier accumulation of $YM1^+$ M2 macrophages and higher *Cxcl1* mRNA levels (Small, Hadoke et al. 2005; McSweeney, Hadoke et al. 2010).

Protection from atherosclerosis in *Apoe*$^{-/-}$ artheroslerosis-prone mice by 11β-HSD1 inhibition was first reported by Merck researchers (Hermanowski-Vosatka, Balkovec et al. 2005). A recent study from Merck by 11β-HSD1 inhibition suggested decreased inflammatory gene expression in the vasculature as a protective mechanism against atherosclerosis (Luo, Thieringer et al. 2013). This has been further confirmed in globally 11β-HSD1 knockout mice on an *Apoe*$^{-/-}$ background by 2 independent groups, both of whom attributed this to 11β-HSD1 knockout in bone marrow-derived macrophages based on bone marrow transfer experiments (Garcia, Search et al. 2013; Kipari, Hadoke et al. 2013). The mechanism may involve accumulation of cholesterol in macrophages. In one study, increased cholesterol efflux was reported in 11β-HSD1 deficient macrophages via up-regulation of *ATP-binding cassette transporter (ABCA) 1*, *ABCG1* and *Apoe* gene expression (Kipari, Hadoke et al. 2013). Consistent with this, reduced foam cell formation was found in the peritoneal macrophages from 11β-HSD1-deficient mice in an *Apoe*$^{-/-}$ background in the other study (Garcia, Search et al. 2013). Reduced circulating MCP-1 levels were found in all the above 4 studies, and Kipari etc. found decreased *Mcp1* expression in the mesenteric adipose tissues (Kipari, Hadoke et al. 2013). However, it is unknown of the tissue contributions of MCP-1 generation.

Similar to myocardial infarction (Small, Hadoke et al. 2005), inhibition or knockout of 11β-HSD1 was shown to accelerate skin wound healing in several studies. Topical application of 11β-HSD1 inhibitor promoted skin wounding healing by increasing proliferation of normal epidermal keratinocytes and fibroblasts (Terao, Murota et al. 2011). Topical 11β-HSD1 inhibition could also overcome stress or exogenous GC-

induced delays in wound healing, with synergistic effects of liver X receptor activators (Youm, Park et al. 2013). 11β-HSD1 deficient mice showed reduced aging induced skin thinning as well as increased wound healing, pointing to a negative role of GC on collagen synthesis (Tiganescu, Tahrani et al. 2013).

1.4.4 11β-HSD1 in inflammation

11β-HSD1 is widely expressed in the immune system. In mice, expression of 11β-HSD1 has been reported in macrophages (Gilmour, Coutinho et al. 2006), $CD4^+$, $CD8^+$ and $B220^+$ lymphocytes (Zhang, Ding et al. 2005) , mast cells (Coutinho, Brown et al. 2013) and neutrophils (Chapman 2011). The levels of 11β-HSD1 are much higher in myeloid cells than in lymphoid cells (reviewed by (Chapman, Coutinho et al. 2013). No *HSD11B1* expression was found in healthy human blood cells, but it was induced upon differentiation of human blood monocytes to macrophages or dendritic cells (Thieringer, Le Grand et al. 2001; Freeman, Hewison et al. 2005)

11β-HSD1 expression is dynamically regulated by activated state in mouse immune cells. 11β-HSD1 levels are very low in naïve monocytes/macrophages and tissue resident macrophages, but can be greatly induced by inflammatory stimuli (Gilmour, Coutinho et al. 2006). Phagocytosis of apoptotic neutrophils decreases human monocytes derived macrophage 11β-HSD1 expression (Chapman, Coutinho et al. 2009). Expression of neutrophil 11β-HSD1 is increased during inflammation but is absent in apoptosis (reviewed by (Chapman, Holmes et al. 2013)). During *in vitro* polarisation of human $CD14^+$ monocytes, IL-4 has a much stronger effect to induce *HSD11B1* expression than classic inflammatory stimuli (Thieringer, Le Grand et al. 2001). The effect of IL4 is further potentiated by peroxisome proliferator activated receptor-γ (PPAR-ϒ) activation (Chinetti-Gbaguidi, Bouhlel et al. 2012). In contrast, immunosuppressive TGF-β2, alpha melanocyte stimulating hormone (α-MSH) and vasoactive intestinal peptide (VIP) are not able to induce *HSD11B1* expression in human monocytes (Varajini Joganathan 2008). There is no information on the role of IL4 or TGF-β upon mouse macrophage 11β-HSD1 expression to my knowledge.

The induction of 11β-HSD1 expression by inflammatory stimuli is generally conceived to be a protective mechanism to suppress inflammation (reviewed by (Chapman, Coutinho et al. 2013)). Exaggerated inflammation is usually found in situations of 11β-HSD1 deficiency or inhibition, although it is not clear to what extent the induction of 11β-HSD1 in activated myeloid cells contributes to this,

because similar induction effect happens in other cells as well, especially fibroblasts (Escher, Galli et al. 1997; Hardy, Filer et al. 2006; Hardy, Rabbitt et al. 2008; Ahasan, Hardy et al. 2012). In globally 11β-HSD1 deficient mice, there is a greater inflammatory response to LPS induced endotoxin inflammation, in the K/BxN serum transfer model of arthritis, in thioglycollate elicited peritonitis and in carrageenan-induced pleurisy (Zhang and Daynes 2007; Coutinho, Gray et al. 2012). In an arthritis study on rats, it was found that synovial 11β-HSD1 activity was increased in association with increased IL-1 and TNFα (Ergang, Leden et al. 2010; Sesti-Costa, Baccan et al. 2010). Additionally, in a human arthritis study, increased 11β-HSD1 activity was associated with disease progression and both were decreased by treatment with disease modifying drugs or anti-TNFα antibodies (Hardy, Rabbitt et al. 2008; Beyeler, Dick et al. 2012; Nanus, Filer et al. 2013)

A possible role for 11β-HSD1 in macrophages is suggested by changed macrophage functions in studies on globally 11β-HSD1 deficient mice and with selective 11β-HSD1 inhibitor treatment, as described below. Delayed acquisition of macrophage phagocytic ability was first reported in globally 11β-HSD1 deficient mice in our lab (Gilmour, Coutinho et al. 2006). In the myocardial infarction model, there were earlier infiltration of YM-1^{+} (M2) macrophages and greater numbers of macrophages in globally 11β-HSD1 deficient mice associated with greater neutrophil influx into the infarcted area (McSweeney, Hadoke et al. 2010). In 11β-HSD1 deficient macrophages, the pro-inflammatory M1 response was found to be increased following *in vitro* LPS stimulation (Gilmour, Coutinho et al. 2006; Zhang and Daynes 2007). In contrast, in diet induced obesity or atherosclerosis, where the inflammation is widely accepted to be mediated by macrophages, 11β-HSD1 deficient mice consistently show less inflammatory gene expression in gene arrays (Wamil, Battle et al. 2011; Garcia, Search et al. 2013), with similar gene array result in an 11β-HSD1 inhibitor study (Luo, Thieringer et al. 2013).

Given the wide spread induction of 11β-HSD1 in different tissues by inflammatory stimuli, the changed disease course associated with inflammation in 11β-HSD1 deficient mice or following 11β-HSD1 inhibitor treatment, and strong indications of

a regulatory effect of 11β-HSD1 on macrophage functions, it is crucial to dissect role of macrophage 11β-HSD1 in these inflammatory processes in order to find the target tissue of 11β-HSD1 inhibition. To this end, macrophage-specific *Hsd11b1* knockout mice (*LysM-Cre Hsd11b1*$^{flox/flox}$) were generated (Zhang 2011) for use in the studies described in this thesis.

1.5 Hypothesis and Aims of the study

Hypothesis: 11β-HSD1 amplification of intracellular GC levels in macrophages is responsible for major effects of global 11β-HSD1 deficiency during inflammation. It is predicted that macrophage specific 11β-HSD1 deletion would worsen inflammatory disease development, but protect against metabolic disease.

Aims: 1. To examine the effects of macrophage 11β-HSD1 deficiency upon M1/M2 polarisation and response to hypoxia to mimic tissue injury situations *in vitro*.

2. To examine whether macrophage 11β-HSD1 was efficiently deleted in myeloid cell-specific *Hsd11b1* knockout mice (*LysM-Cre Hsd11b1*$^{flox/flox}$).

3. To study the *in vivo* effects of macrophage 11β-HSD1 deficiency in inflammatory diseases, including inflammatory angiogenesis, arthritis and high fat diet induced obesity.

Chapter 2: Materials and Methods

2.1 Materials and solutions

All chemicals and reagents were purchased from Sigma-Aldrich Company Ltd, (Poole, UK) or Invitrogen Life Technologies (Paisley, UK), unless otherwise stated. To prepare buffers and solutions, double deionized water (ddH_2O) was used, unless otherwise stated.

Buffers and solutions:

Phosphate buffered saline (PBS) solution: for 1 x PBS solution, a PBS tablet (Oxoid Limited, Hampshire, UK) was dissolved in 200ml ddH_2O to give 8g/l NaCl, 0.2g/L KCl, 1.15g/L Na_2HPO_3 and 0.2g/L NaH_2PO_3.

Culture medium: Dulbeco's modified Eagle's medium (DMEM) with 10% heat inactivated fetal calf serum (FCS) and 1% penicillin/streptomycin.

10 x TBE buffer: 56g tris, 57.5g boric acid, 20ml 0.5M EDTA were dissovled into a total volume of 500ml with ddH_2O and autoclaved before use.

10 x TBS buffer: 24.4g Trizma base, 80g sodium chloride were dissolved in 1L of distilled water, with 0.5M HCl to adjust the final ph to 7.6.

C buffer: 63g glycerol, 8.77g NaCl, 186mg EDTA and 3.03g tris were dissolved in 500ml ddH_2O, and the pH was adjusted to 7.7 with HCl and NaOH.

Homogenization buffer: 100g glycerol, 300mg Tris and 186mg EDTA were dissolved in 500ml ddH_2O, and the pH adjusted to 7.5 with HCl. The buffer was stored at 4℃. 7.7mg dithiothreitol (DTT) was added before use to 50ml of the buffer for a working solution, which was kept on ice.

Borate buffer: 8.25g boric acid and 7.2g NaOH were dissolved in 1L ddH_2O. The pH was adjusted to 7.4 with HCl. Then 5g bovine serum albumin (BSA) was added to a final concentration of 0.5% and stored at -20℃.

Krebs-ringer buffer: In 1L H_2O, 118mM NaCl, 5mM KCl, 1.2mM $MgSO_4$, 3mM NaH_2PO_4, 12mM Na_2HPO4 and 0.9mM $CaCl_2$ were dissolved with a final Ph of 7.4. The solution was filtered to satirize it before being kept at 4℃ until use, when 0.1g glucose and 1g BSA was added. Once glucose and BSA were added, the solution could be kept 4℃ for 1 week at maximum.

RNase free water (DEPC-treated water): ddH_2O was mixed with diethylpyrocarbonate (DEPC) at a proportion of 1 drop DEPC to 100ml ddH_2O. The solution was mixed and left overnight before being autoclaved.

Placental homogenate: 2 Wistar rat placentas were mechanically homogenied in 1ml homogenization buffer and then 300µl aliquoted into tubes and stored at -80℃.

Nicotinamide adenine dinucleotide phosphate (NADP): 1.1mg nicotinamide adenine dinucleotide sodium salt was dissolved into 1684µl C buffer to give a final concentration of 2mM. This solution was made freshly and kept on ice.

Nicotinamide adenine dinucleotide (NAD): 17.1mg of NAD was dissolved in 1ml C buffer (25mM). This solution was made freshly and kept on ice.

10% Thioglycollate solution: 10g of Brewer's thioglycollate powder (DIFCO, Detroit, MI, USA) was dissolved in 0.1L PBS. The solution was autoclaved, then stored at 4℃ and "aged" for at least 3d before use.

^{3}H-Corticosterone: A commercial stock solution of ^{3}H-corticosterone in ethanol was purchased from Amersham Pharmacia Biotech, Buckingham, UK (specific activity ~80Ci/mmol, concentration 13.7nM).

^{3}H-Dehydrocorticosterone: ^{3}H-dehydrocorticosterone was synthesized in-house according to the procedures described in 2.6, below.

2.2 Animal breeding

Globally 11β-HSD1 deficient mice were generated by homologous recombination technique (Kotelevtsev, Holmes et al. 1997) and were crossed with C57Bl/6 mice for >10 generations. *Hsd11b1*$^{del/del}$ mice were generated by Cre/loxP technique (Zhang 2010). The latter has better deletion efficiency, especially in tissues where 11β-HSD1 was expressed from the P1 promoter. *LysM-Cre HSD11b1*$^{flox/flox}$ transgenic mice were generated as previously described (Zhang 2010) and crossed with *HSD11b1*$^{flox/flox}$ mice. In the offspring, *LysM-Cre HSD11b1*$^{flox/flox}$ mice were the conditional knockout mice, and *HSD11b1*$^{flox/flox}$ littermates were their controls.

All mice were bred and maintained in the Biomedical Research Facility, Little France, Edinburgh, UK. Mice were kept in groups of 1-8 per cage under controlled conditions (12h light/dark cycle, 21℃), with *ad libitum* access to water and standard rodent chow (Special Diet Services, UK). All procedures were carried out under the auspices of the Animal (Scientific Procedures) Act UK 1986 after prior approval by the local ethical committee.

2.3 Breeding and genotyping of *LysM-Cre Hsd11b1*$^{flox/flox}$ mice

The line of MKO mice were maintained by breeding *LysM-Cre Hsd11b1*$^{flox/flox}$ (Zhang 2010) with *Hsd11b1*$^{flox/flox}$ mice. In the offsprings, *LysM-Cre Hsd11b1*$^{flox/flox}$ mice were predicted to carry myeloid cell specific deletion allele of *Hsd11b1*, with its normal expression in control *Hsd11b1*$^{flox/flox}$ mice. Ear and tail samples were used for genotyping, in which deleted allele of *Hsd11b1* is predicted to be present in circulating myeloid cells or in the resident tissue macrophages present in the biopsies (e.g. skin), while other cells bearing the un-recombined floxed allele of *Hsd11b1*.

Primers were designed as shown in Figure 2-1A. MKO mice were identified with *Cre* genotyping (*Cre*$^{+}$, Figure 2-1B). *Flox* genotyping was carried out to check the homozygous state of the *flox* transgene in these mice (Figure 2-1C). And *Hsd11b1* gene genotyping was done to detect the deleted allele of *Hsd11b1* (Figure 2-1D). Cre

genotyping was done routinely in all samples, while flox and hsd11b1 genotyping examined occasionally in well-established breeding lines.

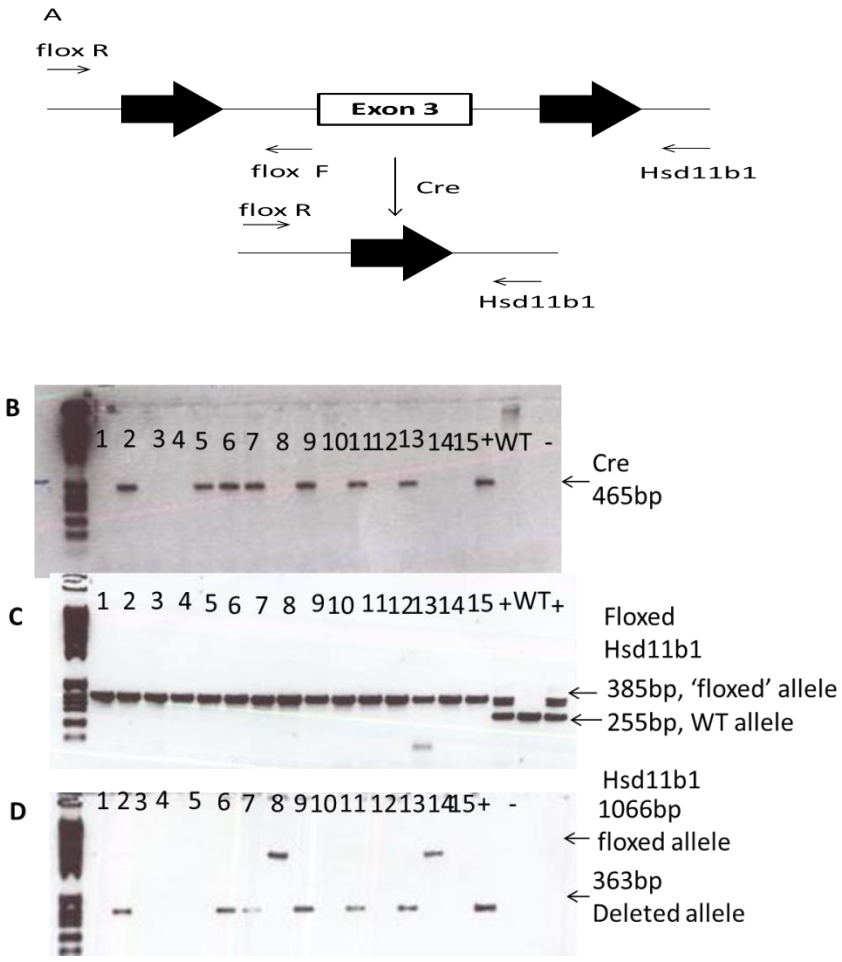

Figure 2-1 Primer design and representative gels showing genotyping results of MKO mice.

(A) 2 LoxP sites (black arrow) flank exon 3. Cre mediated recombination removes exon 3. With flox F and flox R primers, wild-type *Hsd11b1* allele (255bp) and 'floxed' *Hsd11b1* allele (385bp) can be distinguished. With flox R primer and deleted *Hsd11b1* primer, deleted *Hsd11b1* allele (363bp) and 'floxed' *Hsd11b1* allele (1066bp) can be distinguished. (B) Genotyping for Cre transgene (465bp product) showed that mice 2, 5, 6, 7, 9, 11 and 13 carried this gene, while the rest not. (C) Genotyping for the 'floxed' allele of *Hsd11b1* showed that all the mice were homozygous (flox/flox) for the 'floxed' allele. (D) Deleted

bands of *Hsd11b1* (363bp product) were detected in mice 2, 6, 7, 9, 11 and 13, whose genotypes were all Cre^{+} $Hsd11b1^{flox/flox}$; 'floxed' band of *Hsd11b1* were detected in mice 1, 3, 8, 12, 14 and 15, whose genotypes were Cre^{-} $Hsd11b1^{flox/flox}$. Deleted allele in mouse 5 was confirmed in a later repeated PCR, which carried the *Cre* transgene. '+' indicates the positive control, WT wild-type and '-' H_2O control.

2.4 PCR genotyping

All DNA samples were extracted using Qiagen DNeasy blood & tissue kit (Qiagen, West Sussex, UK). Samples were either ear punch samples (for ID) or both ear and tail biopsies. The DNA extraction method was according to the protocol enclosed with the kit, except that in the last step, each sample was dissolved in 100µl instead of 200µl AE buffer (supplied with the kit). The PCR reaction for each sample composed 2.5µl $MgCl_2$ free buffer (supplied with the Qiagen Taq kit), 2.25µl $MgCl_2$ (supplied with the Qiagen Taq kit), 1µl dNTP solution (10mM), 1µl forward primer solution (10pmol/µl), 1µl reverse primer solution (10pmol/µl), 0.2µl Taq DNA polymerase (Qiagen, West Sussex, UK), 15.55µl deionised H_2O and 1.5µl DNA sample solution. Primer sequences and PCR conditions are shown in table 1. In each case, the final step comprised a final extention 72℃ for 10 minutes followed by 4℃ hold.

Table 1 List of PCR primers and reaction conditions

	Flox	*Cre*	*Hsd11b1*
Primers			
Forward	cttgcatgtgtttggtgttgg	gaccgtacaccaaaatttgcctg	gtgatgtcagactacagaagg
Reverse	cccacaatgcatttggaaacatt	ttacgtatatcctggcagcgatc	cccacaatgcatttggaaacatt
Running			
Denature	96℃, 10mins	94℃, 10mins	95℃, 5 mins
cycle	35	32	29
Step 1	95℃ , 30s	94℃, 1 min	95℃, 1min
Step2	60℃, 30s	64℃, 1 min	61℃, 1 min
Step 3	72℃, 1min	72℃, 1 min	72℃, 1 min
Product size	WT: 255bp Flox:385bp	465pb	Deleted band: 363bp WT: 1066bp Floxed: 1196bp

2.5 Thioglycollate-induced sterile peritonitis

Thioglycollate (TG)-induced sterile peritonitis is a mild and self-resolving model of systemic inflammation, which lasts for 5 days (Gallily, Warwick et al. 1964), and allows for isolation of immune cells at the onset, peak and resolution stages of inflammation. Neutrophils are the predominant cell type recruited in the peritoneal in the first 24h after i.p. intraperitoneal injection of thioglycollate, whereas macrophages predominate at later stages, especially at 4 days (Melnicoff, Horan et al. 1989).

300µl of 10% thioglycollate was injected i.p. into each mouse, with a 0.5ml syringe. Mice were killed by a schedule 1 method (cervical dislocation), either 24h following injection for isolation of total cells and/or neutrophil purification, or 96h following injection for macrophage enrichment. Peritoneal cells were lavaged as follows. First, the abdominal skin was dissected apart from the peritoneum. In this process, hemostatic forceps were kept ready to keep the peritoneum intact in case of cleavage of the peritoneum. For each mouse, 5ml cold 1 x PBS was injected (i.p.) into the peritoneum with a 19G needle. The peritoneum was gently massaged, and then as much as possible of the fluid was drawn back into the syringe. For each mouse, harvested solution was put in a 15ml conical tube on ice. Generally, 4ml was collected from each mouse. Following transfer to the laboratory, the solution was gently pipeted up and down for several times to suspend cells. Then the cells were counted using a haemocytometer (Neubauer) and centrifuged for 5 minutes at 300g, 4℃ (Labofuge 400R Centrifuge, Heraeus, Essex, UK). After that, the supernatant was discarded, and the cells were resuspended in the culture medium at the required concentration (usually 1×10^6 cells/ml).

Resident cells in the peritoneal cavity were harvested in the same way without thioglycollate injection. After returning to the laboratory, cells were resuspended in the culture medium and seeded in 6 well plates, 1 mouse per well. After 1-2h incubation at 37℃, 5% CO_2, the cells were washed with PBS to remove floating cells and the attached macrophage cells were used for further experiment.

2.6 Macrophage polarisation under normal oxygen and hypoxia conditions

Male 11β-HSD1 deficient and wild type (WT) mice (8-14 weeks old) were i.p. injected with 10% thioglycollate, 300μl/mouse. And peritoneal lavage was done after 3 days with 5ml ice cold PBS. Cells were centrifuged and supernatants poured off. After another wash with PBS, cells were suspended in DMEM alone on bacteria degrade petri-dishes (no serum) and placed in the cell incubator for 1 or 2 hours for macrophage attachment. Then medium was poured off and plates washed again with PBS without calcium and magnesium to remove non-adhering cells. To remove macrophages from plates, detachment buffer (1mM glucose, 3mM EDTA in calcium and magnesium free PBS) was added into the plate and left in the cell incubator for 15 minutes. Cells were centrifuged and re-suspended in PBS. With the cell number being counted with neucleocasstte, they were suspended in either M1 or M2 conditioning medium ($1x10^6$ cells/ml, 7ml per plate).

M1 medium was made up with LPS and IFN-ϒ, 100ng/ml and 10U/ml respectively. M2 medium was made up with IL-4, 20ng/ml. Both groups were incubated for overnight (~20 hours) at 37℃ before harvest. For hypoxia experiment, M1 macrophages were cultured in the hypoxia chamber (COY Laboratory Inc., Michigan, the USA) with 1% O_2. It was set up with help from Miss Kathryn Wilson and Professor Martin Denvir. The medium was collected and frozen at -80℃ and cells frozen in Trizol after being washed with PBS.

ELISA was done according to the enclosed protocols (Go-Ready ELISA, eBioscience, see Chapter 2 for detailed description). RNA was extracted from samples containing Trizol with RNeasy kit (Qiagen) according to the protocol except RLT buffer being replaced by Trizol here and chloroform used before samples transferred into columns (see Chapter 2 for detailed description). Quantitative PCR (qPCR) was done with gene specific primers and probe in Universal Probe Library (UPL) (see Chapter 2 for detailed description).

2.7 Tissue homogenization and protein assay

2.5.1 Tissue homogenization

Mice were killed by a schedule 1 method and tissues were quickly dissected and frozen on dry ice before being stored at -80℃ until use. Tissues were mechanically homogenized (Dispergierstation T8.10, IKA Instruments, Staufen, Germany) in a 2.5ml tube containing 500-800µl homogenizing buffer, which was kept on ice as far as possible. The amount of tissue used varied, dependant on the protein level and the expected level of 11β-HSD1 in each tissue. The homogenizing time was minimized to avoid protein degradation. The homogenate was aliquoted: 10-30µl in one 0.5ml tube for protein assay (which was done on the same day) and 50-80µl in 3 x 0.5ml tubes for activity assay, which were kept at -80℃ until the activity assay.

2.5.2 Protein assay

Before protein assay of all the samples, a test assay was conducted to choose the proper dilution to use for each tissue. The concentration for each tissue that gave a reading within the standard curve was then used for all samples of that tissue. Then, in a 96 well plate, 5µl of each sample or standard solution was added to duplicate or triplicate wells. Protein standard solutions were made from bovine serum albumin (BSA, Bio-Rad Laboratories, Hertfordshire, UK) stock solution in ddH_2O as 0, 0.1, 0.2, 0.4, 0.6, 0.8, 1.0, 1.2 and 1.4mg/ml. Then 25µl Biorad reagent A (Bio-Rad Laboratories, Hertfordshire, UK) and 200µl Biorad reagent B (Bio-Rad Laboratories, Hertfordshire, UK) were added into each well. The plate was left at room temperature for 15-60 minutes. Then it was read in a plate reader (OPTImax tunable microplate reader, Molecular Devices, Downingtown, PA, USA) at a wavelength of 750nm.

2.8 Synthesis of ^{3}H-11-dehydrocorticosterone

As ^{3}H-11-dehydrocorticosterone is not commercially available, it was made in-house from ^{3}H-corticosterone using rat placenta as a source of 11β-HSD2 to convert ^{3}H-corticosterone into ^{3}H-11-dehydrocorticosterone, as described before (Ehrchen, Steinmuller et al. 2007). 2 rat placentas were homogenized in 1ml of homogenizing buffer as described above (2.5.1, tissue homogenization) and 300µl aliquots stored at -80℃. 120µl stock ^{3}H-corticosterone was dried at 60℃ under gaseous nitrogen and reconstituted in 50µl 100% ethanol in a glass tube or bottle. The following reagents were then prepared in a glass vial: 50µl reconstituted ^{3}H-corticosterone, 200µl 25nM NAD, 300µl placental homogenate and 4.45ml C buffer. The solution was mixed by votexing (Rotamixer, Hook & Tucker Instruments Ltd., Croydon, UK) and split equally into 2 glass tubes. Both were incubated in a water bath at 37℃ for 4 h. The solutions in the 2 glass tubes were further divided equally into 4 glass tubes. 4ml of ethyl acetate was added into each tube, and after mixing in a vortex, they were centrifuged at 1700rpm for 10 minutes at 4℃. The top organic layer containing the steroids in each tube was transferred into a fresh glass vial and dried in a hot block at 60℃ under gaseous nitrogen. When the vials were half dried, the contents of 2 glass vials were combined together. This step was repeated, so all the solutions were finally combined in one glass vial. Another 4ml ethyl acetate was added into the other 3 dried tubes to extract remaining steroids and the above procedures repeated. Finally, the dried steroids were reconstituted in 100µl ethanol and stored at -20℃.

1µl of the solution was used for HPLC to measure the purity of ^{3}H-11-dehydrocorticosterone and another 1µl was added to 1ml scintillation solution to count the amount of radioactivity using a β-counter (Wallac 1450 Microbeta Plus liquid scintillation counter, Milton Keynes, UK).

2.9 11β-HSD1 enzyme activity assay

11β-HSD1 enzyme activity was calculated by measuring the conversion of ^{3}H-11-dehydrocorticosterone to ^{3}H-11-corticosterone (reductase assay) and the conversion of ^{3}H-11-corticosterone into ^{3}H-11-dehydrocorticosterone (dehydrogenase activity),

as described before (Low, Chapman et al. 1994). The reductase assay was carried out in intact cells and the dehydrogenase activity in the homogenates of tissues. The latter assay did not distinguish between 11β-HSD1 and 11β-HSD2, both of which have dehydrogenase activity in homogenates.

2.7.1 Reductase activity assay

Cells were resuspended in culture medium at a density of 10^6 cells/ml. Then 10^6 cells were seeded into each well of a 24 well culture plate, with 0.65 µl (around 5nM) ^{3}H-11-dehydro-corticosterone only or together with 200nM non-radioactive labeled 11dehydro-corticosterone. Samples were assayed in duplicate or triplicate. A negative control contained the culture medium and ^{3}H-11-dehydrocorticosterone only, without cells. Cells were incubated at 37 ℃, 5% CO_2 (CO_2 water jacketed incubator, Forma Scientific, London, UK) for the duration of the experiment. 200 µl of the culture medium was collected at each time point: 30 minutes, 1h, 2h, 4-6h, 16h or 24h (depending on the enzyme activity of each cell type, the time points were adjusted) and frozen at -20 ℃ until analysis (see 2.73 and 2.74).

2.7.2 Steroid extraction

For steroid extraction, samples were thawed and transferred into glass tubes, each capable of holding 2ml (usually 10 times the sample volume, and at least 4 times the sample volume) ethyl acetate. The tubes were vortexed for about 10 s and left for about 1h to separate into organic and aqueous phases. The glass pipet was then used to transfer the upper organic layer to a clean glass tube. The tubes were then left to evaporate in the hood overnight or dried in a 65 ℃ heat block under air or N_2. When the tubes were dry, steroids were on the wall and in the bottom of the tube, ready to be reconstituted in 100% ethanol.

2.7.3 TLC analysis

50µl of 100% ethanol was added into each tube and vortexed for about 15s. The reconstituted steroid was applied onto a thin layer chromatography (TLC) plate (TLC silica gel 60 F_{254}, Merck, Darmstadt, Germany), 5µl at a time until there was none left. Then the TLC plate underwent chromatographic separation in a closed chamber containing 92ml chloroform and 8ml 100% ethanol. In about 45 min, when around 80% of the plate was wet, it was taken out and dried in air. Finally, the TLC plate was placed in a cassette and exposed to a phosphorimager tritium image screen (Fujifilm, Tokyo, Japan). After 1 or 3 days, the screen was taken out and read in a Fujifilm FLA-2000 Image Reader (Fujifilm UK Ltd., Bedford, UK) and quantified by Aida Image Analyzer v.3.44 software (Raytek Scientific Ltd., Sheffield, UK). Enzyme activity was calculated as % conversion of substrate to product: 100 x [product] / ([product] + [substrate]).

2.10 Western blotting

Primary cells were collected and washed with PBS. Cell samples were then centrifuged at 1000rpm, 4℃ for 8 minutes. Supernatants were poured off and cell pellets frozen at -80 ℃. To lysis cells, RIPA cell lysis buffer (R0278, Sigma, UK) with 1% proteinase inhibitor cocktail (P8340, Sigma, UK) was used, 50µl for 10^7 cells. Protein levels were then measured by Bradford protein assay according to the enclosed protocol with the product (Bio-Rad Laboratories Ltd, Herts, UK), as described in 2.5.2.

For each sample, 20-30µg of protein was used for western blotting. All the western blotting reagents were from Invitrogen (Invitrogen Ltd, Paisley, UK) and the experiments were done according to the manufactory's protocols with products. Briefly, protein samples were mixed with sample buffer (10x) and reducing agent (2.5X), and heated at 70℃ for 10 minutes, then loaded onto a 4-12% Bis-Tris Gel (Invitrogen Ltd, Paisley, UK) with 6.5µl of rainbow full range protein ladder (GE Healthcare Life Sciences, Buckinghamshire, UK). The gel running time was 40-60 min at 200v. And transferring time was 60mins at 30 voltages using wet transfer method. First antibodies were incubated with the membrane overnight at 4℃ or 1h at

room temperature. After being washed 3 X 10 min in TBST, the membrane was incubated with the second antibodies for 1h at room temperature. Secondary antibodies from Li-cor were diluted in 5% milk in 1 x TBST solution, working concentration at 1:10,000, and 11β-HSD1 first antibody (kindly provided by Dr. Scott Webster) was used at a working concentration of 1:1,000. Primary antibodies from Santa Cruz were usually used at 1:300-500 dilution, and STAT6 antibodies from Cell signalling were used at 1:1000 dilution.

Membranes were scanned in an Odyssey® Infrared Imaging System (LI-COR Biotechnology - UK Ltd, Cambridge, UK) and the protein bands were quantified with the Odyssey V3 software.

For western blotting of neutrophils, GAPDH was chosen as the internal control because of cross-reaction between antibodies. Both the 11β-HSD1 first antibody and the secondary antibody to β-tubulin were raised in sheep. The problem emerged that secondary antibody of 11β-HSD1 (anti-sheep Ig G), reacted with both antibodies mentioned above. First antibody of GAPDH raised in rabbit did not have this problem. But the band is very close to that of 11β-HSD1. So rabbit-anti-mouse Ig G was used as the secondary antibody for β-tubulin in later experiments.

2.11 ELISA

Ready-Set-Go!® ELISA kits (il-1β 88-7013-22, il6 88-7064-22, il12 p40 88-7120-22, il23 88-7230-22 and tnf-α 88-7324-22) are purchased from eBioscience (Hatfield, UK). The experiments were performed according to the enclosed protocols. Briefly, 96 well plates were coated with detection antibody in 100µl coating buffer overnight in the cold room at 4℃. Solutions were poured off and plates washed with PBST for 3 times before 100µl sample buffer were added to block. After 1h incubation at room temperature, solutions were poured off and plates washed 3 times with PBST. 100µl of sample buffer containing standard or sample dilutions were added into each well and left to incubate at room temperature for 2h. It's recommend to use 2 steps for high samples dilutions, for example, to make 1/800

dilution of samples, dilute first 20 times and then 40 times to reach final 1/800 dilution. Solution were poured off and plated washed 3 times with PBST before 100µ sample buffer containing detection antibody was added. After 1h incubation at room temperature, solutions were poured off and plated washed 3 times with PBST. Then 100µl of sample buffer containing streptavidin-HRP was added into each well for 30 minutes incubation at room temperature. Solutions were poured off and plated washed 5 times before 100µl TMP solution containing HRP substrates were added for 15 minutes incubation at room temperature. The reaction was stopped by adding 50µl of stopping solution. The plates were read in and data were collected by subtracting values in 570nm from values in 450nm with standard curve generated by either 4-parameter standard curve or best fit linear line.

2.12 Magnetic-activated cell sorting (MACS)

MACS is a method which uses magnetic bead-linked antibody to sort out a particular type of cell with the corresponding antigen, from a mixed cell population. The antibody used here for neutrophils was Ly6G (OGUSHI, ENDO et al. 1999). Immune cells were harvested by peritoneal lavage using 5ml PBS, 24h after injection of 300µl of 10% thioglycollate, as described above. The lavaged cells from 4 mice were pooled together and the cells counted using a hemocytometer. The cell density was adjusted to between 1×10^6 and 1×10^7 cells per ml, then 0.5µl of the antibody (Ly6G-PE) was added into every 200µl of sample. The samples were left to incubate on ice in the dark for 1h, after which cells were centrifuged at 300g for 5 min and resuspended in 80µl the MACS running buffer (Miltenyi Biotec, Bergisch Gladbach, Germany) per 10^7 cells. Then, secondary antibody (anti-PE MACS antibody, Miltenyi Biotec, Bergisch Gladbach, Germany) was added (20µl per 10^7 cells) and samples were incubated in the dark at 4℃ for 15 minutes. After centrifuging for 10 min at 300g, 4℃, cells were resuspended in 500µl MACS running buffer. At this time, cells were ready to apply to the MACS column (Miltenyi Biotec, Bergisch Gladbach, Germany), which was kept at 4℃ before use.

The cold column was placed in the magnet (Miltenyi Biotec, Bergisch Gladbach, Germany), and a 50 ml collecting tube was placed under the column. The column was washed with 3ml of MACS running buffer. Then the cell solution was added to the column and the flow through ($Ly6G^-$ cells) collected. The column was washed 3 more times, with 3 ml of the MACS running buffer each time and the flow through collected in the same tube as above. At this time, the column was taken off the magnet, and another 50 ml collecting tube placed below the column. 5 ml of PBS was added to the column to collect the $Ly6G^+$ cells, using the plunge to push the solution through. $Ly6G^+$ and $Ly6G^-$ cells were then counted with a hemocytometer and their density adjusted to 1×10^6 cells per ml. 100-200µl of the cell suspension was cytocentrifuged onto slides with a speed of 300rpm for 3 min. After air drying, the slides were stained with Diff Quick (placed in methanol for 2 minutes, 40 seconds in the Diff Quick Red dye, 40 seconds in the Diff Quick Blue dye and washed in water) and mounted with DPX resin. This was used to evaluate the separating efficiency.

2.13 Adipose stromal vascular cells (SVCs) separation

Adipose tissues harvested from mice were kept in 50ml falcon tubes with about 10ml Krebs-ringer buffer. The tubes were kept warm in a beaker of warm water. Back in laboratory, lymph nodes were dissected out and tissues were weighed to make sure less than 3g of adipose in one sample. Collagenase type I (Worthington Biochemical Corporation, NJ, the USA) was dissolved in Krebs-ringer buffer at 2mg/ml. In a plastic bottle, 10ml of the collagenase I buffer with one adipose tissue sample were put in. The adipose tissue were cut into small pieces with scissors before the bottle was incubated in shaking water bath at 37℃ for 45 mins (swirl the bottle every 15 mins). The reaction was stopped by adding 10-20ml Krebs-ringer buffer to dilute the enzyme concentration.

The solution was passed through mesh into 50ml falcon tubes and then centrifuged at 600g for 10 mins at room temperature. After removing adipocytes in the top layers

and solutions in the middle, ~500µl solution was left with SVCs inside (Optionally, pass the SVCs in10ml Krebs-ringer buffer through pre-wetted 100µm filters, which was washed with another 10ml Krebs-ringer buffer in the end). Red blood cells were lysed by incubating with 2ml lysis buffer (R7757, Sigma, UK) for at least 1 min at room temperature. The lysing was stopped by adding 10ml PBS and cells were recovered after centrifudge at 600g for 10 mins. The cell pellets were resuspended in 2ml PBS buffer before being passed through a 30µm filter, which was washed with 3ml PBS buffer. The cells were pelleted and resuspended in 1ml PBS solution.

2.14 Flow cytometry

In a 12x75 mm, 5 ml polystyrene round bottom test tube, ~10^6cells were incubated in ~ 100µl PBS (the volume left after gently pouring off solutions in the tube) with 10% mouse serum (to block non-specific binding) for 30mins on ice. Then about 3ml PBS were added into the tube to wash the cells. After centrifuge the tube for 5 mins at 300-500g and pouring off the solutions, fluorescence conjugated antibodies and matched iso-type IgG were added into sample and iso-type control tubes respectively, to incubate on ice for 30min in the dark. A tube of cell sample without antibodies was included as well for gating and examining auto-fluorescence in the analysis. The volume of antibody used per test tube was 0.25-0.5µl (otherwise, according to the suggestions of the suppliers). All antibodies were from ebioscience or BD. The cells were washed in 3ml PBS and recovered by centrifugation at 300g for 5min prior to analysis in flow cytometry machines (FACScan or FACScalibur, Becton Dickinson, Oxford, UK). Usually 100µl of 10% neutral formalin solution was added into each tube to preserve the samples at 4°C before analysis within 1 week.

Compensation among different fluorescence was determinded either by auto-compensation with compensation beads (OneComp eBeads, 01-1111-42, eBioscience, UK) or manually set up with all the single antibody stained samples. Gating of cells was done in FSC (forward scatter) and SSC (side scatter) view, which was determined by cell size and granularity respectively. Specific and non-specific fluorescence was determined by processing ≥5000 cells/sample, using Cellquest

software (BD). Data analysis was performed using FlowJo software (Treestar, Oregon, USA) on cell singlets determined by gating in FSC area and FSC height view.

Intracellular staining was done with FIX & PERM® Cell Fixation & Cell Permeabilization Kit (GAS004, Invitrogen, UK) according to the protocol enclosed with the product. Briefly, after surface staining, cells of a sample were fixed in 100µl of the fix buffer at room temperature in dark. After washing with PBS, 100µl of perm buffer (to make pores in cell membrane) with un-conjugated antibodies (1:50 for YM-1 and 1:200 for purified 11β-HSD1 antibody) was added, to incubate in room temperature for 15 mins in dark. Then perm buffer (00-8333-56, eBioscience) was used to wash samples (3ml/tube). PBS washing could lead to failure of staining as all intra-cellular antibodies (specific or non-specific) would be trapped inside cells when the cell membrane closes in PBS. A different perm buffer was used to lower the cost as large quantity of perm buffer used for washing. Recovered cell samples were then incubated with matched fluorescence conjugated secondary antibodies (1:300-500 dilutions) in 100µl of perm buffer at room temperature for 15 mins in dark. Samples were washed again with perm buffer (00-8333-56, eBioscience) and analysed within 1 day.

Blood cell preparation for flow cytometry analysis is done as described below. Tail nick was done with a scalpel and 30µ of blood was collected in to an eppendorf tube with 30µl of 3.9% sodium citrate buffer for anti-coagulation. 30-50µl of the above solution was put into each test tube and antibodies were added to incubate 25 mins on ice in dark. No blocking step was needed as there was serum present in the blood. Red blood cells were lysed with 1ml 1X lysing buffer per sample (BD Pharm Lyse™, 555899, BD, UK) for 8 mins at room temperature in dark. After centrifuge, cells were preserved for flow cytometry analysis.

2.15 RNA extraction, reverse transcription and real-time PCR assay

Cell or samples were usually kept in Trizol (Invitrogen Ltd., Paisley, UK, <107cells/ml) and stored at -80℃ for later RNA extraction. Total RNA was extracted using the Qiagen RNeasy mini kit according to the protocols enclosed with the products, except that Trizol and chloroform were used to lyse the cells instead of the RLT buffer. Obtained RNA was quantified in the NanoDrop ND-1000 spectrophotometer (NanoDrop products, Wilmington, DE 19810, USA).

To make cDNA, SuperScript® III Reverse Transcriptase (Invitrogen Ltd., Paisley, UK) was used according to the protocol enclosed with the product. Usually 1 μg of RNA was used together with 1 μl of mixed dNTPs (Promega, Southampton, United Kingdom), 0.5 μl of random primers (Invitrogen Ltd., Paisley, UK) in a volume of 13 μl, which were heated at 65℃ for 5 min. Then 4 μl of the first strand buffer, 1 μl of the DTT solution, 1 μl of the transcriptase and 1 μl of the RNase-out (Promega, Southampton, United Kingdom) were added into each sample and reverse transcription carried out using the conditions specified in the product sheet (Samples were incubated at 25 ℃ for 5min, then 50 ℃ for 60min and 70 ℃ for 15min). A control with water but no RNA was included in the reaction.

For mRNA measurement, real-time PCR reactions were all carried out in the LightCycler 480 System (Roche Diagnostics Ltd., Burgess Hill, UK) with fluorescent probes in the Universal Probe library (Roche Diagnostics Ltd., Burgess Hill, UK). cDNA samples were prepared in triplicates. For each one, 2 μl of the diluted sample was used together with 5 μl of Roche master mix solution, 2.7 μl of distilled water, 0.1 μl of probes (10μM) and 0.1 μl of the primers (10-40μM) in the following running. The Lightcycler 480 PCR programme was as follows: pre-incubation at 95 ℃, 5min, amplification for 50 cycles (95 ℃, 10s; 60 ℃, 30s; 72 ℃, 1s) and cooling, 40 ℃ for 30s. Data were calculated by the 2nd derivative maximum method. This method determined the Ct (cycle of threshold) of a sample as the point where the sample's fluorescence curve turns sharply upward, the maximum of the

second derivative of the amplification curve and the value were calculated by the LightCycler ® 480 Software automatically.

SYBR green assays were used in qPCR as well with LightCycler® 480 SYBR Green I Master (04 707 516 001, Roche, Switzerland). In each assay, 5µl Master with 2.8µl water and 0.1µ of forward and reverse primer respectively were mixed with 2µl of cDNA. The assay was run in the same machine with a different programme according to the enclosed protocol. There was 1 cycle pre-incubation (95℃ 10 mins), 45 cycle amplification, 1 cycle melting cure and 1 cycle cooling (40℃, 10s). In each amplification, there were denature 95℃, annealing 20s and extension 72℃ 30s. Fluorescence acquisition was done at the extension step. In the melting curve step, there was 95℃ 10s, 65℃ 1min and 97℃ continuous acquisition.

Gene concentration of samples was assigned according to the standard curve and then gene expression was relative to housekeeping gene expression. Usually 3 housekeeping genes were included in each experiment.

Table 2 List of qPCR primers and probes

Gene	Primers	UPL Probe No.
hprt	Forward: tcctcctcagaccgctttt Reverse: cctggttcatcatcgctaatc	95
TBP	Forward: gggagaatcatggaccagaa Reverse: gatgggaattccaggagtca	97
18s	Forward: ctcaacacgggaaacctcac Reverse: cgctccaccaactaagaacg	77
Actb	Forward: ctaaggccaaccgtgaaaag Reverse: accagaggcatacagggaca	64
Hsd11b1	Forward: tctacaaatgaagagttcagaccag Reverse: gccccagtgacaatcacttt	1
Il1a	Forward: ttggttaaatgacctgcaaca Reverse: gagcgctcacgaacagttg	52
Il1b	Forward: tgtaatgaaagacggcacacc Reverse: tcttctttgggtattgcttgg	78
Il6	Forward: gctaccaaactggatataatcagga Reverse: ccaggtagctatggtactccagaa	6
Il10	Forward: cagagccacatgctcctaga	41

	Reverse: tgtccagctggtcctttgtt	
Il12b	Forward: gactccaggggacaggcta	27
	Reverse: ggagatggttagcttctgagga	
tnf	Forward: tcttctcattcctgcttgtgg	49
	Reverse: ggtctgggccatagaactga	
Nos2	Forward: ctttgccacggacgagac	13
	Reverse: tcattgtactctgagggctgac	
Ccl5	Forward: tgcagaggactctgagacagc	110
	Reverse: gagtggtgtccgagccata	
Cx3cl1	Forward: ccgcgttcttccatttgt	84
	Reverse: cacatgatttcgcatttcgt	
Ifnr	Forward: ggaggaactggcaaaaggat	21
	Reverse: ttcaagacttcaaagagtctgagg	
Icam1	Forward: cccacgctacctctgctc	81
	Reverse: gatggatacctgagcatcacc	
Vcam1	Forward: tggtgaaatggaatctgaacc	34
	Reverse: cccagatggtggtttcctt	
Cd68	Forward: gacctacatcagagcccgagt	96
	Reverse: cgccatgaatgtccactg	
Emr1	Forward: cctggacgaatcctgtgaag	1

	Reverse: ggtgggaccacagagagttg	
Pparg	Forward: tgctgttatgggtgaaactctg	2
	Reverse: ctgtgtcaaccatggtaatttctt	
Retnla	Forward: ccctccactgtaacgaagactc	
(Fizz1)	Reverse: cacacccagtagcagtcatcc	
Chi3l3	Forward: gaacactgagctaaaaactctcctg	88
(Ym1)	Reverse: gaccatggcactgaacga	
Mrc1	Forward: ggacgagcaggtgcagtt	47
	Reverse: caacacatcccgcctttc	
Arg1	Forward: cctgaaggaactgaaaggaaag	2
	Reverse: ttggcagatatgcagggagt	
Ang1	Forward: ggaagatggaagcctggat	12
	Reverse: accagagggattcccaaaac	
Ang2	Forward: cacactgaccttccccaact	82
	Reverse: cccacgtccatgtcacagta	
Cdh5	Forward: tcatcaaacccacgaagtcc	42
	Reverse: ggtctgtggcctcaatgtaga	
Shh	Forward: ctggccagatgttttctggt	SYBR green
	Reverse; gatgtcggggttgtaattgg	assay
Ihh	Forward: cgctgcaaggaccgtctgaa	SYBR green

	Reverse: cgtgggccttggactcgtaa	assay
Gli1	Forward: gaaggaattcgtgtgccatt Reverse: gcaaccttcttgctcacaca	SYBR green assay
Patched	Forward: aagcagactacccgaatatcca Reverse: caggagtttgtaagcgaggac	SYBR green assay
Human Hsd11b1	Forward: caatggaagcattgttgtcg Reverse: ggcagcaaccattggataag	20
Human 18s	Forward: ctcaacacgggaaacctcac Reverse: cgctccaccaactaagaacg	77
Human Rpl32	Forward: catctccttctcggcatca Reverse: aaccctgttgtcaatgcctc	SYBR green assay

2.16 Subcutaneous sponge implantation induced angiogenesis and Chalkley counting of blood vessels

Mice (male, 8-12 weeks old, MKO and littermates control) were anesthetized with halothane and a horizon wound cut behind the neck. One sterile sponge cylinder (0.5 cmx1 cm, Caligen Foam, Accrington, Lancashire, U.K.) were implanted s.c. into each flank, away apart from the middle line. Wound was checked in the first 7 days after surgery and the sponges were harvested after 20 days. The sponges in the left were cut apart in the middle with half fixed in 10% formalin, the other half frozen in Trizol at -80℃ and the sponge in the right frozen in Trizol at -80℃ as well. Fixed sponges were embedded in paraffin after being washed in 70% ethanol. 5μm paraffin sections were cut and the slides were processed into H&E staining as described in Chapter 2. The frozen sponges were used for RNA extraction and real-time PCR to measure relevant gene expressions as described in Chapter 2.

To quantify blood vessel growth in the H&E sections, Chalkley counting method was used as described before (Fox, Leek et al. 1995). Basically, a transparent round plate with 25 random dots was fitted into the field of the microscope. 3 most vascularized areas (usually in the surroundings of the sponges) in each section were chosen in low magnification (X125) and examined at high magnification power (X312.5). When a dot in the plate covers the position of a blood vessel, it's counted as 1. The plate can be rotated and as many as possible blood vessels covered by the dots are desired to make the counting. Two sections from one sample were examined and the average of the 6 numbers is assigned as the Chalkey count value of the sample.

2.17 K/BxN serum transfer induced arthritis

In-house K/BxN serum was collected from 60 day old offspring of KRN and NOD breeding pairs, when the anti-G6PI antibody levels are highest (Monach, Mathis et al. 2008). Serum was pooled and stored in 500μl aliquots at -80℃. A single i.p. injection of 125μl serum per mouse (males, 7-9 weeks old) was used to induce arthritis on day 0. The body weight of mice was checked before injection and mice

weighed less than 23g were excluded from the experiments. Clinical scoring was carried out blind to genotype for 21 continuous days as described (Chou, Kim et al. 2010). Briefly, a score in a range of 0-3 was given to each paw and ankle joint, with 0 representing no inflammation (red and swelling), 1 localised inflammation, 2 extended inflammation and 3 inflammation in the whole circumference of the joint. The value of the 4 scores added together is assigned as the clinical score for the mouse (a maximum of 12 for one mouse). Data from MKO and 'floxed' littermate control groups were assessed by repeated measurement 2 way ANOVA in Prism GraphPad 5.0, as well as Bonferroni post-test. Area under the curve (AUC) was calculated for each mouse and compared in different genotypes by unpaired t-test.

On day 21 or day 15, mice were culled and joints fixed in 10% formalin for 1 day, before decalcification in 10% EDTA solution (pH 7.4) in room temperature for 2 months or more until the bone was easy to bend. After embedding in paraffin (with sagittal plane of the leg parallel to the glass surface), joints were sectioned (4μm) and processed for H&E staining. Joint pathology was examined with help from David G. Brownstein (Mouse Pathology Core Lab, Queen's Medical Research Institute) and Donald Salter (Pathology Department, University of Edinburgh).

2.18 High fat diet feeding, glucose tolerance test (GTT) and plasma glucose, insulin measurement

Male MKO and littermate control mice (8 weeks old) were put on high fat diet (58% mixed fat, Research Diet, U.S.A) for 14 weeks. Body weight was measured weekly and fasting glucose level, glucose tolerant test (GTT) was done a week before culling. Mice were culled by neck dislocation and blood collected in EDTA tubes for plasma collection. Subcutaneous (SC), epididymis (Epi), mesenteric (Mes) and brown adipose, liver, spleen, muscle and adrenals were harvested and weighed before being fixed in 10% formalin or frozen at -80℃.

Mice were housed individually several days before GTT experiment to adjust them to the environment and reduce stress levels. Mice underwent a 6 hour fast to achieve

a ‘baseline’ blood glucose level and then glucose solution (2g glucose/kg bodyweight using 25% (w/v) D-glucose in PBS) was injected into the peritoneal cavity. Blood glucose levels were measured with a handheld glucometer (OneTouch Ultra,LifeScan,USA) on a drop of tail vein blood according to the protocol enclosed. Blood samples from each mouse were collected into EDTA coated Microvette CB 300 tubes (Sarstedt,Leicester, UK) at 0, 30, 60, and 120 minutes after glucose administration for glucose and insulin analysis.

Glucose levels were quantified using an Infinity Glucose Hexokinase Liquid Stable Reagent (Thermo Electron, Pittsburgh, USA). Serial dilutions of glucose were prepared (50 – 400mg/dl) from the standard using distilled water, with distilled water used as a blank. 2µl of sample and standards was added to each well of 96-well plates, followed by addition of the reagent (200µl). Atfer15 min incubation in the dark at room temperature, the absorbance at 340nm was measured the concentration calculated with reference to the standard curve.

Plasma insulin level was measured with Mouse insulin ELISA kit (Crystal chem, US) according to the enclosed protocol. Briefly, an insulin standard curve (25.6, 12.8, 6.4, 3.2, 1.6, 0.8, 0.4, 0.2, 0.1, 0ng/ml insulin) was made by diluting 25.6ng/ml mouse insulin stock standard solution. In each well of a 96 well plate, 95µl of sample diluent buffer and 5 µ l of sample or standards was added to incubate for 2 hours at 4 ℃. Solutions were then aspirated and the wells washed 5 times with washing buffer (300 µ l per well). 100 µ l of anti-insulin enzyme conjugate solution was added into each well. After incubation for 30mins at room temperature, solutions were aspirated and the wells washed 7 times as described above. Then 100 µ l of enzyme substrate solution was added into each well. After 40mins reaction at room temperature without exposure to light, it was stopped by adding 100 µ l per well of stop solution. The plate was read within 30 minutes using a plate reader machine (Spectrophotometer) at wavelengths of 450 and 630nm. The reading subtraction results (A450-A630) were compared to the standard curve to calculate the sample concentrations.

2.19 Statistics

All statistics analysis was conducted using Graphpad Prism 5.0, unpaired t-tests was often used, sometimes with Welch's correction when the variances between groups are not equal. One way ANOVA and 2 way repeated measurement ANOVA were used as well. Significance is set at $p<0.05$. Data are means $\pm$ standard error of means (SEM).

Chapter 3: *In vitro* studies of 11β-HSD1 deficient macrophages

3.1 Introduction

Evidence is accumulating to suggest that 11β-HSD1 deficiency or inhibition influences macrophage functions. For example, delayed acquisition of phagocytic ability was observed in 11β-HSD1 deficient macrophages (Gilmour, Coutinho et al. 2006) and YM-1 positive cells (indicative of more M2 polarised macrophages) accumulated earlier in the infarcted area of the heart of 11β-HSD1 deficient mice following coronary artery ligation (McSweeney, Hadoke et al. 2010). An increased inflammatory response was reported in LPS treated (M1 polarised) primary 11β-HSD1 deficient peritoneal or spleen macrophages, but not bone marrow derived macrophages (BMDMs). The difference between genotypes was postulated to be from secondary effect of increased circulating GC levels on macrophage differentiation, while no influence of circulating GCs on BMDMs experiments *in vitro* (Gilmour, Coutinho et al. 2006; Zhang and Daynes 2007). In contrast, selective 11β-HSD1 inhibitor treatment of macrophages showed decreased inflammatory responses by LPS, although there were no GC substrate for 11β-HSD1 added in the experiment (Ishii, Masuzaki et al. 2007). There are no reported direct *in vitro* studies on role of 11β-HSD1 in IL-4 induced M2 macrophage polarisation. Thus, there has been no conclusion so far on role of 11β-HSD1 in M1/M2 macrophage polarisation.

The role of macrophage 11β-HSD1 in hypoxia is also worthy of study. Hypoxia is closely linked to macrophage-driven fibrosis and angiogenesis and both of them are influenced in globally 11β-HSD1 deficient mice (refer to Section 1.4). More angiogenesis and less fibrosis was reported in the adipose tissues of 11β-HSD1 deficient mice following high fat diet feeding (Michailidou, Turban et al. 2012), but more inflammation and fibrosis were found in their lungs following bleomycin treatment (Yang 2010) and in livers following CCl4 treatment (Xiantong Zou 2013). Treatment with 11β-HSD1 inhibitor was shown to promote the proliferation of human dermal fibroblasts and accelerate skin wound healing (Terao, Murota et al.

2011). Again, there is no conclusion as to the part played by macrophage 11β-HSD1 deficiency in these studies.

Based on the above studies, it is important to elucidate the role of 11β-HSD1 in macrophage polarisation and in hypoxic response. As mentioned above, there is no intrinsic difference in LPS induced inflammatory responses between 11β-HSD1-deficient and wild-type BMDMs. So, TG elicited macrophages (differentiated from monocytes *in vivo*) were chosen for the studies reported here.

3.2 Hypothesis and aims

Hypothesis:

1. 11β-HSD1 deficiency will favour an increased M1 and decreased M2 response in macrophages.

2. The response to hypoxia will be augmented in 11β-HSD1 deficient macrophages, leading to greater inflammatory, angiogenic and fibrotic response.

Aims:

1. To investigate whether 11β-HSD1 is differentially regulated in wild-type M1 and M2 macrophages.

2. To investigate the effects of 11β-HSD1 deficiency upon M1/M2 macrophage polarisation *in vitro*.

3. To investigate the effects of 11β-HSD1 deficiency in the response of macrophages to hypoxia *in vitro*.

3.3 Results

3.3.1 *Hsd11b1* mRNA levels are higher in M1 than M2 wild-type macrophages but without change in protein levels

To study the role of 11β-HSD1 in M1/M2 macrophage polarisation, day 3 TG elicited macrophages from 11β-HSD1 deficient and C57Bl/6 mice were treated with LPS + IFN-γ and IL4 to induce M1 and M2 polarised macrophages, respectively, as described in Chapter 2.

First, 11β-HSD1 expression in M1 and M2 wild-type macrophages was examined. RNA sequence data from Professor Judith Allen's group suggest down-regulation of *Hsd11b1* in peritoneal macrophages following nematode infection (an IL4 mediated M2 response), compared to *Hsd11b1* mRNA levels in TG elicited macrophages from naïve BALB/c mice. Moreover, the levels of *Hsd11b1* mRNA in wild type cells were lower than those in *Il4ra* knockout mice (Thomas, Ruckerl et al. 2012). In agreement with this, *Hsd11b1* mRNA levels are found to be higher in M1 than M2 polarised macrophages in this experiment (Figure 3-1A). However, surprisingly there is no change in 11β-HSD1 protein levels (Figure 3-1B).

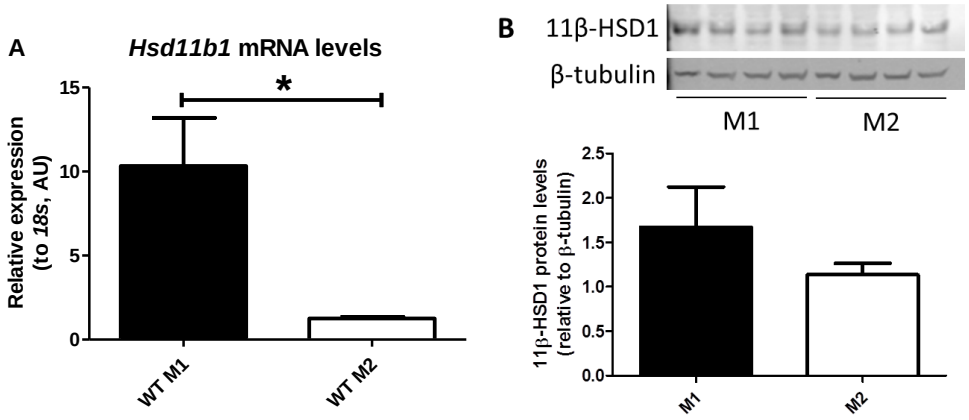

Figure 3-1 Higher *Hsd11b1* mRNA but similar 11β-HSD1 protein levels in M1 than M2 polarised macrophages.

Peritoneal macrophages were elicited from C57Bl/6 mice 3 days after TG injection. LPS (100ng/ml) + IFN-γ (10U/ml) and IL4 (20ng/ml) were used to polarise macrophages into M1 and M2 macrophages, respectively. After overnight treatment, RNA and proteins were extracted from these cells and analysed by qPCR and western blotting. (A) *Hsd11b1* levels were measured by qPCR, relative to the levels of *18S* rRNA. Data are means ± SEM and were analysed by un-paired t-test. N=6/group; *, $p<0.05$. (B) 11β-HSD1 protein levels were measured by western blotting. The band densities were quantified in the graph below. Each lane contains 20μg of protein from one mouse. N=4/group. Data are means ± SEM and were analysed by un-paired t-test with significance set at $p<0.05$. There is no difference between genotypes.

3.3.2 11β-HSD1 protein levels in TG elicited macrophage are not increased by inflammatory stimulation

The previous experiment addressed expression of 11β-HSD1 in M1 verse M2 polarized macrophages but did not address whether LPS + IFNϒ increases 11β-HSD1 levels in untreated TG elicited peritoneal macrophages. In studies on the macrophage cell lines, LPS induced 11β-HSD1 expression (Thieringer, Le Grand et al. 2001; Ishii, Masuzaki et al. 2007). Whether 11β-HSD1 protein levels can be increased by inflammatory stimulation of TG elicited macrophages, similar to that in macrophage cell lines has not been reported, although TG is known to increase 11β-HSD1 expression in peritoneal cells, which include macrophages (Gilmour, Coutinho et al. 2006).

Western blotting was carried out compare 11β-HSD1 levels in untreated TG elicited peritoneal macrophages from C57Bl/6 mice and following treatment with LPS or LPS plus IFNϒ treatment groups. IFNϒ synergistically regulates LPS induced inflammatory response (Held, Xiao et al. 1999).

11β-HSD1 protein levels in macrophages treated with LPS or LPS+IFN-γ did not differ from levels in untreated cells, although IFN-γ modestly increased 11β-HSD1 expression in LPS treated macrophages (Figure 3-2). This reveals different 11β-HSD1 modulation by inflammatory stimuli between primary macrophages and macrophage cell lines.

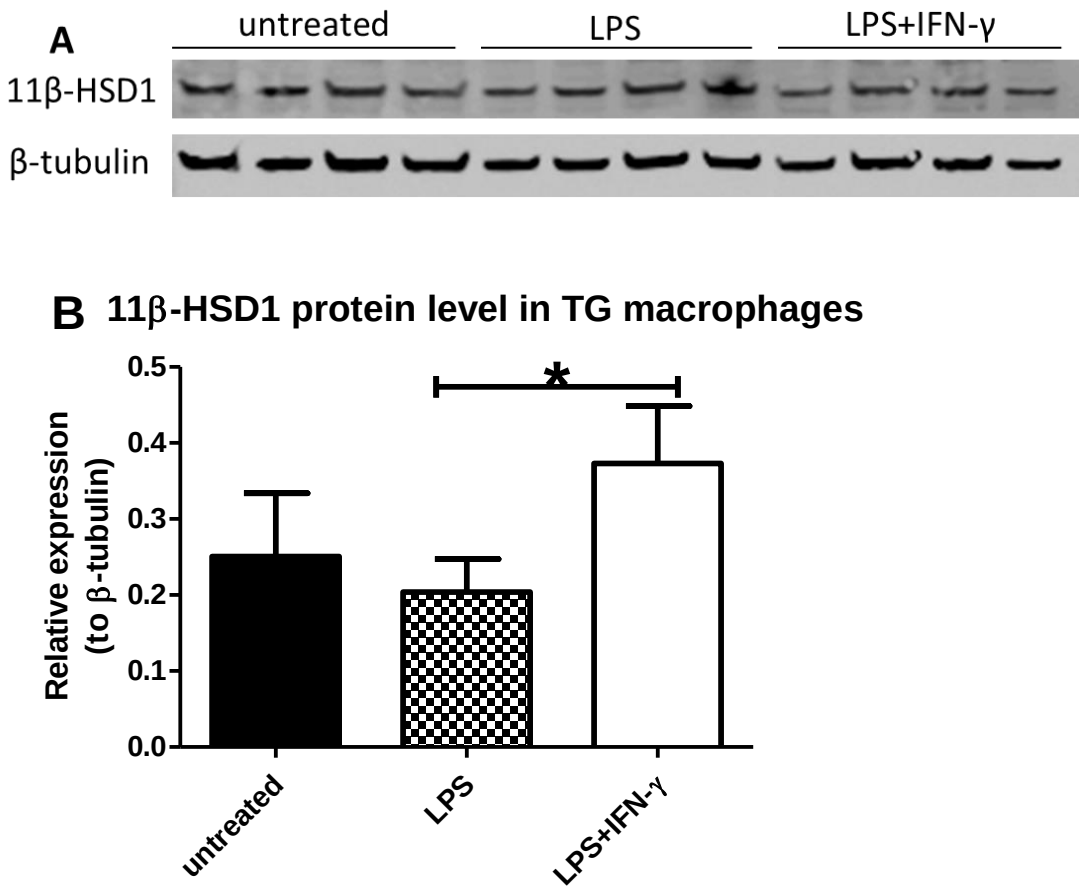

Figure 3-2 11β-HSD1 protein levels are not higher in TG elicited macrophages following LPS, or LPS plus IFN-ϒ treatment compared to untreated cells.

Western blotting of 11β-HSD1 was carried out in day 3 TG elicited peritoneal macrophages from C57Bl/6 mice following *ex vivo* treatment with LPS or LPS+IFN-γ. (A) A representative image of 11β-HSD1 western blotting. Each lane contained 30μg of protein from one mouse. (B) The bands in figure (A) were quantified and plotted into the graph. Data are means ± SEM and were analysed by one way ANOVA with Tukey post-test. N=4 in each group. *, $p<0.05$.

3.3.3 Levels of inflammatory gene mRNAs are increased in 11β-HSD1 deficient macrophages, but without corresponding increase in protein levels.

The next question was to test the effect of macrophage 11β-HSD1 deficiency on M1/M2 polarisation. To test the inflammatory M1 response, *Il1b*, *Il6*, *Tnfa*, *Nos2* and *Il12b* mRNA levels were examined in TG elicited macrophages from 11β-HSD1 deficient and control C57Bl/6 mice polarised *ex vivo* with LPS + IFNγ treatment. Among the examined genes, *Il1b*, *Tnfa* and *Nos2* mRNA levels are significantly higher in 11β-HSD1 deficient (KO) macrophages compared to WT controls (Figure 3-3).

Other mRNAs were measured to explore the mechanism. *Cox2* induction leads to elevated levels of prostanoids in inflammation and has been found to be GC regulated (Masferrer, Reddy et al. 1994). Annexin A1 (encoded by *Anxa1*) is a downstream effector of GC that supresses inflammation (Perretti and D'Acquisto 2009). *Trib1* and *Cop1* are linked to control of IL12 p40 production (Yamamoto, Uematsu et al. 2007). There is no difference in *Cox2*, *Anxa1*, *Fcgr2b*, *Fcgr3*, *Patched*, *Trib1* (tribbles pseudokinase 1) or *Cop1* (constitutive photomorphogenic 1) expression between the 2 genotypes, but *Ccl2* and *Nr3c1* (encoding the GR protein) mRNAs are found to be lower in 11β-HSD1 deficient M1 macrophages (Figure 3-4). Lower *Nr3c1* expression may account for the increased inflammatory gene expression.

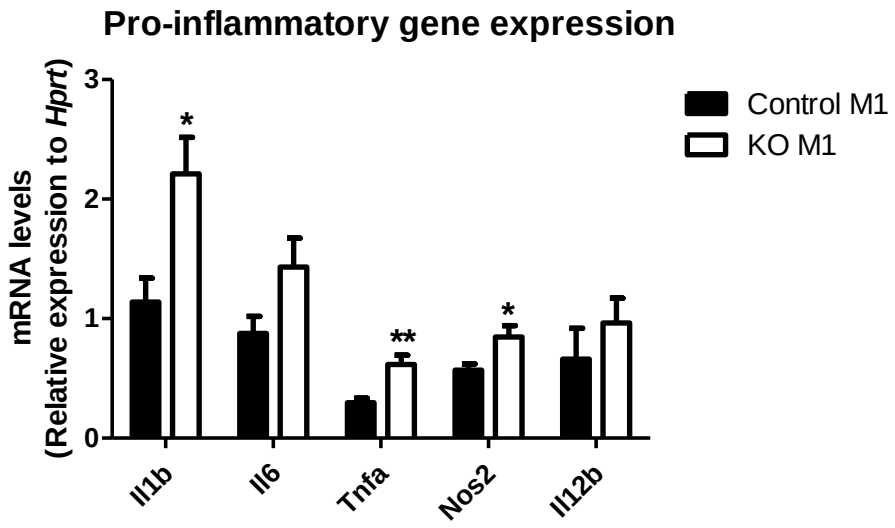

Figure 3-3 Levels of mRNA encoding pro-inflammatory markers are increased in *Hsd11b1* deficient M1 macrophages.

Day 3 TG elicited peritoneal macrophages from globally 11β-HSD1 deficient (white bar) and C57Bl/6 mice (black bar) were treated with 100ng/ml LPS and 10U/ml IFNγ *ex vivo.* After overnight treatment, inflammatory mRNA levels were measured by qPCR. Data are means ± SEM and were analysed by un-paired t-test to compare the 2 groups for each gene with significance set at $p<0.05$. *, $p<0.05$; **, $p<0.01$. N=8 in each group, except for *Il12b* (N=4-6). 'KO', *Hsd11b1* deficient.

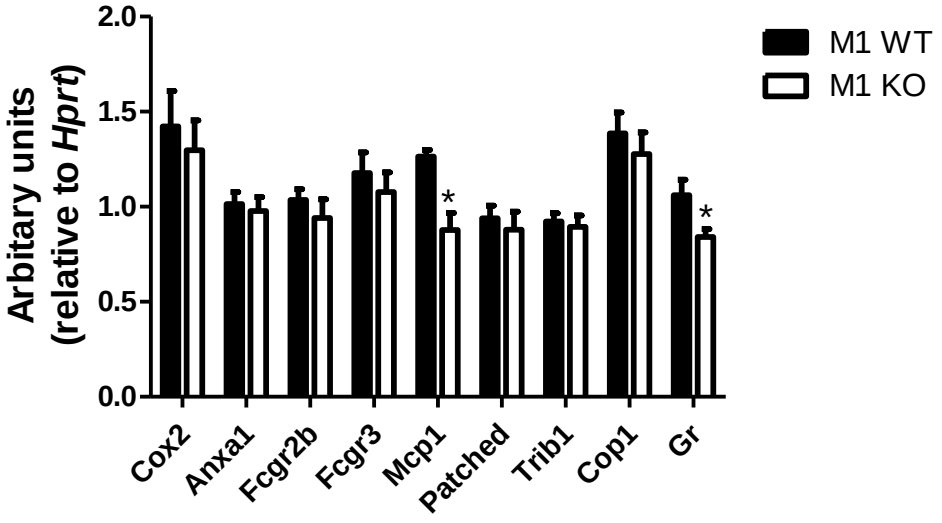

Figure 3-4 Levels of mRNAs encoding CCL2 and GR are decreased in M1 polarised macrophages from 11β-HSD1 deficient mice.

In the same experiment as shown Figure 3-3, a number of other mRNA expression levels were examined by qPCR to compare the two genotypes (white bar, 11β-HSD1 deficient macrophages; black bar, wild-type macrophages). Data are means ± SEM and were analysed by un-paired t-test for each gene with significance set at $p<0.05$. N=6/group; *, $p<0.05$.

To check whether increased levels of inflammatory mRNAs translated into corresponding changes in peptide and protein levels in 11β-HSD1 deficient macrophages, ELISA and western blotting were carried out in the cell culture medium and cell homogenates, respectively. However, there was no difference in IL1β or IL6 cytokine levels in the medium. Instead, IL12 p40 was decreased (Figure 3-5A). Western blotting of iNOS (encoded by *Nos2*) also showed no difference in its protein levels (Figure 3-5B), in contrast to the increased *Nos2* mRNA levels in 11β-HSD1 deficient macrophages.

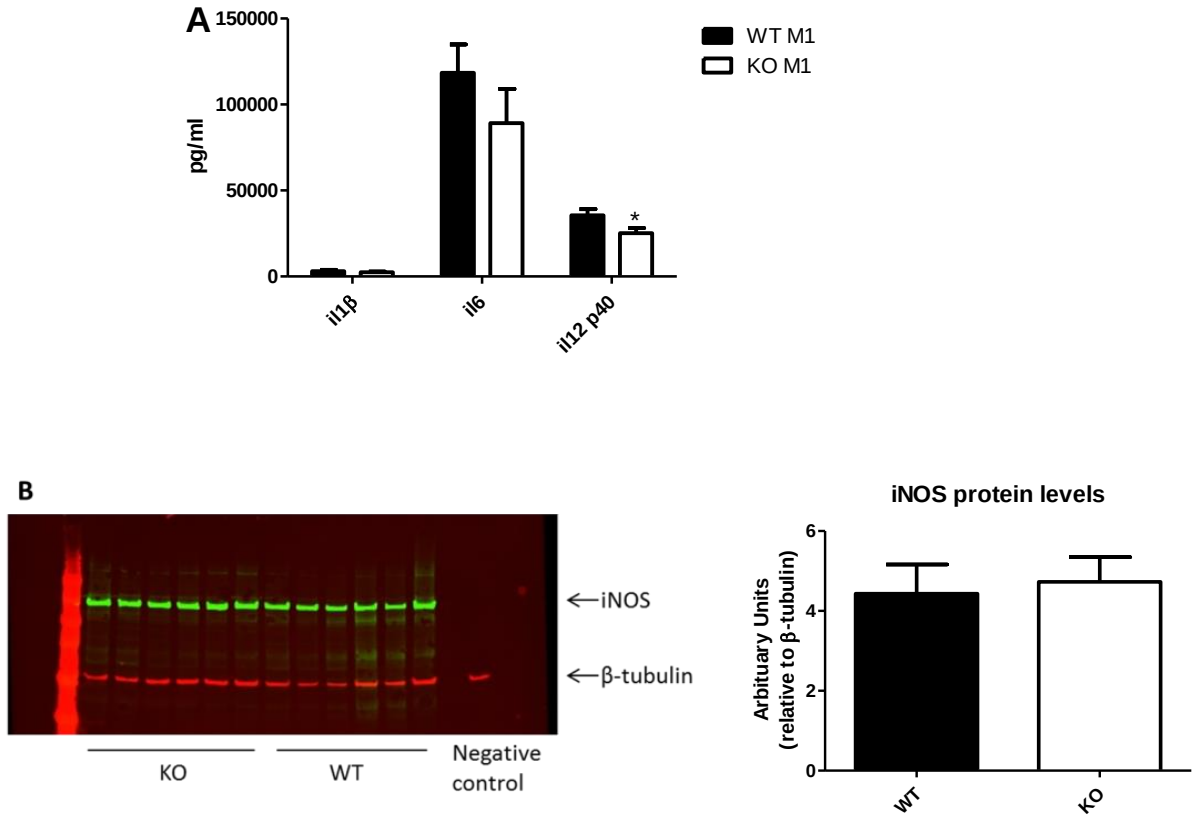

Figure 3-5 Levels of the secreted cytokines IL1β, IL6 and intracellular iNOS protein levels in M1 macrophages were not different between the two genotypes, but IL12 p40 secretion from 11β-HSD1 deficient macrophages was decreased.

In the *ex vivo* M1 macrophage polarisation as described in Figure 3-3, cell culture medium was saved for ELISA and cell homogenates for western blotting. (A) ELISA results for IL1β, IL6 and IL12 p40. (B) Western blotting of iNOS. Density of bands was quantified in the graph to the right of the western blot image. Each lane contains 30μg of protein from 1 mouse. Data are means ± SEM and were analysed by unpaired t-test with significance set at $p<0.05$. N=7-8, *, $p<0.05$.

3.3.4 Increased levels of C/EBPβ protein in 11β-HSD1 deficient M1 macrophages despite lower levels of encoding mRNA.

Because C/EBPβ is a negative regulator of IL12 p40 expression (Gorgoni, Maritano et al. 2002) and IL12 p40 levels are decreased in 11β-HSD1 deficient M1 polarized macrophages, C/EBPβ was measured in M1 macrophages. C/EBPβ protein levels are higher in 11β-HSD1 deficient M1 macrophages (Figure 3-6A&B), possibly explaining the decreased IL12 p40 levels. However, the encoding *Cebpb* mRNA levels are lower in 11β-HSD1 deficient macrophages without changes in *Cebpa* or *Cebpd* mRNA levels (Figure 3-6C).

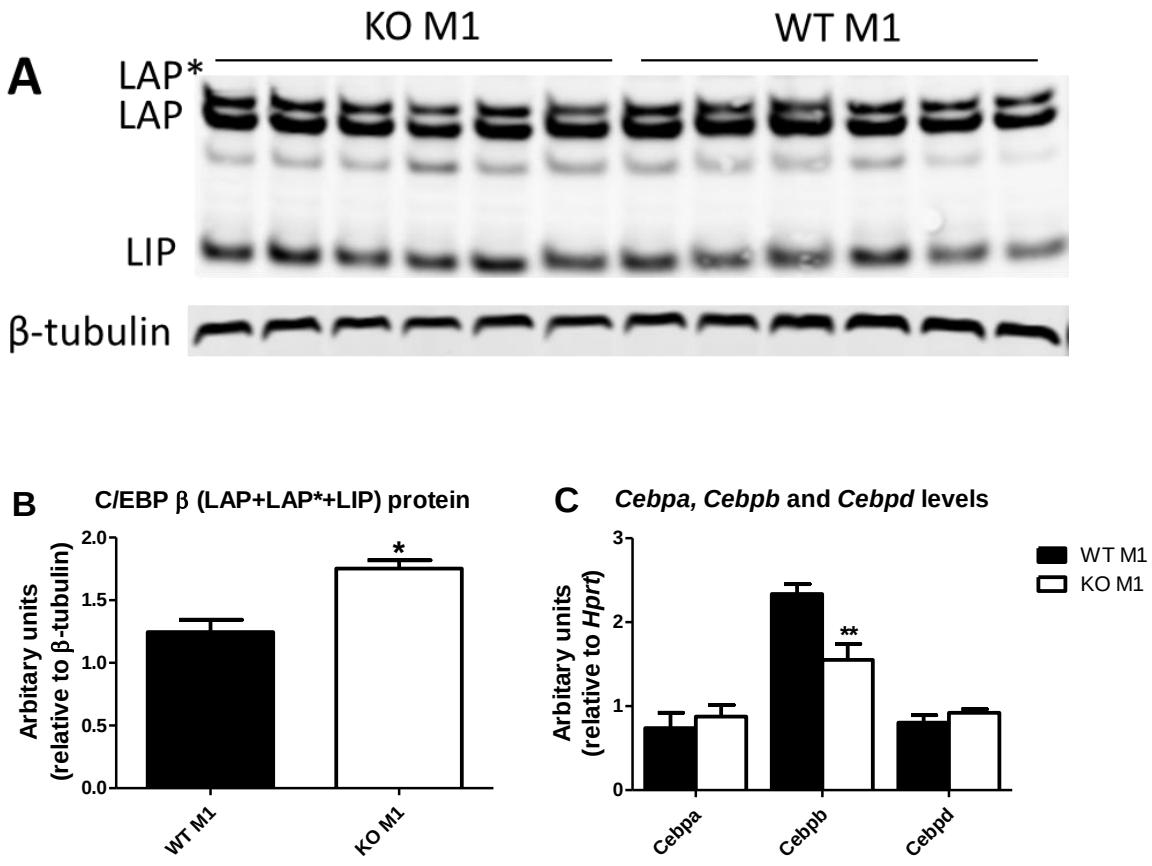

Figure 3-6 C/EBPβ levels are higher in 11β-HSD1 deficient M1 macrophages, albeit a lower *cebpb* RNA expression.

In the same M1 polarisation experiment described in Figure 3-3 to 3-5, C/EBPβ protein levels were examined by western blotting in the cell homogenates and *Cebpa, Cebpb, Cebpd* mRNA levels were measured by qPCR in the extracted RNA. (A) Image of the western blot of C/EBPβ and β-tubulin. All 3 isoforms of C/EBPβ (LAP*, LAP and LIP) were detected. Each lane contains 30μg protein from 1 mouse. (B) Density of the bands were quantified and plotted. Data are means ± SEM, n=6 in each group. Un-paired t-test. *, $p<0.05$. (C) *Cebpb* mRNA levels were lower in 11β-HSD1 deficient M1 macrophages. No differences in *Cebpa* or *Cebpd* were detected. Data are means ± SEM, n=6 in each group. Un-paired t-test. **, $p<0.01$.

3.3.5 Decreased levels of mRNA encoding M2 markers in 11β-HSD1 deficient macrophages without change in phospho-STAT6 or intracellular YM1 protein levels.

To test whether 11β-HSD1 deficiency affects M2 macrophage polarization, day 3 TG elicited peritoneal macrophages from globally 11β-HSD1 deficient and C57Bl/6 mice were treated with IL4 overnight to induce M2 macrophage polarization. RNA and protein were harvested at the end of the experiment to study M2 markers.

Some of the examined mRNA levels were reduced in 11β-HSD1 deficient macrophages such as *Chi3l3*, *Arg1* and *Il10*, but no differences in *Retnla*, *Pparg* or *Tgfb1* were detected (Figure 3-7).

To investigate the responsible signalling pathway and confirm altered levels of M2 markers, western blotting was carried out to detect phosphorylated STAT6 (phospho-STAT6) and intracellular YM-1 (encoded by *Chi3l3*). STAT6 is the transcription factor that directs IL4 induced M2 gene transcription (reviewed by (Lawrence and Natoli 2011)). Unfortunately, no difference was found in levels of either phosphor-STAT6 or YM-1 (Figure 3-8).

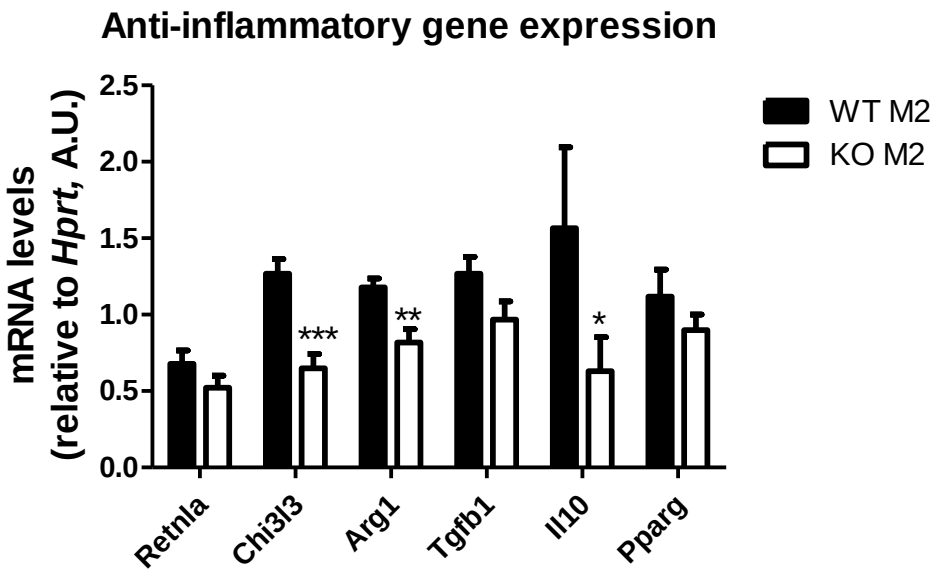

Figure 3-7 Levels of mRNA encoding markers of M2 polarised macrophages were decreased in 11β-HSD1 deficient macrophages.

Day 3 TG elicited macrophages from 11β-HSD1 deficient and C57Bl/6 wild type mice were treated overnight with 20ng/ml IL4. RNA was harvested for qPCR to compare M2 marker mRNA levels in the 11β-HSD1 deficient macrophages (KO M2, white bar) and control wild type macrophages (WT M2, black bar). Data are means ± SEM and were analysed by un-paired t-test for each gene. N=6 in each group; *, $p<0.05$,**, $p<0.01$, ***, $p<0.001$.

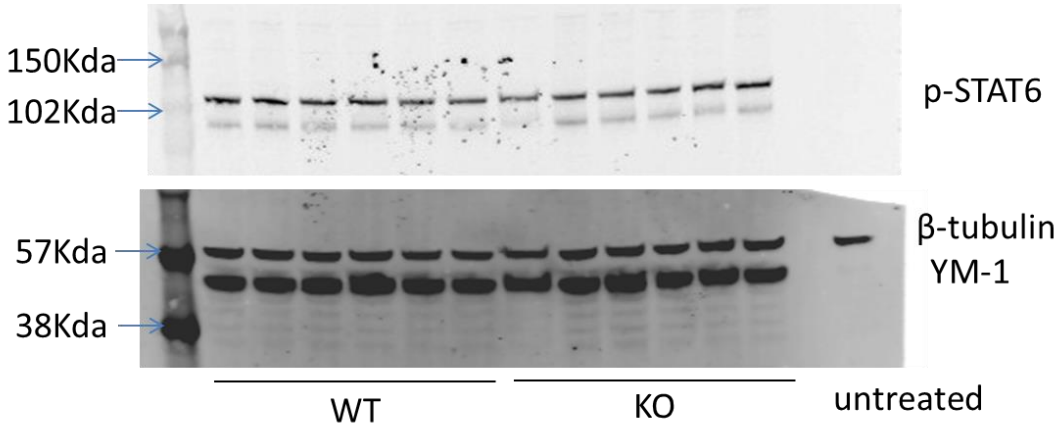

Figure 3-8 No difference in p-STAT6 or YM-1 protein levels between 11β-HSD1 deficient and C57Bl/6 M2 macrophages.

In the same M2 macrophage polarisation experiment as shown in Figure 3-7, cell homogenates were used for western blotting. This is a representative image of a membrane, which was cut into 2 parts for separate first antibody staining. The left lane contains a protein ladder (band sizes indicated). The first 6 lanes next to the ladder are WT samples, and the neighbouring 6 samples in the right are 11β-HSD1 deficient samples ('KO'). The lane at the right end contains an untreated control, which showed a band of β-tubulin (50kDa), but not p-STAT6 (110kDa) or YM-1 (45kDa, encoded by *Chi3l3*). Each lane contained 30μg protein from 1 mouse. No difference in phospho-STAT6 or YM-1 protein levels between the 2 groups was detected after quantifying the bands (quantified results not shown).

3.3.6 Decreased levels of *Patched* mRNA encoding the hedgehog ligand receptor in 11β-HSD1 deficient M2 macrophages

RNA sequence data on aortas of globally 11β-HSD1 deficient mice on an *Apoe*$^{-/-}$ genetic background showed higher *Gli1* (glioma-associated oncogene homologue 1) and *Hhip* (hedgehog interacting protein) mRNA levels, compared to *ApoE*$^{-/-}$ controls (unpublished data, Professor Karen Chapman). Both *Gli1* and *Hhip* are in the hedgehog pathway. In this pathway, *Gli1* is the main induced transcription factor after hedgehog ligands Indian hedgehog (*Ihh*), Sonic hedgehog (*Shh*) or Desert hedgehog (*Dhh*) bind to the receptor *Patched* (reviewed by (Kasper, Regi et al. 2006)). The hedgehog interacting protein could sequester the hedgehog ligands (Bosanac, Maun et al. 2009). This pathway is emerging as an important regulator of inflammatory tissue remodeling underlying liver fibrosis and osteophyte formation (Ruiz-Heiland, Horn et al. 2012; Pereira, Xie et al. 2013).

Therefore, related genes were examined in M1 and M2 polarized macrophage samples. Expression of *Patched* and *Ihh* were detected in M2 macrophages but not in M1 macrophages (*Dhh* and *Shh* are too low to be detected in both M1 and M2 RNA samples). *Patched* mRNA levels were decreased while there was a trend to higher *Ihh* expression levels in 11β-HSD1 deficient M2 macrophages, compared to wild type M2 macrophages (Figure 3-9). However, western blotting failed to detect Indian hedgehog in M2 macrophages (data not shown).

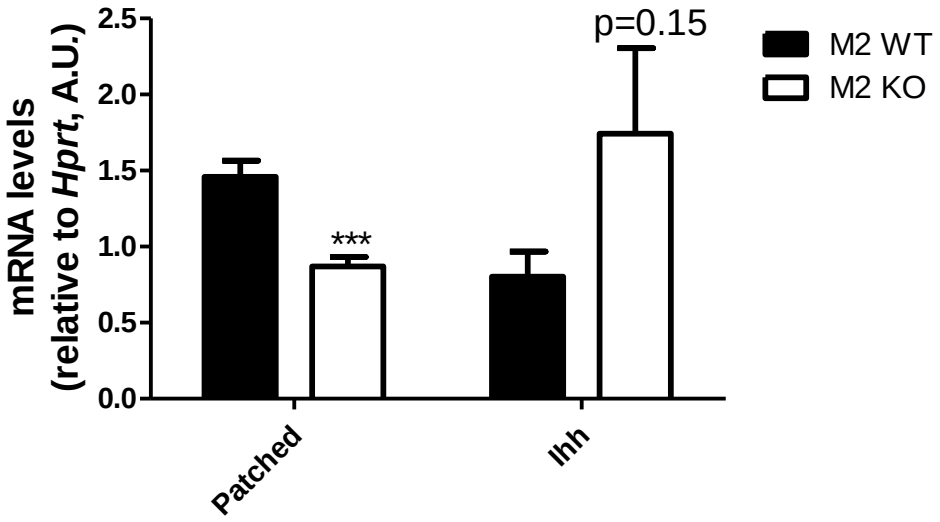

Figure 3-9 Decreased *Patched* and a trend to higher *Ihh* levels in 11β-HSD1 deficient M2 macrophages.

In the M2 macrophage polarisation experiment described in Figure 3-7 and 3-8, *Patched* and *Ihh* mRNA levels in the macrophages were measured by qPCR. Data are means ± SEM and were analysed by un-paired t-test for each gene. N=7-8 mice/group. ***, $p<0.001$.

3.3.7 The response of M1 macrophages under hypoxic conditions is largely unaffected by 11β-HSD1 deficiency

Hypoxia is an important factor influencing inflammatory, fibrotic and angiogenic responses (Cramer, Yamanishi et al. 2003; Halberg, Khan et al. 2009; Imtiyaz, Williams et al. 2010). To mimic the *in vivo* hypoxic conditions macrophages are exposed to during inflammation and to investigate whether 11β-HSD1 deficiency alters the macrophage response to hypoxia, M1 macrophage polarization was carried out under hypoxic conditions (1% O_2 level) in 11β-HSD1 deficient and control macrophages. However, neither *Hif1a* nor its target genes differed between genotypes, including the glucose transporter gene *Glut1*, inflammatory genes, angiogenesis gene *Vegfa* and genes related to fibrosis, such as *Tgfb1*, *Timp1*. However, *Patched* was increased (Figure 3-10).

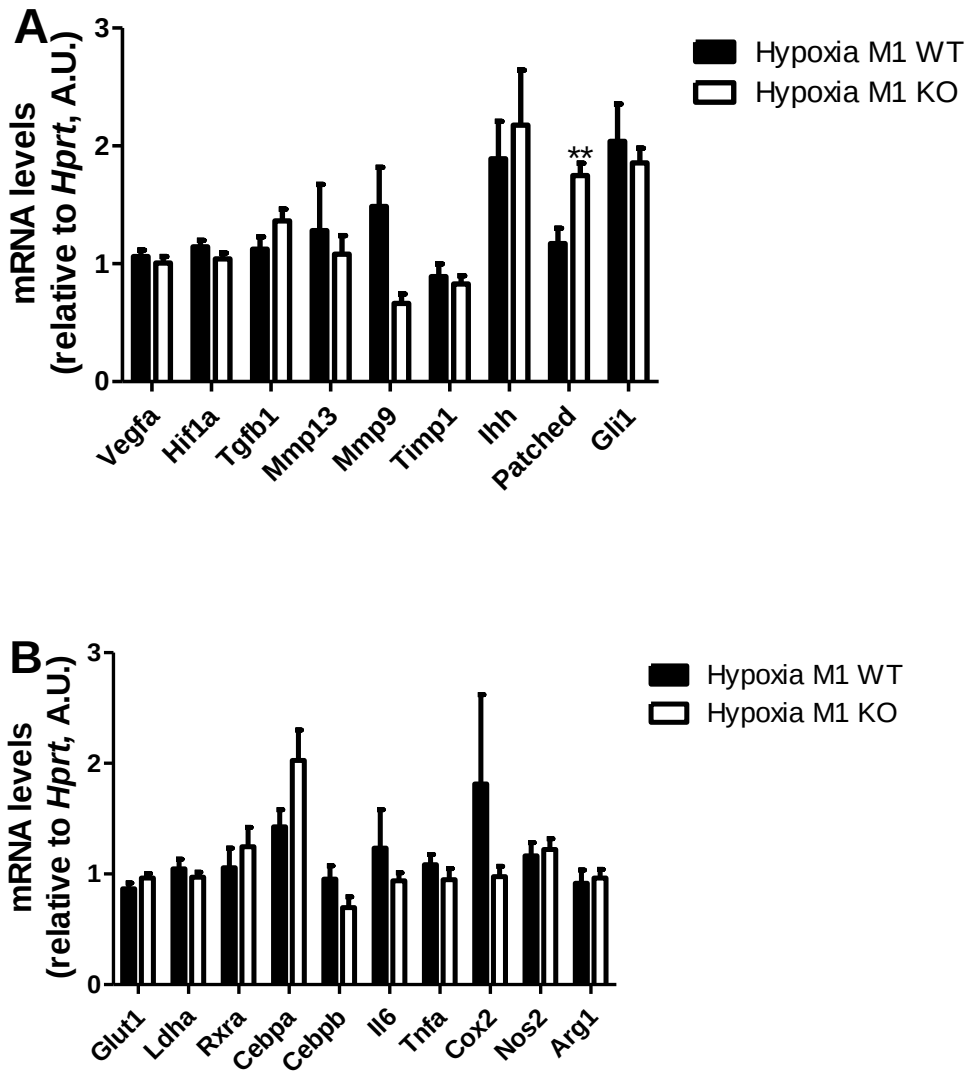

Figure 3-10 Similar gene expression levels in response to hypoxia between 11β-HSD1 deficient and wild-type M1 macrophages.

TG elicited peritoneal macrophages from 11β-HSD1 deficient and control wild type mice were treated with 100ng/ml LPS and 10U/ml IFN-ϒ under hypoxic conditions (1% oxygen) overnight before the cells were harvested for RNA analysis by qPCR. (A) *Vegf1, Hif1a, Tgf1a, Mmp9, 13, Timp1* and *Gli1* mRNA levels are not different between genotypes, but *Patched* levels are higher in the 11β-HSD1 deficient macrophages. (B) *Glut1, Ldha, Rxr1, Cebpa, Cebpb, Il6, Tnfa, Cox2, Nos2* and *Arg1* mRNA levels are not different between the 2 genotypes in the same experiment as in (A). Data are means ± SEM and were analysed by un-paired t-test for each gene. N=6-7; **, $p<0.01$.

3.4 Discussion

Hsd11b1 mRNA is differentially expressed in M1 and M2 polarised TG elicited peritoneal macrophages from C57/Bl6 mice as hypothesised, with higher levels in M1 than M2 macrophages. But surprisingly, no difference was found in the 11β-HSD1 protein levels, which may suggest that the protein translation is blocked or newly synthesised protein is quickly degraded. Equal 11β-HSD1 protein levels in M1 and M2 polarised macrophages does not support a role for 11β-HSD1 to support one direction but oppose the other in M1/M2 macrophage polarisation.

11β-HSD1 expression was induced very robustly in the J774.1 macrophage cell line by LPS stimulation (examined by qPCR and enzyme activity assay) (Ishii, Masuzaki et al. 2007; Wang, Liu et al. 2012). A dynamic 11β-HSD1 expression change is also seen in TG elicited peritoneal cells. 11β-HSD1 enzyme activity is increased with time in TG elicited peritoneal cells during the first 24h (when neutrophils and monocytes are dominating populations) and remains at high levels during day 1-day4 (when monocyte differentiates into macrophages) but it returns to normal levels by day 5 (when macrophages are fully matured) (Gilmour, Coutinho et al. 2006). However, compared to untreated day 3 TG elicited peritoneal macrophages, LPS only or LPS+IFNϒ treatment failed to increase 11β-HSD1 expression examined by western blotting. This shows that TG elicited macrophages are different to the J774.1 macrophage cell line in terms of 11β-HSD1 expression in response to inflammatory challenges.

In terms of M1/M2 polarised TG elicited peritoneal macrophages, although RNA data showed some increased M1 markers and some decreased M2 markers in 11β-HSD1 deficient macrophages, there were no changes in corresponding cytokine and protein levels. In the M1 polarisation study, *Il1b*, *Tnfa* and *Nos2* mRNA levels were modestly increased in 11β-HSD1 deficient macrophages (less than 2 fold), but there were no difference in IL-1β or iNOS protein levels. A similar phenomenon was found in the M2 polarisation study. *Chi3l3*, *Arg1* and *Il10* mRNA levels were modestly higher in 11β-HSD1 deficient macrophages than wild type control macrophages, but YM-1 protein (encoded by *Chi3l3*) levels were not different

between the 2 groups. The M2 response is dominated by the phospho-STAT6 transcription factor, the expression levels of which were not changed either. These data argue against important role of 11β-HSD1 in M1/M2 polarization of macrophages. Similarly, in macrophages isolated from adipose tissues of 11β-HSD1 deficient and control wild type mice, mRNA levels of M1/M2 marker genes are similar, as well as cytokine levels (Wamil, Battle et al. 2011).

In the reports based on *in vitro* macrophage 11β-HSD1 studies, which advocate a pro-inflammatory role of 11β-HSD1 (Ishii, Masuzaki et al. 2007; Wang, Liu et al. 2012; Garcia, Search et al. 2013), 11β-HSD1 substrate concentration is a big concern. There is no 11β-HSD1 substrate or the substrate concentration deviates from the *in vivo* conditions. The first 2 papers used J774.1 macrophage cell line to study LPS induced inflammatory response with 11β-HSD1 inhibitors. In the report of Ishii, et al., there was no added 11β-HSD1 substrate, 11-dehydrocorticosterone, in the culture medium, the levels of which is very low in fetal calf serum. In the paper of Wang, et al., it was revealed that the pro-inflammatory role of 11β-HSD1 in macrophages is exhibited when 11-dehydrocorticosterone level is <0.1nM (no effects between 1-1000nM and anti-inflammatory effects at 10μM) in the absence of any active GCs. Also, the effects are very mild with about 0.25 fold change of *Il6* mRNA levels by these treatments. Primary peritoneal macrophages elicited by TG from 11β-HSD1 knockout mice in *Apoe*$^{-/-}$ genetic background were used in the third report and showed a decreased inflammatory response to copper-oxidized LDL, compared to *Apoe*$^{-/-}$ controls. The effect was produced when macrophages were incubated with 200nM 11-DHC in culture medium for 5h and then overnight incubation with 200nM 11-DHC and oxidized LDL.

It is very hard to predict the levels of the 11β-HSD1 substrates *in vivo*, which is under the control of the HPA axis to generate active GCs and 11β-HSD2 to generate inert GCs. Inflammation induces a change in HPA axis activity and 11β-HSD2 activity was decreased by inflammation (Chisaka, Johnstone et al. 2005). Therefore it is hard to judge how well these reported changes *in vitro* mimic what happens *in vivo*.

The data showing increased inflammatory cytokine levels in macrophages from 11β-HSD1 deficient mice after LPS stimulation (Gilmour, Coutinho et al. 2006; Zhang and Daynes 2007) were not reproduced in the current experiments. In the second report, primary macrophages from 11β-HSD1 deficient mice, either TG elicited macrophages or spleen macrophages but not BMDMs, showed increased cytokines secretion upon LPS treatment, compared to wild type controls. (Zhang and Daynes 2007). This was associated with lower Iκ Bα protein levels in 11β-HSD1 deficient spleen macrophages upon LPS treatment, while p-Akt, p-p38, p-ERK44/42 and SHIP1 were increased in them. The authors proposed higher SHIP1 expression may stimulate pro-inflammatory cytokine production, but this contrasts with the normally accepted view of SHIP1 to be a negative regulator of inflammatory cytokines (An, Xu et al. 2005), as the authors discussed. The increased SHIP1 levels were attributed to induction of TGFβ by higher circulating GC levels in the 11β-HSD1 deficient mice. However, the reported higher circulating GC levels in 11β-HSD1 deficient mice are not observed in the same line of mice measured in our centre (Carter, Paterson et al. 2009).

The ELISA cytokine pattern observed here is unusual, with unchanged IL1 and IL6, but decreased IL12 p40 levels. However, a similar pattern was reported in macrophages from *Trib1*$^{-/-}$ mice. After LPS stimulation of *Trib1*$^{-/-}$ macrophages, the only difference detected was reduced IL12 p40 release associated with increased C/EBPβ protein expression (Yamamoto, Uematsu et al. 2007). Western blotting did show increased C/EBPβ expression in macrophages from *Hsd11b1* deficient macrophages, but with lower *Cebpb* mRNA levels. There was no change in levels of *Trib1* or *Cop1* mRNA (encoding an E3-ubiquitin ligase, which docks on Trib1 protein) and this does not support an influence of 11β-HSD1 deficiency on *Trib1* or *Cop1*. With hindsight, it is found that selective IL12 p40 was also reported in 12/15 lipoxygenase deficient macrophages (Zhao, Cuff et al. 2002) and IL12 p40 is also negatively regulated by SHIP-1 (Hadidi, Antignano et al. 2012), but these have not been explored in the 11β-HSD1 deficient macrophages.

In terms of alternative activation of macrophages, increased M2 polarisation in the 11β-HSD1 deficient macrophages was hypothesised, as early accumulation of YM-1 positive cells were observed in the infarcted area of the hearts of 11β-HSD1 deficient mice following myocardial infarction (McSweeney, Hadoke et al. 2010). However, the in *vitro* polarisation experiment does not support this. Although mRNA levels of most M2 gene tested are lower in the 11β-HSD1 deficient macrophages, there was no difference in phospho-STAT6 or YM-1 protein levels. However, there are limitations in the western blotting studies. YM-1 is a secreted protein and only intracellular YM-1 is represented in western blotting. Additionally, measurement of phospho-STAT6 at early time points would be more informative, such as 1h time point post IL4 stimulation used in the study of ABCA1 (Pradel, Mitchell et al. 2009) rather than 20h in the current experiment.

Hypoxia is a strong modulator of macrophage function. *Hif1a* and *Hif2a* were shown to be necessary for a macrophage inflammatory response (Cramer, Yamanishi et al. 2003; Imtiyaz, Williams et al. 2010). In terms of hypoxic regulation of 11β-HSD1, HIF1α has been shown to negatively regulate 11β-HSD1 expression in adipocytes (Lee, Gao et al. 2013). But when 11β-HSD1 deficient and control macrophages were tested in the hypoxia environment, surprisingly most genes were unchanged at the mRNA level, including genes involved in angiogenesis, fibrosis, energy metabolism and inflammatory responses.

The interest in Hedgehog signalling came from RNA-sequence data from atherosclerotic aortas of 11β-HSD1 deficient mice (Professor Karen Chapman, unpublished data). There are several reports of effects of GC on hedgehog activity (Heine and Rowitch 2009; Wang, Lu et al. 2010), and cortisol is reported to have a stronger ability than cortisone to positively sensitize cells to hedgehog ligand stimulation *in vitro* (Wang, Davidow et al. 2012). The preliminary data here on the effect of 11β-HSD1 deficiency in macrophages upon hedgehog signalling are not conclusive. The trend to higher *Ihh* mRNA levels with significantly lower *Patched* mRNA levels is suggestive of higher hedgehog signalling from11β-HSD1 deficient

M2 macrophages. However, no IHH protein was detected in M2 proteins by western blotting, the levels of which may be too low.

In summary, there is little evidence to support an important role of 11β-HSD1 in M1/M2 macrophage polarisation or in the response to hypoxia, as least when studied *in vitro*. These *in vitro* experiments lack the dynamic 11β-HSD1 substrate level changes *in vivo* and are not able to explain the 'changed' macrophage function in globally 11β-HSD1 deficient mice. Therefore, macrophage specific 11β-HSD1 knockout mice provide a good tool to examine the role of macrophage 11β-HSD1 within *in vivo* settings.

Chapter 4: Characterisation of *LysM-Cre Hsd11b1*$^{flox/flox}$ mice

4.1 Introduction

Studies carried out in globally *Hsd11b1* deficient mice (Kotelevtsev, Holmes et al. 1997) have shown that 11β-HSD1 deficiency promotes angiogenesis in a model of subcutaneous sponge implantation (Small, Hadoke et al. 2005) and improves outcome of atherosclerosis and myocardial infarction (McSweeney, Hadoke et al. 2010; Kipari, Hadoke et al. 2013). However, 11β-HSD1 deficiency increases the severity of acute inflammation and worsens outcome in K/BxN serum induced arthritis (Coutinho, Gray et al. 2012). Macrophages were suggested to play a role in these processes. For example, 11β-HSD1 deficient mice have more YM-1^{+} macrophage infiltration after myocardial infarction (McSweeney, Hadoke et al. 2010), fewer macrophages in the atherosclerosis plaque area (Kipari, Hadoke et al. 2013) and delayed acquisition of macrophage phagocytosis (Gilmour, Coutinho et al. 2006). However, these experiments do not distinguish between cause and effect. Given the wide range of 11β-HSD1 expression (Whorwood, Sheppard et al. 1993; Tomlinson, Walker et al. 2004), it is hard to distinguish the contribution of different cells in a particular model. In addition, a role for changed HPA axis activity or regulation, shown to be dependent on mouse genetic background, in globally 11β-HSD1 deficient mice is not ruled out (Harris, Kotelevtsev et al. 2001; Carter, Tworowska et al. 2006; Carter, Paterson et al. 2009).

To avoid disturbance of HPA axis activity and dissect the function of 11β-HSD1 function in myeloid cells, cre/loxP recombination technology was introduced. In *LysM-Cre* mice, Cre expression is under the control of the *LysM* (*Lyz2*) promoter, which has been shown to be highly expressed in myeloid cells; mainly neutrophils and monocytes/macrophages (Clausen, Burkhardt et al. 1999). By crossing *LysM-Cre* mice with *Hsd11b1*$^{flox/flox}$ mice, *LysM-Cre Hsd11b1*$^{flox/flox}$ (MKO) mice were generated as part of a previous study (Zhang 2011), but were not characterized. In

this chapter, 11β-HSD1 deletion efficiency was examined in different sources of myeloid cells from MKO and control littermate mice by measuring levels of *Hsd11b1* mRNA, 11β-HSD1 protein and enzyme activity.

4.2 Aim

To determine efficiency of 11β-HSD1 deletion in different populations of myeloid phagocytes in MKO mice.

4.3 Results

4.3.1 Thioglycollate elicited peritoneal cells from MKO mice show reduced *Hsd11b1* mRNA levels but no corresponding reduction in 11β-HSD1 protein or enzyme activity levels.

To determine whether *Hsd11b1* mRNA levels were reduced as predicted in myeloid cells of MKO mice, peritoneal cells were lavaged 24h after intraperitoneal (i.p.) thioglycollate (TG) injection (when neutrophils and monocytes/macrophages are the majority of the population), or 96h after TG injection (when macrophages are the majority population, >95%). Additionally, as *LysM-Cre* mediated recombination is reported to be ~100% in neutrophils (Clausen, Burkhardt et al. 1999), neutrophils purified from peritoneal cells lavaged 24h after TG injection were examined as well.

Compared to littermate control 'floxed' mice, MKO mice showed an 81% reduction in *Hsd11b1* mRNA in peritoneal macrophages lavaged 96h after TG injection (Figure 4-1A) and a 71% reduction in peritoneal cells lavaged 24h after TG injection (Figure 4-1B). In the purified neutrophils, there was 83% reduction in *Hsd11b1* mRNA levels (Figure 4-1C).

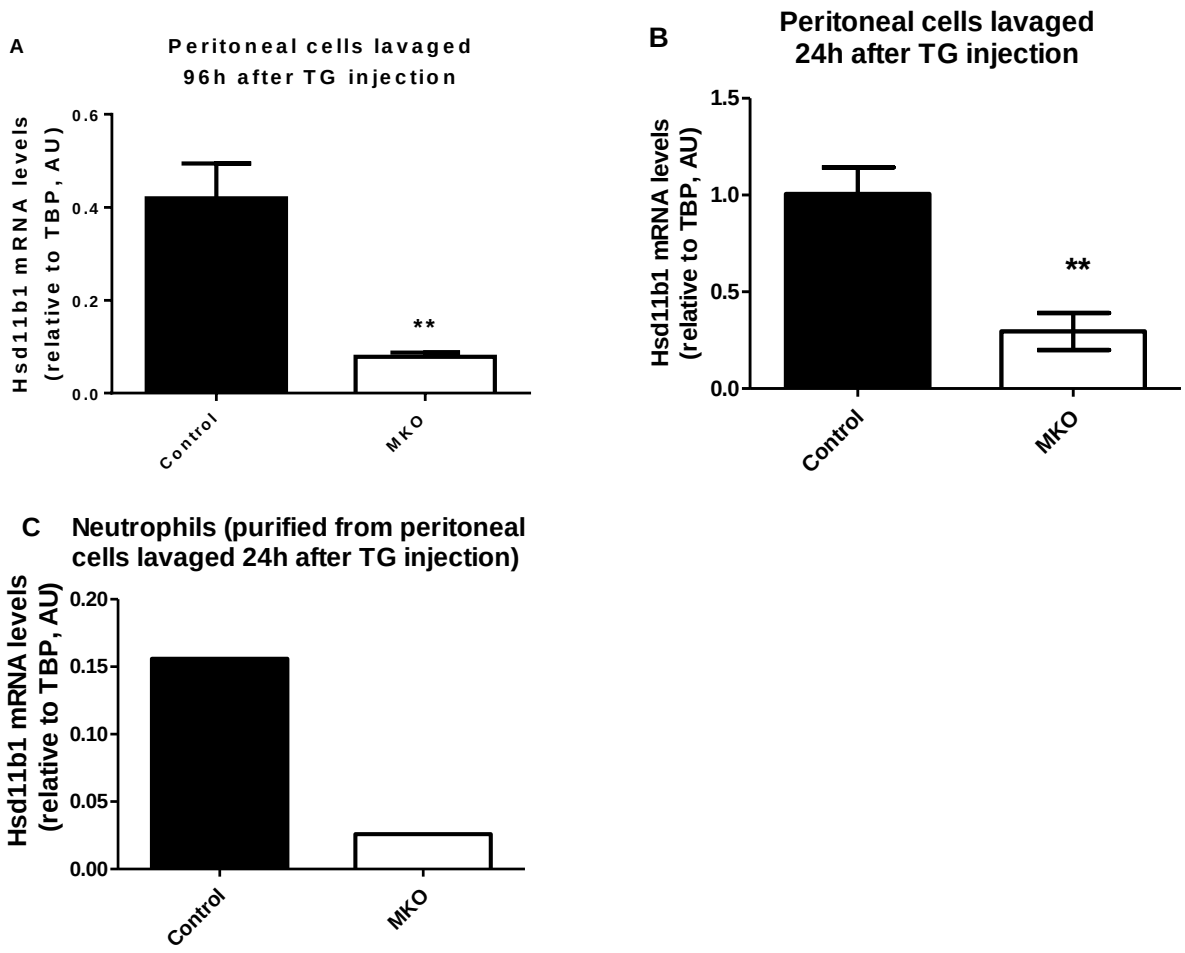

Figure 4-1 *Hsd11b1* mRNA levels are reduced in TG elicited myeloid cells from MKO mice.

*Hsd11b1*mRNA levels were measured by qPCR, with TBP mRNA as internal control. (A) In peritoneal cell lavaged 96h after TG injection, there were lower *Hsd11b1* mRNA levels in the MKO group than 'floxed' littermate controls (** $p<0.01$, unpaired t-test, n=4-5/group). (B) In peritoneal cells lavaged 24h after TG injection, there was a significant reduction in *Hsd11b1* mRNA levels of MKO mice ($p<0.01$, unpaired t-test, n=6 in each group). (C) In the neutrophils, a reduction was also observed, although the n number in the MKO group was 2 (n=3 in control group), too few for statistical test. Data are means ± SEM.

To determine whether reduced *Hsd11b1* mRNA levels were associated with decreased 11β-HSD1 enzyme activity, enzyme activity assays were conducted in myeloid cells from MKO and control mice. Samples were the same as above, including peritoneal macrophages lavaged 96h after TG injection (Figure 4-2A), peritoneal cells lavaged 24h after TG injection (monocytes and neutrophils, Figure 4-2B) and neutrophils purified from total peritoneal cells at 24h (Figure 4-2C). Surprisingly, there was no difference in 11β-HSD1 enzyme activity levels between the 2 genotypes in the macrophage and neutrophil groups. However, a modest decrease was observed at one time point of the assay in the mixed cell population lavaged at 24h.

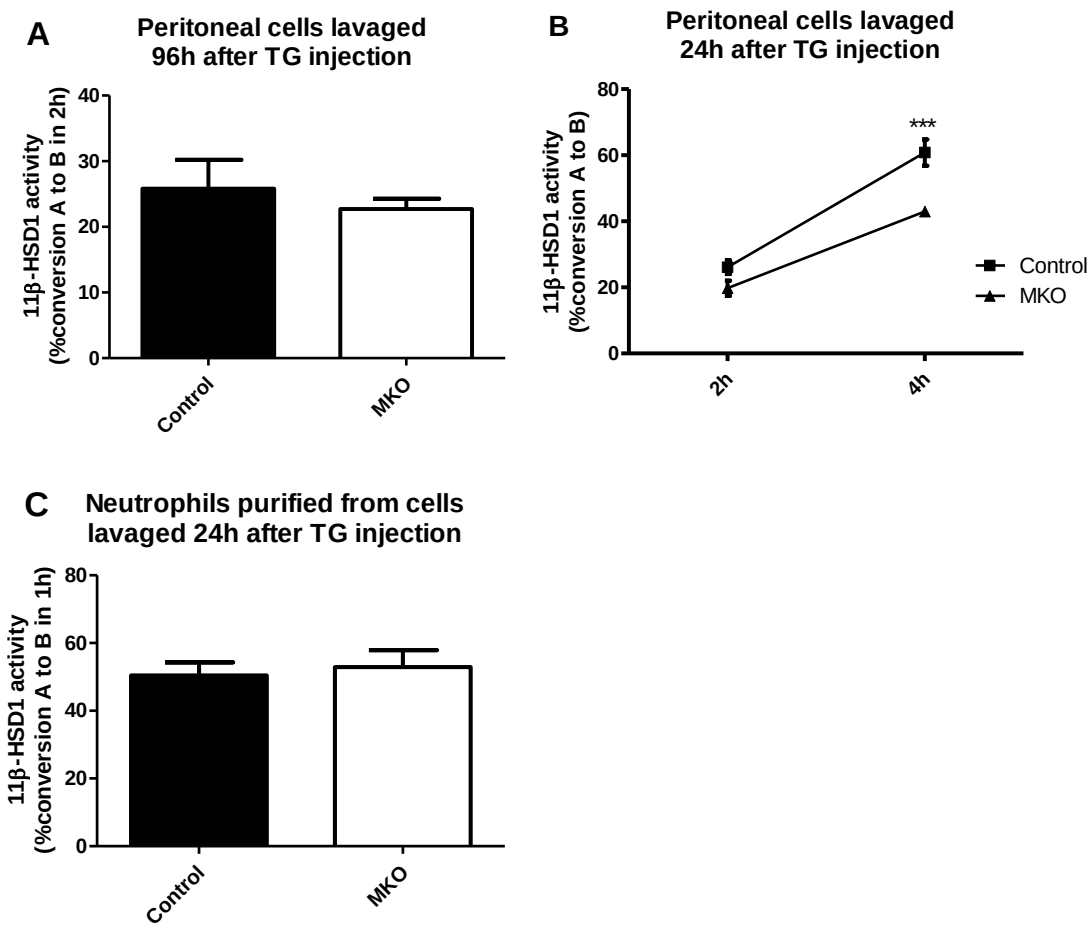

Figure 4-2 11β-HSD1 reductase activity did not differ between TG elicited myeloid cells from MKO and control mice.

11β-HSD1 activity was measured by the conversion of ^{3}H-11-dehydrocorticosterone (B) to ^{3}H-corticosterone (A) in the medium by intact cells. (A) In peritoneal macrophages lavaged 96h after TG injection, there was no significant difference in 11β-HSD1 reductase activity levels between MKO and control mice ($p=0.43$, unpaired t-test, $n=4$ in the control group and $n=8$ in the MKO group). (B) In repeated samplings of the culture medium during the enzyme activity assay of peritoneal cells lavaged 24h after TG injection, 2 way repeated measurement ANOVA showed a significant interaction between genotypes and time. Bonferroni post-test showed significant difference at the 4h time point, but not at the 2h time point. ($n=4$ in each group). (C) In the purified neutrophils, there was no significant difference in 11β-HSD1 reductase activity levels ($p=0.72$, unpaired t-test, $n=3$/group). Data are means ± SEM.

To address the discrepancy between reduced *Hsd11b1* mRNA levels and nearly normal 11β-HSD1 enzyme activity levels in TG elicited myeloid cells form MKO mice, the encoded 11β-HSD1 protein levels were measured. Western blotting of 11β-HSD1 showed 33% reduction in peritoneal macrophages lavaged 96h after TG injection (Figure 4-3A), 31% reduction in cells lavaged 24h after TG injection (Figure 4-3B) and 38% reduction in purified neutrophils (Figure 4-3C), although the difference in neutrophils is not significant, likely due to small n number (n=3).

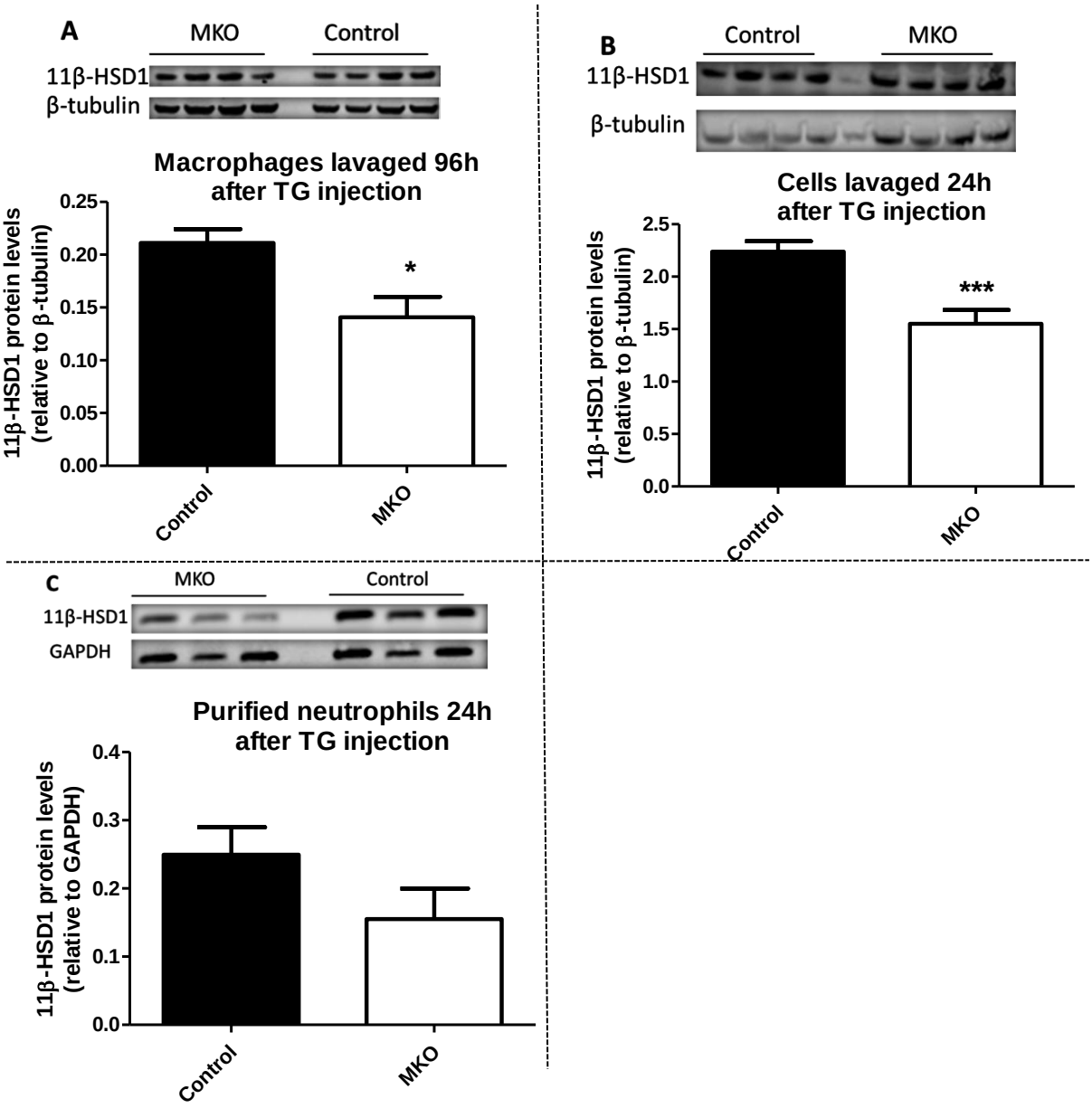

Figure 4-3 11β-HSD1 protein levels were decreased modestly in TG elicited myeloid cells of MKO mice.

Western blotting was used to measure 11β-HSD1 protein levels, relative to β-tubulin or GAPDH. (A) 11β-HSD1 protein levels were reduced in peritoneal macrophages lavaged 96h after TG injection in MKO mice, compared to controls (* $p<0.05$, unpaired t-test, n=4 in each group). (B) 11β-HSD1 protein levels were reduced in peritoneal cells lavaged 24h after TG injection in MKO mice, compared to controls (*** $p<0.001$, unpaired t-test, n=4 in each group). (C) There was a trend to reduced levels of 11β-HSD1 protein in purified neutrophils

from MKO mice, but did not achieve significance (p=0.19, unpaired t-test, n=3 in each group). Data shown are means ± SEM.

4.3.2 Cre protein is expressed in peritoneal cells lavaged 24h after TG injection

The modest reduction in 11β-HSD1 protein levels of myeloid cells from MKO group was disappointing. To make sure that Cre protein is expressed in myeloid cells lavaged from MKO mice, western blotting of Cre protein was conducted. In a separate experiment, peritoneal cells lavaged 24h after TG injection were harvested from MKO and control mice. Although several bands appeared, a band unique to the MKO group of the correct size of Cre protein (38kDa) was present in the MKO group (Figure 4-4).

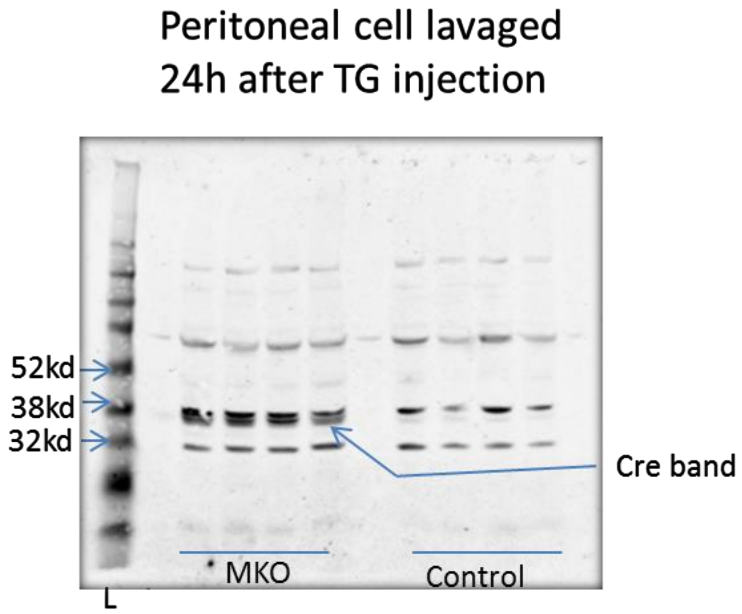

Figure 4-4 Cre protein is expressed in MKO peritoneal myeloid cells lavaged 24h after TG injection in MKO group.

Western blotting was done to detect Cre protein. Each lane contains 20μg protein from one mouse. The left lane ('L') contains a protein ladder with 3 sizes marked. Arrow indicates a band of the right size for Cre, which is present in the MKO group, but not in the control group. Predicted Cre protein size is 38kDa.

4.3.3 Moderate deletion efficiency in day 7 bone marrow derived macrophages from MKO mice

The absence of the expected reduction in 11β-HSD1 enzyme activity in TG elicited myeloid cells from MKO mice was puzzling. Therefore, another population of macrophages was examined: bone marrow derived macrophages (BMDM, day 7). BMDMs from MKO mice showed a trend for a 45% reduction in *Hsd11b1* mRNA levels (Figure 4-5A) and 54% reduction in 11β-HSD1 enzyme activity levels (Figure 4-5B).

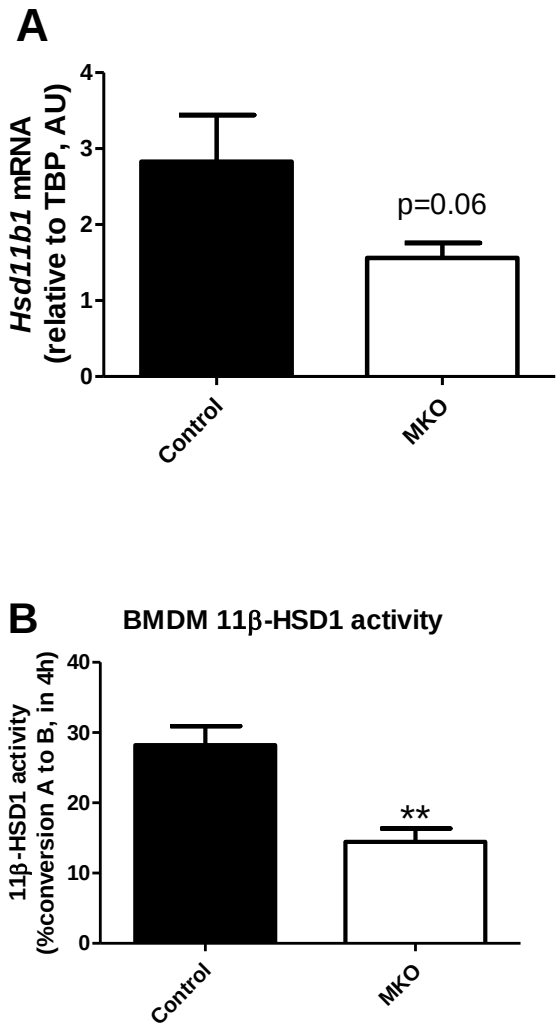

Figure 4-5 11β-HSD1 activity was reduced in BMDMs from MKO mice, compared to Cre$^-$ littermate controls.

Level of *Hsd11b1* mRNA was measured by qPCR and 11β-HSD1 enzyme activity was measured by conversion of ^{3}H-11-dehydrocorticosterone (B) to ^{3}H-corticosterone (A) in the medium by intact cells. (A) *Hsd11b1* mRNA showed a trend of 45% reduction in the MKO group (n=5-6, no significant difference, unpaired t-test with Welch's correction). (B) 11β-HSD1 enzyme activity was reduced by 54% in BMDMs from MKO group (n=5-6, ** $p<0.01$, unpaired t-test). Data are means ± SEM.

4.3.4 11β-HSD1 protein is reduced by ~50% in TG elicited macrophages from *LysM-Cre Hsd11b1*$^{del/flox}$ (MKO/Δ) mice

The poor deletion efficiency observed in the above experiments may be due to insufficient Cre-mediated recombination. To try to improve this, *LysM-Cre Hsd11b1*$^{del/flox}$ (MKO/Δ) mice (with one 'floxed' and one null allele of *Hsd11b1*) were generated by crossing *LysM-Cre Hsd11b1*$^{flox/flox}$ mice with *Hsd11b1*$^{del/del}$ mice. However, western blotting on peritoneal macrophages lavaged 96h after TG injection showed that there was still ~50% 11β-HSD1 protein expression remaining in macrophages from MKO mice compared to controls (Figure 4-6). The experiment was repeated a second time, with similar results.

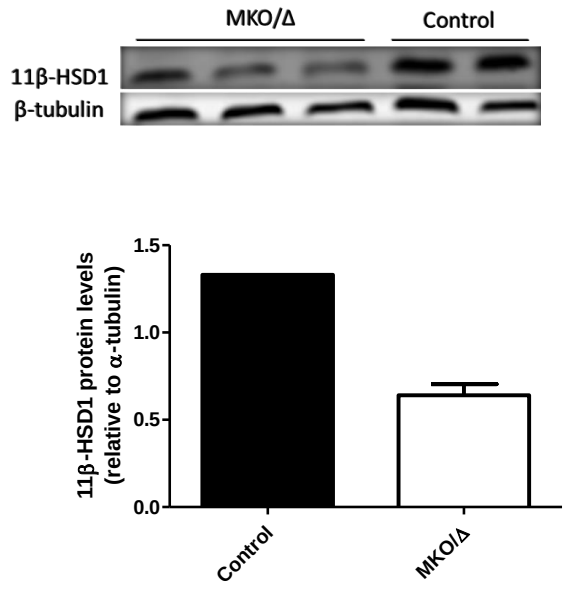

Figure 4-6 11β-HSD1 protein levels in MKO/Δ mice were reduced by ~50% in peritoneal macrophages lavaged 96h after TG injection.

Western blotting was done to detect 11β-HSD1 protein in macrophage homogenates. In the picture, 11β-HSD1 protein is clearly visible in MKO/Δ mouse samples. Each lane contained 30μg of protein from one mouse. Data shown are the mean of the control group and mean ± SEM of the MKO group (n=2 and 3, respectively).

To address whether the observed ~50% reduction in MKO/Δ mice simply reflects loss of an allele of *Hsd11b1*, 11β-HSD1 protein and *Hsd11b1* mRNA levels were measured in *Hsd11b1*$^{del/+}$ heterozygous mice and control 'floxed' mice. In peritoneal cells lavaged from *Hsd11b1*$^{del/+}$ heterozygous mice 24h after TG injection, there was ~50% reduction in *Hsd11b1* mRNA levels and 11β-HSD1 protein levels (data not shown). This confirms the lack of efficient *LysM-Cre* mediated deletion of 11β-HSD1 protein and rules out post-translational regulation of 11β-HSD1 protein to increase 11β-HSD1 protein expression in myeloid cells as the source of discrepancy between *Hsd11b1* mRNA and 11β-HSD1 enzyme activity levels.

4.3.5 11β-HSD1 enzyme activity is markedly reduced in resident peritoneal macrophages from MKO mice.

Previous studies using siRNA to reduce *Hsd11b1* expression *in vitro* (Bujalska, Draper et al. 2005; Aubry and Odermatt 2009) showed a similar discrepancy between mRNA and 11β-HSD1 protein expression to that observed here, in TG-elicited myeloid cells from MKO mice. A long half-life of 11β-HSD1 protein was suggested to account for this (Aubry and Odermatt 2009). It was reasoned that the discrepancy between *Hsd11b1* mRNA and 11β-HSD1 protein in the current study was because of a recent Cre-mediated recombination of *Hsd11b1* gene, sufficient to decrease mRNA, but not the long-lived 11β-HSD1 protein in short-living circulating myeloid cells. Therefore, the long-lived resident peritoneal macrophage population was chosen to measure 11β-HSD1 protein and enzyme activity in MKO mice.

In a pilot experiment, it was found that 11β-HSD1 protein was undetectable in resident peritoneal macrophages from a single MKO mouse (Figure 4-7A). The limited cell number (about 1 million) obtained from each mouse and the method of collecting macrophages (which attach firmly in the tissue culture plate during the purification process) constrained amount of concentrated proteins for western blotting study. Instead, 11β-HSD1 enzyme activity was examined in these cells. As 11β-HSD1 activity in resident macrophages is much lower than in TG elicited myeloid cells, a 20h assay time was used. It was evident that 11β-HSD1 enzyme activity was greatly reduced in MKO mice, compared to the littermate controls (Figure 4-7B and C).

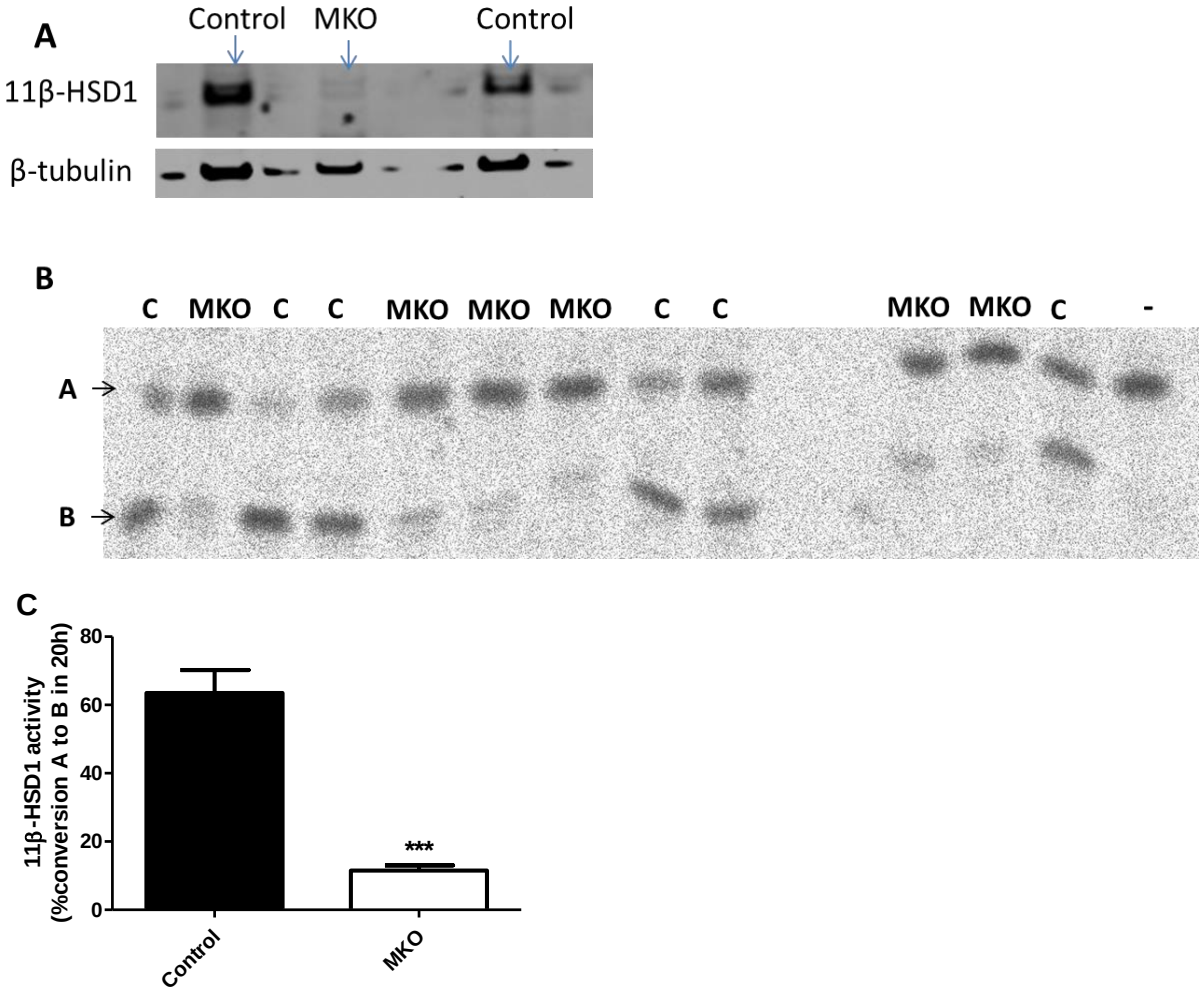

Figure 4-7 11β-HSD1 enzyme activity is markedly reduced in resident peritoneal macrophages from MKO mice.

(A) Western blotting showed a lack of immuno-reactive 11β-HSD1 in resident peritoneal macrophages from a naïve MKO mouse. Each lane contains ~10 µg protein from one mouse. Only the 3 labelled lanes were loaded. (Because the maximum volume was loaded into the wells, sample overload caused spillage into neighbouring wells.) (B) Image of the phosphorimager tritium image screen showed little or no conversion of 11-dehydrocorticosterone (A) to corticosterone (B) by resident peritoneal macrophages from MKO mice. 'C', control; '-', no cells. Each lane represents one mouse except for the lane marked as '-'. (C) Quantification of 11β-HSD1 activity shown in (B) showed 82% reduction in MKO macrophages, compared to those from littermate controls (unpaired t-test, n=6, *** $p<0.0001$).

To examine other tissue resident macrophages, 11β-HSD1 western blotting was carried out in alveolar macrophages and adipose stromal vascular cells (SVCs) from naïve mice. However, no 11β-HSD1 protein was detectable in alveolar macrophages, even in control mice (Figure 4-8A). In macrophages harvested from adipose SVCs ($CD11b^+$ population), there did not appear to be an obvious decrease in 11β-HSD1 protein levels (Figure 4-8B). Limited cell number constrained protein harvest in both cases and anti-β-tubulin antibody failed to work in the SVC experiment.

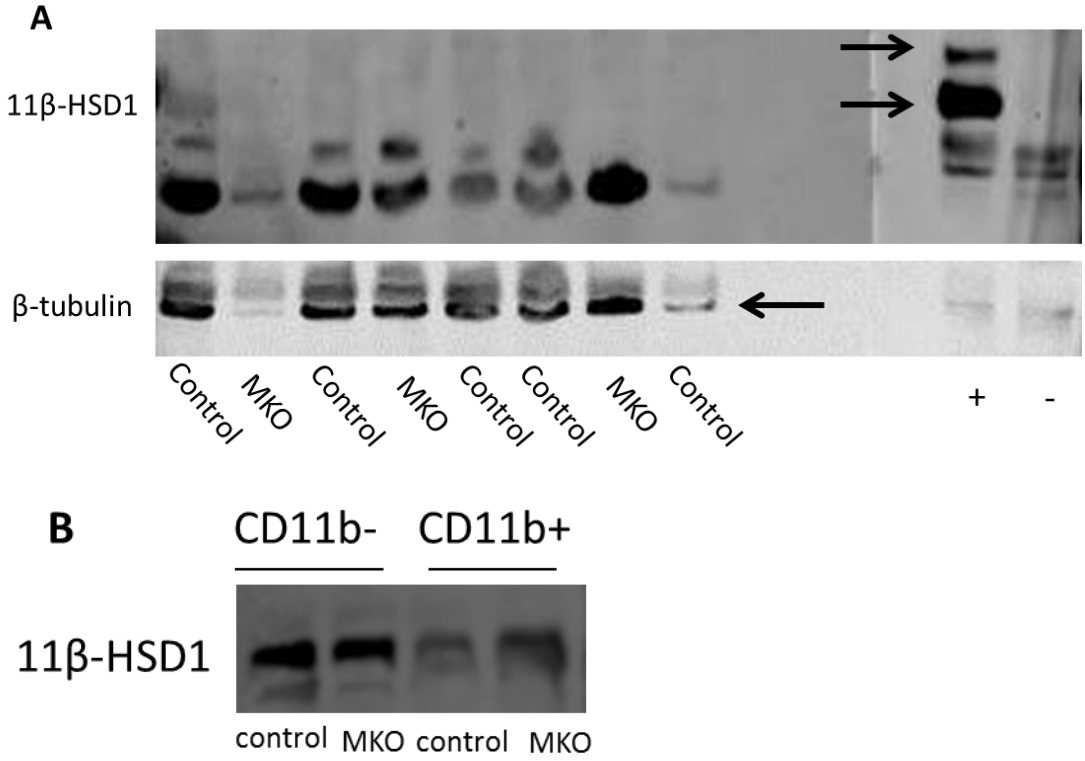

Figure 4-8 11β-HSD1 protein was undetectable in alveolar macrophages from either control or MKO mice and the expression levels in macrophages in the adipose SVCs of MKO mice were not obviously different to those controls.

(A) Comparison to the positive control (wild-type lung total protein sample; '+') and negative control (*Hsd11b1*$^{del/del}$ lung total protein sample; '-') showed that 11β-HSD1 was undetectable in alveolar macrophages from either MKO or control mice. Each lane contains ~10μg of protein and represents one mouse. Arrows indicate the bands of target proteins. For 11β-HSD1, there are 2 bands detected with the lower band as glycosylated form of 11β-HSD1. (B) In neither $CD11b^+$ nor $CD11b^-$ cells isolated from adipose SVCs, 11β-HSD1 protein levels were obviously decreased in MKO mice. However, failure to detect β-tubulin confounded the interpretation of this experiment. Each sample was obtained by pooling SVCs from 2 or 3 mice of the same genotype.

4.4 Discussion

In this line of MKO mice, it is likely that there is good Cre-mediated *Hsd11b1* recombination at the genomic level in target cells, reflected by ~80% reduction in *Hsd11b1* mRNA levels in macrophages lavaged 96h after TG injection, as well as total peritoneal cells lavaged 24h after TG injection and in purified neutrophils. However, 11β-HSD1 protein and enzyme activity were reduced by less than 50% at best in these cells. In contrast, substantial reduction in 11β-HSD1 protein and enzyme activity levels was observed in resident peritoneal macrophages.

The possible discrepancy between *Hsd11b1* mRNA and encoded protein expression in the TG-elicited myeloid cells was first attributed to a post-transcriptional regulation mechanism, to maintain normal levels of 11β-HSD1 protein in response to reduced *Hsd11b1* mRNA levels. However, the fact that myeloid cells from heterozygous *Hsd11b1* globally knockout mice (*Hsd11b1*$^{del/+}$) contain approximately half the levels of *Hsd11b1* mRNA and encoded protein of the control 'floxed' mice does not support this.

An alternative explanation for the discrepancy between *Hsd11b1* mRNA and 11β-HSD1 protein levels in TG elicited myeloid cells is the long half-life of 11β-HSD1 protein. A similar persistence in 11β-HSD1 enzyme activity was described in mouse C2C12 myotubes, following down-regulation of *Hsd11b1* mRNA by incubation with retinoic acid (Aubry and Odermatt 2009). Similarly, when siRNA was used to knock down *HSD11B1* in HEK 293T1 cells, despite >52% reduction in *HSD11B1* mRNA, 85% of 11β-HSD1 enzyme activity remained (Bujalska, Draper et al. 2005). The half-life of *Hsd11b1* mRNA in 3T3-L1 adipocytes is reported to be 21h under basal conditions (Balachandran, Guan et al. 2008), but so far, little information about 11β-HSD1 protein half-life is available to my knowledge. In a proteomics study after 6 month of protein labelling with N^{15} (Toyama, Savas et al. 2013), 11β-HSD1 scored the top 5% in terms of being "exceptionally long lived" (personal communication, Dr. Jeffrey N. Savas, Lab of John Yates, Scripps Institute, the US). The half-life of myeloid cells in *vivo* is another factor to consider. For TG elicited myeloid cells and circulating myeloid cells, the rapid clearance *in vivo* probably constrains the

observation of protein decrease. For example, the half-life of circulating neutrophils is reported to be about 6-8 hours in one report (Summers, Rankin et al. 2010).

It is puzzling that there was little reduction in 11β-HSD1 enzyme activity levels in neutrophils and macrophages from MKO mice than control mice, albeit ~30% decrease in 11β-HSD1 protein levels. Moreover, enzyme activity was modestly reduced in peritoneal cells lavaged 24h after TG injection at 4h of the assay but not at 2h. In the case of cells lavaged 24h after TG injection, monocytes and neutrophils are in the majority, it is likely that during the assay, 11β-HSD1 expression was synthesised *de novo* in the control but not the MKO group. It is known that monocytes up-regulate 11β-HSD1 expression during differentiation into macrophages (Thieringer, Le Grand et al. 2001; Gilmour, Coutinho et al. 2006). This could be the reason for the difference of activity assay at 4h but not at 2h. Alternatively, the 'missed' difference in enzyme activity assay may be due to limited n number (n=3 -8) and big intra-group variance. With hindsight, it is realised that small n number usually used in the literature is enough for detecting the expected big difference (>80%, for example) but has limited power to uncover small differences. However, even if there was a 30% difference in enzyme activity levels between MKO and controls, this small decrease probably would not produce a phenotype in the macrophages.

The poor deletion efficiency of target genes by *LysM-Cre* has been described previously. The original paper described very high deletion efficiency in the LysM-Cre mice, but it is of note that the method they used to detect target gene expression change was only southern blotting. For the 2 tested target genes, deletion efficiency was lower for one than the other. An on-going deletion process was found in bone marrow derived macrophages (Clausen, Burkhardt et al. 1999). This may explain the observation of about 50% deletion of *Hsd11b1* mRNA and11β-HSD1 protein in BMDMs from MKO mice. Other researchers have noted varying efficiency of *LysM-Cre* mediated gene 'knock-out' in different monocyte/macrophage populations. By examining *LysM-Cre ROSA26-GFP* mice, it was found that there was 80% deletion of the target gene in resident peritoneal macrophages but only about 50% in TG

elicited ones (day 3) and BMDMs (from day 1 and day 7) by flow cytometry examination ((Osterreicher, Penz-Osterreicher et al. 2011)). In another study, researchers crossed *LysM-Cre* mice with *ROSA26*STOP*DTR (DTR, diphtheria-toxin receptor) mice, aiming to specifically deplete macrophages after DT administration. When DT was administered to the *LysM*-Cre/DTR mice, it was only the resident macrophages (such as those in the skin and liver) that were markedly reduced, not the circulating monocytes (Goren, Allmann et al. 2009). Comparison of *LysM* and *Cre* mRNA expression showed higher levels of both in $CD11b^{+}$, $F4/80^{high}$ macrophages than in the $CD11b^{+}$, $Lys6C^{high}$ monocyte precursors. This suggests that *LysM-Cre* expression increases with the maturation of monocytes and macrophages.

Why is good deletion efficiency achieved in resident peritoneal macrophages? In a recent study, resident macrophages from different anatomical sites (brain, liver, lung and peritoneal cavity) were examined by microarray. Interestingly, *Lyz2* (*LysM*) is found to be expressed at markedly higher levels in resident peritoneal macrophages than in all the other tissue resident macrophages (Gautier, Shay et al. 2012). This may explain the high deletion efficiency of 11β-HSD1 activity in resident peritoneal macrophages.

It remains to be investigated whether other tissue resident macrophages have good 11β-HSD1 deletion in MKO mice or whether some of them do not express 11β-HSD1. 11β-HSD1 seems to be expressed in different levels among different populations of tissue resident macrophages. There is no 11β-HSD1 protein detected from alveolar macrophages in the current study, although low levels of *Hsd11b1* mRNA have been detected previously, which may be due higher sensitivity of qPCR (Yang 2010). Immunohistology staining only detect very low 11β-HSD1 expression in adipose tissue macrophages (De Sousa Peixoto, Turban et al. 2008) or in microglial cells (personal communication, Miss Mei Xuan Lye, University of Edinburgh). Weak enzyme activity in peritoneal resident macrophages found in this study is similar to what was reported in a previous study (Gilmour, Coutinho et al. 2006). Whether adipose tissue SVC macrophages are tissue resident macrophage or

bone marrow derived macrophages are not defined yet (personal communication, Frederic Geissman, King's College of London).

Different to tissue resident macrophages, TG-elicited peritoneal macrophages are bone marrow derived macrophages (Van Furth, Diesselhoff-den Dulk et al. 1973). Peritoneal macrophages lavaged after TG injection are generally thought to be not fully activated in the first instance. Accordingly, they are usually further stimulated with LPS, etc. to study macrophage polarisation (Usher, Duan et al. 2010).

The attempt to achieve better deletion in *LysM-Cre Hsd11b1l*$^{flox/\Delta}$ mice is not successful, although this method was shown to work well for other target genes (Huang, Perlman et al. 2010). With hind sight, Cre deletion efficiency does not appear to be the problem in the MKO mice; instead, it is likely to be owing to that 11β-HSD1 protein has a long half-life, relative to that of the circulating myeloid cells.

In summary, macrophage-specific 11β-HSD1 knockout is achieved in peritoneal resident macrophages, but not in TG-elicited myeloid cells in MKO mice. These mice will be therefore suitable to assess the role of 11β-HSD1 in certain tissue resident macrophages in inflammation, but may not be suitable for the investigation of 11β-HSD1 in inflammatory cells recruited from bone marrow during acute inflammation. Moreover, in inflammatory models such as wound healing, diet induced obesity, atherosclerosis and K/BxN serum induced arthritis, inflammation evolves in a much longer time period with possible involvement of resident macrophages and thus these models may be suitable to study the effect of 11β-HSD1 deficiency on macrophage function in MKO mice.

Chapter 5: Increased angiogenesis in macrophage-specific 11β-HSD1 knockout MKO mice

5.1 Introduction

Angiogenesis is a process of capillary branching formation from big blood vessels. It is important in both embryo development and tissue remodelling to ensure an appropriate supply of oxygen and nutrition. It is a rigorously regulated process, as either inadequate (as in ischemic diseases) or excess (as in tumour growth) blood vessel growth poses a threat to the body. Glucocorticoids (GCs) have been shown to effectively inhibit angiogenesis (Folkman, Langer et al. 1983). Local amplification of GC action by 11β-HSD1 is also demonstrated to assert a negative role on angiogenesis, demonstrated in globally 11β-HSD1 deficient mice (Small, Hadoke et al. 2005).

The cell type responsible for increased angiogenesis in globally 11β-HSD1 deficient mice has not been identified. By qPCR in different parts of the mouse aorta, *Hsd11b1* was shown to be localised in the smooth muscles and the adventitial tissues (where macrophages and other cells resides), but not in endothelial cells (Christy, Hadoke et al. 2003). Later, immunohistology staining showed that 11β-HSD1 was in endothelial cells (Gong, Morris et al. 2008; Luo, Thieringer et al. 2013). But the existence of 11β-HSD1 in endothelial cells is still controversial, as 11β-HSD2 is expressed there and 11β-HSD1 and 11β-HSD2 rarely co-localise (Hadoke, Macdonald et al. 2006; Hadoke, Kipari et al. 2013). Specificity of 11β-HSD1 antibodies for immunohistology is another concern (Coutinho 2009; Liu, Srikant et al. 2011).

As mentioned in the Section 1.1.3 and 1.4.3, inflammation is closely associated with angiogenesis and changed macrophage polarisation was indicated in previous angiogenesis studies on globally 11β-HSD1 deficient mice (McSweeney, Hadoke et al. 2010). To dissect the contribution of resident macrophage 11β-HSD1 deficiency to the increased angiogenesis phenotype in globally *Hsd11b1* deficient mice,

angiogenesis was studied in MKO mice using a model of subcutaneous (s.c.) sponge implantation.

5.2 Hypothesis

Myeloid cell 11β-HSD1 ablation increases angiogenesis *in vivo*.

5.3 Results

5.3.1 Blood vessel formation in the sponge implantation model on MKO and control mice.

To investigate the role of myeloid cell 11β-HSD1 in angiogenesis, MKO and control mice were subjected to s.c. sponge implantation. In the experiment, one piece of sponge was inserted subcutaneously in each flank. After 21 days, sponges were removed for analysis, one for histology and the other for RNA extraction. The colour of sponges is indicative of haemoglobin content and thus blood vessel number (Yoshida, Amano et al. 2003). Although images of fresh sponges were not taken, Figure 5-1 shows images of sponges in the paraffin blocks. The gross appearance of the sponge shows that those from MKO mice display a darker colour than those from control mice. One globally 11β-HSD1 knockout mouse ('Del I') was included in the experiment for comparison.

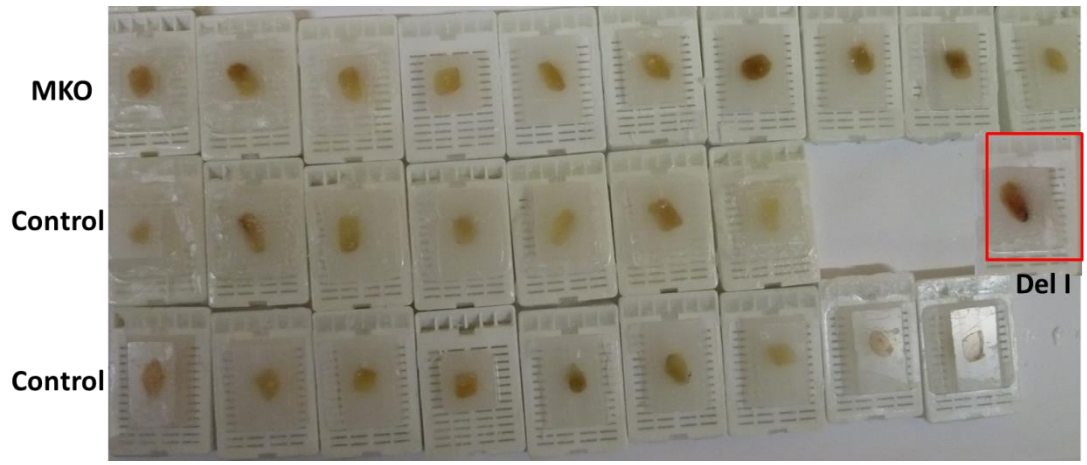

Figure 5-1 Representative images of sponges from MKO and control mice in paraffin blocks.

Samples in the first row are from MKO mice, with those in the 2nd and 3rd row from control mice (except the one within a red box). Each block shows one sponge from one mouse. 'Del I', globally 11β-HSD1 knockout mouse.

5.3.2 Increased angiogenesis in sponges from MKO mice.

To visualise blood vessels in the sponges, H&E staining was carried out on paraffin sections. Circle or tube-like shaped structures usually with red blood cells inside were considered to be blood vessels. Chalkley counting was performed to count the number of blood vessels, blind to genotype, as described in Section 2.16. As shown in Figure 5-2A, blood vessel numbers are higher in MKO mice than in littermate controls. This was confirmed by measuring an endothelial cell specific marker, *Cdh5* (encoding VE-cadherin) (Figure 5-2B). Examples of H&E stained section are shown in Figure 5-2C.

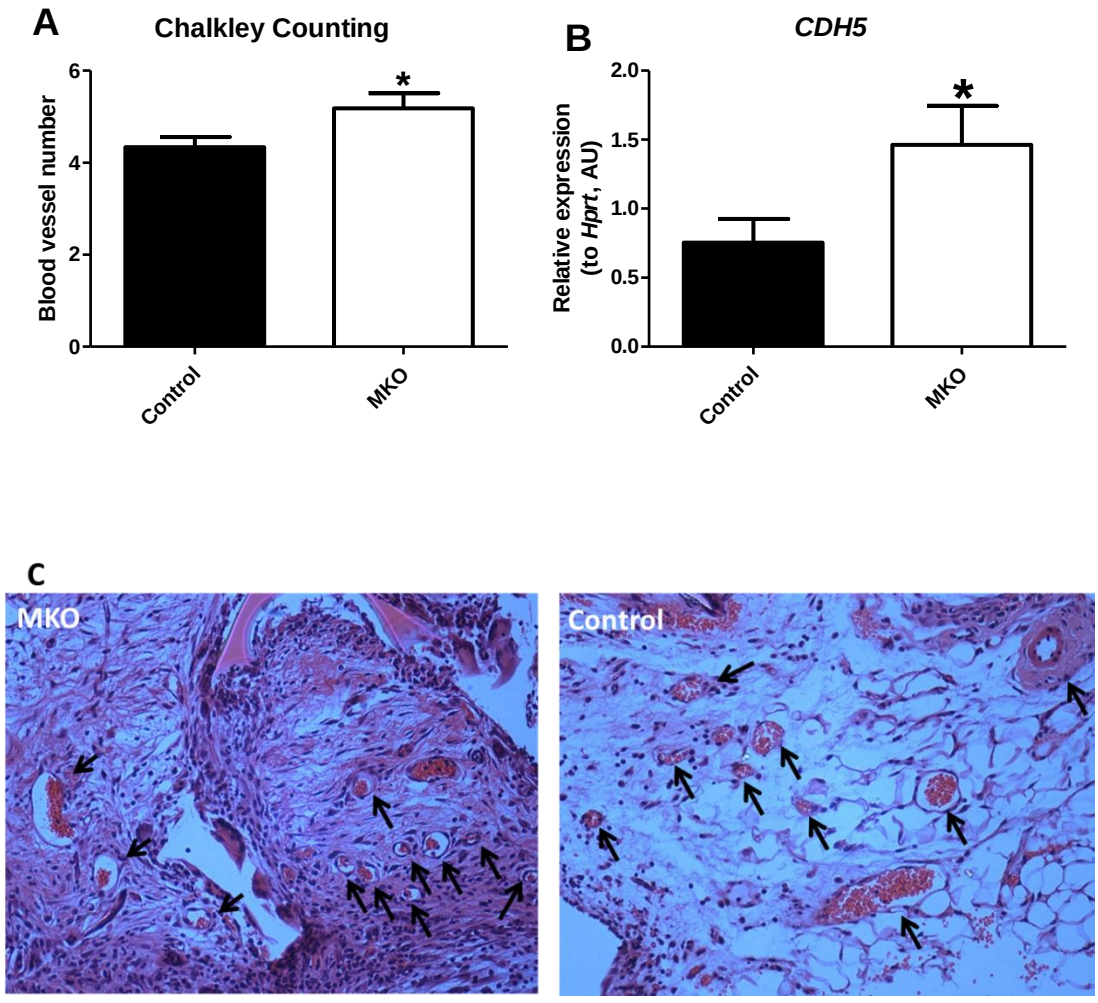

Figure 5-2 MKO mice show more angiogensesis than littermate controls.

(A) Chalkley counting on H&E stained sections of day 21 sponges showed more blood vessel formation in MKO mice than controls. Scoring was carried out blind to genotype and the average number of 6 fields from 2 sections was assigned to each sample. (B) *Cdh5* mRNA (encoding VE-Cadherin) levels were higher in sponges from MKO mice than controls. (C) Representive images of H&E stained sections of sponges from MKO and control mice, with blood vessels indicated by arrows. Data are means ± SEM and analysed by unpaired t-test, with significance set at $p<0.05$; *, $p<0.05$. N=9-11.

5.3.3 No difference in the cell proliferation marker *Ki67* or the angiogenic factor *Vegfa* between MKO and control mice

Increased cell proliferation (especially endothelial cells) may underline the increased blood vessel growth phenotype. However, measurement of mRNA encoding cell proliferation marker *Ki67* did not support this (Figure 5-3A).

VEGF and angiopoietin are crucial regulators of endothelial cell proliferation and migration, and thus angiogenesis (Welti, Loges et al. 2013). The presence of both was examined by qPCR on RNA from the sponges. There was no difference in *Vegfa* mRNA levels between MKO and control groups (Figure 5-3B), although with a trend to higher angiopoietin RNA levels in the MKO group ($p=0.09$ for *Angpt1*, Figure 5-3C).

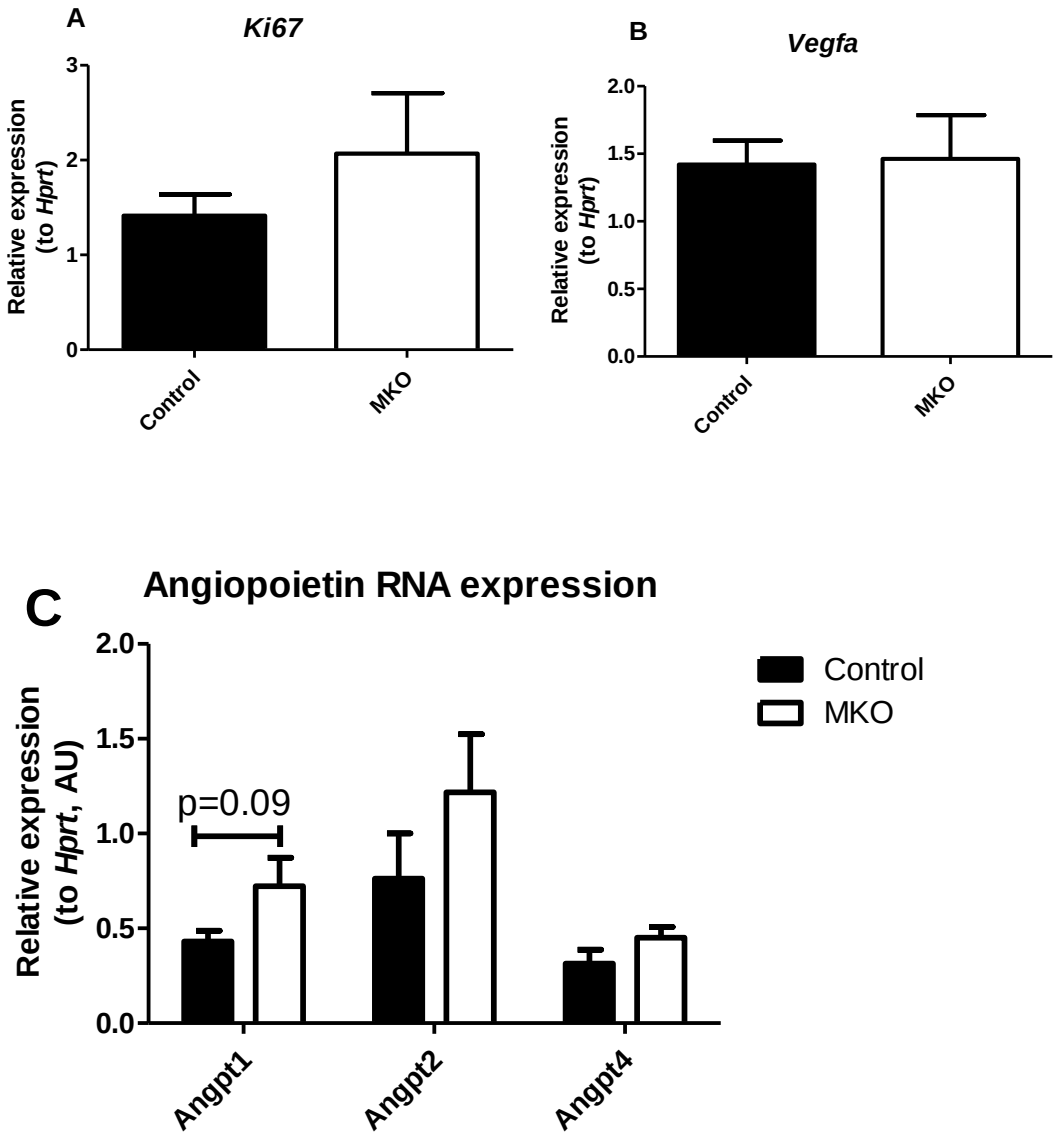

Figure 5-3 qPCR measurement of *ki67, Vegfa* and *Angpt1, 2* and *4* gene expression in MKO and control mice.

Expression of cell proliferation maker *Ki67* (A) and angiogenesis factors *Vegfa* (B) were similar between MKO and control mice. There was a trend to higher *Angpt1* mRNA levels in MKO mice, but not significant, the same as *Angpt2* and *Angpt4*. Data are means ± SEM, n=7-11 in each group. Data were analysed by unpaired t-test, or un-paired t-test with Welch's correction in case of *Angpt1*.

5.3.4 Higher *Il1b* and lower *Icam1* mRNA levels in sponge from MKO.

Because the sponge implantation model is usually considered to be an inflammation-driven model of angiogenesis (Zhang, Modi et al. 2012), inflammatory and other relevant gene expressions were examined. Of the inflammatory genes examined, only *Il1b* expression levels are significantly higher in the MKO group, and no difference is detected in *Il6*, *Ifng*, *Tnfa* or *Ccl5* expression levels (Figure 5-4A). No *Il12b* gene expression is detected. There is little difference in the relevant gene expression levels, such as hedgehog receptor *Patched*, anti-inflammatory *Tgfb1*, etc., except for lower *Icam1* in the MKO group (Figure 5-4B).

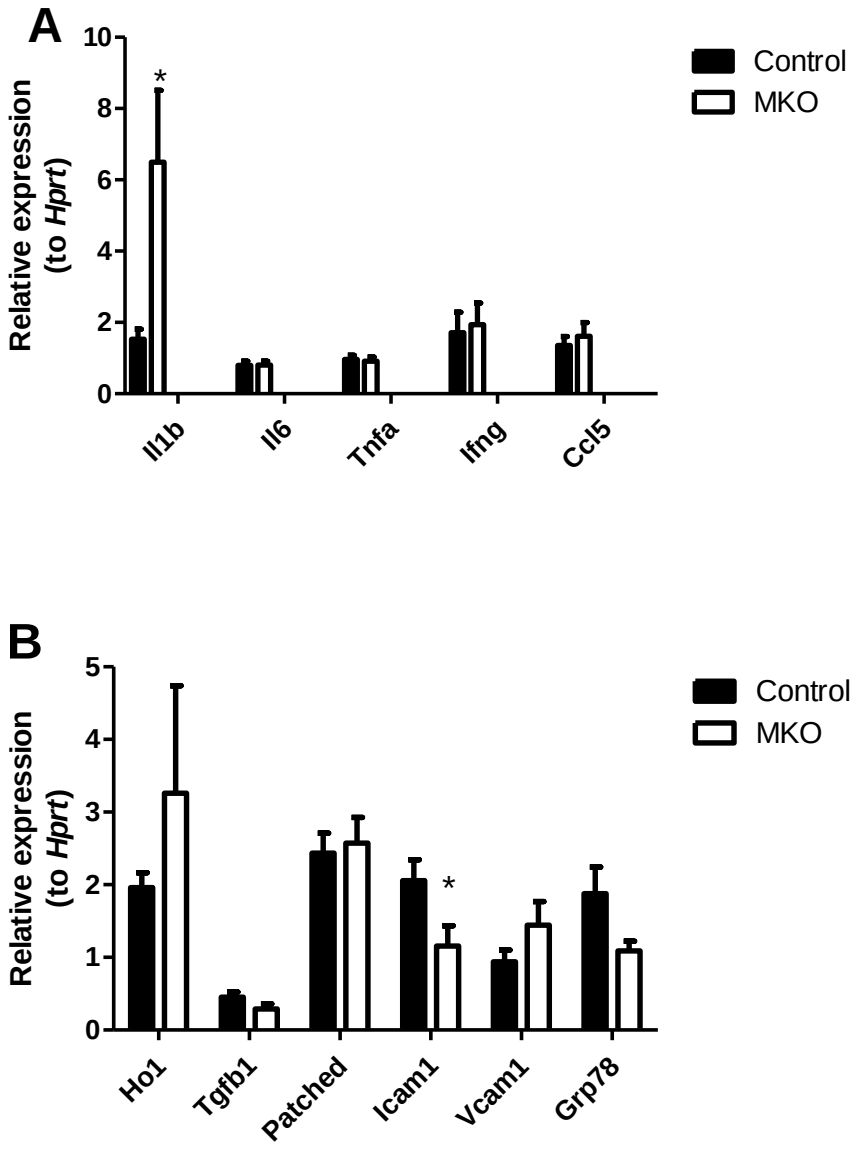

Figure 5-4 Increased *Il1b* and decreased *Icam1* mRNA levels in the sponges from MKO mice.

(A) qPCR measurement of *Il1b*, *Il6*, *Ifng*, *Tnfa* and *Ccl5* gene expression. (B) qPCR measurement of *Ho1*, *Tgfb1*, *Patched*, *Icam1*, *Vcam1* and *Grp78* expression. Data are means ± SEM, n=7-11. Each gene expression data are analysed by unpaired t-test individually to compare MKO and control groups with significance set at $p<0.05$; *, $p<0.05$. When the intergroup variance is not equal, un-paired t-test with Welch correction is used to analyse the data in the case of *Il1b* and *Ho1*.

5.3.5 Evidence for similar recruitment and alternative polarization state of macrophages in the sponges from MKO and control mice.

Inflammation is accompanied by immune cell infiltration. Given the previous evidence of changed inflammatory state in MKO mice (higher *Il1b* expression), macrophage number and polarisation were investigated by qPCR in the sponges from MKO and control mice. However, levels of macrophage marker *Cd68* mRNA was not different between genotypes (Figure 5-5), nor was expression of macrophage alternative polarisation status marker *Retnla* (Figure 5-5). *Ym1* mRNA was undetectable (data not shown).

Myeloid cell 11β-HSD1 ablation may result in decreased total *Hsd11b1* mRNA levels in the sponges from MKO mice. However, total *Hsd11b1* mRNA levels in the sponges did not differ between MKO and control groups (Figure 5-5C).

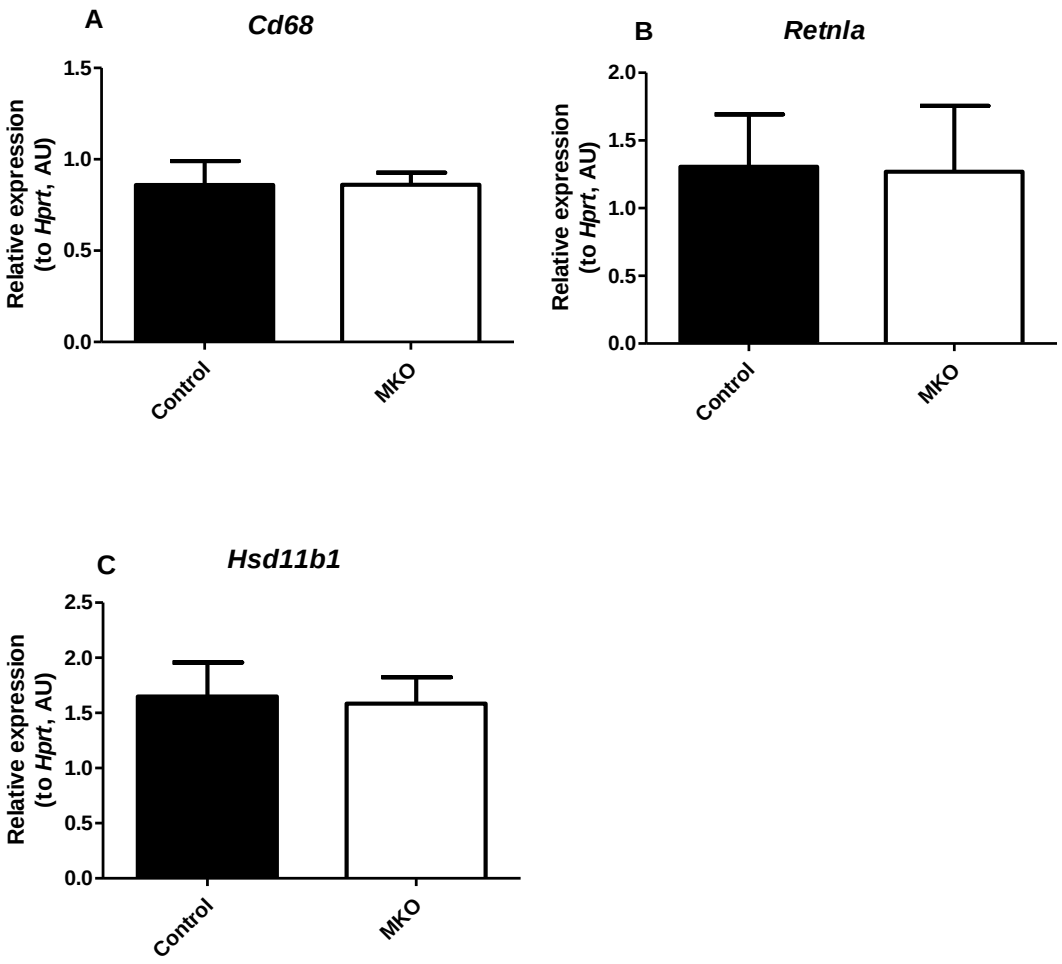

Figure 5-5 Macrophage markers are not different in mRNA levels between genotypes.

The pan-macrophage marker *CD68* (A), alternative polarisation state maker *Retnla* (B) and *Hsd11b1* mRNA levels (C) in the sponges were measured by qPCR. Data are means ± SEM, n=7-8. Data were analysed by unpaired t-test, with significance set at $p<0.05$.

5.4 Discussion

The s.c. sponge implantation experiment offered an *in vivo* insight into the role of macrophages in the increased angiogenic response of globally 11β-HSD1 deficient mice. As hypothesised, MKO mice showed increased angiogenesis in the sponge implantation model. These data highlight the important function of macrophage 11β-HSD1 in limiting angiogenesis. It contrasts with little effect of smooth muscle specific 11β-HSD1 ablation on angiogenesis in the same model (personal communication, Dr. Patrick Hadoke, University of Edinburgh).

The angiogenesis of sponge implantation is considered to be an 'inflammatory' model. It is a chronic granulomatous response accompanied by angiogenesis and infiltration of inflammatory cells. Molecules involved include VEGF, PDGF, IL-1β, TNF-α, TGF-β, fibroblast growth factor 2, NO, COX2 and angiotensin-converting enzyme, many of which are from macrophages (Alam 2008). Endogenous GCs generated by 11β-HSD1 inhibit this angiogenesis process (Small, Hadoke et al. 2005). When synthetic dexamethasone-loaded polyurethane implants were inserted in the sponge, reductions neovascularization, macrophage recruitment and collagen deposition were observed, with no change in neutrophil infiltration (Moura, Lima et al. 2011). Lack of GC signalling within macrophages of MKO mice may worsen acute inflammation. Higher *Il1* mRNA levels of MKO mice support this. However, there is no indication of a general difference in inflammation, as other inflammatory genes such as *Il6*, *Ifna* and *Tnfa* were not differently expressed. Validation of this at the protein level, using ELISA or western blotting would enhance this conclusion. However, attempts to do western blotting on whole sponge homogenates failed. Western blotting on cells isolated by collagenase digestion of the sponges may be helpful.

Study of the angiogenesis in more time windows, especially at earlier times, may help reveal possible gene expression differences. In an *in vivo* nemotade infection model, there are more alternative polarised macrophages in globally 11β-HSD1 deficient mice on day 8, but not later time points. Angiogenesis is controlled in a coordinated way. The early step of invasive capillary sprouting is induced by

VEGF/VEGF receptor and Notch/Notch ligand pathways. Subsequently, neurovascular guidance molecules (ephrins, slits, netrins, semaphorins) induce 3D vessel assembly and lumen formation. Maturation and vascular remodelling in the final stage of angiogenesis is controlled by angiopoietins, PDGF, and TGF-β families (Felcht, Luck et al. 2012). In past studies on globally 11β-HSD1 deficient mice, *Vegfa* mRNA levels were shown to be increased in the s.c. adipose tissues after high fat diet feeding (Michailidou, Turban et al. 2012), but this was not found in hearts 7 days post myocardial infarction (McSweeney, Hadoke et al. 2010) or in the angiogenesis of sponge implantation model (personal communication, Dr. Patrick Hadoke). In the current study, neither *Vegfa* nor the proliferation maker *Ki67* was differently expressed between genotypes, but the day 21 data represent only a snapshot of the late stage of the whole angiogenesis process. On day 21, angiogenic activity is likely to have switched from sprouting of new blood vessel formation to maturation of blood vessels in MKO mice. The trend to higher *Angpt1* expression levels is likely to reflect enhanced angiogenesis. It would be worth examining gene expressions at earlier time points, when the angiogenic activity is just initiated.

In the s.c. environment where the sponges are implanted, resident macrophage number may be very limited. And other infiltrating cells of the sponges, such as fibroblasts and neutrophils could highly express 11β-HSD1. This may explain why the total *Hsd11b1* mRNA in the sponge is not different between the 2 groups. But there is no direct evidence to show the deletion efficiency in sponge macrophages of the MKO mice anyway.

In summary, the data from MKO mice in the angiogenesis model of s.c. sponge implantation show that generation of active GCs by myeloid cell 11β-HSD1 suppresses angiogenesis, by regulating Il-1β and possibly angiopoietin-1 expression. This indicates that endocrine and immune systems work closely to regulate angiogenesis.

Chapter 6: Impaired resolution of K/BxN serum transfer induced arthritis in MKO mice

6.1 Introduction

Synthetic GCs have been used in arthritis treatment for over 60 years and remain widely used in clinics to suppress a wide range of inflammatory diseases. However, the role of endogenous GCs in inflammatory responses remains eclusive.

11β-HSD1 expression is usually increased in joints of arthritic subjects, a possible mechanism to suppress inflammation. A study in RA patients demonstrated a positive correlation between donor erythrocyte sedimentation rate (SER) and 11β-HSD1 enzyme activity in the synovium (Hardy, Rabbitt et al. 2008). A rat study in adjuvant arthritis showed increased synovial *Hsd11b1* mRNA and 11β-HSD1 reductase activity, which was decreased by treatment with TNF-α and IL-1β antagonists (Ergang, Leden et al. 2010). A human study of urine steroid metabolites revealed higher 11β-HSD1 enzyme activity during RA progression, which was decreased after treatment with disease modifying drugs (Beyeler, Dick et al. 2012).

The protective role of endogenous GCs was confirmed in studies of globally 11β-HSD1 deficient mice. A previous study in the lab on these mice revealed a more severe onset and delayed resolution of K/BxN serum transfer induced arthritis (Coutinho, Gray et al. 2012). To further dissect contributions of different cell populations to this phenotype, myeloid cell specific *Hsd11b1* KO mice (*LysM-Cre Hsd11b1*$^{flox/flox}$, MKO) and their littermate controls (*Hsd11b1*$^{flox/flox}$, Control) were studied in this model.

K/BxN serum induced arthritis was chosen because this model is reported to be lymphoid cell independent (Ji, Ohmura et al. 2002). As K/BxN serum contains autoantibody against glucose-6-phosphate isomerase, arthritis is initiated by immune complex formation, eliciting myeloid cells without T cell activation or B cell

producing antibodies (Ditzel 2004). In this way, myeloid cell functions in inflammation can be studied separately from lymphocytes. Moreover, globally 11β-HSD1 deficient mice are maintained on the C57Bl/6 strain genetic background, in which the K/BxN serum transfer induced arthritis (K/BxN arthritis) model works well (in contrast to other arthritis models, such as collagen induced arthritis) (Coutinho 2009).

6.2 Results

6.2.1 11β-HSD1 expression is modestly decreased in circulating neutrophils and monocytes of MKO mice during K/BxN serum transfer induced arthritis

Increased *LysM-Cre* mediated gene deletion efficiency with inflammation development has been reported *(Cho, Hong et al. 2008)*. It was predicted that in the K/BxN serum induced arthritis model, 11β-HSD1 deletion efficiency would be boosted by development of inflammation. This was tested by flow cytometry to measure levels of 11β-HSD1 in blood neutrophils and monocytes.

K/BxN serum transfer induced arthritis (abbreviated as K/BxN arthritis below) was induced as described in Section 2.17. In a pilot experiment, on day 3, 6, 9 and 12 after K/BxN serum injection, blood was collected by a tail nick from 2 mice in each group; C57/BL6 ('WT'), *Hsd11b1*$^{del/del}$ ('Del'), MKO and 'floxed' littermate ('Control'). Blood cells were stained with CD45, CD11B and Ly6G antibodies before intracellular staining of 11β-HSD1 as described in Section 2.14

An in-house sheep anti-11β-HSD1 antibody was kindly provided by Dr. Scott Webster. Staining with this antibody was specific as shown, by comparing the staining in *Hsd11b1*$^{del/del}$ ('Del') samples (negative control for 11β-HSD1 expression), isotype sheep IgG staining and unstained samples (Figure 6-1A). Examples of myeloid cell 11β-HSD1 staining in 'floxed' control and MKO mice are shown in Figure 6-1B and 6-1C, respectively.

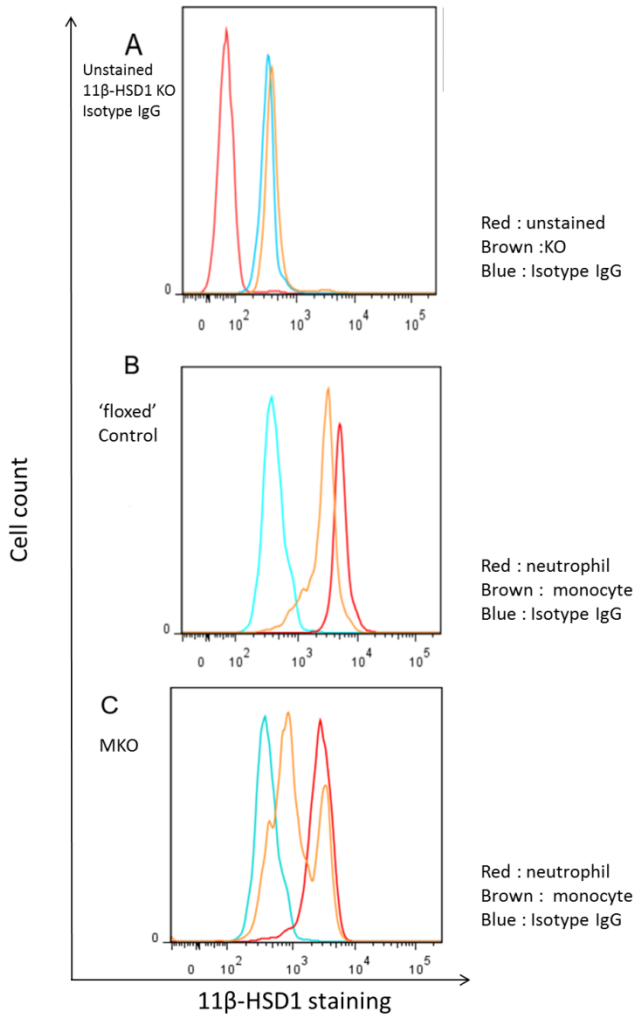

Figure 6-1 Flow cytometry measurement of blood myeloid cell 11β-HSD1.

Levels of 11β-HSD1 in the blood myeloid cells were measured by flow cytometry following induction of K/BxN arthritis. Total leukocytes were stained with anti-CD45 antibody, myeloid cells with anti-CD11B antibody, neutrophils with anti-Ly6G and monocytes assigned as $CD11B^{+}$ $Ly6G^{-}$. (A) 11β-HSD1 flow cytometry staining in unstained cells (red), negative control *Hsd11b1*$^{del/del}$ cells (brown) and isotype IgG staining (blue) in 'floxed' control mice. (B) An example of neutrophil (red) and monocyte (brown) 11β-HSD1 staining in a 'floxed' mouse, compared to isotype control staining (blue). (C) An example of neutrophil (red) and monocyte (brown) 11β-HSD1 staining in a MKO mouse, compared to isotype control staining (blue).

This pilot experiment to measure 11β-HSD1 levels showed that there was no improvement in 11β-HSD1 deletion efficiency in circulating neutrophils or monocytes of MKO mice during the study period, with about 50% reduction in neutrophils and monocytes (Figure 6-2). Peak expression of 11β-HSD1 on day 6 corresponded to the peak in inflammation following induction of arthritis.

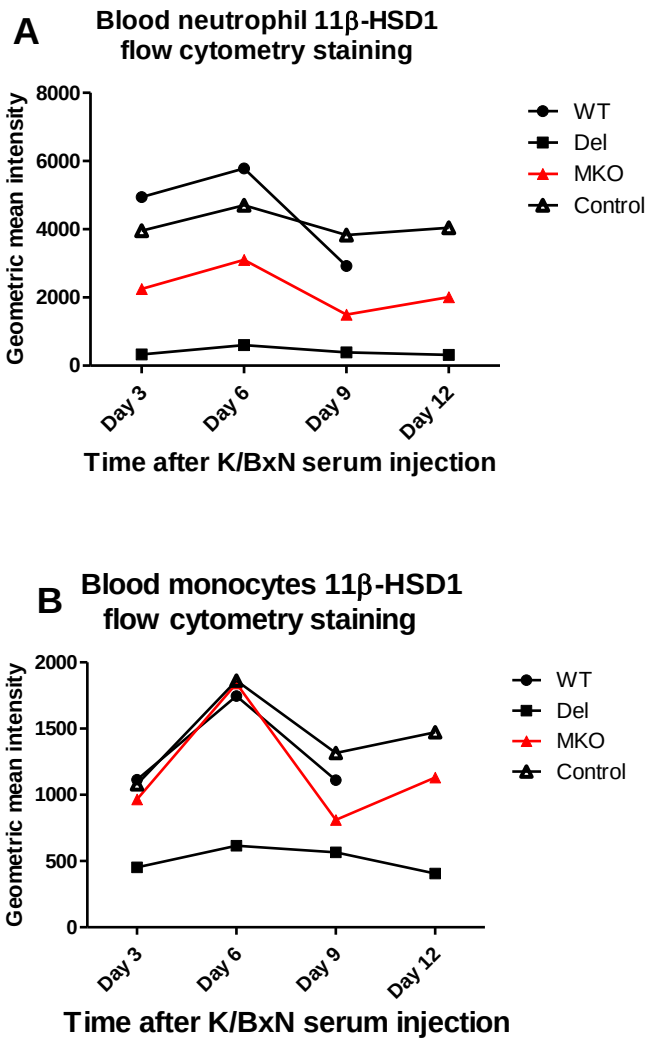

Figure 6-2 No increase in 11β-HSD1 deletion efficiency in circulating neutrophils and monocytes from MKO mice during K/BxN arthritis.

Levels of 11β-HSD1 in blood myeloid cells were measured by flow cytometry on day 3, 6, 9 and 12 following induction of K/BxN arthritis. Geometric means of 11β-HSD1 staining were used to plot the figure, which reflected average levels of 11β-HSD1 in the cells. Day 3-12 blood neutrophil (A) and monocyte (B) 11β-HSD1 staining in C57/BL6 ('WT', black squares), *Hsd11b1*$^{del/del}$ ('Del', circles), MKO (filled triangles) and 'floxed' littermate control s(empty triangles) mice were plotted into the lines. N=2/group. Data are means. No data of day 12 in WT mice were obtained.

The low deletion efficiency in circulating myeloid cells was subsequently confirmed in a larger group of mice on day 9 after i.p. K/BxN serum injection. As shown in Figure 6-3, about 50% reduction in 11β-HSD1 staining was found in neutrophils of MKO mice with little change in monocytes. These data suggests a limited contribution of 11β-HSD1 deletion in circulating myeloid cells to the effects of *LysM-Cre* mediated 11β-HSD1 deletion upon arthritis development in MKO mice.

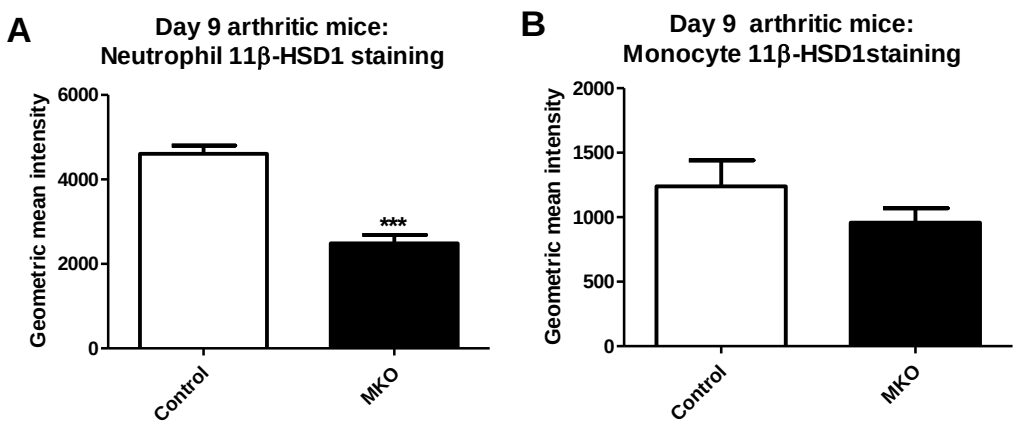

Figure 6-3 11β-HSD1 staining was modestly reduced in circulating myeloid cells of MKO mice on day 9 following K/BxN serum injection.

MKO and littermate 'floxed' control mice were injected with 125µl K/BxN serum and 9d later, 11β-HSD1 levels in the circulating neutrophils and monocytes were measured. Geometric means of 11β-HSD1 staining were calculated for each sample after deduction of background staining (the average value of the staining in *Hsd11b1*$^{del/del}$ samples). (A) There was a significant reduction in 11β-HSD1 staining in neutrophils from the MKO group. (B) There was no significant difference in blood monocyte 11β-HSD1 staining between MKO and control groups. Data are means ± SEM and were analyzed by un-paired t-test with significance set at $p<0.05$. ***, $p<0.0001$; n=7-10 per group, including *Hsd11b1*$^{del/del}$ mice group.

6.2.2 Resolution of arthritis was impaired in the MKO mice, indistinguishable from that of *Hsd11b1*$^{del/del}$ mice

Despite the lack of efficient deletion of 11β-HSD1 in circulating myeloid cells, 11β-HSD1 is successfully deleted in resident peritoneal macrophages and possibly other resident macrophages in MKO mice. To investigate whether deletion of 11β-HSD1 in tissue macrophages alter the course of K/BxN serum induced arthritis, young adult male MKO, 'floxed' littermate controls and *Hsd11b1*$^{del/del}$ mice (with 'null' alleles of *Hsd11b1*, see Section 2.2) were i.p. injected with 125μl K/BxN serum per mouse. Clinical scoring was used to assess joint inflammation in the following 21 days. Ankle joints were harvested for histopathological examination at the end of the experiment.

As shown in Figure 6-4, during the arthritis onset, clinical scores were similar between MKO and 'floxed' control mice. However, from day 9 onwards, MKO mice exhibited a trend to higher clinical scores than 'floxed' control mice, which was significant from day 13 to day 18 and indistinguishable from that of *Hsd11b1*$^{del/del}$ mice.

The experiment was repeated in another cohort of mice using a slightly higher dose of serum (150μl/mouse), which showed a very similar pattern of arthritis development (data not shown).

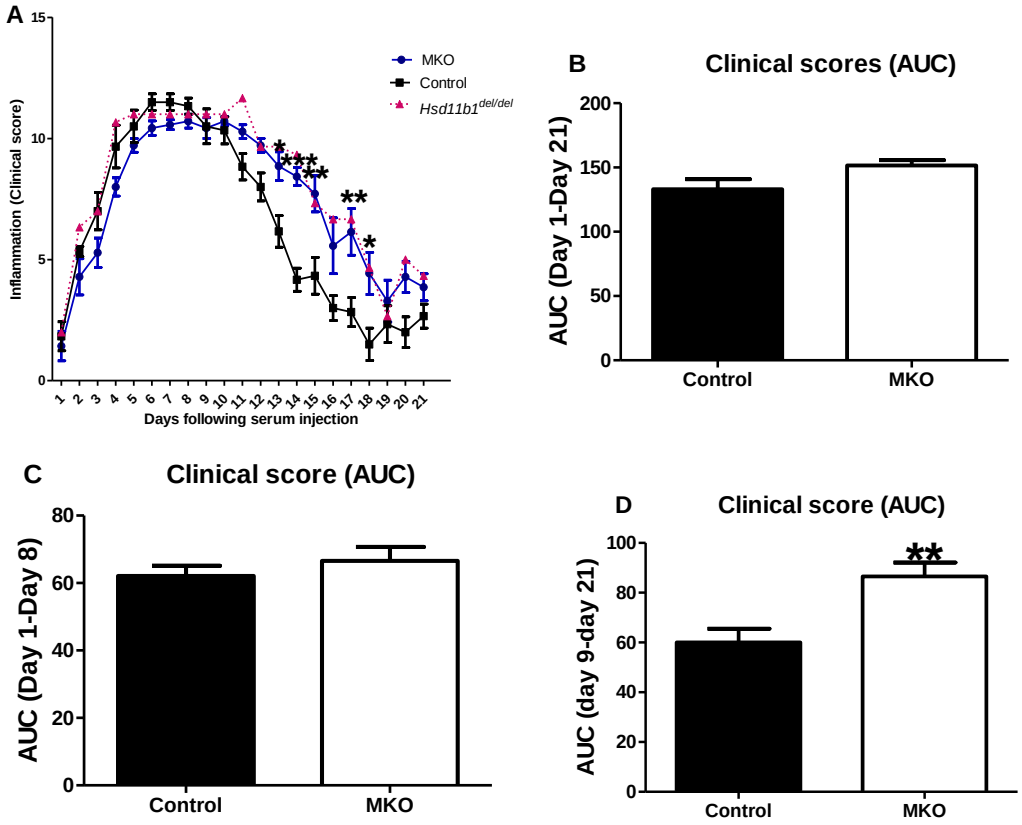

Figure 6-4 Worse inflammation resolution reflected by higher clinical scores in MKO compared to control littermate mice during the resolution phase of K/BxN arthritis.

MKO (n=7), 'floxed' control (n=6) and *Hsd11b1*$^{del/del}$ (n=3) mice were injected with 125µl K/BxN serum and joint inflammation was assessed by clinical scoring for 21 continual days, blind to genotype. (A) Clinical scores over 21 days. Data in the MKO and control groups are means ± SEM and were analysed by repeated measurement 2 way ANOVA with Bonferroni post-test. The p value for interaction between time and genotype is $p<0.0001$. Post-test shows a significant difference between MKO and 'floxed' control mice from day 13 to day 18(except day 16). *, $p<0.05$, **, $p<0.01$, ***, $p<0.001$. Only the mean is shown for the *Hsd11b1*$^{del/del}$ group. (B) There was no significant difference in the AUC of clinical scores in the MKO and control mice from day 1 to day 21 or (C) from day 1 to day 8. (D) There was a higher AUC of clinical scores in MKO mice from day 9 to day 21 compared to controls. AUC was calculated when input data were in XY form, then the calculated total area was plotted and data were analysed by unpaired t-test. Data are means ± SEM. N=6-7/group; *, $p<0.05$.

6.2.3 More advanced fibroplasia in the mesenchymal tissue around the joints of MKO mice

Ankle joints were collected on day 21 after K/BxN serum injection, processed for H & E staining and examined for pathological changes with help from Professor Donald Salter. More severe pathological changes were found in MKO and *Hsd11b1*$^{del/del}$ mice than in 'floxed' controls. There was more advanced fibroplasia in the mesenchymal tissue surrounding the joint and tendon sheath in MKO and *Hsd11b1*$^{del/del}$ mice than in controls, with new bone (exostosis) and blood vessel formation (Figure 6-5).

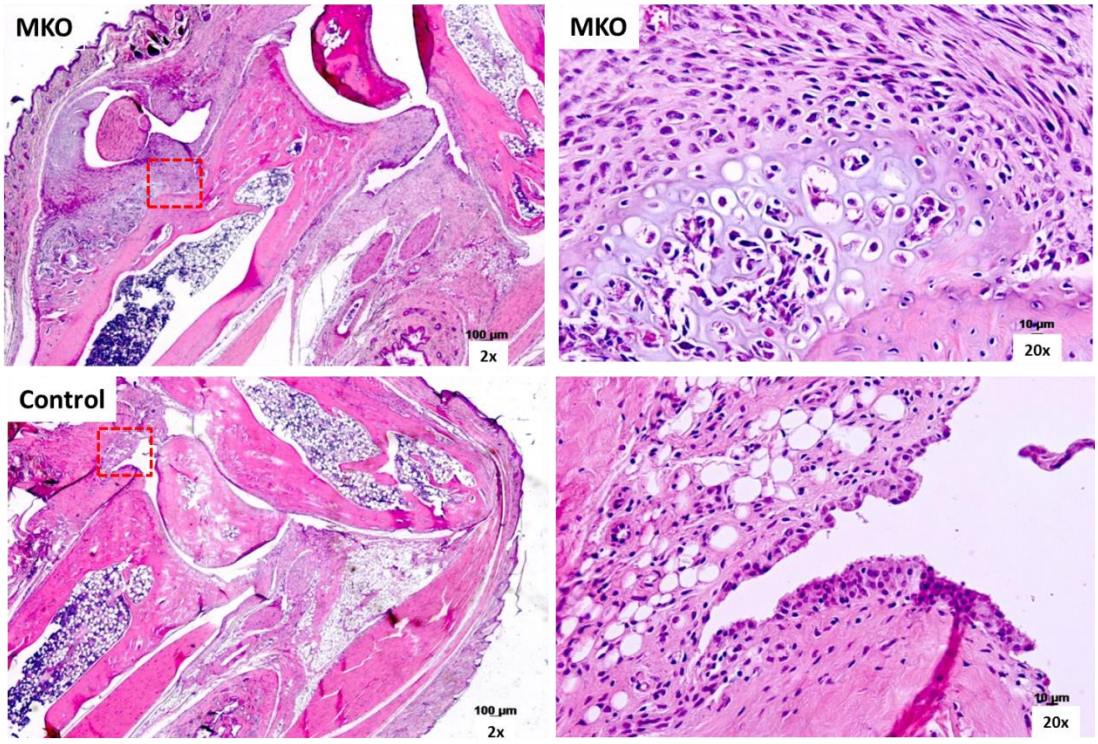

Figure 6-5 Worse fibroplasia and new bone formation in ankle joints of MKO mice.

In the experiment described in Figure 6-4, ankle joints after 21 days of K/BxN serum injection were harvested and processed for H & E staining. The top 2 pictures are representative images of joints in one MKO mouse and the bottom 2 are from a control mouse. The pictures in the left are taken at 2x magnification and those in the right are taken from the boxed area in the left pictures at 20x magnification. Fibroplasia and new bone formation are evident in the MKO mouse, not in the control mouse.

6.2.4 Synovial fluid leukocyte populations do not differ between MKO and control mice

Synovial fluid leukocyte infiltration dominates the development of K/BxN arthritis, with neutrophils and monocytes/macrophages in particular (Ji, Ohmura et al. 2002; Chou, Kim et al. 2010; Alexander V. Misharin 2012). A pilot study of synovial fluid leukocytes on day 12 following K/BxN serum injection showed that the percentage of $CD11b^{+}$ cells (mainly neutrophils and monocytes/macrophages) decreased from about 90% of total leukocytes in *Hsd11b1*$^{del/del}$ and 60% in MKO mice, to about 30% in littermate 'floxed' controls (each sample was pooled from 2 mice) (Figure 6-6). This suggested that high synovial fluid leukocyte count was associated with higher clinical scores.

Therefore, a larger cohort was used to investigate synovial fluid leukocytes in MKO, *Hsd11b1*$^{del/del}$ and WT mice. Unfortunately, on day 11, there were no differences in ratios of $CD11b^{+}$ myeloid cells, $Ly6g^{+}$ neutrophils, $Ly6c^{high}$ or $Ly6c^{low}$ monocytes/macrophages between genotypes (Figure 6-7).

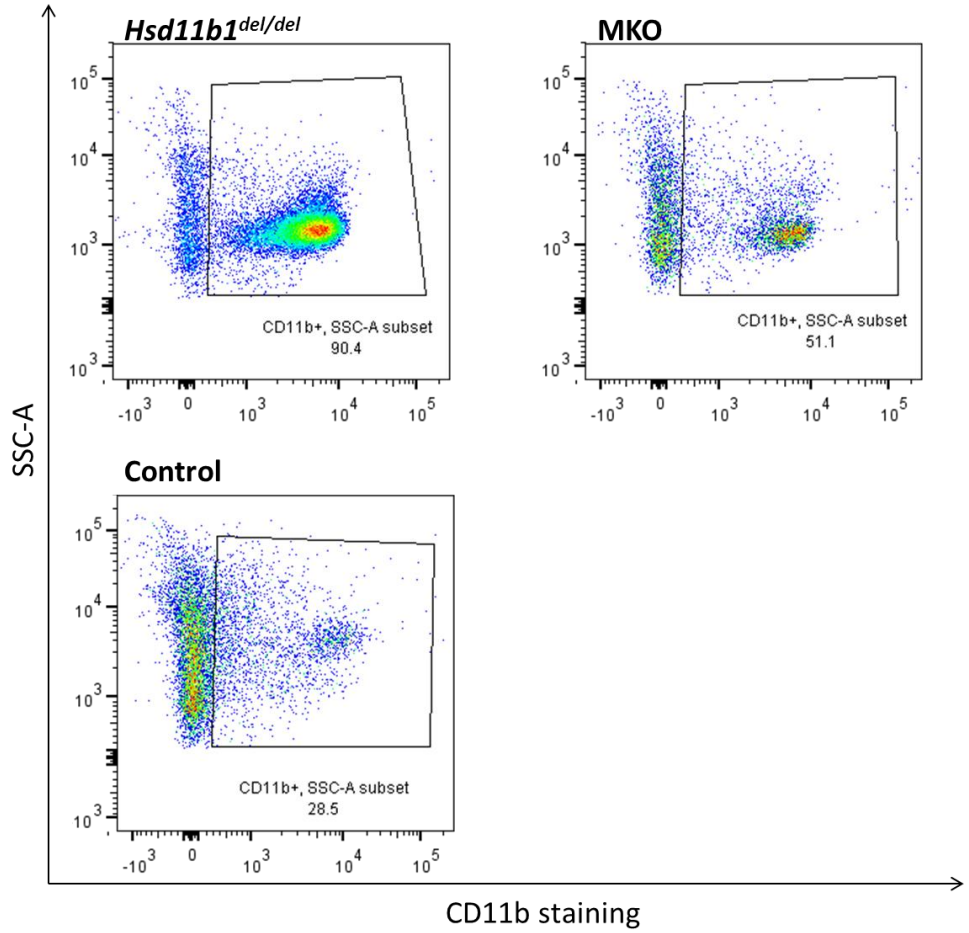

Figure 6-6 Higher CD11b$^+$ cell ratios in total synovial fluid leukocytes from *Hsd11b1*$^{del/del}$ (Del I) and MKO mice than 'floxed' control mice.

Synovial fluid leukocytes were harvested 12 days after K/BxN serum injection. The percentage of CD11b$^+$ cells of total single cells in the synovial fluid is shown for (A) *Hsd11b1*$^{del/del}$ (Del I), (B) MKO and (C) 'floxed' control mice. In each graph, a single sample was pooled from 2 mice.

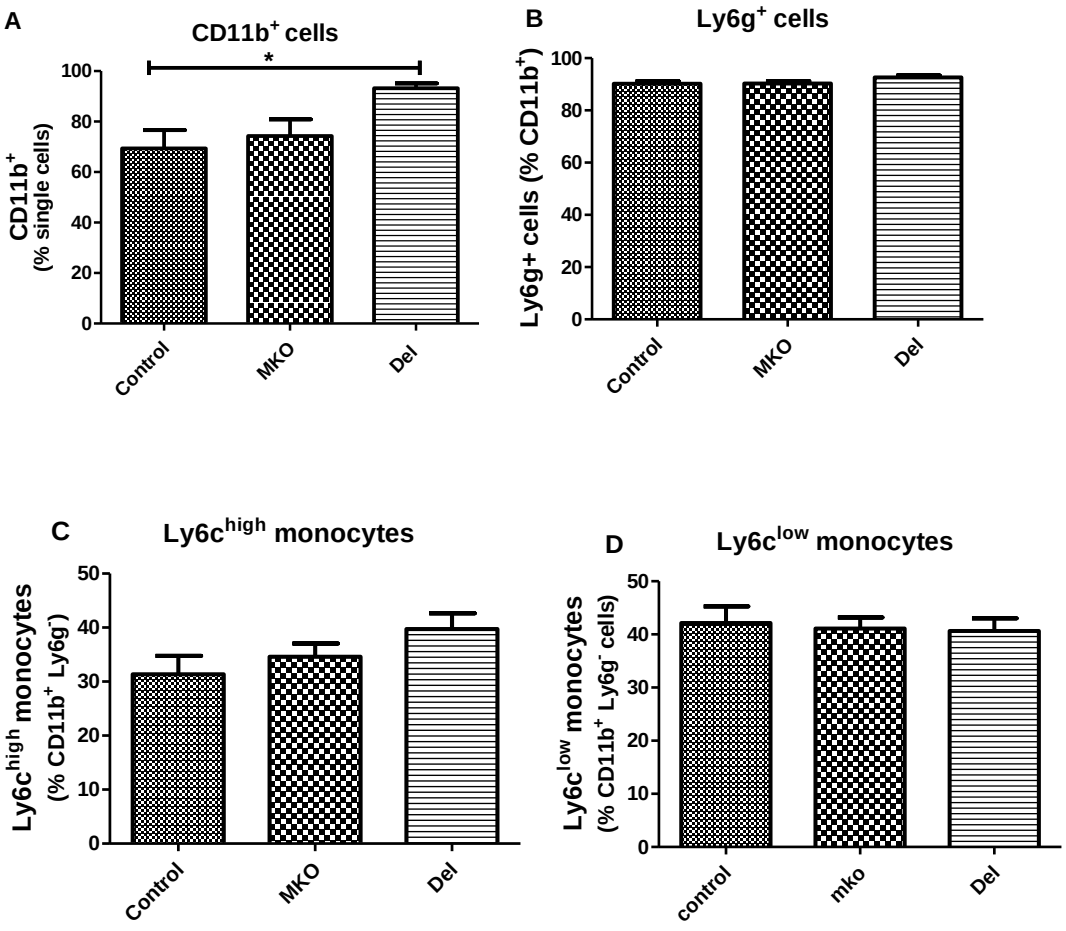

Figure 6-7 No difference in percentage of myeloid cell populations in synovial fluid from control, MKO and *Hsd11b1*$^{del/del}$ mice ('Del') on day 11 after K/BxN serum injection.

Synovial fluid leukocytes harvested 11 days after K/BxN serum injection were analysised by flow cytometry to study total myeloid cells (CD11b^{+}), neutrophils (CD11b^{+} Ly6g^{+}) and 2 populations of monocytes (CD11b^{+} Ly6g^{-} Ly6c^{high} monocytes, CD11b^{+} Ly6g^{-} Ly6c^{low} monocytes). (A) CD11b^{+} cells as a percenatge of all the single cells. (B) Ly6g^{+} neutrophils as a percentage of all the CD11b^{+} cells. (C) Ratios of Ly6c^{high} cells in the total moncytes (CD11b^{+} Ly6g^{-}). (D) Ratios of Ly6c^{low} cells in the total monocytes. No differences were detected by one way ANNOVA in any of the cell populations except in Figure 6-7A (but no difference between any 2 genotypes was found in by Tukey post test). Data are means ± SEM. N=6-9 in each group; *, $p<0.05$.

6.3 Discussion

Neutrophils and macrophages are the main effector cells in the K/BxN serum transfer induced arthritis model with arthritis induction dependant on neutrophil expression of FcRϒ, C5aR and CD11a/LFA-1 (Monach, Nigrovic et al. 2010). In this model, neutrophils are recruited by the lipid mediator LTB4, the cytokine IL-1, and CCR1 and CXCR2 chemokine ligands (Chou, Kim et al. 2010). The importance of monocytes and macrophages in the initiation and resolution of K/BxN arthritis was revealed by *in vivo* cell depletion studies, including studies on CD11b-DTR mice (Rajasekaran 2005; Solomon, Rajasekaran et al. 2005; Alexander V. Misharin 2012). Although mast cells were initially thought to be important for arthritis initiation from studies in mast cell deficient *c-kit*$^{W/Wv}$ mice (Nigrovic, Binstadt et al. 2007), mast cells were later revealed to be redundant in this model, using mast cell deficient *c-kit*$^{Sh/Sh}$ mice (Elliott, Van Ziffle et al. 2011). The initial findings of impaired arthritis initiation in mast cell deficient *c-kit*$^{W/Wv}$ mice were subsequently attributed to impaired neutrophil function in the former line of mice.

There was a trend for lower clinical scores during the onset phase of arthritis in MKO mice, although there was no significant difference detected by post-test of repeated measurement 2 way ANOVA or by t-test to examine the AUC. This may reflect low levels of 11β-HSD1 expression or poor 11β-HSD1 deletion efficiency in circulating myeloid cells from MKO mice at the early time of arthritis development, or little effect of resident macrophage 11β-HSD1 deletion on the arthritis initiation.

In the K/BxN arthritis model, resolution of inflammation is less studied than the initiation of the disease. Most studies aim to decrease the peak of inflammation during arthritis development. Given that failed resolution often causes chronic disease, it is important to elucidate the mechanisms of inflammation resolution. In the resolution phase of inflammation, phagocytosis of apoptotic cells by macrophages is essential for inflammation resolution (Uderhardt, Herrmann et al. 2012). A previous study demonstrated delayed acquisition of macrophage phagocytic ability in globally 11β-HSD1 deficient mice (Gilmour, Coutinho et al. 2006). This may be due to decreased GC signalling within macrophages, which promotes

macrophage phagocytosis (Giles, Ross et al. 2001). As shown here, impaired resolution without higher inflammatory altitude in MKO mice resulted in worse pathological fibroplasia, more new bone formation and greater angiogenesis. This may reflect deficient phagocytic ability of 11β-HSD1 deficient macrophages in clearing inflammatory neutrophils in MKO mice and it is possible that 11β-HSD1 deficiency in tissue resident macrophages contributes to this phenotype. So far, evidence supports good deletion of 11β-HSD1 protein in tissue resident macrophages (as shown in Chapter 4), while there is only about 50% deletion of 11β-HSD1 in circulating neutrophils and little deletion in monocytes. In a previous bone marrow transfer experiment between globally 11β-HSD1 deficient and C57Bl/6 mice, a trend of impaired arthritis resolution was seen in globally 11β-HSD1 deficient mice re-constituted with wild type bone marrow cells, compared to C57Bl/6 recipient mice receiving 11β-HSD1 deficient bone marrow cells (Coutinho 2009).

Similar results were found in another inflammatory model in globally 11β-HSD1 knockout mice. In a study of LPS induced lung inflammation, there was no difference in the peak inflammation between global 11β-HSD1 knockout and control wild-type mice, but in the resolution phase, a significant accumulation of apoptotic neutrophils and $CD11b^+$ $CD11c^+$ monocytes was found in the lungs of the knockout mice, indicative of failed inflammation resolution (Lax, Wilson et al. 2012).

The lack of change in myeloid cell populations in the synovial fluid between MKO and control mice awaits further investigation. There were some problems in the current experiment. For example, when the $CD11b^+$ $Ly6G^+$ neutrophil population was plotted in the side scatter channel (SSC) and forward scatter channel (FSC), there were 2 distinct populations of cells, which was not observed in the pilot experiment and puzzling. The reason was not clear. Cytospin examination of synovial fluid leukocytes may help clarify this. In addition, there was also likely some contamination with blood, as red cells were observed after centrifugation.

In a human RA study, 11β-HSD1 enzyme activity was positively correlated with erythrocyte sedimentation rate, a marker of disease activity (Hardy, Rabbitt et al. 2008). Increased 11β-HSD1 may be a protective mechanism to suppress

inflammation by generating more active GC. However, in that study, 11β-HSD1 expression was shown by immunofluorescence staining, to be located in fibroblasts rather than macrophages, whilst 11β-HSD2 was localised in macrophages. Up-regulation of *Hsd11b2* mRNA in the blood monocytes was reported in early RA patients (Olsen, Sokka et al. 2004). This is an interesting phenomenon, as mouse macrophages usually express 11β-HSD1 but not 11β-HSD2 (Gilmour, Coutinho et al. 2006; Usher, Duan et al. 2010) and human monocytes from healthy donors expressed 11β-HSD1 during *in vitro* differentiation into macrophages (Thieringer, Le Grand et al. 2001; Chinetti-Gbaguidi, Bouhlel et al. 2012). The presence of 11β-HSD2 but not 11β-HSD1 in synovial macrophages of RA patients may be a result of disease modification or drug treatment. However, it is possible that immunostaining is not sensitive enough to pick up the lower 11β-HSD1 levels in macrophages than those in fibroblasts. The study here indicates that the anti-inflammatory effects of 11β-HSD1 in K/BxN arthritis should be attributed to macrophages, rather than fibroblasts, although there is a chance that induction of fibroblast 11β-HSD1 is impaired by macrophage 11β-HSD1 deficiency in the current study.

Without a clear aetiology of RA, all current animal models have drawbacks in mimicking the human disease, including the K/BxN serum induced arthritis model (reviewed by (Wekerle, Flugel et al. 2012)). Therefore, a possible role of fibroblast 11β-HSD1 in other types of arthritis models is not excluded. First, the auto-antibody is not generated *de novo* in mice, but administered artificially. The disease development is self-limited and highly depends on the titration of the antibody. Second, the inflammation mainly depends on neutrophils and macrophages, not T or B cells. This is more like self-resolving arthritis and other none-RA arthritis in humans rather than RA. Last, but not least, is that fibroplasia in K/BxN arthritis is wide-spread and extends beyond the joint, involving the mesenchymal tissue along the bones and tendon sheath. Indeed, the damage in this area is more pronounced than in the joint itself (personal communication, Dr. David Brownstein and Professor Donald Salter).

A limitation of this study is that circulating neutrophils showed about 50% deletion of 11β-HSD1. Actually the current study cannot dissect the roles of macrophages and neutrophils. What's more, it is not entirely clear that the phenotype is down to an altered GC signalling pathway, although this is the putative pathway altered by 11β-HSD1. A study on *LysM-Cre GR*$^{flox/flox}$ mice in adjuvant induced arthritis showed no difference in arthritis development (both initiation and resolution) compared to control 'floxed' mice (Baschant, Frappart et al. 2011). This suggests that in arthritis models involving both innate and adaptive immune cells, the influence of endogenous GC action in myeloid cells is limited. To test whether this phenotype is because of GC signalling in macrophages, in addition to a K/BxN arthritis study in *LysM-Cre GR*$^{flox/flox}$ mice, macrophage specific delivery of GCs by liposome encapsulation could be administered into MKO mice during arthritis resolution to test whether this would promote arthritis resolution.

In summary, clinical scoring indicated impaired resolution of K/BxN arthritis in MKO mice with advanced histopathological changes in the joint with pronounced fibroplasia in the mesenchymal tissues surrounding the joints, possibly due to tissue resident macrophage 11β-HSD1 deficiency. It suggests that impaired resolution alone, without increased peak inflammation, could result in a poor prognosis and that GC signalling in tissue resident macrophages can boost the ability of macrophages to dampen inflammation.

Chapter 7: Less subcutaneous adipose fibrosis in high fat fed MKO mice

7.1 Introduction

Increased adipose tissue 11β-HSD1 activity has been implicated in the pathogenesis of metabolic syndrome (Engeli, Bohnke et al. 2004). The predominant theory to explain the link between high 11β-HSD1 enzyme activity and metabolic diseases, supported by evidence from transgenic mice overexpressing *Hsd11b1* in adipose tissue, is that elevated 11β-HSD1 activity increases GC signalling in adipocytes, which in turn antagonizes insulin signalling, leading to dysregulated glucose and lipid homeostasis and accumulation of visceral adipose tissue (Morton and Seckl 2008). As several clinical trials of 11β-HSD1 inhibitors are on-going for treatment of metabolic diseases, it is crucial to gain more understanding of the underlying mechanisms through basic research, for example, identification of the target tissue to inhibit 11β-HSD1 to generate beneficial effects upon metabolism.

The liver gained attention as a target in studies related to glucose homoeostasis and type 2 diabetes, as 11β-HSD1 is most highly expressed in the liver and the original paper describing the globally 11β-HSD1 deficient mice showed lower fasting glucose levels with decreased liver glucose 6-phosphatase (G6Pase) and phosphoenolpyruvate carboxykinase (PEPCK) activity, key enzymes in gluconeogenesis (Kotelevtsev, Holmes et al. 1997). However, liver specific *Hsd11b1* KO mice failed to recapitulate these phenotypes (Lavery, Zielinska et al. 2012), although they were protected against 11-dehydrocorticosterone induced insulin resistance (Harno, Cottrell et al. 2013).

Several ‘metabolically protective’ mechanisms conferred by 11β-HSD1 deficiency in high fat fed mice have been uncovered in the white adipose tissue, including more lipid oxidation and less inflammation (Wamil, Battle et al. 2011), more angiogenesis and less fibrosis (Michailidou, Turban et al. 2012). However, it is unknown whether

this reflects an effect in adipocytes themselves or in the residing immune cells, especially macrophages.

Adipose tissue macrophages are important to maintain of normal insulin sensitivity, with a protective role for alternatively activated macrophages (M2) and a harmful role for classically activated macrophages (M1) (Wu, Molofsky et al. 2011; Molofsky, Nussbaum et al. 2013). Secreted inflammatory cytokines from accumulated inflammatory macrophages activate NFκB signalling in adipocytes, which is possible to blunt the insulin signalling pathway (Olefsky and Glass 2010; Tabas and Glass 2013).

To dissect the *in vivo* effect of macrophage 11β-HSD1 deficiency upon metabolic disease, a high fat diet (HFD) induced obesity experiment was carried out in MKO and control mice. Male MKO and littermate control 'floxed' mice (8-10 weeks old) were subject to 14 week HFD feeding. Body weight was measured weekly from the first week until week 14. A glucose tolerance test (GTT) was carried out in week 13 before the mice were culled for tissue collection in week 14.

7.2 Hypothesis

Myeloid cell 11β-HSD1 deficiency partly or fully accounts for the metabolic protective effects of global 11β-HSD1 deficiency, such as improved insulin sensitivity, increased angiogenesis and less fibrosis in the adipose tissue.

7.3 Results

7.3.1 Similar body weight and tissue weight between MKO and control mice

There was no difference in body weight between MKO and control mice through the HFD experiment. Tissues were collected and weighed before being fixed or frozen at the end of the experiment. There was no difference in tissue to body weight ratios between MKO and control groups in any of the tissues examined: subcutaneous adipose tissue (Figure 7-2A), epididymal adipose tissue (Figure 7-2B), mesenteric adipose tissue (Figure 7-2C), liver (Figure 7-2D) or spleen (Figure 7-2E).

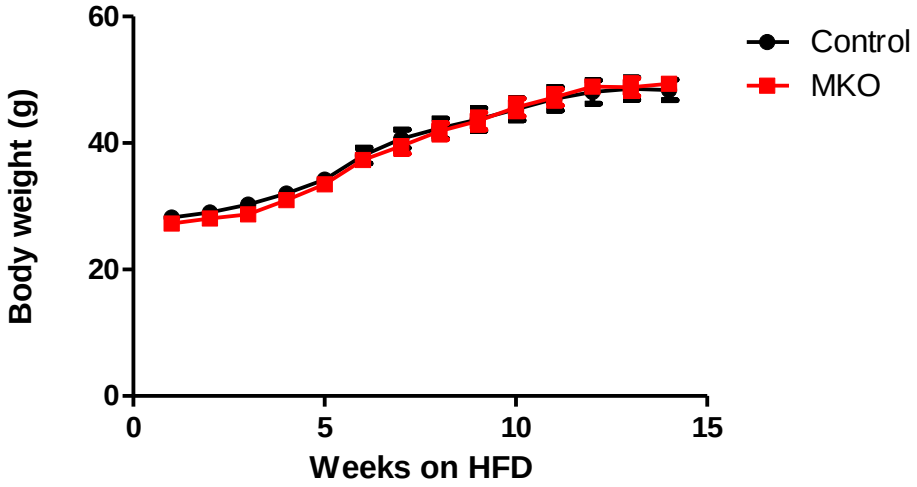

Figure 7-1 Similar body weight between MKO and control mice during 14 weeks of high fat diet feeding.

Body weight was monitored weekly during 14 week high fat diet feeding. Red square symbols show MKO mice and black round symbols show control mice. Data are means ± SEM, n=5-7. Data were analysed by repeated measurement 2-way ANOVA. There was no significant interaction between genotype and time.

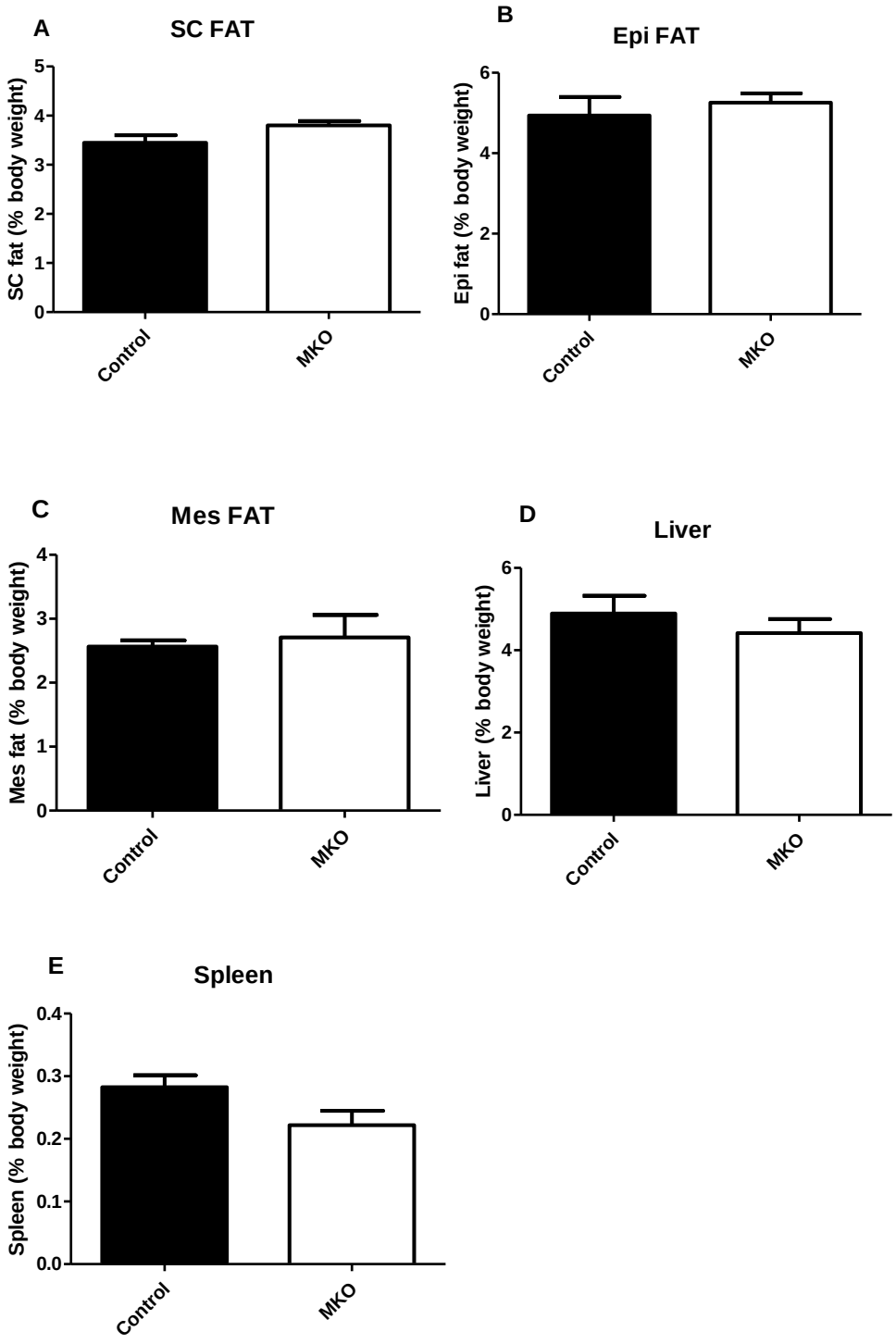
A
SC FAT
SC fat (% body weight)
0
1
2
3
4
5
Control
MKO
B
Epi FAT
Epi fat (% body weight)
0
2
4
6
Control
MKO
C
Mes FAT
Mes fat (% body weight)
0
1
2
3
4
Control
MKO
D
Liver
Liver (% body weight)
0
2
4
6
Control
MKO
E
Spleen
Spleen (% body weight)
0.0
0.1
0.2
0.3
0.4
Control
MKO

Figure 7-2 Similar tissue and organ weights in MKO and control mice.

At the end of the 14 week HFD experiment, tissues were harvested from the mice and weighted. There was no difference in (A) subcutaneous (SC), (B) epididymal (Epi) or (C) mesenteric adipose tissue (MES), (D) liver or (E) spleen tissue to body weight ratios between genotypes. Data are means ± SEM, n=5-7. Data were analysed by unpaired t-test with significance set at $p<0.05$.

7.3.2 Similar circulating glucose and insulin levels during GTT in MKO and control mice

A GTT was carried out in week 13 of the experiment. Tail bleeding was carried out at each time point to collect blood for plasma glucose and insulin measurement in the lab, in addition to the onsite measurement of whole blood glucose levels with a glucose meter. Plasma glucose and insulin measurements were carried out by Dr. Sophie Turban.

The limited detection range of the glucose meter resulted in some readings of 'HI' without a numerical value, whereas in the plasma glucose ELISA assay, haemoglobin contamination in some samples caused artificially high glucose levels. For these situations, the relevant data were excluded from the analysis. As some data points were missing, no statistical tests were performed in the glucose measurements. There did not appear to be any difference in glucose levels between MKO and control mice (Figure 7-3), but the missing data may alter the current judgement.

Insulin levels in plasma samples from each time point were measured and there was no difference between MKO and control groups by repeated measurement 2 way ANOVA (7-4A) or by comparing the area under the curve (AUC, Figure 7-4B).

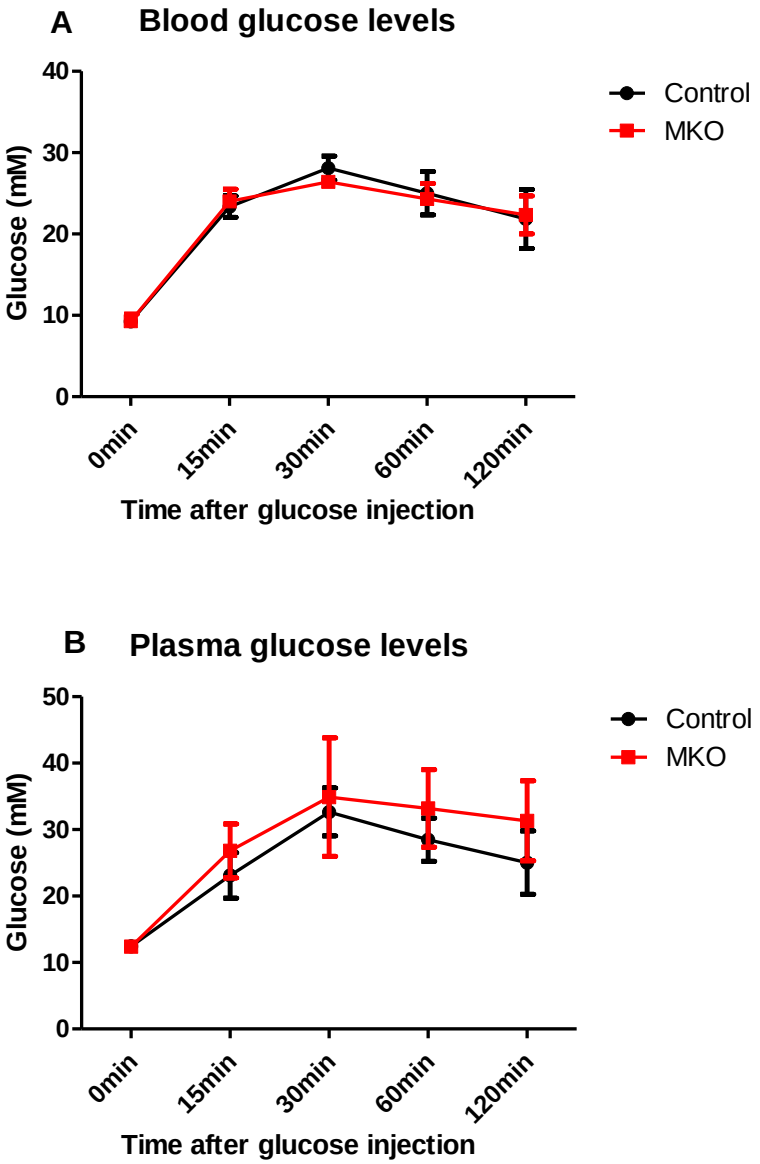

Figure 7-3 Similar blood and plasma glucose levels during GTT between MKO and control mice.

Young male MKO and control littermate mice were subject to a 14 week HFD experiment with GTT carried out in week 13. Circulating glucose levels were measured by glucose meter in blood (A) and by ELISA in the plasma (B). There are 3 out of 25 and 35 readings in the MKO and control groups unavailable in (A), respectively. There are 6-8 out of 25 and 35 readings unavailable in the MKO and control groups in (B), respectively. Data are means ± SEM, n=5-7/group.

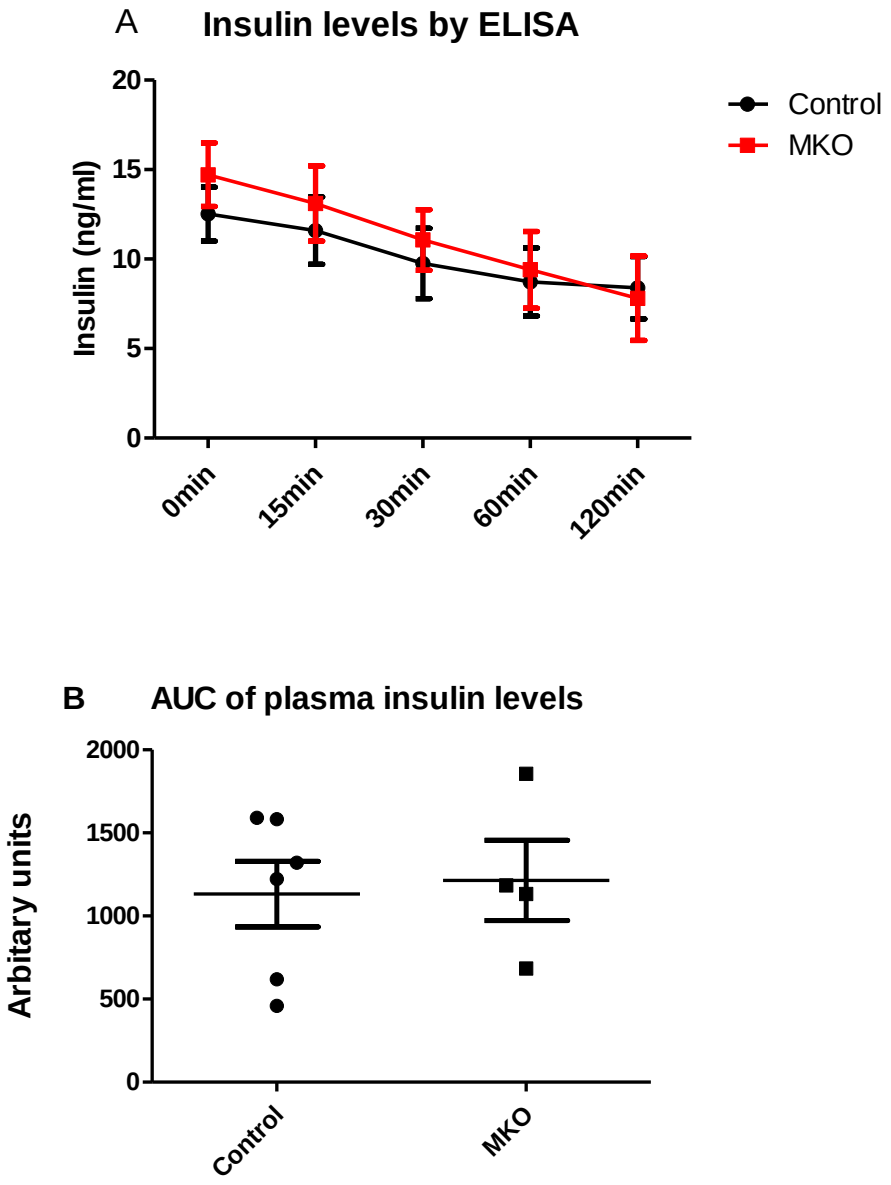

Figure 7-4 Similar plasma insulin levels during GTT between MKO and control mice.

During the experiment described in Figure 7-3, plasma insulin levels were measured by GTT. (A) There was no significant difference between genotypes by repeated measurement 2-way ANOVA. (B) The AUC of insulin levels between MKO and control mice during GTT was not different by unpaired t-test. Data are means ± SEM, n=4-6/group. There was 1out of 25 and 35 readings unavailable in the MKO and control groups, respectively and thus all the readings from the same mouse are not included in the graph.

7.3.3 No difference in macrophage related gene expression in mesenteric adipose tissue between MKO and control mice

Mesenteric adipose tissue was chosen for RNA analysis because inflammation is considered to be more pronounced here than in subcutaneous adipose tissue (Wamil, Battle et al. 2011). Between MKO and control mice, there was no difference in levels of the macrophage marker *Cd68*, the hypoxia response marker *Hif1a*, the angiogenic factor *Vegfa*, or in inflammatory M1 makers *Tnfa* or *Nos2* (*Il6* expression was too low to measure). There was no difference in alternative M2 markers *Mrc1* (mannose receptor) or *Fizz1* (*Ym1* was not detected) (Figure 7-5).

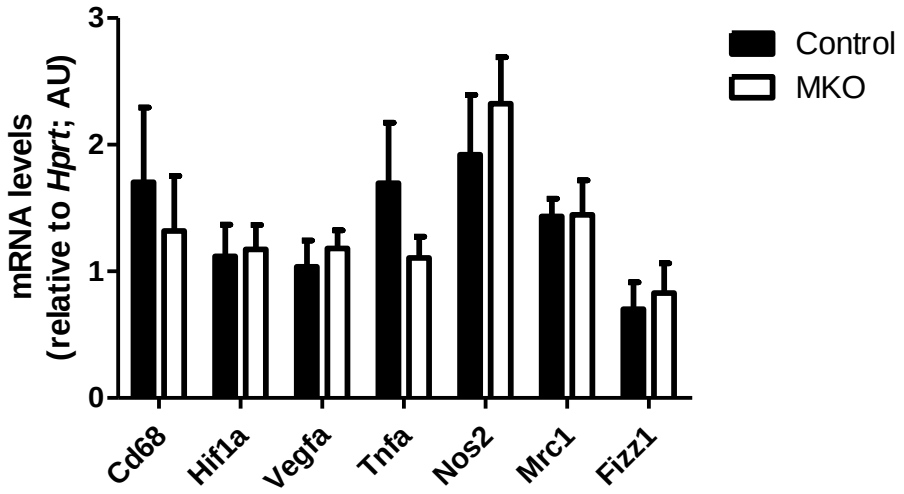

Figure 7-5 No difference in macrophage related gene expression levels in mesenteric adipose tissues from MKO and control mice.

At the end of the 14 week HFD experiment, tissues were harvested for analysis with mensentric adipose tissue gene expression examined by qPCR. There was no difference in levels of *Cd68, Hif1a, Vegfa, Tnfa, Nos2, Mrc1* or *Fizz1* mRNA between genotypes. Data are means ± SEM, N=5-7/group. Data were analysed by un-paired t-test for each individual gene, with significance set at $p<0.05$.

7.3.4 Subcutaneous adipose tissue from MKO mice shows decreased fibrosis but similar cell size to control mice.

To further study adipose tissue remodeling, picrosirius red staining was carried out on sections from subcutaneous inguinal depots to visualize collagen deposition, a key feature of fibrosis. In addition, cell size was also measured in these sections. The quantification of the staining was done by Mr. Oliver Brown, an undergraduate project student. There was less collagen deposition in adipose tissue from MKO mice, but no difference in cell sizes was found between genotypes (Figure 7-6).

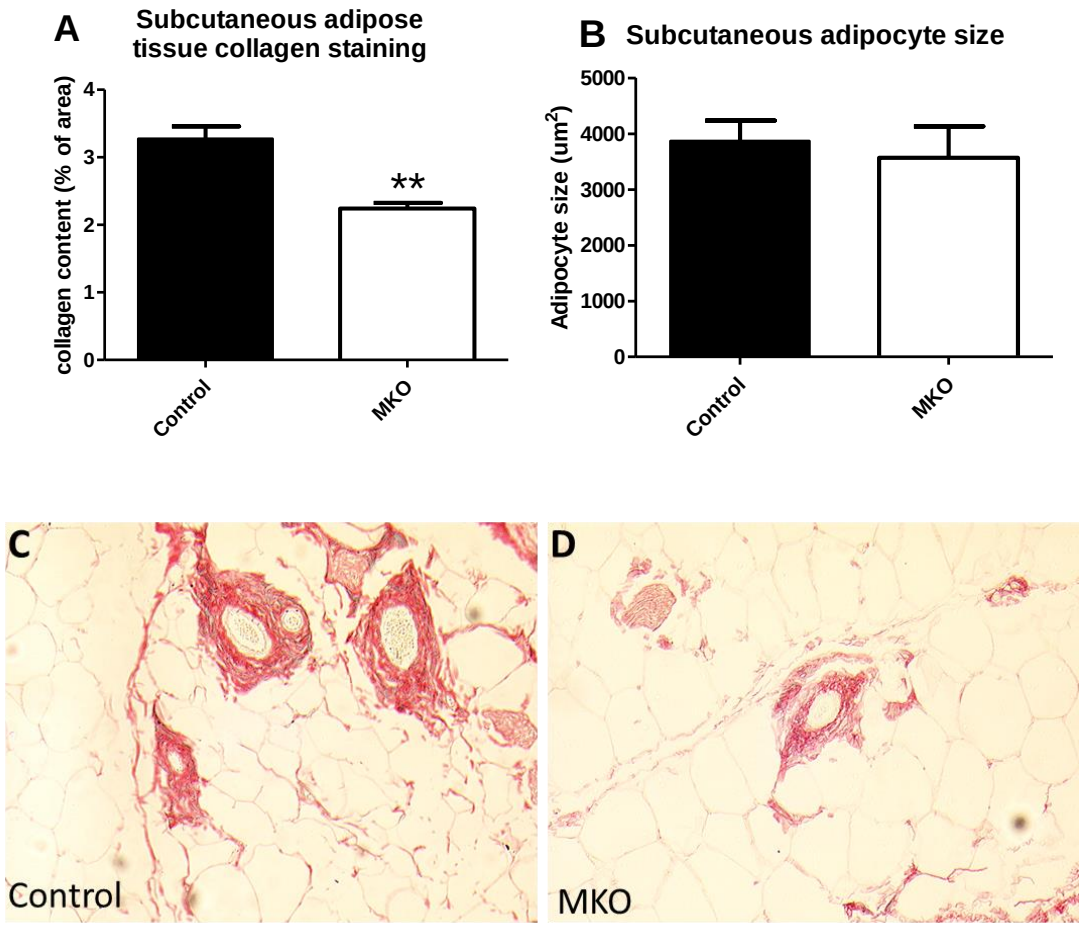

Figure 7-6 Reduced collagen content but similar adipocyte size in the subcutaneous adipose tissues from MKO mice, compared to littermate controls.

Picrosirius red staining was performed on sections of subcutaneous adipose tissues collected after 14 week HFD and collagen content and adipocyte size were analysed by ImageJ. (A) There was reduced collagen content in MKO mice compared to controls. Data were analysed by unpaired t-test, with significance set at $p<0.05$. Data are means ± SEM, n=3-5/group. **, $p<0.01$. (B) There was no difference in adipocyte sizes between genotypes. Data are means ± SEM, n=3/group. Data were analysed by unpaired t-test, with significance set at $p<0.05$. (C and D) Representative picrosirius red staining in control and MKO mice.

7.4 Discussion

MKO mice showed a similar body weight to their littermate controls during the 14 week HFD experiment. This was associated with similar organ and tissue weights at the end of the experiment. The results differed from previous data in globally 11β-HSD1 deficient mice which showed reduced body weight gain and reduced mesenteric adipose tissue weight after HFD, compared to wild type controls (Morton, Paterson et al. 2004; Wamil, Battle et al. 2011). However, both the original 11β-HSD1 deficient mice and *Hsd11b1*$^{del/del}$ mice (with null alleles of *Hsd11b1*) failed to show the previous difference in an HFD experiment in parallel to this one (data not shown). In terms of glucose metabolism, the GTT data are not conclusive in MKO mice but there is no suggestion that their glucose or insulin levels differed from control littermates. This again contrasts with globally 11β-HSD1 deficient mice which showed lower glucose levels during both GTT and insulin tolerance test (ITT) (Morton, Paterson et al. 2004).

In the gene analysis of mesenteric adipose tissues, there were no differences found between genotypes, whereas higher *Vegfa* and lower *Hif1a* were reported in the white adipose tissues of HFD fed globally 11β-HSD1 deficient mice compared to wild type controls (Michailidou, Turban et al. 2012). Although a gene array from a previous study concluded that inflammation was reduced in mesenteric adipose of 11β-HSD1 deficient mice after HFD feeding, the reported changes were not in the familiar immune genes examined in the current study, such as *Tnfa, Mcp1, Il6, Il10* or *Arg* (Wamil, Battle et al. 2011). It awaits future examination whether the reported decreased levels of *Marco, Stat4* and *L-sel* mRNA occurred in the MKO adipose tissues. Decreased macrophage infiltration was reported in the same paper, but again this is not suggested by *Cd68* mRNA measurement in the current study on MKO mice. It is of note that CD11b as a marker for adipose macrophages in the report is likely to be unspecific, as neutrophils are also evident in the cytospins of separated CD11b^{+} cells (data not shown here). However, the reduction in tissue fibrosis in subcutaneous adipose tissue of MKO mice is similar to that previously described in globally 11β-HSD1 deficient mice (Michailidou, Turban et al. 2012). These results

suggest that macrophage 11β-HSD1 deficiency contributes to only part of the adipose tissue phenotype of globally 11β-HSD1 deficient mice.

There are several suggestions that macrophage 11β-HSD1 may not play an important role in HFD induced obesity. Inflammation in the adipose tissue of 11β-HSD1 deficient mice was found to be reduced in the microarray study with reduced infiltration of cytotoxic T cells and macrophages. But in separated macrophages from the adipose tissue, there were no differences in levels of inflammatory mRNA or cytokine release (Wamil, Battle et al. 2011). In terms of 11β-HSD1 expression in adipose tissue stromal cells, a previous immunofluorescence staining study from the lab has shown that 11β-HSD1 co-localises with $p27^{kip1}$ positive pre-adipocytes with little 11β-HSD1 expression in the F4/80 positive macrophage population (De Sousa Peixoto, Turban et al. 2008). These studies do not support an important role of adipose macrophage 11β-HSD1 to reduce inflammation in globally 11β-HSD1 deficient mice.

However, the experiment is restricted in some ways and does not allow a final conclusion. First, the n number in each group is low. There were only 5 MKO mice and 7 littermate controls and some data were missing in the GTT results. Second, in a parallel HFD experiment to the study, no reported improved insulin signalling was found in the globally 11β-HSD1 deficient mice (data not shown here). Third, most infiltrated macrophages in the adipose tissue arise from bone marrow derived monocytes (Koh, Kang et al. 2007) and 11β-HSD1 deletion efficiency is not likely to be high in these macrophages.

Searching for the target tissue which confers the beneficial metabolic effect in globally 11β-HSD1 deficiency has turned out to be a challenging task. So far, brain, adipose, liver and macrophage specific 11β-HSD1 deficient mice have failed to replicate the phenotype (Lavery, Zielinska et al. 2012; Erika Harno 2013) (unpublished data from our lab). Given the recent discovery that osteocalcin from osteoblasts underlies the protection from GC induced glucose intolerance in Col2.3-11β-HSD2 Tg mice (Brennan-Speranza, Henneicke et al. 2012), it is reasonable to

propose a role for bone 11β-HSD1 in glucose metabolism. Another possible target is skeletal muscle. Previous studies showed a role for muscle 11β-HSD1 in insulin signalling and protein degradation (Morgan, Sherlock et al. 2009; Biedasek, Andres et al. 2011). Combined deletion of 11β-HSD1 in liver and adipose tissue may be needed to recapitulate the phenotype of globally 11β-HSD1 deficient mice, as 11β-HSD1 is highly expressed in both places and there is a possible cross-talk between liver and adipose tissue 11β-HSD1 (unpublished data, Professor Karen Chapman).

In summary, the preliminary data from MKO mice on 14 week HFD experiment do not show differences in body or tissue weights, or GTT results compared to controls. Thus myeloid cell 11β-HSD1 deficiency does not contribute to improved insulin signalling in globally 11β-HSD1 deficient mice. However, the study does reveal reduced fibrosis in subcutaneous adipose of MKO mice after HFD feeding, which supports role of macrophage 11β-HSD1 in tissue remodelling.

Chapter 8: Summary and Discussion

8.1 Summary

In this thesis, the role of 11β-HSD1 in macrophages was first studied during *in vitro* M1/M2 macrophage polarisation and hypoxic conditioning experiments, to compare day 3 TG elicited macrophages from 11β-HSD1 deficient and control C57Bl/6 mice. In control macrophages, levels of 11β-HSD1 protein were found to be similar between M1 and M2 polarised macrophages, despite higher *Hsd11b1* mRNA levels in M1 than M2 polarised macrophages. It is also surprising that although expression of some M1 genes was increased and that of some M2 genes decreased in 11β-HSD1 deficient macrophages, compared to controls, no evidence of changed M1/M2 polarisation was found in ELISA or western blotting measurements (except for decreased IL-12 p40). Upon inflammatory stimulation under hypoxic conditions, 11β-HSD1 deficient and control macrophages showed similar expression levels of genes related to inflammatory, angiogenic, fibrotic and metabolic responses.

To directly study macrophage 11β-HSD1 in *vivo,* macrophage specific *Hsd11b1* knockout mice (MKO) were introduced. The deletion efficiency of 11β-HSD1 was examined in different macrophage populations. There was no effective deletion (>50%) at 11β-HSD1 protein or enzyme activity levels in TG elicited myeloid cells from MKO mice, albeit decreased *Hsd11b1* mRNA levels (>80%). A modest decrease was found in bone marrow derived macrophages of MKO mice (~50% in both enzyme activity and mRNA levels). However, resident peritoneal macrophages from MKO mice exhibited >80% reduction in 11β-HSD1 enzyme activity and protein levels. Other tissue resident macrophage populations were studied as well, but there was no detectable 11β-HSD1 protein in alveolar macrophages and no evidence of high deletion efficiency in adipose macrophages.

The inflammatory angiogenesis response was studied in MKO and control ‘floxed’ littermate mice using subcutaneous implanted sponges. In the sponges harvested 21 days later, evidence of increased angiogenesis was found in the MKO mice by both

Chakley counting of blood vessels and qPCR measurement of the endothelial marker *Cdh5*. In qPCR measurements, no difference in *Vegfa* levels was found, nor was there a difference in levels of mRNA encoding the macrophage marker *Cd68* or other inflammatory genes with the notable exception of higher pro-angiogenic *Il1b* mRNA in MKO mice.

The role of macrophage 11β-HSD1 in an inflammatory response was studied using the K/BxN serum transfer induced arthritis model. A longitudinal blood flow cytometry study to measure levels of myeloid cell 11β-HSD1 failed to show increased 11β-HSD1 deletion with arthritis development in MKO mice, with a consistent ~50% deletion in neutrophils and much less in monocytes of MKO mice. Using clinical scoring to access joint inflammation, it was found that arthritis resolution is impaired in MKO mice. Histopathological examination of ankle joints confirmed this and pointed out more advanced fibroplasia in the mesenchymal tissues around the joints. Examination of joint RNA showed higher levels of yhr endothelial cell marker *Cdh5*, suggesting increased angiogenesis activity. However, a flow cytometry study of day 11 joint synovial fluid leukocytes did not detect the expected increase in composition of myeloid cells in MKO.

To study metabolic diseases associated with chronic GC excess, MKO and control littermate 'floxed' mice were subjected to high fat diet feeding to generate obesity. After 14 weeks of high fat diet feeding, there was no difference in body weight or organ weight between genotypes, nor was there a difference in blood glucose or insulin levels in a GTT. There was no change in levels of mRNA encoding inflammatory markers in the mesenteric adipose tissue between genotypes either. The only phenotype related to protection from metabolic diseases found in obese MKO mice was reduced fibrosis in the subcutaneous adipose tissue, with no change in adipocyte size.

8.2 Macrophage 11β-HSD1 in inflammatory signalling study

The lack of difference during *in vitro* macrophage studies on TG elicited peritoneal 11β-HSD1 deficient and wild type macrophages is not able to explain the changed inflammatory disease course in the MKO mice. The effects of macrophage 11β-HSD1 deficiency would be more interpretable if studied *in vivo* with simpler inflammatory models, such as LPS or zymosan induced peritonitis. For example, the inflammation onset and resolution phases of both zymosan induced peritonitis have been well characterised, with macrophage phenotypes similar to M1 and M2 (Bystrom, Evans et al. 2008). Poor 11β-HSD1 deletion efficiency in recruited macrophages of MKO mice hindered such studies. However, resident peritoneal macrophages were suggested to be involved in zymosan induced peritonitis, in which macrophages showed the characteristic proliferation behaviour of resident macrophages (Davies, Rosas et al. 2011); this model would be worthy of study. Alternatively, effective 11β-HSD1 deficiency restricted to immune cells (including macrophages) can be achieved with bone marrow transfer experiment between 11β-HSD1 deficient and wild type mice. However, bone marrow radiation is not specific to deplete bone marrow derived monocytes/macrophages. In addition, irradiation may have its own effect and tissue resident macrophages may also be affected.

The active GC generated by 11β-HSD1 in macrophages may act through GR or MR to modulate inflammation development. It was shown in an *in vitro* study that a low dose of corticosterone (<1nM) increases inflammation and high dose of corticosterone (>10nM) suppresses inflammation, both effects of which are elicited by GR, not MR (Lim, Muller et al. 2007). Given the fact of basal circulating active GC levels *in vivo*, it is likely that MR is saturated and GR exerts anti-inflammatory effects in physiological situations. Therefore, 11β-HSD1 generated active GC in macrophages is likely to bind with GR to suppress inflammation, but this awaits examination. As 11β-HSD1 can also metabolise cholesterol and bile acids, apart from GR and MR, LXR and FXR are also possible affected targets in 11β-HSD1 deficient macrophages. More information on this topic will be discussed in Section 8.4.

The hedgehog pathway in macrophages is worth further study. In addition to the hedgehog ligands (IHH, SHH and DHH) and receptor patched measurement, it is important to measure the induced transcription factor Gli1 at target cells. In tissues *in vivo*, macrophages are more likely to be a source of the hedgehog ligands to act on the surrounding cells, such as endothelial cells, pericytes or fibroblasts. Co-culture of macrophages and target cells or using the macrophage culture medium to stimulate target cells is a way to further study influence of macrophage 11β-HSD1 deficiency on this signalling pathway.

8.3 Macrophage 11β-HSD1 in cardiovascular study

It was surprising that increased angiogenesis was observed in the MKO mice in the angiogenesis assay of sponge implantation. *Hsd11b1* mRNA is expressed in smooth muscle cells of the aorta (Christy, Hadoke et al. 2003), but angiogenesis experiments carried out in *Sm22-Cre Hsd11b1*$^{flox/flox}$ mice did not show a difference in either *in vivo* (hind leg ischaemic model) or *in vitro* models (aorta ring assay) (personal communication, Dr. Patrick Hadoke, University of Edinburgh). The results from MKO mice highlighted the importance of macrophage 11β-HSD1 in regulation of angiogenesis. However, the extent of increased angiogenesis in MKO mice is likely to be smaller than globally 11β-HSD1 deficient mice, by comparing with the reported day 21 Chalkley counting data (Small, Hadoke et al. 2005). What's more, in a myocardial infarction experiment carried out in MKO mice by Dr. Gillian Gray's group, there was no improvement in cardiac performance of MKO mice, in contrast to globally 11β-HSD1 deficient mice. It is unknown whether incomplete macrophage 11β-HSD1 deficiency in MKO mice or 11β-HSD1 deficiency in other places in globally 11β-HSD1 deficient mice is responsible for the differences. Role of endothelial cell 11β-HSD1 awaits future examination, the expression of which was confirmed by immunohistochemical staining in blood vessels (Luo, Thieringer et al. 2013).

In terms of atherosclerosis, a bone marrow transfer experiment between 11β-HSD1 KO and wild type mice revealed protection against atherosclerosis by 11β-HSD1 KO

bone marrow cells, suggesting macrophages are involved in atherosclerosis with 11β-HSD1 deficiency (Garcia, Search et al. 2013; Kipari, Hadoke et al. 2013). Other candidates include liver and adipose tissue, which are important places for lipid and cholesterol metabolism and highly enriched for 11β-HSD1. However, myeloid cell, but not liver or adipose specific 11β-HSD1 knockout mice (using LysM-Cre, Albumin-Cre and Ap2-Cre, respectively) in the *Apoe*$^{-/-}$ genetic background were protected from atherosclerosis development (unpublished data, Professor Karen Chapman). Whether macrophage 11β-HSD1 has a direct role in cholesterol metabolism can be investigated by lipomics analysis of the atherosclerosis plaque or foam macrophages from 11β-HSD1 deficient and wild type mice, but data from Kipari et al support increased cholesterol efflux in 11β-HSD1 deficient macrophages.

8.4 Macrophage 11β-HSD1 in arthritis

The impaired resolution of K/BxN serum transfer induced arthritis found in MKO mice appear to be in contrast to a previous report of lack of difference with *LysM-Cre* mediated GR knockout during glucose-6-phosphate isomerase antigen induced arthritis (Baschant, Frappart et al. 2011), although the latter involves not only innate but also adaptive immune cells. It raised the question that whether endogenous GCs are important in some type of arthritis (inflammatory arthritis) but not others (rheumatoid arthritis). This was similar to findings in an atherosclerosis study, where no protection against atherosclerosis was observed in *Ldlr*$^{-/-}$ mice receiving *LysM-Cre Nr3c1*$^{flox/flox}$ bone marrow cells but with reduced blood vessel calcification (Preusch, Rattazzi et al. 2008). Protection from atherosclerosis in *LysM-Cre Hsd11b1*$^{flox/flox}$ mice suggests that the effect of 11β-HSD1 in macrophages may not be via the classic substrate 11-DHC, or 11β-HSD1 generated GCs in macrophages bind to MR rather than GR. In addition, the drawback of the experiment is bone marrow transfer method is inclusive on role of resident macrophage GR.

Study on myeloid cell MR or GR knockout mice in the K/BxN arthritis model will give help clarify the target of 11β-HSD1. Myeloid cell MR knockout mice are protected from several types of inflammation associated-adverse tissue remodelling

(Rickard, Morgan et al. 2009; Frieler, Meng et al. 2011; Frieler, Ray et al. 2012). Studies of neural inflammation in brain of *LysM-Cre Nr3c1*$^{flox/flox}$ mice yielded conflicting results on role of macrophage GR expression. In studies from Sheela Vyasa' group, these mice suffered from more dopaminergic neuron loss following 1-methyl-4-phenyl-1,2,3,6-tetrahydropyridine intoxication treatment (Ros-Bernal, Hunot et al. 2011) and worse inflammation following LPS treatment (Carrillo-de Sauvage, Maatouk et al. 2013), whereas studies from Robert M. Sapolsky's group showed little or even protective effect of myeloid cell GR deletion in kainic acid induced excitotoxic injury model and focal cerebral ischemia model (Sorrells, Caso et al. 2013).

It is also worth noting that although very successful in relieving the inflammatory symptoms for a short time period, they have limited long term efficacy on disease progression (Townsend and Saag 2004). This is different to rodent studies, where disease progression is usually dramatically regressed associated with reduced inflammation following GC treatment. An understanding of the underlying mechanism behind the difference of GC's effects on animal and human arthritis would be helpful in clinics. Although there may be simple explanations such as more complex pathological activities in human arthritis, it is also possible that repeated administration of GCs in humans causes GC to lose properties required to modify disease progression but retain the ability to suppress inflammation.

8.5 Macrophage specific 11β-HSD1 deficiency in metabolism

Although preliminary data did not suggest a difference in GTT between MKO and control mice, it would be good to repeat the experiment with a larger group of mice. Based on the increased 'inflammatory' angiogenesis and impaired resolution of K/BxN arthritis, more inflammation and possible worse glucose metabolism would be expected in MKO mice on high fat diet feeding. However, less subcutaneous adipose fibrosis in MKO mice after HFD feeding is an indication of better adipose

remodelling, similar to that reported in the globally 11β-HSD1 deficient mice (Michailidou, Turban et al. 2012).

There is some evidence supporting that some degree of inflammation can be beneficial for glucose metabolism, although inflammation is generally believed to disrupt insulin sensitivity. For example, overexpression of NF-kB p65 (RelA) in adipose tissue in aP2-p65 transgenic mice or global inactivation of NF-kB p50 (NF-kB1) are both protective against insulin resistance with HFD feeding, despite elevated inflammatory cytokines (TNFα and IL6) in adipose tissues and serum (Tang, Zhang et al. 2010). Conversely, *Il6*$^{-/-}$ mice develop obesity, hepatosteatosis, liver inflammation and insulin resistance (Matthews, Allen et al. 2010) and IL6 was shown to be able to stimulate glucagon-like peptide-1 secretion (Ellingsgaard, Hauselmann et al. 2011). The IL6 secretion from adipocytes of globally 11β-HSD1 deficient mice was lower in chow fat diet feeding than the controls, but increased after HFD feeding, in contrast to the decrease in controls (Wamil, Battle et al. 2011).

8.6 Future studies

Increased 11β-HSD1 by various cytokines in leukocytes, especially in macrophages, is a possible endogenous brake to limit inflammation development. One of the likely mechanisms is that amplified GC action in macrophages would enhance the ability of macrophage phagocytosis to clear inflammatory cells. A better understanding of human monocyte/macrophage 11β-HSD1 expression in physiological and pathological conditions would help to exploit this for inflammatory disease treatment.

Healthy human monocytes can be induced to express 11β-HSD1 by in *vitro* treatment with IL4, TNFα, etc. and don't express 11β-HSD2 (Thieringer, Le Grand et al. 2001; Chinetti-Gbaguidi, Bouhlel et al. 2012). In human rheumatoid arthritis patients, blood monocyte 11β-HSD2 is transiently up-expressed in the early disease development (Olsen, Sokka et al. 2004) and synovial macrophages are found to co-express 11β-HSD1 and 11β-HSD2 (Schmidt, Weidler et al. 2005) or only 11β-HSD2

(Hardy, Rabbitt et al. 2008). This shift from 11β-HSD1 to 11β-HSD2 expression in macrophages between healthy and rheumatoid arthritis donors may be due to disease modification or drug treatment. And reduced ability to generate active GCs would perpetuate inflammation development. Ways of reversing this expression pattern, for example large dose of GC administration may benefit patients, as it reduces 11β-HSD2 but increases 11β-HSD1 expression (reviewed by (Chapman, Holmes et al. 2013)). It would be interesting to examine leukocyte, especially macrophage 11β-HSD1/11β-HSD2 expression in other inflammatory diseases such as systemic lupus erythematosus.

As evidence for high induction of 11β-HSD1 by inflammation in activated neutrophils is emerging (Chapman 2011), another area worthy of study is neutrophil 11β-HSD1 function. Neutrophil specific gene deletion can be achieved using *Mrp8-Cre* mice (Elliott, Van Ziffle et al. 2011). Although cortisone is showing little effect in delaying healthy human neutrophil apoptosis after overnight incubation (my data, not shown here), it appears possible that during inflammatory disease settings, 11β-HSD1 activity would be induced in neutrophils as happened at the RNA level after LPS stimulation (my data, not shown here).

From a translational point of view, one of the important implications from the study is that macrophages represent good targets for GCs. Macrophage targeted GC administration such as liposome encapsulated GC (which is already on the way (Crielaard, Lammers et al. 2011)), could provide lots of similar benefits to that of systemic GC use such as anti-inflammation and suppression of angiogenesis. In this way, metabolic side effects of GC use in clinics may be avoided. Regarding the use of 11β-HSD1 inhibitors to treat metabolic disease, this study raises caution of their possible side effects to delay recovery from inflammatory diseases.

References

(2011). "The Nobel Prize in Physiology or Medicine 2011." from http://www.nobelprize.org/nobel_prizes/medicine/laureates/2011/press.html.

Abraham, S. M., T. Lawrence, A. Kleiman, P. Warden, M. Medghalchi, J. Tuckermann, J. Saklatvala and A. R. Clark (2006). "Antiinflammatory effects of dexamethasone are partly dependent on induction of dual specificity phosphatase 1." Journal Of Experimental Medicine **203**(8): 1883-1889.

Adams, M., O. C. Meijer, J. A. Wang, A. Bhargava and D. Pearce (2003). "Homodimerization of the glucocorticoid receptor is not essential for response element binding: Activation of the phenylethanolamine N-methyltransferase gene by dimerization-defective mutants." Molecular Endocrinology **17**(12): 2583-2592.

Aguzzi, A., B. Barres and M. L. Bennett (2013). "Microglia: Scapegoat, Saboteur, or Something Else?" Science **339**(6116): 156-161.

Ahasan, M. M., R. Hardy, C. Jones, K. Kaur, D. Nanus, M. Juarez, S. A. Morgan, Z. Hassan-Smith, C. Benezech, J. H. Caamano, M. Hewison, G. Lavery, E. H. Rabbitt, A. R. Clark, A. Filer, C. D. Buckley, K. Raza, P. M. Stewart and M. S. Cooper (2012). "Inflammatory regulation of glucocorticoid metabolism in mesenchymal stromal cells." Arthritis and Rheumatism **64**(7): 2404-2413.

Ahasan, M. M., R. Hardy, C. Jones, K. Kaur, D. Nanus, M. Juarez, S. A. Morgan, Z. Hassan-Smith, C. Benezech, J. H. Caamano, M. Hewison, G. Lavery, E. H. Rabbitt, A. R. Clark, A. Filer, C. D. Buckley, K. Raza, P. M. Stewart and M. S. Cooper (2012). "Inflammatory regulation of glucocorticoid metabolism in mesenchymal stromal cells." Arthritis Rheum **64**(7): 2404-2413.

Alam, C. A. C.-N., Paul; Seed, Michael P. (2008). Modelling angiogenesis in inflammation. Angiogenesis in Inflammation: Machanisms and Clinical Correlates. D. A. W. Micheael P. Seed. Basel, Birkhäuser Verlag AG**:** 99-148.

Alexander V. Misharin, G. K. H. I. a. H. R. P. (2012). Non Classical Monocytes Are Required for Initiation Phase While Macrophages Are Necessary for the Resolution Phase in the K/BxN Murine of Inflammatory Arthritis. Annual Conference of Rheumatology, Washington.

Almeida, O. F. X., G. L. Conde, C. Crochemore, B. A. Demeneix, D. Fischer, A. H. S. Hassan, M. Meyer, F. Holsboer and T. M. Michaelidis (2000). "Subtle shifts in the ratio between pro- and antiapoptotic molecules after activation of corticosteroid receptors decide neuronal fate." Faseb Journal **14**(5): 779-790.

An, H., H. Xu, M. Zhang, J. Zhou, T. Feng, C. Qian, R. Qi and X. Cao (2005). "Src homology 2 domain-containing inositol-5-phosphatase 1 (SHIP1) negatively regulates TLR4-mediated LPS response primarily through a phosphatase activity- and PI-3K-independent mechanism." Blood **105**(12): 4685-4692.

Arriza, J. L., C. Weinberger, G. Cerelli, T. M. Glaser, B. L. Handelin, D. E. Housman and R. M. Evans (1987). "Cloning of human mineralocorticoid receptor complementary DNA: structural and functional kinship with the glucocorticoid receptor." Science **237**(4812): 268-275.

Arthur, N. (1958). Process for production of dienes by corynebacteria The United States, SCHERING CORP

Ashwell, J. D., F. W. M. Lu and M. S. Vacchio (2000). "Glucocorticoids in T cell development and function." Annual Review of Immunology **18**: 309-345.

Aubry, E. M. and A. Odermatt (2009). "Retinoic acid reduces glucocorticoid sensitivity in C2C12 myotubes by decreasing 11{beta}-hydroxysteroid dehydrogenase type 1 and glucocorticoid receptor activities." Endocrinology %R 10.1210/en.2008-1618: en.2008-1618.

Aubry, E. M. and A. Odermatt (2009). "Retinoic Acid Reduces Glucocorticoid Sensitivity in C2C12 Myotubes by Decreasing 11β-Hydroxysteroid Dehydrogenase Type 1 and Glucocorticoid Receptor Activities." Endocrinology **150**(6): 2700-2708.

Balachandran, A., H. Guan, M. Sellan, S. van Uum and K. Yang (2008). "Insulin and dexamethasone dynamically regulate adipocyte 11beta-hydroxysteroid dehydrogenase type 1." Endocrinology **149**(8): 4069-4079.

Baschant, U., L. Frappart, U. Rauchhaus, L. Bruns, H. M. Reichardt, T. Kamradt, R. Brauer and J. P. Tuckermann (2011). "Glucocorticoid therapy of antigen-induced arthritis depends on the dimerized glucocorticoid receptor in T cells." Proceedings of the National Academy of Sciences of the United States of America **108**(48): 19317-19322.

Baschant, U., L. Frappart, U. Rauchhaus, L. Bruns, H. M. Reichardt, T. Kamradt, R. Brauer and J. P. Tuckermann (2011). "Glucocorticoid therapy of antigen-induced arthritis depends on the dimerized glucocorticoid receptor in T cells." Proc Natl Acad Sci U S A **108**(48): 19317-19322.

Baschant, U., N. E. Lane and J. Tuckermann (2012). "The multiple facets of glucocorticoid action in rheumatoid arthritis." Nature Reviews Rheumatology **8**(11): 645-655.

Baschant, U., N. E. Lane and J. Tuckermann (2012). "The multiple facets of glucocorticoid action in rheumatoid arthritis." Nat Rev Rheumatol **8**(11): 645-655.

Bertini, R., M. Bianchi and P. Ghezzi (1988). "Adrenalectomy sensitizes mice to the lethal effects of interleukin 1 and tumor necrosis factor." J Exp Med **167**(5): 1708-1712.

Beyeler, C., B. Dick, B. H.A. and B. M. Frey (2012). "Regulation of 11β-Hydroxysteroid Dehydrogenase Type 1 and 2 in Rheumatoid Arthritis." International Journal of Clinical Medicine **3**(4): 254-262.

Bhattacharyya, S., D. E. Brown, J. A. Brewer, S. K. Vogt and L. J. Muglia (2007). "Macrophage glucocorticoid receptors regulate Toll-like receptor-4-mediated inflammatory responses by selective inhibition of p38 MAP kinase." Blood **109**: 4313-4319.

Bhattacharyya, S., D. E. Brown, J. A. Brewer, S. K. Vogt and L. J. Muglia (2007). "Macrophage glucocorticoid receptors regulate toll-like receptor 4-mediated inflammatory responses by selective inhibition of p38 MAP kinase." Blood **109**(10): 4313-4319.

Biedasek, K., J. Andres, K. Mai, S. Adams, S. Spuler, J. Fielitz and J. Spranger (2011). "Skeletal muscle 11beta-HSD1 controls glucocorticoid-induced

proteolysis and expression of E3 ubiquitin ligases atrogin-1 and MuRF-1." PLoS One **6**(1): e16674.
Binstadt, B. A., P. R. Patel, H. Alencar, P. A. Nigrovic, D. M. Lee, U. Mahmood, R. Weissleder, D. Mathis and C. Benoist (2006). "Particularities of the vasculature can promote the organ specificity of autoimmune attack." Nat Immunol **7**(3): 284-292.
Bittencourt, D., D. Y. Wu, K. W. Jeong, D. S. Gerke, L. Herviou, I. Ianculescu, R. Chodankar, K. D. Siegmund and M. R. Stallcup (2012). "G9a functions as a molecular scaffold for assembly of transcriptional coactivators on a subset of Glucocorticoid Receptor target genes." Proceedings of the National Academy of Sciences of the United States of America **109**(48): 19673-19678.
Bolt, M. J., F. Stossi, J. Y. Newberg, A. Orjalo, H. E. Johansson and M. A. Mancini (2013). "Coactivators enable glucocorticoid receptor recruitment to fine-tune estrogen receptor transcriptional responses." Nucleic Acids Research **41**(7): 4036-4048.
Bosanac, I., H. R. Maun, S. J. Scales, X. H. Wen, A. Lingel, J. F. Bazan, F. J. de Sauvage, S. G. Hymowitz and R. A. Lazarus (2009). "The structure of SHH in complex with HHIP reveals a recognition role for the Shh pseudo active site in signaling." Nature Structural & Molecular Biology **16**(7): 691-U628.
Brattsand, R. L., B. T. Af Ekenstam, K. G. Claeson and B. A. Thalen (1975). Steroids, processes for their manufacture and preparations containing same AB Bofors **3929768**
Brennan-Speranza, T. C., H. Henneicke, S. J. Gasparini, K. I. Blankenstein, U. Heinevetter, V. C. Cogger, D. Svistounov, Y. Zhang, G. J. Cooney, F. Buttgereit, C. R. Dunstan, C. Gundberg, H. Zhou and M. J. Seibel (2012). "Osteoblasts mediate the adverse effects of glucocorticoids on fuel metabolism." J Clin Invest **122**(11): 4172-4189.
Bridgham, J. T., S. M. Carroll and J. W. Thornton (2006). "Evolution of hormone-receptor complexity by molecular exploitation." Science **312**(5770): 97-101.
Bujalska, I. J., N. Draper, Z. Michailidou, J. W. Tomlinson, P. C. White, K. E. Chapman, E. A. Walker and P. M. Stewart (2005). "Hexose-6-phosphate dehydrogenase confers oxo-reductase activity upon 11β-hydroxysteroid dehydrogenase type 1." Journal of Molecular Endocrinology **34**(3): 675-684.
Bujalska, I. J., N. Draper, Z. Michailidou, J. W. Tomlinson, P. C. White, K. E. Chapman, E. A. Walker and P. M. Stewart (2005). "Hexose-6-phosphate dehydrogenase confers oxo-reductase activity upon 11β-hydroxysteroid dehydrogenase type 1." J Mol Endocrinol **34**(3): 675-684.
Buren, J., Y. C. Lai, M. Lundgren, J. W. Eriksson and J. Jensen (2008). "Insulin action and signalling in fat and muscle from dexamethasone-treated rats." Archives of Biochemistry and Biophysics **474**(1): 91-101.
Bystrom, J., I. Evans, J. Newson, M. Stables, I. Toor, N. van Rooijen, M. Crawford, P. Colville-Nash, S. Farrow and D. W. Gilroy (2008). "Resolution-phase macrophages possess a unique inflammatory phenotype that is controlled by cAMP." Blood **112**(10): 4117-4127.
Carrick, D. M., W. S. Lai and P. J. Blackshear (2004). "The tandem CCCH zinc finger protein tristetraprolin and its relevance to cytokine mRNA turnover and arthritis." Arthritis Research & Therapy **6**(6): 248-264.

Carrillo-de Sauvage, M. A., L. Maatouk, I. Arnoux, M. Pasco, A. Sanz Diez, M. Delahaye, M. T. Herrero, T. A. Newman, C. F. Calvo, E. Audinat, F. Tronche and S. Vyas (2013). "Potent and multiple regulatory actions of microglial glucocorticoid receptors during CNS inflammation." Cell Death Differ.

Carter, R. N., J. M. Paterson, U. Tworowska, D. J. Stenvers, J. J. Mullins, J. R. Seckl and M. C. Holmes (2009). "Hypothalamic-Pituitary-Adrenal Axis Abnormalities in Response to Deletion of 11 beta-HSD1 is Strain-Dependent." Journal of Neuroendocrinology **21**(11): 879-887.

Carter, R. N., J. M. Paterson, U. Tworowska, D. J. Stenvers, J. J. Mullins, J. R. Seckl and M. C. Holmes (2009). "Hypothalamic-Pituitary-Adrenal Axis Abnormalities in Response to Deletion of 11β-HSD1 is Strain-Dependent." J Neuroendocrinol **21**(11): 879-887.

Carter, R. N., U. Tworowska, J. R. Seckl and M. C. Holmes (2006). "11β-hydroxysteroid dehydrogenase modulation of HPA function - importance of genetic background." Endocrine Abstracts (2006) 11 OC39 **OC39**.

Chapman, A. E. C. T. K. Z. Z. C. E. J. S. G. J.-F. C. J. H. J. R. S. J. S. S. K. E. (2011). Dynamic Regulation of 11β-Hydroxysteroid Dehydrogenase Type 1 in Neutrophils during an Inflammatory Response ENDO Meeting 2011.

Chapman, K., M. Holmes and J. Seckl (2013). "11beta-hydroxysteroid dehydrogenases: intracellular gate-keepers of tissue glucocorticoid action." Physiol Rev **93**(3): 1139-1206.

Chapman, K. E., A. E. Coutinho, M. Gray, J. S. Gilmour, J. S. Savill and J. R. Seckl (2009). "The role and regulation of 11beta-hydroxysteroid dehydrogenase type 1 in the inflammatory response." Mol Cell Endocrinol **301**(1-2): 123-131.

Chapman, K. E., A. E. Coutinho, Z. Zhang, T. Kipari, J. S. Savill and J. R. Seckl (2013). "Changing glucocorticoid action: 11beta-Hydroxysteroid dehydrogenase type 1 in acute and chronic inflammation." J Steroid Biochem Mol Biol.

Chen, G. Y. and G. Nunez (2010). "Sterile inflammation: sensing and reacting to damage." Nat Rev Immunol **10**(12): 826-837.

Chinetti-Gbaguidi, G., M. A. Bouhlel, C. Copin, C. Duhem, B. Derudas, B. Neve, B. Noel, J. Eeckhoute, P. Lefebvre, J. R. Seckl and B. Staels (2012). "Peroxisome proliferator-activated receptor-gamma activation induces 11beta-hydroxysteroid dehydrogenase type 1 activity in human alternative macrophages." Arterioscler Thromb Vasc Biol **32**(3): 677-685.

Chisaka, H., J. F. Johnstone, M. Premyslova, Z. Manduch and J. R. Challis (2005). "Effect of pro-inflammatory cytokines on expression and activity of 11beta-hydroxysteroid dehydrogenase type 2 in cultured human term placental trophoblast and human choriocarcinoma JEG-3 cells." J Soc Gynecol Investig **12**(5): 303-309.

Cho, I. H., J. Hong, E. C. Suh, J. H. Kim, H. Lee, J. E. Lee, S. Lee, C. H. Kim, D. W. Kim, E. K. Jo, K. E. Lee, M. Karin and S. J. Lee (2008). "Role of microglial IKK in kainic acid-induced hippocampal neuronal cell death." Brain **131**: 3019-3033.

Chou, R. C., N. D. Kim, C. D. Sadik, E. Seung, Y. Lan, M. H. Byrne, B. Haribabu, Y. Iwakura and A. D. Luster (2010). "Lipid-Cytokine-Chemokine Cascade

Drives Neutrophil Recruitment in a Murine Model of Inflammatory Arthritis." Immunity **33**(2): 266-278.
Christy, C., P. W. Hadoke, J. M. Paterson, J. J. Mullins, J. R. Seckl and B. R. Walker (2003). "11beta-hydroxysteroid dehydrogenase type 2 in mouse aorta: localization and influence on response to glucocorticoids." Hypertension **42**(4): 580-587.
Christy, C., P. W. F. Hadoke, J. M. Paterson, J. J. Mullins, J. R. Seckl and B. R. Walker (2003). "11β-Hydroxysteroid Dehydrogenase Type 2 in Mouse Aorta." Hypertension **42**(4): 580-587.
Clark, A. R. (2007). "Anti-inflammatory functions of glucocorticoid-induced genes." Mol Cell Endocrinol **275**(1-2): 79-97.
Clausen, B. E., C. Burkhardt, W. Reith, R. Renkawitz and I. Forster (1999). "Conditional gene targeting in macrophages and granulocytes using LysMcre mice." Transgenic Research **8**(4): 265-277.
Constant, S. L. and K. Bottomly (1997). "Induction of Th1 and Th2 CD4+ T cell responses: the alternative approaches." Annu Rev Immunol **15**: 297-322.
Costa, C., J. Incio and R. Soares (2007). "Angiogenesis and chronic inflammation: cause or consequence?" Angiogenesis **10**(3): 149-166.
Coutinho, A. E. (2009). Consequences of 11β-hydroxysteroid dehydrogenase deficiency during inflammatory responses. Ph.D, The University of Edinburgh.
Coutinho, A. E., J. K. Brown, F. Yang, D. G. Brownstein, M. Gray, J. R. Seckl, J. S. Savill and K. E. Chapman (2013). "Mast cells express 11beta-hydroxysteroid dehydrogenase type 1: a role in restraining mast cell degranulation." PLoS One **8**(1): e54640.
Coutinho, A. E., M. Gray, D. G. Brownstein, D. M. Salter, D. A. Sawatzky, S. Clay, J. S. Gilmour, J. R. Seckl, J. S. Savill and K. E. Chapman (2012). "11β-Hydroxysteroid Dehydrogenase Type 1, But Not Type 2, Deficiency Worsens Acute Inflammation and Experimental Arthritis in Mice." Endocrinology **153**(1): 234-240.
Cox, G. (1995). "Glucocorticoid Treatment Inhibits Apoptosis in Human Neutrophils - Separation of Survival and Activation Outcomes." Journal of Immunology **154**(9): 4719-4725.
Cramer, T., Y. Yamanishi, B. E. Clausen, I. Forster, R. Pawlinski, N. Mackman, V. H. Haase, R. Jaenisch, M. Corr, V. Nizet, G. S. Firestein, H. P. Gerber, N. Ferrara and R. S. Johnson (2003). "HIF-1 alpha is essential for myeloid cell-mediated inflammation (vol 112, pg 648, 2003)." Cell **113**(3): 419-419.
Cramer, T., Y. Yamanishi, B. E. Clausen, I. Forster, R. Pawlinski, N. Mackman, V. H. Haase, R. Jaenisch, M. Corr, V. Nizet, G. S. Firestein, H. P. Gerber, N. Ferrara and R. S. Johnson (2003). "HIF-1alpha is essential for myeloid cell-mediated inflammation." Cell **112**(5): 645-657.
Crielaard, B. J., T. Lammers, M. E. Morgan, L. Chaabane, S. Carboni, B. Greco, P. Zaratin, A. D. Kraneveld and G. Storm (2011). "Macrophages and liposomes in inflammatory disease: friends or foes?" Int J Pharm **416**(2): 499-506.
Dahlman-Wright, K., A. Wright, J. A. Gustafsson and J. Carlstedt-Duke (1991). "Interaction of the glucocorticoid receptor DNA-binding domain with DNA

as a dimer is mediated by a short segment of five amino acids." J Biol Chem **266**(5): 3107-3112.
Daley, J. M., S. K. Brancato, A. A. Thomay, J. S. Reichner and J. E. Albina (2010). "The phenotype of murine wound macrophages." Journal of Leukocyte Biology **87**(1): 59-67.
David, T., N. L. Wendler and H. L. Slates (1962). Novel 16-alkyl and 16-alkylene steroids and processes,. The United States, MERCK & CO INC **3053865**.
Davies, L. C., M. Rosas, P. J. Smith, D. J. Fraser, S. A. Jones and P. R. Taylor (2011). "A quantifiable proliferative burst of tissue macrophages restores homeostatic macrophage populations after acute inflammation." European Journal of Immunology **41**(8): 2155-2164.
De Palma, M., M. A. Venneri, R. Galli, L. S. Sergi, L. S. Politi, M. Sampaolesi and L. Naldini (2005). "Tie2 identifies a hematopoietic monocytes required for tumor lineage of proangiogenic vessel formation and a mesenchymal population of pericyte progenitors." Cancer Cell **8**(3): 211-226.
De Sousa Peixoto, R. A., S. Turban, J. H. Battle, K. E. Chapman, J. R. Seckl and N. M. Morton (2008). "Preadipocyte 11β-Hydroxysteroid Dehydrogenase Type 1 Is a Keto-Reductase and Contributes to Diet-Induced Visceral Obesity in Vivo." Endocrinology **149**(4): 1861-1868.
Dessaud, E., A. P. McMahon and J. Briscoe (2008). "Pattern formation in the vertebrate neural tube: a sonic hedgehog morphogen-regulated transcriptional network." Development **135**(15): 2489-2503.
Diamond, M. I., J. N. Miner, S. K. Yoshinaga and K. R. Yamamoto (1990). "Transcription factor interactions: selectors of positive or negative regulation from a single DNA element." Science **249**(4974): 1266-1272.
Dickmeis, T. (2009). "Glucocorticoids and the circadian clock." Journal of Endocrinology **200**(1): 3-22.
Ditzel, H. J. (2004). "The K/BxN mouse: a model of human inflammatory arthritis." Trends in molecular medicine **10**(1): 40-45.
Draper, N., S. M. Echwald, G. G. Lavery, E. A. Walker, R. Fraser, E. Davies, T. I. A. Sorensen, A. Astrup, J. Adamski, M. Hewison, J. M. Connell, O. Pedersen and P. M. Stewart (2002). "Association studies between microsatellite markers within the gene encoding human 11 beta-hydroxysteroid dehydrogenase type 1 and body mass index, waist to hip ratio, and glucocorticoid metabolism." Journal of Clinical Endocrinology & Metabolism **87**(11): 4984-4990.
Duffield, J. S., S. J. Forbes, C. M. Constandinou, S. Clay, M. Partolina, S. Vuthoori, S. Wu, R. Lang and J. P. Iredale (2005). "Selective depletion of macrophages reveals distinct, opposing roles during liver injury and repair." J Clin Invest **115**(1): 56-65.
Duffield, J. S., S. J. Forbes, C. M. Constandinou, S. Clay, M. Partolina, S. Vuthoori, S. J. Wu, R. Lang and J. P. Iredale (2005). "Selective depletion of macrophages reveals distinct, opposing roles during liver injury and repair." Journal of Clinical Investigation **115**(1): 56-65.
Dujic, T., T. Bego, B. Mlinar, S. Semiz, M. Malenica, B. Prnjavorac, B. Ostanek, J. Marc and A. Causevic (2012). "Association between 11beta-hydroxysteroid

dehydrogenase type 1 gene polymorphisms and metabolic syndrome in Bosnian population." Biochem Med (Zagreb) **22**(1): 76-85.
Echelard, Y., D. J. Epstein, B. Stjacques, L. Shen, J. Mohler, J. A. Mcmahon and A. P. Mcmahon (1993). "Sonic-Hedgehog, a Member of a Family of Putative Signaling Molecules, Is Implicated in the Regulation of Cns Polarity." Cell **75**(7): 1417-1430.
Ehrchen, J., L. Steinmuller, K. Barczyk, K. Tenbrock, W. Nacken, M. Eisenacher, U. Nordhues, C. Sorg, C. Sunderkotter and J. Roth (2007). "Glucocorticoids induce differentiation of a specifically activated, anti-inflammatory subtype of human monocytes." Blood **109**(3): 1265-1274.
Ellingsgaard, H., I. Hauselmann, B. Schuler, A. M. Habib, L. L. Baggio, D. T. Meier, E. Eppler, K. Bouzakri, S. Wueest, Y. D. Muller, A. M. K. Hansen, M. Reinecke, D. Konrad, M. Gassmann, F. Reimann, P. A. Halban, J. Gromada, D. J. Drucker, F. M. Gribble, J. A. Ehses and M. Y. Donath (2011). "Interleukin-6 enhances insulin secretion by increasing glucagon-like peptide-1 secretion from L cells and alpha cells." Nature Medicine **17**(11): 1481-U1500.
Elliott, E. R., J. A. Van Ziffle, P. Scapini, B. M. Sullivan, R. M. Locksley and C. A. Lowell (2011). "Deletion of Syk in Neutrophils Prevents Immune Complex Arthritis." The Journal of Immunology **187**(8): 4319-4330.
Elliott, E. R., J. A. Van Ziffle, P. Scapini, B. M. Sullivan, R. M. Locksley and C. A. Lowell (2011). "Deletion of Syk in Neutrophils Prevents Immune Complex Arthritis." Journal of Immunology **187**(8): 4319-4330.
Engeli, S., J. Bohnke, M. Feldpausch, K. Gorzelniak, U. Heintze, J. Janke, F. C. Luft and A. M. Sharma (2004). "Regulation of 11 beta-HSD genes in human adipose tissue: Influence of central obesity and weight loss." Obesity Research **12**(1): 9-17.
Ergang, P., P. Leden, K. Vagnerova, P. Klusonova, I. Miksik, J. Jurcovicova, M. Kment and J. Pacha (2010). "Local metabolism of glucocorticoids and its role in rat adjuvant arthritis." Mol Cell Endocrinol **323**(2): 155-160.
Ergang, P., P. Leden, K. Vagnerová, P. Klusonová, I. Miksík, J. Jurcovicová, M. Kment and J. Pácha (2010). "Local metabolism of glucocorticoids and its role in rat adjuvant arthritis." Molecular and Cellular Endocrinology **323**(2): 155-160.
Erika Harno, E. C. C., Joanne DeSchoolmeester, Andrew V Turnbull, Brendan Leighton, Anne White (2013). Knockdown of brain 11β-HSD1 does not lower body weight or improve insulin sensitivity. Society for Endocrinology BES 2013, Harrogate, UK.
Escher, G., I. Galli, B. S. Vishwanath, B. M. Frey and F. J. Frey (1997). "Tumor necrosis factor alpha and interleukin 1beta enhance the cortisone/cortisol shuttle." J Exp Med **186**(2): 189-198.
Esteves, C. L., V. Kelly, V. Begay, T. Y. Man, N. M. Morton, A. Leutz, J. R. Seckl and K. E. Chapman (2012). "Regulation of adipocyte 11beta-hydroxysteroid dehydrogenase type 1 (11beta-HSD1) by CCAAT/enhancer-binding protein (C/EBP) beta isoforms, LIP and LAP." PLoS One **7**(5): e37953.
Fadok, V. A., D. L. Bratton, A. Konowal, P. W. Freed, J. Y. Westcott and P. M. Henson (1998). "Macrophages that have ingested apoptotic cells in vitro

inhibit proinflammatory cytokine production through autocrine/paracrine mechanisms involving TGF-beta, PGE2, and PAF." Journal of Clinical Investigation **101**(4): 890-898.

Fantin, A., J. M. Vieira, G. Gestri, L. Denti, Q. Schwarz, S. Prykhozhij, F. Peri, S. W. Wilson and C. Ruhrberg (2010). "Tissue macrophages act as cellular chaperones for vascular anastomosis downstream of VEGF-mediated endothelial tip cell induction." Blood **116**(5): 829-840.

Felcht, M., R. Luck, A. Schering, P. Seidel, K. Srivastava, J. H. Hu, A. Bartol, Y. Kienast, C. Vettel, E. K. Loos, S. Kutschera, S. Bartels, S. Appak, E. Besemfelder, D. Terhardt, E. Chavakis, T. Wieland, C. Klein, M. Thomas, A. Uemura, S. Goerdt and H. G. Augustin (2012). "Angiopoietin-2 differentially regulates angiogenesis through TIE2 and integrin signaling." Journal of Clinical Investigation **122**(6): 1991-2005.

Feng, Y., S. L. Huang, W. Dou, S. Zhang, J. H. Chen, Y. Shen, J. H. Shen and Y. Leng (2010). "Emodin, a natural product, selectively inhibits 11beta-hydroxysteroid dehydrogenase type 1 and ameliorates metabolic disorder in diet-induced obese mice." Br J Pharmacol **161**(1): 113-126.

Flaster, H., J. Bernhagen, T. Calandra and R. Bucala (2007). "The macrophage migration inhibitory factor-glucocorticoid dyad: Regulation of inflammation and immunity." Molecular Endocrinology **21**(6): 1267-1280.

Flavell, S. J., T. Z. Hou, S. Lax, A. D. Filer, M. Salmon and C. D. Buckley (2008). "Fibroblasts as novel therapeutic targets in chronic inflammation." British Journal of Pharmacology **153**: S241-S246.

Folkman, J., R. Langer, R. J. Linhardt, C. Haudenschild and S. Taylor (1983). "Angiogenesis Inhibition and Tumor-Regression Caused by Heparin or a Heparin Fragment in the Presence of Cortisone." Science **221**(4612): 719-725.

Freedman, L. P. (1999). "Increasing the complexity of coactivation in nuclear receptor signaling." Cell **97**(1): 5-8.

Freeman, L., M. Hewison, S. V. Hughes, K. N. Evans, D. Hardie, T. K. Means and R. Chakraverty (2005). "Expression of 11beta-hydroxysteroid dehydrogenase type 1 permits regulation of glucocorticoid bioavailability by human dendritic cells." Blood **106**(6): 2042-2049.

Friedman, J. E., J. S. Yun, Y. M. Patel, M. M. Mcgrane and R. W. Hanson (1993). "Glucocorticoids Regulate the Induction of Phosphoenolpyruvate Carboxykinase (Gtp) Gene-Transcription during Diabetes." Journal of Biological Chemistry **268**(17): 12952-12957.

Frieler, R. A., H. Meng, S. Z. Duan, S. Berger, G. Schutz, Y. He, G. Xi, M. M. Wang and R. M. Mortensen (2011). "Myeloid-specific deletion of the mineralocorticoid receptor reduces infarct volume and alters inflammation during cerebral ischemia." Stroke **42**(1): 179-185.

Frieler, R. A., J. J. Ray, H. Meng, S. P. Ramnarayanan, M. G. Usher, E. J. Su, S. Berger, D. J. Pinsky, D. A. Lawrence, M. M. Wang and R. M. Mortensen (2012). "Myeloid mineralocorticoid receptor during experimental ischemic stroke: effects of model and sex." J Am Heart Assoc **1**(5): e002584.

Funder, J. W., D. Feldman and I. S. Edelman (1973). "The roles of plasma binding and receptor specificity in the mineralocorticoid action of aldosterone." Endocrinology **92**(4): 994-1004.
Funder, J. W., P. T. Pearce, R. Smith and A. I. Smith (1988). "Mineralocorticoid action: target tissue specificity is enzyme, not receptor, mediated." Science **242**(4878): 583-585.
Gaillard, D., M. Wabitsch, B. Pipy and R. Negrel (1991). "Control of terminal differentiation of adipose precursor cells by glucocorticoids." J Lipid Res **32**(4): 569-579.
Gallily, R., A. Warwick and F. B. Bang (1964). "Effect of Cortisone of Genetic Resistance to Mouse Hepatitis Virus in Vivo and in Vitro." Proc Natl Acad Sci U S A **51**: 1158-1164.
Gambineri, A., F. Tomassoni, A. Munarini, R. H. Stimson, R. Mioni, U. Pagotto, K. E. Chapman, R. Andrew, V. Mantovani, R. Pasquali and B. R. Walker (2011). "A combination of polymorphisms in HSD11B1 associates with in vivo 11{beta}-HSD1 activity and metabolic syndrome in women with and without polycystic ovary syndrome." Eur J Endocrinol **165**(2): 283-292.
Garcia, R. A., D. J. Search, J. A. Lupisella, J. Ostrowski, B. Guan, J. Chen, W. P. Yang, A. Truong, A. He, R. Zhang, M. Yan, S. E. Hellings, P. S. Gargalovic, C. S. Ryan, L. M. Watson, R. A. Langish, P. A. Shipkova, N. L. Carson, J. R. Taylor, R. Yang, G. C. Psaltis, T. W. Harrity, J. A. Robl and D. A. Gordon (2013). "11beta-hydroxysteroid dehydrogenase type 1 gene knockout attenuates atherosclerosis and in vivo foam cell formation in hyperlipidemic apoE(-)/(-) mice." PLoS One **8**(2): e53192.
Garcia, R. A., D. J. Search, J. A. Lupisella, J. Ostrowski, B. Guan, J. Chen, W. P. Yang, A. Truong, A. Q. He, R. G. Zhang, M. J. Yan, S. E. Hellings, P. S. Gargalovic, C. S. Ryan, L. M. Watson, R. A. Langish, P. A. Shipkova, N. L. Carson, J. R. Taylor, R. Yang, G. C. Psaltis, T. W. Harrity, J. A. Robl and D. A. Gordon (2013). "11 beta-Hydroxysteroid Dehydrogenase Type 1 Gene Knockout Attenuates Atherosclerosis and In Vivo Foam Cell Formation in Hyperlipidemic apoE(-/-) Mice." PLoS One **8**(2).
Gathercole, L. L., G. G. Lavery, S. A. Morgan, M. S. Cooper, A. J. Sinclair, J. W. Tomlinson and P. M. Stewart (2013). "11beta-Hydroxysteroid Dehydrogenase 1: Translational and Therapeutic Aspects." Endocr Rev.
Gautier, E. L., T. Shay, J. Miller, M. Greter, C. Jakubzick, S. Ivanov, J. Helft, A. Chow, K. G. Elpek, S. Gordonov, A. R. Mazloom, A. Ma'ayan, W. J. Chua, T. H. Hansen, S. J. Turley, M. Merad, G. J. Randolph and I. G. Consortium (2012). "Gene-expression profiles and transcriptional regulatory pathways that underlie the identity and diversity of mouse tissue macrophages." Nature Immunology **13**(11): 1118-1128.
Geissmann, F., S. Gordon, D. A. Hume, A. M. Mowat and G. J. Randolph (2010). "Unravelling mononuclear phagocyte heterogeneity." Nature Reviews Immunology **10**(6): 453-U492.
Georges, M., B. Roland and J. Jean (1961). Process for the fluorination of 9beta, 11beta-epoxy and 5alpha, 6alpha-epoxy steroids The United States, Lab, Francais Chimiotherapie DE. .

Giles, K. M., K. Ross, A. G. Rossi, N. A. Hotchin, C. Haslett and I. Dransfield (2001). "Glucocorticoid augmentation of macrophage capacity for phagocytosis of apoptotic cells is associated with reduced p130Cas expression, loss of paxillin/pyk2 phosphorylation, and high levels of active Rac." Journal of Immunology **167**(2): 976-986.

Gilmour, J. S., A. E. Coutinho, J. F. Cailhier, T. Y. Man, M. Clay, G. Thomas, H. J. Harris, J. J. Mullins, J. R. Seckl, J. S. Savill and K. E. Chapman (2006). "Local amplification of glucocorticoids by 11 beta-hydroxysteroid dehydrogenase type 1 promotes macrophage phagocytosis of apoptotic leukocytes." J Immunol **176**(12): 7605-7611.

Gilmour, J. S., A. E. Coutinho, J. F. Cailhier, T. Y. Man, M. Clay, G. Thomas, H. J. Harris, J. J. Mullins, J. R. Seckl, J. S. Savill and K. E. Chapman (2006). "Local amplification of Glucocorticoids by 11 beta-hydroxysteroid dehydrogenase type 1 promotes macrophage phagocytosis of apoptotic leukocytes." Journal of Immunology **176**(12): 7605-7611.

Gilmour, J. S., A. E. Coutinho, J. F. Cailhier, T. Y. Man, M. Clay, G. Thomas, H. J. Harris, J. J. Mullins, J. R. Seckl, J. S. Savill and K. E. Chapman (2006). "Local amplification of glucocorticoids by 11β-hydroxysteroid dehydrogenase type 1 promotes macrophage phagocytosis of apoptotic leukocytes." J Immunol **176**(12): 7605-7611.

Gomez, F., E. R. De Kloet and A. Armario (1998). "Glucocorticoid negative feedback on the HPA axis in five inbred rat strains." American Journal of Physiology-Regulatory Integrative and Comparative Physiology **274**(2): R420-R427.

Gong, R., D. J. Morris and A. S. Brem (2008). "Variable expression of 11β Hydroxysteroid dehydrogenase (11β-HSD) isoforms in vascular endothelial cells." Steroids **73**(11): 1187-1196.

Gordon, S. (2012). "Macrophage Heterogeneity A Personal Scientific Journey." Arteriosclerosis Thrombosis and Vascular Biology **32**(6): 1339-1342.

Gordon, S. and F. O. Martinez (2010). "Alternative Activation of Macrophages: Mechanism and Functions." Immunity **32**(5): 593-604.

Goren, I., N. Allmann, N. Yogev, C. Schurmann, A. Linke, M. Holdener, A. Waisman, J. Pfeilschifter and S. Frank (2009). "A Transgenic Mouse Model of Inducible Macrophage Depletion: Effects of Diphtheria Toxin-Driven Lysozyme M-Specific Cell Lineage Ablation on Wound Inflammatory, Angiogenic, and Contractive Processes." Am J Pathol **175**(1): 132-147.

Goren, I., N. Allmann, N. Yogev, C. Schurmann, A. Linke, M. Holdener, A. Waisman, J. Pfeilschifter and S. Frank (2009). "A transgenic mouse model of inducible macrophage depletion: effects of diphtheria toxin-driven lysozyme M-specific cell lineage ablation on wound inflammatory, angiogenic, and contractive processes." Am J Pathol **175**(1): 132-147.

Gorgoni, B., D. Maritano, P. Marthyn, M. Righi and V. Poli (2002). "C/EBP beta gene inactivation causes both impaired and enhanced gene expression and inverse regulation of IL-12 p40 and p35 mRNAs in macrophages." J Immunol **168**(8): 4055-4062.

Grontved, L., S. John, S. Baek, Y. Liu, J. R. Buckley, C. Vinson, G. Aguilera and G. L. Hager (2013). "C/EBP maintains chromatin accessibility in liver and

facilitates glucocorticoid receptor recruitment to steroid response elements." EMBO J **advance online publication**.
H, P. G., B. B. M, S. I. P and W. Christopher (1982). Androstane carbothioates, Glaxo Group. **4335121**.
Hadidi, S., F. Antignano, M. R. Hughes, S. K. Wang, K. Snyder, G. M. Sammis, W. G. Kerr, K. M. McNagny and C. Zaph (2012). "Myeloid cell-specific expression of Ship1 regulates IL-12 production and immunity to helminth infection." Mucosal Immunol **5**(5): 535-543.
Hadoke, P. W., T. Kipari, J. R. Seckl and K. E. Chapman (2013). "Modulation of 11beta-hydroxysteroid dehydrogenase as a strategy to reduce vascular inflammation." Curr Atheroscler Rep **15**(5): 320.
Hadoke, P. W., L. Macdonald, J. J. Logie, G. R. Small, A. R. Dover and B. R. Walker (2006). "Intra-vascular glucocorticoid metabolism as a modulator of vascular structure and function." Cell Mol Life Sci **63**(5): 565-578.
Halberg, N., T. Khan, M. E. Trujillo, I. Wernstedt-Asterholm, A. D. Attie, S. Sherwani, Z. V. Wang, S. Landskroner-Eiger, S. Dineen, U. J. Magalang, R. A. Brekken and P. E. Scherer (2009). "Hypoxia-inducible factor 1alpha induces fibrosis and insulin resistance in white adipose tissue." Mol Cell Biol **29**(16): 4467-4483.
Hammond, G. L., C. L. Smith, N. A. M. Paterson and W. J. Sibbald (1990). "A Role for Corticosteroid-Binding Globulin in Delivery of Cortisol to Activated Neutrophils." Journal of Clinical Endocrinology & Metabolism **71**(1): 34-45.
Hardy, R., E. H. Rabbitt, A. Filer, P. Emery, M. Hewison, P. M. Stewart, N. J. Gittoes, C. D. Buckley, K. Raza and M. S. Cooper (2008). "Local and systemic glucocorticoid metabolism in inflammatory arthritis." Ann Rheum Dis **67**(9): 1204-1210.
Hardy, R., E. H. Rabbitt, A. Filer, P. Emery, M. Hewison, P. M. Stewart, N. J. Gittoes, C. D. Buckley, K. Raza and M. S. Cooper (2008). "Local and systemic glucocorticoid metabolism in inflammatory arthritis." Annals of the Rheumatic Diseases **67:**: 1204-1210.
Hardy, R. S., A. Filer, M. S. Cooper, G. Parsonage, K. Raza, D. L. Hardie, E. H. Rabbitt, P. M. Stewart, C. D. Buckley and M. Hewison (2006). "Differential expression, function and response to inflammatory stimuli of 11beta-hydroxysteroid dehydrogenase type 1 in human fibroblasts: a mechanism for tissue-specific regulation of inflammation." Arthritis Res Ther **8**(4): R108.
Hardy, R. S., M. J. Seibel and M. S. Cooper (2013). "Targeting 11beta-hydroxysteroid dehydrogenases: a novel approach to manipulating local glucocorticoid levels with implications for rheumatic disease." Curr Opin Pharmacol.
Harno, E., E. C. Cottrell, B. G. Keevil, J. DeSchoolmeester, M. Bohlooly-Y, H. Andersén, A. V. Turnbull, B. Leighton and A. White (2013). "11-Dehydrocorticosterone causes metabolic syndrome which is prevented when 11β-HSD1 is knocked-out in livers of male mice." Endocrinology.
Harno, E. and A. White (2010). "Will treating diabetes with 11beta-HSD1 inhibitors affect the HPA axis?" Trends Endocrinol Metab **21**(10): 619-627.
Harris, H. J., Y. Kotelevtsev, J. J. Mullins, J. R. Seckl and M. C. Holmes (2001). "Intracellular regeneration of glucocorticoids by 11 beta-hydroxysteroid

dehydrogenase (11 beta-HSD)-1 plays a key role in regulation of the hypothalamic-pituitary-adrenal axis: Analysis of 11 beta-HSD-1-deficient mice." Endocrinology **142**(1): 114-120.

Harris, H. J., Y. Kotelevtsev, J. J. Mullins, J. R. Seckl and M. C. Holmes (2001). "Intracellular Regeneration of Glucocorticoids by 11{beta}-Hydroxysteroid Dehydrogenase (11{beta}-HSD)-1 Plays a Key Role in Regulation of the Hypothalamic-Pituitary-Adrenal Axis: Analysis of 11{beta}-HSD-1-Deficient Mice." Endocrinology **142**(1): 114-120.

Hashimoto, D., A. Chow, C. Noizat, P. Teo, M. B. Beasley, M. Leboeuf, C. D. Becker, P. See, J. Price, D. Lucas, M. Greter, A. Mortha, S. W. Boyer, E. C. Forsberg, M. Tanaka, N. van Rooijen, A. Garcia-Sastre, E. R. Stanley, F. Ginhoux, P. S. Frenette and M. Merad (2013). "Tissue-resident macrophages self-maintain locally throughout adult life with minimal contribution from circulating monocytes." Immunity **38**(4): 792-804.

Hawes, A. S., C. S. Rock, C. V. Keogh, S. F. Lowry and S. E. Calvano (1992). "In vivo effects of the antiglucocorticoid RU 486 on glucocorticoid and cytokine responses to Escherichia coli endotoxin." Infect Immun **60**(7): 2641-2647.

Heck, S., M. Kullmann, A. Gast, H. Ponta, H. J. Rahmsdorf, P. Herrlich and A. C. Cato (1994). "A distinct modulating domain in glucocorticoid receptor monomers in the repression of activity of the transcription factor AP-1." EMBO J **13**(17): 4087-4095.

Heine, V. M. and D. H. Rowitch (2009). "Hedgehog signaling has a protective effect in glucocorticoid-induced mouse neonatal brain injury through an 11 beta HSD2-dependent mechanism." Journal of Clinical Investigation **119**(2): 267-277.

Held, T. K., W. H. Xiao, Y. Liang, D. V. Kalvakolanu and A. S. Cross (1999). "Gamma interferon augments macrophage activation by lipopolysaccharide by two distinct mechanisms, at the signal transduction level and via an autocrine mechanism involving tumor necrosis factor alpha and interleukin-1." Infection and Immunity **67**(1): 206-212.

Hench, P. S., C. H. Slocumb, H. F. Polley and E. C. Kendall (1950). "Effect of Cortisone and Pituitary Adrenocorticotropic Hormone (Acth) on Rheumatic Diseases." Jama-Journal of the American Medical Association **144**(16): 1327-1335.

Hermanowski-Vosatka, A., J. M. Balkovec, K. Cheng, H. Y. Chen, M. Hernandez, G. C. Koo, C. B. Le Grand, Z. Li, J. M. Metzger, S. S. Mundt, H. Noonan, C. N. Nunes, S. H. Olson, B. Pikounis, N. Ren, N. Robertson, J. M. Schaeffer, K. Shah, M. S. Springer, A. M. Strack, M. Strowski, K. Wu, T. Wu, J. Xiao, B. B. Zhang, S. D. Wright and R. Thieringer (2005). "11beta-HSD1 inhibition ameliorates metabolic syndrome and prevents progression of atherosclerosis in mice." J Exp Med **202**(4): 517-527.

Hinz, B. and G. Gabbiani (2010). "Fibrosis: recent advances in myofibroblast biology and new therapeutic perspectives." F1000 Biol Rep **2**: 78.

Holmes, M. C., R. N. Carter, J. Noble, S. Chitnis, A. Dutia, J. M. Paterson, J. J. Mullins, J. R. Seckl and J. L. Yau (2010). "11beta-hydroxysteroid dehydrogenase type 1 expression is increased in the aged mouse

hippocampus and parietal cortex and causes memory impairments." J Neurosci **30**(20): 6916-6920.
Horn, A., K. Palumbo, C. Cordazzo, C. Dees, A. Akhmetshina, M. Tomcik, P. Zerr, J. Avouac, J. Gusinde, J. Zwerina, H. Roudaut, E. Traiffort, M. Ruat, O. Distler, G. Schett and J. H. W. Distler (2012). "Hedgehog signaling controls fibroblast activation and tissue fibrosis in systemic sclerosis." Arthritis Rheum **64**(8): 2724-2733.
Huang, Q. Q., H. Perlman, Z. Huang, R. Birkett, L. Kan, H. Agrawal, A. Misharin, S. Gurbuxani, J. D. Crispino and R. M. Pope (2010). "FLIP: a novel regulator of macrophage differentiation and granulocyte homeostasis." Blood **116**(23): 4968-4977.
Hui, C. C. and S. Angers (2011). "Gli Proteins in Development and Disease." Annual Review of Cell and Developmental Biology, Vol 27 **27**: 513-537.
Hutchison, N., C. Fligny and J. S. Duffield (2013). "Resident mesenchymal cells and fibrosis." Biochimica Et Biophysica Acta-Molecular Basis of Disease **1832**(7): 962-971.
Ignatova, I. D., R. M. Kostadinova, C. E. Goldring, A. R. Nawrocki, F. J. Frey and B. M. Frey (2009). "Tumor necrosis factor-alpha upregulates 11beta-hydroxysteroid dehydrogenase type 1 expression by CCAAT/enhancer binding protein-beta in HepG2 cells." Am J Physiol Endocrinol Metab **296**(2): E367-377.
Imtiyaz, H. Z., E. P. Williams, M. M. Hickey, S. A. Patel, A. C. Durham, L. J. Yuan, R. Hammond, P. A. Gimotty, B. Keith and M. C. Simon (2010). "Hypoxia-inducible factor 2alpha regulates macrophage function in mouse models of acute and tumor inflammation." J Clin Invest **120**(8): 2699-2714.
Ingham, P. W., Y. Nakano and C. Seger (2011). "Mechanisms and functions of Hedgehog signalling across the metazoa." Nature Reviews Genetics **12**(6): 393-406.
Ishii, T., H. Masuzaki, T. Tanaka, N. Arai, S. Yasue, N. Kobayashi, T. Tomita, M. Noguchi, J. Fujikura, K. Ebihara, K. Hosoda and K. Nakao (2007). "Augmentation of 11beta-hydroxysteroid dehydrogenase type 1 in LPS-activated J774.1 macrophages--role of 11beta-HSD1 in pro-inflammatory properties in macrophages." Febs Letters **581**(3): 349-354.
Ishii, T., H. Masuzaki, T. Tanaka, N. Arai, S. Yasue, N. Kobayashi, T. Tomita, M. Noguchi, J. Fujikura, K. Ebihara, K. Hosoda and K. Nakao (2007). "Augmentation of 11β-hydroxysteroid dehydrogenase type 1 in LPS-activated J774.1 macrophages - role of 11β-HSD1 in pro-inflammatory properties in macrophages." FEBS Lett **581**(3): 349-354.
Ishmael, F. T., X. Fang, M. R. Galdiero, U. Atasoy, W. F. C. Rigby, M. Gorospe, C. Cheadle and C. Stellato (2008). "Role of the RNA-binding protein tristetraprolin in glucocorticoid-mediated gene regulation." Journal of Immunology **180**(12): 8342-8353.
Jenkins, S. J., D. Ruckerl, P. C. Cook, L. H. Jones, F. D. Finkelman, N. van Rooijen, A. S. MacDonald and J. E. Allen (2011). "Local Macrophage Proliferation, Rather than Recruitment from the Blood, Is a Signature of T(H)2 Inflammation." Science **332**(6035): 1284-1288.

Ji, H., K. Ohmura, U. Mahmood, D. M. Lee, F. M. Hofhuis, S. A. Boackle, K. Takahashi, V. M. Holers, M. Walport, C. Gerard, A. Ezekowitz, M. C. Carroll, M. Brenner, R. Weissleder, J. S. Verbeek, V. Duchatelle, C. Degott, C. Benoist and D. Mathis (2002). "Arthritis critically dependent on innate immune system players." Immunity **16**(2): 157-168.

Jilma, B., P. Stohlawetz, T. Pernerstorfer, H. G. Eichler, C. Mullner and S. Kapiotis (1998). "Glucocorticoids dose-dependently increase plasma levels of granulocyte colony stimulating factor in man." J Clin Endocrinol Metab **83**(3): 1037-1040.

Jilma, B., J. Voltmann, S. Albinni, P. Stohlawetz, I. Schwarzinger, C. H. Gleiter, A. Rauch, H. G. Eichler and O. F. Wagner (1997). "Dexamethasone down-regulates the expression of L-selectin on the surface of neutrophils and lymphocytes in humans." Clin Pharmacol Ther **62**(5): 562-568.

Joanny, M.-E. (2011). THE ROLE OF DUAL SPECIFICITY PHOSPHATASE 1 IN THE ANTI-INFLAMMATORY EFFECTS OF THE GLUCOCORTICOID RECEPTOR. Ph.D, Imperial College London.

Kasper, M., G. Regi, A. M. Frischauf and F. Aberger (2006). "GLI transcription factors: Mediators of oncogenic Hedgehog signalling." European Journal of Cancer **42**(4): 437-445.

Kawamura, H., X. J. Li, K. Goishi, L. A. van Meeteren, L. Jakobsson, S. Cebe-Suarez, A. Shimizu, D. Edholm, K. Ballmer-Hofer, L. Kjellen, M. Klagsbrun and L. Claesson-Welsh (2008). "Neuropilin-1 in regulation of VEGF-induced activation of p38MAPK and endothelial cell organization." Blood **112**(9): 3638-3649.

Kipari, T., P. W. Hadoke, J. Iqbal, T. Y. Man, E. Miller, A. E. Coutinho, Z. Zhang, K. M. Sullivan, T. Mitic, D. E. Livingstone, C. Schrecker, K. Samuel, C. I. White, M. A. Bouhlel, G. Chinetti-Gbaguidi, B. Staels, R. Andrew, B. R. Walker, J. S. Savill, K. E. Chapman and J. R. Seckl (2013). "11beta-hydroxysteroid dehydrogenase type 1 deficiency in bone marrow-derived cells reduces atherosclerosis." FASEB J **27**(4): 1519-1531.

Kipari, T., P. W. F. Hadoke, J. Iqbal, T. Y. Man, E. Miller, A. E. Coutinho, Z. G. Zhang, K. M. Sullivan, T. Mitic, D. E. W. Livingstone, C. Schrecker, K. Samuel, C. I. White, M. A. Bouhlel, G. Chinetti-Gbaguidi, B. Staels, R. Andrew, B. R. Walker, J. S. Savill, K. E. Chapman and J. R. Seckl (2013). "11 beta-hydroxysteroid dehydrogenase type 1 deficiency in bone marrow-derived cells reduces atherosclerosis." Faseb Journal **27**(4): 1519-1531.

Kobayashi, T., D. W. Soegiarto, Y. Z. Yang, B. Lanske, E. Schipani, A. P. McMahon and H. M. Kronenberg (2005). "Indian hedgehog stimulates periarticular chondrocyte differentiation to regulate growth plate length independently of PTHrP." Journal of Clinical Investigation **115**(7): 1734-1742.

Koh, Y. J., S. Kang, H. J. Lee, T. S. Choi, H. S. Lee, C. H. Cho and G. Y. Koh (2007). "Bone marrow-derived circulating progenitor cells fail to transdifferentiate into adipocytes in adult adipose tissues in mice." Journal of Clinical Investigation **117**(12): 3684-3695.

Kotelevtsev, Y., M. C. Holmes, A. Burchell, P. M. Houston, D. Schmoll, P. Jamieson, R. Best, R. Brown, C. R. Edwards, J. R. Seckl and J. J. Mullins (1997). "11beta-hydroxysteroid dehydrogenase type 1 knockout mice show

attenuated glucocorticoid-inducible responses and resist hyperglycemia on obesity or stress." Proc Natl Acad Sci U S A **94**(26): 14924-14929.
Kotelevtsev, Y., M. C. Holmes, A. Burchell, P. M. Houston, D. Schmoll, P. Jamieson, R. Best, R. Brown, C. R. W. Edwards, J. R. Seckl and J. J. Mullins (1997). "11β-Hydroxysteroid dehydrogenase type 1 knockout mice show attenuated glucocorticoid-inducible responses and resist hyperglycemia on obesity or stress." Proceedings of the National Academy of Sciences of the United States of America **94**(26): 14924-14929.
Kugler, D. G., P. R. Mittelstadt, J. D. Ashwell, A. Sher and D. Jankovic (2013). "CD4+ T cells are trigger and target of the glucocorticoid response that prevents lethal immunopathology in toxoplasma infection." The Journal of Experimental Medicine.
Kuziel, W. A., S. J. Morgan, T. C. Dawson, S. Griffin, O. Smithies, K. Ley and N. Maeda (1997). "Severe reduction in leukocyte adhesion and monocyte extravasation in mice deficient in CC chemokine receptor 2." Proc Natl Acad Sci U S A **94**(22): 12053-12058.
Lam, D., D. Harris and Z. Y. Qin (2013). "Inflammatory Mediator Profiling Reveals Immune Properties of Chemotactic Gradients and Macrophage Mediator Production Inhibition during Thioglycollate Elicited Peritoneal Inflammation." Mediators of Inflammation.
Lavery, G. G., A. E. Zielinska, L. L. Gathercole, B. Hughes, N. Semjonous, P. Guest, K. Saqib, M. Sherlock, G. Reynolds, S. A. Morgan, J. W. Tomlinson, E. A. Walker, E. H. Rabbitt and P. M. Stewart (2012). "Lack of Significant Metabolic Abnormalities in Mice with Liver-Specific Disruption of 11β-Hydroxysteroid Dehydrogenase Type 1." Endocrinology.
Lawrence, T. and G. Natoli (2011). "Transcriptional regulation of macrophage polarization: enabling diversity with identity." Nature Reviews Immunology **11**(11): 750-761.
Lawrence, T. and G. Natoli (2011). "Transcriptional regulation of macrophage polarization: enabling diversity with identity." Nat Rev Immunol **11**(11): 750-761.
Lax, S., M. Wilson, M. Takata, P. Stewart and D. Thickett (2012). "S54 The Role of Pre-Receptor Glucocorticoid Metabolism in Regulating the Severity and Persistence of Murine Lung Injury." Thorax **67**(Suppl 2): A28.
Lee, J. H., Z. Gao and J. Ye (2013). "Regulation of 11beta-HSD1 expression during adipose tissue expansion by hypoxia through different activities of NF-kappaB and HIF-1alpha." Am J Physiol Endocrinol Metab **304**(10): E1035-1041.
Lee, S. B. and R. Kalluri (2010). "Mechanistic connection between inflammation and fibrosis." Kidney International **78**: S22-S26.
Leibovich, S. J. and R. Ross (1975). "The role of the macrophage in wound repair. A study with hydrocortisone and antimacrophage serum." Am J Pathol **78**(1): 71-100.
Leo, C. and J. D. Chen (2000). "The SRC family of nuclear receptor coactivators." Gene **245**(1): 1-11.
Lightman, S. L., C. C. Wiles, H. C. Atkinson, D. E. Henley, G. M. Russell, J. A. Leendertz, M. A. McKenna, F. Spiga, S. A. Wood and B. L. Conway-

Campbell (2008). "The significance of glucocorticoid pulsatility." Eur J Pharmacol **583**(2-3): 255-262.
Ligresti, G., A. C. Aplin, P. Zorzi, A. Morishita and R. F. Nicosia (2011). "Macrophage-Derived Tumor Necrosis Factor-alpha Is an Early Component of the Molecular Cascade Leading to Angiogenesis in Response to Aortic Injury." Arteriosclerosis Thrombosis and Vascular Biology **31**(5): 1151-U1555.
Lim, H. Y., N. Muller, M. J. Herold, J. van den Brandt and H. M. Reichardt (2007). "Glucocorticoids exert opposing effects on macrophage function dependent on their concentration." Immunology **122**(1): 47-53.
Lin, E. Y., J. F. Li, L. Gnatovskiy, Y. Deng, L. Zhu, D. A. Grzesik, H. Qian, X. N. Xue and J. W. Pollard (2006). "Macrophages regulate the angiogenic switch in a mouse model of breast cancer." Cancer Research **66**(23): 11238-11246.
Liu, J., X. Kong, L. Wang, H. Qi, W. Di, X. Zhang, L. Wu, X. Chen, J. Yu, J. Zha, S. Lv, A. Zhang, P. Cheng, M. Hu, Y. Li, J. Bi, F. Hu, Y. Zhong, Y. Xu and G. Ding (2013). "Essential roles of 11beta-HSD1 in regulating brown adipocyte function." J Mol Endocrinol **50**(1): 103-113.
Liu, J. L., C. B. Srikant and S. Chowdhury (2011). "Is 11 beta-HSD1 expressed in islet beta-cells and regulated by corticotropin-releasing hormone?" Proceedings of the National Academy of Sciences of the United States of America **108**(51): E1390-E1390.
Liu, W. H., J. Wang, G. Q. Yu and D. Pearce (1996). "Steroid receptor transcriptional synergy is potentiated by disruption of the DNA-binding domain dimer interface." Molecular Endocrinology **10**(11): 1399-1406.
Lokmic, Z., J. Musyoka, T. D. Hewitson and I. A. Darby (2012). Chapter three - Hypoxia and Hypoxia Signaling in Tissue Repair and Fibrosis. International Review of Cell and Molecular Biology. W. J. Kwang, Academic Press. **Volume 296:** 139-185.
Low, S. C., K. E. Chapman, C. R. W. Edwards and J. R. Seckl (1994). "'Liver-type' 11{beta}-hydroxysteroid dehydrogenase cDNA encodes reductase but not dehydrogenase activity in intact mammalian COS-7 cells." J Mol Endocrinol **13**(2): 167-174.
Lucas, T., A. Waisman, R. Ranjan, J. Roes, T. Krieg, W. Muller, A. Roers and S. A. Eming (2010). "Differential roles of macrophages in diverse phases of skin repair." J Immunol **184**(7): 3964-3977.
Luo, M. J., R. Thieringer, M. S. Springer, S. D. Wright, A. Hermanowski-Vosatka, A. Plump, J. M. Balkovec, K. Cheng, G. J. Ding, D. W. Kawka, G. C. Koo, C. B. Grand, Q. Luo, M. M. Maletic, L. Malkowitz, K. Shah, I. Singer, S. T. Waddell, K. K. Wu, J. Yuan, J. Zhu, S. Stepaniants, X. Yang, P. Y. Lum and I. M. Wang (2013). "11beta-HSD1 inhibition reduces atherosclerosis in mice by altering proinflammatory gene expression in the vasculature." Physiol Genomics **45**(1): 47-57.
Luo, M. J., R. Thieringer, M. S. Springer, S. D. Wright, A. Hermanowski-Vosatka, A. Plump, J. M. Balkovec, K. Cheng, G. J. Ding, D. W. Kawka, G. C. Koo, C. B. L. Grand, Q. Luo, M. M. Maletic, L. Malkowitz, K. Shah, I. Singer, S. T. Waddell, K. K. Wu, J. Yuan, J. Zhu, S. Stepaniants, X. Yang, P. Y. Lum and I.-M. Wang (2013). "11β-HSD1 inhibition reduces atherosclerosis in

mice by altering proinflammatory gene expression in the vasculature." Physiological Genomics **45**(1): 47-57.
Macfarlane, D. P., S. Forbes and B. R. Walker (2008). "Glucocorticoids and fatty acid metabolism in humans: fuelling fat redistribution in the metabolic syndrome." J Endocrinol **197**(2): 189-204.
Majno, G. (1975). The Healing Hand - Man and wound in the ancient world. Cambridge, MA, Harvard University Press.
Majno, G. J., I. (2004). Cells, Tissues, and Disease, Oxford University Press, Oxford.
Mantovani, A., A. Sica and M. Locati (2005). "Macrophage polarization comes of age." Immunity **23**(4): 344-346.
Mantovani, A., A. Sica, S. Sozzani, P. Allavena, A. Vecchi and M. Locati (2004). "The chemokine system in diverse forms of macrophage activation and polarization." Trends in Immunology **25**(12): 677-686.
Mantovani, A., A. Sica, S. Sozzani, P. Allavena, A. Vecchi and M. Locati (2004). "The chemokine system in diverse forms of macrophage activation and polarization." Trends Immunol **25**(12): 677-686.
Martin, P., D. D'Souza, J. Martin, R. Grose, L. Cooper, R. Maki and S. R. McKercher (2003). "Wound healing in the PU.1 null mouse - Tissue repair is not dependent on inflammatory cells." Current Biology **13**(13): 1122-1128.
Masferrer, J. L., S. T. Reddy, B. S. Zweifel, K. Seibert, P. Needleman, R. S. Gilbert and H. R. Herschman (1994). "In vivo glucocorticoids regulate cyclooxygenase-2 but not cyclooxygenase-1 in peritoneal macrophages." J Pharmacol Exp Ther **270**(3): 1340-1344.
Mason, H. L., C. S. Myers and E. C. Kendall (1936). "The chemistry of crystalline substances isolated from the suprarenal gland." Journal of Biological Chemistry **114**(3): 613-631.
Masters, S. L., A. Simon, I. Aksentijevich and D. L. Kastner (2009). "Horror autoinflammaticus: the molecular pathophysiology of autoinflammatory disease (*)." Annu Rev Immunol **27**: 621-668.
Masuzaki, H., J. Paterson, H. Shinyama, N. M. Morton, J. J. Mullins, J. R. Seckl and J. S. Flier (2001). "A transgenic model of visceral obesity and the metabolic syndrome." Science **294**(5549): 2166-2170.
Masuzaki, H., H. Yamamoto, C. J. Kenyon, J. K. Elmquist, N. M. Morton, J. M. Paterson, H. Shinyama, M. G. F. Sharp, S. Fleming, J. J. Mullins, J. R. Seckl and J. S. Flier (2003). "Transgenic amplification of glucocorticoid action in adipose tissue causes high blood pressure in mice." The Journal of Clinical Investigation **112**(1): 83-90.
Matthews, V. B., T. L. Allen, S. Risis, M. H. S. Chan, D. C. Henstridge, N. Watson, L. A. Zaffino, J. R. Babb, J. Boon, P. J. Meikle, J. B. Jowett, M. J. Watt, J. O. Jansson, C. R. Bruce and M. A. Febbraio (2010). "Interleukin-6-deficient mice develop hepatic inflammation and systemic insulin resistance." Diabetologia **53**(11): 2431-2441.
Mayosmith, W., C. W. Hayes, B. M. K. Biller, A. Klibanski, H. Rosenthal and D. I. Rosenthal (1989). "Body-Fat Distribution Measured with Ct - Correlations in Healthy-Subjects, Patients with Anorexia-Nervosa, and Patients with Cushing Syndrome." Radiology **170**(2): 515-518.

McEwen, B. S., C. A. Biron, K. W. Brunson, K. Bulloch, W. H. Chambers, F. S. Dhabhar, R. H. Goldfarb, R. P. Kitson, A. H. Miller, R. L. Spencer and J. M. Weiss (1997). "The role of adrenocorticoids as modulators of immune function in health and disease: Neural, endocrine and immune interactions." Brain Research Reviews **23**(1-2): 79-133.

McMahon, B. and C. Godson (2004). "Lipoxins: endogenous regulators of inflammation." Am J Physiol Renal Physiol **286**(2): F189-201.

McSweeney, S. J., P. W. Hadoke, A. M. Kozak, G. R. Small, H. Khaled, B. R. Walker and G. A. Gray (2010). "Improved heart function follows enhanced inflammatory cell recruitment and angiogenesis in 11{beta}HSD1-deficient mice post-MI." Cardiovasc Res.

McSweeney, S. J., P. W. Hadoke, A. M. Kozak, G. R. Small, H. Khaled, B. R. Walker and G. A. Gray (2010). "Improved heart function follows enhanced inflammatory cell recruitment and angiogenesis in 11betaHSD1-deficient mice post-MI." Cardiovasc Res **88**(1): 159-167.

McSweeney, S. J., P. W. F. Hadoke, A. M. Kozak, G. R. Small, H. Khaled, B. R. Walker and G. A. Gray (2010). "Improved heart function follows enhanced inflammatory cell recruitment and angiogenesis in 11βHSD1-deficient mice post-MI." Cardiovascular Research.

Meagher, L. C., J. M. Cousin, J. R. Seckl and C. Haslett (1996). "Opposing effects of glucocorticoids on the rate of apoptosis in neutrophilic and eosinophil granulocytes." Journal of Immunology **156**(11): 4422-4428.

Medzhitov, R. (2010). "Inflammation 2010: new adventures of an old flame." Cell **140**(6): 771-776.

Meijsing, S. H., M. A. Pufall, A. Y. So, D. L. Bates, L. Chen and K. R. Yamamoto (2009). "DNA binding site sequence directs glucocorticoid receptor structure and activity." Science **324**(5925): 407-410.

Melnicoff, M. J., P. K. Horan and P. S. Morahan (1989). "Kinetics of changes in peritoneal cell populations following acute inflammation." Cell Immunol **118**(1): 178-191.

Metchnikoff, E. (1892). "On aqueous humour, micro-organisms, and immunity." The Journal of Pathology and Bacteriology **1**(1): 13-20.

Metselaar, J. M., W. B. van den Berg, A. E. M. Holthuysen, M. H. M. Wauben, G. Storm and P. L. E. M. van Lent (2004). "Liposomal targeting of glucocorticoids to synovial lining cells strongly increases therapeutic benefit in collagen type II arthritis." Annals of the Rheumatic Diseases **63**(4): 348-353.

Michailidou, Z., S. Turban, E. Miller, X. Zou, J. Schrader, P. J. Ratcliffe, P. W. Hadoke, B. R. Walker, J. P. Iredale, N. M. Morton and J. R. Seckl (2012). "Increased angiogenesis protects against adipose hypoxia and fibrosis in metabolic disease-resistant 11beta-hydroxysteroid dehydrogenase type 1 (HSD1)-deficient mice." J Biol Chem **287**(6): 4188-4197.

Michailidou, Z., S. Turban, E. Miller, X. T. Zou, J. Schrader, P. J. Ratcliffe, P. W. F. Hadoke, B. R. Walker, J. P. Iredale, N. M. Morton and J. R. Seckl (2012). "Increased Angiogenesis Protects against Adipose Hypoxia and Fibrosis in Metabolic Disease-resistant 11 beta-Hydroxysteroid Dehydrogenase Type 1 (HSD1)-deficient Mice." Journal of Biological Chemistry **287**(6): 4188-4197.

Miles, K., J. Heaney, Z. Sibinska, D. Salter, J. Savill, D. Gray and M. Gray (2012). "A tolerogenic role for Toll-like receptor 9 is revealed by B-cell interaction with DNA complexes expressed on apoptotic cells." Proceedings of the National Academy of Sciences of the United States of America **109**(3): 887-892.

Mishler, J. M. and P. M. Emerson (1977). "Development of Neutrophilia by serially increasing doses of dexamethasone." Br J Haematol **36**(2): 249-257.

Miyamoto, Y., H. Morisaki, I. Yamanaka, Y. Kokubo, H. Masuzaki, A. Okayama, H. Tomoike, K. Nakao, T. Okamura, Y. Yoshimasa and T. Morisaki (2009). "Association study of 11beta-hydroxysteroid dehydrogenase type 1 gene polymorphisms and metabolic syndrome in urban Japanese cohort." Diabetes Res Clin Pract **85**(2): 132-138.

Molofsky, A. B., J. C. Nussbaum, H. E. Liang, S. J. Van Dyken, L. E. Cheng, A. Mohapatra, A. Chawla and R. M. Locksley (2013). "Innate lymphoid type 2 cells sustain visceral adipose tissue eosinophils and alternatively activated macrophages." J Exp Med **210**(3): 535-549.

Monach, P. A., D. Mathis and C. Benoist (2008). "The K/BxN arthritis model." Curr Protoc Immunol **Chapter 15**: Unit 15 22.

Monach, P. A., P. A. Nigrovic, M. Chen, H. Hock, D. M. Lee, C. Benoist and D. Mathis (2010). "Neutrophils in a mouse model of autoantibody-mediated arthritis: critical producers of Fc receptor gamma, the receptor for C5a, and lymphocyte function-associated antigen 1." Arthritis Rheum **62**(3): 753-764.

Moon, S. S., Y. S. Lee, J. G. Kim, S. W. Kim, J. Y. Jeong, E. J. Jeon, H. A. Seo, S. H. Kwak, K. S. Park and I. K. Lee (2011). "Relationship of 11beta-hydroxysteroid dehydrogenase type 1 and hexose-6-phosphate dehydrogenase gene polymorphisms with metabolic syndrome and type 2 diabetes." Endocr J **58**(11): 949-959.

Morgan, S. A., M. Sherlock, L. L. Gathercole, G. G. Lavery, C. Lenaghan, I. J. Bujalska, D. Laber, A. Yu, G. Convey, R. Mayers, K. Hegyi, J. K. Sethi, P. M. Stewart, D. M. Smith and J. W. Tomlinson (2009). "11beta-hydroxysteroid dehydrogenase type 1 regulates glucocorticoid-induced insulin resistance in skeletal muscle." Diabetes **58**(11): 2506-2515.

Morton, N. M., J. M. Paterson, H. Masuzaki, M. C. Holmes, B. Staels, C. Fievet, B. R. Walker, J. S. Flier, J. J. Mullins and J. R. Seckl (2004). "Novel adipose tissue-mediated resistance to diet-induced visceral obesity in 11β-hydroxysteroid dehydrogenase type 1-deficient mice." Diabetes **53**(4): 931-938.

Morton, N. M., J. M. Paterson, H. Masuzaki, M. C. Holmes, B. Staels, C. Fievet, B. R. Walker, J. S. Flier, J. J. Mullins and J. R. Seckl (2004). "Novel Adipose Tissue–Mediated Resistance to Diet-Induced Visceral Obesity in 11β-Hydroxysteroid Dehydrogenase Type 1–Deficient Mice." Diabetes **53**(4): 931-938.

Morton, N. M. and J. R. Seckl (2008). "11beta-hydroxysteroid dehydrogenase type 1 and obesity." Front Horm Res **36**: 146-164.

Moser, M., T. De Smedt, T. Sornasse, F. Tielemans, A. A. Chentoufi, E. Muraille, M. Van Mechelen, J. Urbain and O. Leo (1995). "Glucocorticoids down-

regulate dendritic cell function in vitro and in vivo." Eur J Immunol **25**(10): 2818-2824.
Mosmann, T. R., H. Cherwinski, M. W. Bond, M. A. Giedlin and R. L. Coffman (1986). "Two types of murine helper T cell clone. I. Definition according to profiles of lymphokine activities and secreted proteins." J Immunol **136**(7): 2348-2357.
Mosser, D. M. and J. P. Edwards (2008). "Exploring the full spectrum of macrophage activation." Nat Rev Immunol **8**(12): 958-969.
Moura, S. A., L. D. Lima, S. P. Andrade, A. Da Silva-Cunha, Jr., R. L. Orefice, E. Ayres and G. R. Da Silva (2011). "Local drug delivery system: inhibition of inflammatory angiogenesis in a murine sponge model by dexamethasone-loaded polyurethane implants." J Pharm Sci **100**(7): 2886-2895.
Munoz, R., C. Carvajal, A. Escalona, C. Boza, G. Perez, L. Ibanez and C. Fardella (2009). "11beta-hydroxysteroid dehydrogenase type 1 is overexpressed in subcutaneous adipose tissue of morbidly obese patients." Obes Surg **19**(6): 764-770.
Muzumdar, M. D., B. Tasic, K. Miyamichi, L. Li and L. Luo (2007). "A global double-fluorescent Cre reporter mouse." genesis **45**(9): 593-605.
Nanus, D. E., A. Filer, B. A. Fisher, P. C. Taylor, P. Stewart, C. D. Buckley, I. McInnes, M. S. Cooper and K. Raza (2013). TNFα directly regulates in vivo corticosteroid metabolism in inflammatory arthritis. Society for Endocrinology BES 2013, Harrogate, UK.
Nashev, L. G., C. Chandsawangbhuwana, Z. Balazs, A. G. Atanasov, B. Dick, F. J. Frey, M. E. Baker and A. Odermatt (2007). "Hexose-6-phosphate dehydrogenase modulates 11beta-hydroxysteroid dehydrogenase type 1-dependent metabolism of 7-keto- and 7beta-hydroxy-neurosteroids." PLoS One **2**(6): e561.
Nathan, C. and A. Ding (2010). "Nonresolving Inflammation." Cell **140**(6): 871-882.
Nieuwenhuis, B., A. Luth, J. Chun, A. Huwiler, J. Pfeilschifter, M. Schafer-Korting and B. Kleuser (2009). "Involvement of the ABC-transporter ABCC1 and the sphingosine 1-phosphate receptor subtype S1P(3) in the cytoprotection of human fibroblasts by the glucocorticoid dexamethasone." J Mol Med (Berl) **87**(6): 645-657.
Nigrovic, P. A., B. A. Binstadt, P. A. Monach, A. Johnsen, M. Gurish, Y. Iwakura, C. Benoist, D. Mathis and D. M. Lee (2007). "Mast cells contribute to initiation of autoantibody-mediated arthritis via IL-1." Proc Natl Acad Sci U S A **104**(7): 2325-2330.
Nishida, S., S. Matsumura, M. Horino, H. Oyama and A. Tenku (1977). "The variations of plasma corticosterone/cortisol ratios following ACTH stimulation or dexamethasone administration in normal men." J Clin Endocrinol Metab **45**(3): 585-588.
Novak, M. L. and T. J. Koh (2013). "Macrophage phenotypes during tissue repair." Journal of Leukocyte Biology **93**(6): 875-881.
Nusslein-Volhard, C. and E. Wieschaus (1980). "Mutations affecting segment number and polarity in Drosophila." Nature **287**(5785): 795-801.
Odegaard, J. I. and A. Chawla (2013). "Pleiotropic Actions of Insulin Resistance and Inflammation in Metabolic Homeostasis." Science **339**(6116): 172-177.

Odermatt, A., T. Da Cunha, C. A. Penno, C. Chandsawangbhuwana, C. Reichert, A. Wolf, M. Dong and M. E. Baker (2011). "Hepatic reduction of the secondary bile acid 7-oxolithocholic acid is mediated by 11beta-hydroxysteroid dehydrogenase 1." Biochem J **436**(3): 621-629.

OGUSHI, F., T. ENDO, K. TANI, K. ASADA, T. KAWANO, H. TADA, K. MANIWA and S. SONE (1999). "Decreased prostaglandin E₂ synthesis by lung fibroblasts isolated from rats with bleomycin-induced lung fibrosis." International Journal of Experimental Pathology **80**(1): 41-49.

Olefsky, J. M. and C. K. Glass (2010). "Macrophages, Inflammation, and Insulin Resistance." Annual Review of Physiology **72**(1): 219-246.

Oliveto, E. P. (1959). "Synthesis of 16alpha-Methyl and 16beta-Methyl Corticoids." Annals of the New York Academy of Sciences **82**(4): 809-820.

Olsen, N., T. Sokka, C. L. Seehorn, B. Kraft, K. Maas, J. Moore and T. M. Aune (2004). "A gene expression signature for recent onset rheumatoid arthritis in peripheral blood mononuclear cells." Ann Rheum Dis **63**(11): 1387-1392.

Olza, J., M. Gil-Campos, R. Leis, A. I. Ruperez, R. Tojo, R. Canete, A. Gil and C. M. Aguilera (2012). "A gene variant of 11beta-hydroxysteroid dehydrogenase type 1 is associated with obesity in children." Int J Obes (Lond) **36**(12): 1558-1563.

Opherk, C., F. Tronche, C. Kellendonk, D. Kohlmuller, A. Schulze, W. Schmid and G. Schutz (2004). "Inactivation of the glucocorticoid receptor in hepatocytes leads to fasting hypoglycemia and ameliorates hyperglycemia in streptozotocin-induced diabetes mellitus." Mol Endocrinol **18**(6): 1346-1353.

Osterreicher, C. H., M. Penz-Osterreicher, S. I. Grivennikov, M. Guma, E. K. Koltsova, C. Datz, R. Sasik, G. Hardiman, M. Karin and D. A. Brenner (2011). "Fibroblast-specific protein 1 identifies an inflammatory subpopulation of macrophages in the liver." Proceedings of the National Academy of Sciences of the United States of America **108**(1): 308-313.

Pal, D., S. Dasgupta, R. Kundu, S. Maitra, G. Das, S. Mukhopadhyay, S. Ray, S. S. Majumdar and S. Bhattacharya (2012). "Fetuin-A acts as an endogenous ligand of TLR4 to promote lipid-induced insulin resistance." Nature Medicine **18**(8): 1279-+.

Park, J. S., S. D. Rhee, W. H. Jung, N. S. Kang, H. Y. Kim, S. K. Kang, J. H. Ahn and K. Y. Kim (2012). "Anti-diabetic and anti-adipogenic effects of a novel selective 11 beta-hydroxysteroid dehydrogenase type 1 inhibitor in the diet-induced obese mice." European Journal of Pharmacology **691**(1-3): 19-27.

Patel, A. S., A. Smith, S. Nucera, D. Biziato, P. Saha, R. Q. Attia, J. Humphries, K. Mattock, S. P. Grover, O. T. Lyons, L. G. Guidotti, R. Siow, A. Ivetic, S. Egginton, M. Waltham, L. Naldini, M. De Palma and B. Modarai (2013). "TIE2-expressing monocytes/macrophages regulate revascularization of the ischemic limb." Embo Molecular Medicine **5**(6): 858-869.

Paterson, J. M., N. M. Morton, C. Fievet, C. J. Kenyon, M. C. Holmes, B. Staels, J. R. Seckl and J. J. Mullins (2004). "Metabolic syndrome without obesity: Hepatic overexpression of 11β-hydroxysteroid dehydrogenase type 1 in transgenic mice." Proceedings of the National Academy of Sciences of the United States of America **101**(18): 7088-7093.

Penno, C. A., S. A. Morgan, A. Vuorinen, D. Schuster, G. G. Lavery and A. Odermatt (2013). "Impaired oxidoreduction by 11beta-hydroxysteroid dehydrogenase 1 results in the accumulation of 7-oxolithocholic acid." J Lipid Res.

Pepicelli, C. V., P. M. Lewis and A. P. McMahon (1998). "Sonic hedgehog regulates branching morphogenesis in the mammalian lung." Current Biology **8**(19): 1083-1086.

Pereira, T. A., G. H. Xie, S. S. Choi, W. K. Syn, I. Voieta, J. Y. Lu, I. S. Chan, M. Swiderska, K. B. Amaral, C. M. Antunes, W. E. Secor, R. P. Witek, J. R. Lambertucci, F. L. Pereira and A. M. Diehl (2013). "Macrophage-derived hedgehog ligands promotes fibrogenic and angiogenic responses in human schistosomiasis mansoni." Liver International **33**(1): 149-161.

Perretti, M. and F. D'Acquisto (2009). "Annexin A1 and glucocorticoids as effectors of the resolution of inflammation." Nature Reviews Immunology **9**(1): 62-70.

Petersen, H. H., T. K. Andreassen, T. Breiderhoff, J. H. Brasen, H. Schulz, V. Gross, H. J. Grone, A. Nykjaer and T. E. Willnow (2006). "Hyporesponsiveness to glucocorticoids in mice genetically deficient for the corticosteroid binding globulin." Molecular and Cellular Biology **26**(19): 7236-7245.

Peterson, D. H. and H. C. Murray (1952). "Microbiological Oxygenation of Steroids at Carbon-11." Journal of the American Chemical Society **74**(7): 1871-1872.

Peterson, R. E. (1957). "The Identification of Corticosterone in Human Plasma and Its Assay by Isotope Dilution." Journal of Biological Chemistry **225**(1): 25-37.

Philips, G. M., I. S. Chan, M. Swiderska, V. T. Schroder, C. Guy, G. F. Karaca, C. Moylan, T. Venkatraman, S. Feuerlein, W. K. Syn, Y. M. Jung, R. P. Witek, S. Choi, G. A. Michelotti, F. Rangwala, E. Merkle, C. Lascola and A. M. Diehl (2011). "Hedgehog Signaling Antagonist Promotes Regression of Both Liver Fibrosis and Hepatocellular Carcinoma in a Murine Model of Primary Liver Cancer." PLoS One **6**(9).

Pollard, J. W. (2009). "Trophic macrophages in development and disease." Nature Reviews Immunology **9**(4): 259-270.

Pradel, L. C., A. J. Mitchell, A. Zarubica, L. Dufort, L. Chasson, P. Naquet, C. Broccardo and G. Chimini (2009). "ATP-binding cassette transporter hallmarks tissue macrophages and modulates cytokine-triggered polarization programs." Eur J Immunol **39**(8): 2270-2280.

Preusch, M. R., M. Rattazzi, C. Albrecht, U. Merle, J. Tuckermann, G. Schutz, E. Blessing, G. Zoppellaro, P. Pauletto, R. Krempien, M. E. Rosenfeld, H. A. Katus and F. Bea (2008). "Critical role of macrophages in glucocorticoid driven vascular calcification in a mouse-model of atherosclerosis." Arterioscler Thromb Vasc Biol **28**(12): 2158-2164.

Pucci, F., M. A. Venneri, D. Biziato, A. Nonis, D. Moi, A. Sica, C. Di Serio, L. Naldini and M. De Palma (2009). "A distinguishing gene signature shared by tumor-infiltrating Tie2-expressing monocytes, blood "resident" monocytes, and embryonic macrophages suggests common functions and developmental relationships." Blood **114**(4): 901-914.

Rajasekaran, N. (2005). Role of cellular and molecular factors involved in the K/BxN sera induced arthritis. Doktors der Naturwissenschaften, Universität Konstanz.

Raubenheimer, P. J., E. A. Young, R. Andrew and J. R. Seckl (2006). "The role of corticosterone in human hypothalamic-pituitary-adrenal axis feedback." Clin Endocrinol (Oxf) **65**(1): 22-26.

Reddy, T. E., F. Pauli, R. O. Sprouse, N. F. Neff, K. M. Newberry, M. J. Garabedian and R. M. Myers (2009). "Genomic determination of the glucocorticoid response reveals unexpected mechanisms of gene regulation." Genome Research **19**(12): 2163-2171.

Regard, J. B., D. Malhotra, J. Gvozdenovic-Jeremic, M. Josey, M. Chen, L. S. Weinstein, J. M. Lu, E. M. Shore, F. S. Kaplan and Y. Z. Yang (2013). "Activation of Hedgehog signaling by loss of GNAS causes heterotopic ossification." Nature Medicine **19**(11): 1505-+.

Reichardt, H. M., K. H. Kaestner, J. Tuckermann, O. Kretz, O. Wessely, R. Bock, P. Gass, W. Schmid, P. Herrlich, P. Angel and G. Schütz (1998). "DNA binding of the glucocorticoid receptor is not essential for survival." Cell **93**(4): 531-541.

Reichstein, T. (1936). "The elements of adrenal cortex IV." Helvetica Chimica Acta **19**: 402-412.

Ren, Y., Y. Xie, G. P. Jiang, J. Q. Fan, J. Yeung, W. Li, P. K. H. Tam and J. Savill (2008). "Apoptotic cells protect mice against lipopolysaccharide-induced shock." Journal of Immunology **180**(7): 4978-4985.

Reul, J. M. H. M., A. Gesing, S. Droste, I. S. M. Stec, A. Weber, C. Bachmann, A. Bilang-Bleuel, F. Holsboer and A. C. E. Linthorst (2000). "The brain mineralocorticoid receptor: greedy for ligand, mysterious in function." European Journal of Pharmacology **405**(1-3): 235-249.

Revollo, J. R. and J. A. Cidlowski (2009). "Mechanisms generating diversity in glucocorticoid receptor signaling." Ann N Y Acad Sci **1179**: 167-178.

Rickard, A. J., J. Morgan, G. Tesch, J. W. Funder, P. J. Fuller and M. J. Young (2009). "Deletion of Mineralocorticoid Receptors From Macrophages Protects Against Deoxycorticosterone/Salt-Induced Cardiac Fibrosis and Increased Blood Pressure." Hypertension **54**(3): 537-U180.

Ros-Bernal, F., S. Hunot, M. T. Herrero, S. Parnadeau, J. C. Corvol, L. Lu, D. Alvarez-Fischer, M. A. Carrillo-de Sauvage, F. Saurini, C. Coussieu, K. Kinugawa, A. Prigent, G. Hoglinger, M. Hamon, F. Tronche, E. C. Hirsch and S. Vyas (2011). "Microglial glucocorticoid receptors play a pivotal role in regulating dopaminergic neurodegeneration in parkinsonism." Proc Natl Acad Sci U S A **108**(16): 6632-6637.

Rose, A. J., A. Vegiopoulos and S. Herzig (2010). "Role of glucocorticoids and the glucocorticoid receptor in metabolism: insights from genetic manipulations." J Steroid Biochem Mol Biol **122**(1-3): 10-20.

Rose, A. J., A. Vegiopoulos and S. Herzig (2010). "Role of glucocorticoids and the glucocorticoid receptor in metabolism: Insights from genetic manipulations." Journal Of Steroid Biochemistry and Molecular Biology **122**(1-3): 10-20.

Ruiz-Heiland, G., A. Horn, P. Zerr, W. Hofstetter, W. Baum, M. Stock, J. H. Distler, F. Nimmerjahn, G. Schett and J. Zwerina (2012). "Blockade of the hedgehog

pathway inhibits osteophyte formation in arthritis." Annals of the Rheumatic Diseases **71**(3): 400-407.
Ryan, G. B. and G. Majno (1977). "Acute inflammation. A review." Am J Pathol **86**(1): 183-276.
Sadik, C. D. and A. D. Luster (2012). "Lipid-cytokine-chemokine cascades orchestrate leukocyte recruitment in inflammation." Journal of Leukocyte Biology **91**(2): 207-215.
Saffar, A. S., H. Ashdown and A. S. Gounni (2011). "The molecular mechanisms of glucocorticoids-mediated neutrophil survival." Curr Drug Targets **12**(4): 556-562.
Sai, S., C. L. Esteves, V. Kelly, Z. Michailidou, K. Anderson, A. P. Coll, Y. Nakagawa, T. Ohzeki, J. R. Seckl and K. E. Chapman (2008). "Glucocorticoid regulation of the promoter of 11beta-hydroxysteroid dehydrogenase type 1 is indirect and requires CCAAT/enhancer-binding protein-beta." Mol Endocrinol **22**(9): 2049-2060.
Sandeep, T. C., J. L. Yau, A. M. MacLullich, J. Noble, I. J. Deary, B. R. Walker and J. R. Seckl (2004). "11Beta-hydroxysteroid dehydrogenase inhibition improves cognitive function in healthy elderly men and type 2 diabetics." Proc Natl Acad Sci U S A **101**(17): 6734-6739.
Schmidt, M., C. Weidler, H. Naumann, S. Anders, J. Scholmerich and R. H. Straub (2005). "Reduced capacity for the reactivation of glucocorticoids in rheumatoid arthritis synovial cells: possible role of the sympathetic nervous system?" Arthritis Rheum **52**(6): 1711-1720.
Schulz, C., E. G. Perdiguero, L. Chorro, H. Szabo-Rogers, N. Cagnard, K. Kierdorf, M. Prinz, B. S. Wu, S. E. W. Jacobsen, J. W. Pollard, J. Frampton, K. J. Liu and F. Geissmann (2012). "A Lineage of Myeloid Cells Independent of Myb and Hematopoietic Stem Cells." Science **336**(6077): 86-90.
Sebek, O. K. and G. B. Spero (1959). 6-methyl-1-dehydro analogues of cortisone, hydrocortisone and 21-esters thereof The United States, UPJOHN CO **2897218**
Seckl, J. R. and K. E. Chapman (1997). "The 11β-Hydroxysteroid Dehydrogenase System, A Determinant of Glucocorticoid and Mineralocorticoid Action." European Journal of Biochemistry **249**(2): 361-364.
Sesti-Costa, R., G. C. Baccan, S. Chedraoui-Silva and B. Mantovani (2010). "Effects of Acute Cold Stress on Phagocytosis of Apoptotic Cells: The Role of Corticosterone." Neuroimmunomodulation **17**(2): 79-87.
Seymour, B. and W. S. Allen (1957). 16-alpha oxy-delta1, 4-pregnadienes The United States, AMERICAN CYANAMID CO **2806043**
Shen, H., D. Kreisel and D. R. Goldstein (2013). "Processes of sterile inflammation." J Immunol **191**(6): 2857-2863.
Slavin, B. G., J. M. Ong and P. A. Kern (1994). "Hormonal regulation of hormone-sensitive lipase activity and mRNA levels in isolated rat adipocytes." J Lipid Res **35**(9): 1535-1541.
Slocumb, C. H., H. F. Polley, P. S. Hench and E. C. Kendall (1950). "Effects of Cortisone and Acth on Patients with Rheumatoid Arthritis." Proceedings of the Staff Meetings of the Mayo Clinic **25**(17): 476-478.

Small, G. R., P. W. Hadoke, I. Sharif, A. R. Dover, D. Armour, C. J. Kenyon, G. A. Gray and B. R. Walker (2005). "Preventing local regeneration of glucocorticoids by 11β-hydroxysteroid dehydrogenase type 1 enhances angiogenesis." Proc Natl Acad Sci U S A **102**(34): 12165-12170.

Small, G. R., P. W. F. Hadoke, I. Sharif, A. R. Dover, D. Armour, C. J. Kenyon, G. A. Gray and B. R. Walker (2005). "Preventing local regeneration of glucocorticoids by 11β-hydroxysteroid dehydrogenase type 1 enhances angiogenesis." Proceedings of the National Academy of Sciences of the United States of America **102**(34): 12165-12170.

Smit, P., M. J. Dekker, F. J. de Jong, A. W. van den Beld, J. W. Koper, H. A. Pols, A. O. Brinkmann, F. H. de Jong, M. M. Breteler and S. W. Lamberts (2007). "Lack of Association of the 11beta-hydroxysteroid dehydrogenase type 1 gene 83,557insA and hexose-6-phosphate dehydrogenase gene R453Q polymorphisms with body composition, adrenal androgen production, blood pressure, glucose metabolism, and dementia." J Clin Endocrinol Metab **92**(1): 359-362.

Soehnlein, O. and L. Lindbom (2010). "Phagocyte partnership during the onset and resolution of inflammation." Nature Reviews Immunology **10**(6): 427-439.

Solomon, S., N. Rajasekaran, E. Jeisy-Walder, S. B. Snapper and H. Illges (2005). "A crucial role for macrophages in the pathology of K/B x N serum-induced arthritis." European Journal of Immunology **35**(10): 3064-3073.

Sorrells, S. F., J. R. Caso, C. D. Munhoz, C. K. Hu, K. V. Tran, Z. D. Miguel, B. Y. Chien and R. M. Sapolsky (2013). "Glucocorticoid signaling in myeloid cells worsens acute CNS injury and inflammation." J Neurosci **33**(18): 7877-7889.

Spann, N. J., L. X. Garmire, J. G. McDonald, D. S. Myers, S. B. Milne, N. Shibata, D. Reichart, J. N. Fox, I. Shaked, D. Heudobler, C. R. Raetz, E. W. Wang, S. L. Kelly, M. C. Sullards, R. C. Murphy, A. H. Merrill, Jr., H. A. Brown, E. A. Dennis, A. C. Li, K. Ley, S. Tsimikas, E. Fahy, S. Subramaniam, O. Quehenberger, D. W. Russell and C. K. Glass (2012). "Regulated accumulation of desmosterol integrates macrophage lipid metabolism and inflammatory responses." Cell **151**(1): 138-152.

Spero, G. B., B. J. Magerlein, W. P. Schneider and J. A. Hogg (1958). 6-fluoro steroids and process for preparing same The United States, UPJOHN CO **2838538**

Stefater, J. A., I. Lewkowich, S. Rao, G. Mariggi, A. C. Carpenter, A. R. Burr, J. Q. Fan, R. Ajima, J. D. Molkentin, B. O. Williams, M. Wills-Karp, J. W. Pollard, T. Yamaguchi, N. Ferrara, H. Gerhardt and R. A. Lang (2011). "Regulation of angiogenesis by a non-canonical Wnt-Flt1 pathway in myeloid cells." Nature **474**(7352): 511-515.

Stewart, P. M., A. M. Wallace, R. Valentino, D. Burt, C. H. L. Shackleton and C. R. W. Edwards (1987). "Mineralocorticoid Activity of Licorice - 11-Beta-Hydroxysteroid Dehydrogenase-Deficiency Comes of Age." Lancet **2**(8563): 821-824.

Summers, C., S. M. Rankin, A. M. Condliffe, N. Singh, A. M. Peters and E. R. Chilvers (2010). "Neutrophil kinetics in health and disease." Trends Immunol **31**(8): 318-324.

Sunderkotter, C., K. Steinbrink, M. Goebeler, R. Bhardwaj and C. Sorg (1994). "Macrophages and Angiogenesis." Journal of Leukocyte Biology **55**(3): 410-422.

Swirski, F. K. and M. Nahrendorf (2013). "Leukocyte Behavior in Atherosclerosis, Myocardial Infarction, and Heart Failure." Science **339**(6116): 161-166.

Szekanecz, Z., T. Besenyei, A. Szentpetery and A. E. Koch (2010). "Angiogenesis and vasculogenesis in rheumatoid arthritis." Curr Opin Rheumatol **22**(3): 299-306.

Tabas, I. and C. K. Glass (2013). "Anti-Inflammatory Therapy in Chronic Disease: Challenges and Opportunities." Science **339**(6116): 166-172.

Tang, T., J. Zhang, J. Yin, J. Staszkiewicz, B. Gawronska-Kozak, D. Y. Jung, H. J. Ko, H. Ong, J. K. Kim, R. Mynatt, R. J. Martin, M. Keenan, Z. G. Gao and J. P. Ye (2010). "Uncoupling of Inflammation and Insulin Resistance by NF-kappa B in Transgenic Mice through Elevated Energy Expenditure." Journal of Biological Chemistry **285**(7): 4637-4644.

Tauber, A. I. (2003). "Metchnikoff and the phagocytosis theory." Nat Rev Mol Cell Biol **4**(11): 897-901.

Tchen, C. R., J. R. S. Martins, N. Paktiawal, R. Perelli, J. Saklatvala and A. R. Clark (2010). "Glucocorticoid Regulation of Mouse and Human Dual Specificity Phosphatase 1 (DUSP1) Genes UNUSUAL CIS-ACTING ELEMENTS AND UNEXPECTED EVOLUTIONARY DIVERGENCE." Journal of Biological Chemistry **285**(4): 2642-2652.

Teperino, R., S. Amann, M. Bayer, S. L. Mcgee, A. Loipetzberger, T. Connor, C. Jaeger, B. Kammerer, L. Winter, G. Wiche, K. Dalgaard, M. Selvaraj, M. Gaster, R. S. Lee-Young, M. A. Febbraio, C. Knauf, P. D. Cani, F. Aberger, J. M. Penninger, J. A. Pospisilik and H. Esterbauer (2012). "Hedgehog Partial Agonism Drives Warburg-like Metabolism in Muscle and Brown Fat." Cell **151**(2): 414-426.

Terao, M., H. Murota, A. Kimura, A. Kato, A. Ishikawa, K. Igawa, E. Miyoshi and I. Katayama (2011). "11 beta-Hydroxysteroid Dehydrogenase-1 Is a Novel Regulator of Skin Homeostasis and a Candidate Target for Promoting Tissue Repair." PLoS One **6**(9).

Thieringer, R., C. B. Le Grand, L. Carbin, T. Q. Cai, B. Wong, S. D. Wright and A. Hermanowski-Vosatka (2001). "11 Beta-hydroxysteroid dehydrogenase type 1 is induced in human monocytes upon differentiation to macrophages." J Immunol **167**(1): 30-35.

Thomas, G. D., D. Ruckerl, B. H. Maskrey, P. D. Whitfield, M. L. Blaxter and J. E. Allen (2012). "The biology of nematode- and IL4Ralpha-dependent murine macrophage polarization in vivo as defined by RNA-Seq and targeted lipidomics." Blood **120**(25): e93-e104.

Tiganescu, A., A. A. Tahrani, S. A. Morgan, M. Otranto, A. Desmouliere, L. Abrahams, Z. Hassan-Smith, E. A. Walker, E. H. Rabbitt, M. S. Cooper, K. Amrein, G. G. Lavery and P. M. Stewart (2013). "11beta-Hydroxysteroid dehydrogenase blockade prevents age-induced skin structure and function defects." J Clin Invest **123**(7): 3051-3060.

Tiganescu, A., A. A. Tahrani, S. A. Morgan, M. Otranto, A. Desmouliere, L. Abrahams, Z. Hassan-Smith, E. A. Walker, E. H. Rabbitt, M. S. Cooper, K.

Amrein, G. G. Lavery and P. M. Stewart (2013). "11beta-hydroxysteroid dehydrogenase blockade prevents age-induced skin structure and function defects." J Clin Invest.

Tomlinson, J. W., E. A. Walker, I. J. Bujalska, N. Draper, G. G. Lavery, M. S. Cooper, M. Hewison and P. M. Stewart (2004). "11 beta-hydroxysteroid dehydrogenase type 1: A tissue-specific regulator of glucocorticoid response." Endocrine Reviews **25**(5): 831-866.

Tomlinson, J. W., E. A. Walker, I. J. Bujalska, N. Draper, G. G. Lavery, M. S. Cooper, M. Hewison and P. M. Stewart (2004). "11β-hydroxysteroid dehydrogenase type 1: a tissue-specific regulator of glucocorticoid response." Endocr Rev **25**(5): 831-866.

Townsend, H. B. and K. G. Saag (2004). "Glucocorticoid use in rheumatoid arthritis: Benefits, mechanisms, and risks." Clinical and Experimental Rheumatology **22**(5): S77-S82.

Toyama, B. H., J. N. Savas, S. K. Park, M. S. Harris, N. T. Ingolia, J. R. Yates, 3rd and M. W. Hetzer (2013). "Identification of long-lived proteins reveals exceptional stability of essential cellular structures." Cell **154**(5): 971-982.

Tuckermann, J. P., A. Kleiman, R. Moriggl, R. Spanbroek, A. Neumann, A. Illing, B. E. Clausen, B. Stride, I. Forster, A. J. Habenicht, H. M. Reichardt, F. Tronche, W. Schmid and G. Schutz (2007). "Macrophages and neutrophils are the targets for immune suppression by glucocorticoids in contact allergy." J Clin Invest **117**(5): 1381-1390.

Uderhardt, S., M. Herrmann, O. V. Oskolkova, S. Aschermann, W. Bicker, N. Ipseiz, K. Sarter, B. Frey, T. Rothe, R. Voll, F. Nimmerjahn, V. N. Bochkov, G. Schett and G. Kronke (2012). "12/15-lipoxygenase orchestrates the clearance of apoptotic cells and maintains immunologic tolerance." Immunity **36**(5): 834-846.

Uhlenhaut, N. H., G. D. Barish, R. T. Yu, M. Downes, M. Karunasiri, C. Liddle, P. Schwalie, N. Hubner and R. M. Evans (2013). "Insights into Negative Regulation by the Glucocorticoid Receptor from Genome-wide Profiling of Inflammatory Cistromes." Molecular Cell **49**(1): 158-171.

Ulmansky, R., K. Turjeman, M. Baru, G. Katzavian, M. Harel, A. Sigal, Y. Naparstek and Y. Barenholz (2012). "Glucocorticoids in nano-liposomes administered intravenously and subcutaneously to adjuvant arthritis rats are superior to the free drugs in suppressing arthritis and inflammatory cytokines." Journal of Controlled Release **160**(2): 299-305.

Usa, K., R. J. Singh, B. C. Netzel, Y. Liu, H. Raff and M. Liang (2007). "Renal interstitial corticosterone and 11-dehydrocorticosterone in conscious rats." American Journal of Physiology - Renal Physiology **293**(1): F186-F192.

Usher, M. G., S. Z. Duan, C. Y. Ivaschenko, R. A. Frieler, S. Berger, G. Schutz, C. N. Lumeng and R. M. Mortensen (2010). "Myeloid mineralocorticoid receptor controls macrophage polarization and cardiovascular hypertrophy and remodeling in mice." Journal of Clinical Investigation **120**(9): 3350-3364.

Usher, M. G., S. Z. Duan, C. Y. Ivaschenko, R. A. Frieler, S. Berger, G. Schütz, C. N. Lumeng and R. M. Mortensen (2010). "Myeloid mineralocorticoid receptor controls macrophage polarization and cardiovascular hypertrophy

and remodeling in mice." The Journal of Clinical Investigation **120**(9): 3350-3364.
van Berlo, D., A. Wessels, A. W. Boots, V. Wilhelmi, A. M. Scherbart, K. Gerloff, F. J. van Schooten, C. Albrecht and R. P. F. Schins (2010). "Neutrophil-derived ROS contribute to oxidative DNA damage induction by quartz particles." Free Radical Biology and Medicine **49**(11): 1685-1693.
Van Furth, R., M. C. Diesselhoff-den Dulk and H. Mattie (1973). "Quantitative study on the production and kinetics of mononuclear phagocytes during an acute inflammatory reaction." J Exp Med **138**(6): 1314-1330.
Van Furth, R., M. C. Diesselhoff-den Dulk and H. Mattie (1973). "Quantitative study on the production and kinetics of mononuclear phagocytes during an acute inflammatory reaction." The Journal of Experimental Medicine **138**(6): 1314-1330.
van Uum, S. H. M., A. R. M. M. Hermus, P. Smits, T. Thien and J. W. M. Lenders (1998). "The role of 11β-hydroxysteroid dehydrogenase in the pathogenesis of hypertension." Cardiovascular Research **38**(1): 16-24.
Vandevyver, S., L. Dejager, J. Tuckermann and C. Libert (2013). "New Insights into the Anti-inflammatory Mechanisms of Glucocorticoids: An Emerging Role for Glucocorticoid-Receptor-Mediated Transactivation." Endocrinology **154**(3): 993-1007.
Varajini Joganathan, A. A.-H., Saaeha Rauz, Paul M Stewart, Graham R Wallace, Iwona J Bujalska (2008). Local cortisol generation by human macrophage subsets by 11β-hydroxysteroid dehydrogenase type 1 enzyme and its role in ocular immune privilege. Society for Endocrinology BES 2008, Harrogate, UK.
Varin, A. and S. Gordon (2009). "Alternative activation of macrophages: Immune function and cellular biology." Immunobiology **214**(7): 630-641.
Varjosalo, M. and J. Taipale (2008). "Hedgehog: functions and mechanisms." Genes & Development **22**(18): 2454-2472.
Vattakuzhi, Y., S. M. Abraham, A. Freidin, A. R. Clark and N. J. Horwood (2012). "Dual-specificity phosphatase 1-null mice exhibit spontaneous osteolytic disease and enhanced inflammatory osteolysis in experimental arthritis." Arthritis Rheum **64**(7): 2201-2210.
Vegiopoulos, A. and S. Herzig (2007). "Glucocorticoids, metabolism and metabolic diseases." Molecular and Cellular Endocrinology **275**(1–2): 43-61.
Vogeser, M., J. Groetzner, C. Küpper and J. Briegel (2003). "The Serum Cortisol:Cortisone Ratio in the Postoperative Acute-Phase Response." Hormone Research in Paediatrics **59**(6): 293-296.
Walker, B. R. (2006). "Cortisol--cause and cure for metabolic syndrome?" Diabet Med **23**(12): 1281-1288.
Walshe, T. E. and P. A. D'Amore (2008). "The role of hypoxia in vascular injury and repair." Annu Rev Pathol **3**: 615-643.
Wamil, M., J. H. Battle, S. Turban, T. Kipari, D. Seguret, R. de Sousa Peixoto, Y. B. Nelson, D. Nowakowska, D. Ferenbach, L. Ramage, K. E. Chapman, J. Hughes, D. R. Dunbar, J. R. Seckl and N. M. Morton (2011). "Novel Fat Depot–Specific Mechanisms Underlie Resistance to Visceral Obesity and

Inflammation in 11β-Hydroxysteroid Dehydrogenase Type 1–Deficient Mice." Diabetes **60**(4): 1158-1167.
Wang, J., L. S. Barak, R. A. Mook, Jr. and W. Chen (2011). "Glucocorticoid hedgehog agonists in neurogenesis." Vitam Horm **87**: 207-215.
Wang, J., J. Lu, M. C. Bond, M. Chen, X.-R. Ren, H. K. Lyerly, L. S. Barak and W. Chen (2010). "Identification of select glucocorticoids as Smoothened agonists: Potential utility for regenerative medicine." Proceedings of the National Academy of Sciences **107**(20): 9323-9328.
Wang, J. B., J. Y. Lu, M. C. Bond, M. Y. Chen, X. R. Ren, H. K. Lyerly, L. S. Barak and W. Chen (2010). "Identification of select glucocorticoids as Smoothened agonists: Potential utility for regenerative medicine." Proceedings of the National Academy of Sciences of the United States of America **107**(20): 9323-9328.
Wang, L., J. Liu, A. Zhang, P. Cheng, X. Zhang, S. Lv, L. Wu, J. Yu, W. Di, J. Zha, X. Kong, H. Qi, Y. Zhong and G. Ding (2012). "BVT.2733, a selective 11beta-hydroxysteroid dehydrogenase type 1 inhibitor, attenuates obesity and inflammation in diet-induced obese mice." PLoS One **7**(7): e40056.
Wang, Y., L. Davidow, A. C. Arvanites, J. Blanchard, K. Lam, K. Xu, V. Oza, J. W. Yoo, J. M. Y. Ng, T. Curran, L. L. Rubin and A. P. McMahon (2012). "Glucocorticoid Compounds Modify Smoothened Localization and Hedgehog Pathway Activity." Chemistry & Biology **19**(8): 972-982.
Webster, J. I. and J. Carlstedt-Duke (2002). "Involvement of multidrug resistance proteins (MDR) in the modulation of glucocorticoid response." Journal Of Steroid Biochemistry and Molecular Biology **82**(4-5): 277-288.
Wekerle, H., A. Flugel, L. Fugger, G. Schett and D. Serreze (2012). "Autoimmunity's next top models." Nature Medicine **18**(1): 66-70.
Welti, J., S. Loges, S. Dimmeler and P. Carmeliet (2013). "Recent molecular discoveries in angiogenesis and antiangiogenic therapies in cancer." J Clin Invest **123**(8): 3190-3200.
Whorwood, C. B., M. C. Sheppard and P. M. Stewart (1993). "Tissue specific effects of thyroid hormone on 11 beta-hydroxysteroid dehydrogenase gene expression." J Steroid Biochem Mol Biol **46**(5): 539-547.
Williams, L. J., V. Lyons, I. MacLeod, V. Rajan, G. J. Darlington, V. Poli, J. R. Seckl and K. E. Chapman (2000). "C/EBP regulates hepatic transcription of 11beta -hydroxysteroid dehydrogenase type 1. A novel mechanism for cross-talk between the C/EBP and glucocorticoid signaling pathways." J Biol Chem **275**(39): 30232-30239.
Wilson, C. W. and P. T. Chuang (2010). "Mechanism and evolution of cytosolic Hedgehog signal transduction." Development **137**(13): 2079-2094.
Wintersteiner, O. and J. J. Pfiffner (1936). "Chemical studies on the adrenal cortex III. Isolation of two new physiologically inactive compounds." Journal of Biological Chemistry **116**(1): 291-305.
Wu, D., A. B. Molofsky, H. E. Liang, R. R. Ricardo-Gonzalez, H. A. Jouihan, J. K. Bando, A. Chawla and R. M. Locksley (2011). "Eosinophils sustain adipose alternatively activated macrophages associated with glucose homeostasis." Science **332**(6026): 243-247.

Wust, S., J. van den Brandt, D. Tischner, A. Kleiman, J. P. Tuckermann, R. Gold, F. Luhder and H. M. Reichardt (2008). "Peripheral T cells are the therapeutic targets of glucocorticoids in experimental autoimmune encephalomyelitis." Journal of Immunology **180**(12): 8434-8443.

Wynn, T. A. and L. Barron (2010). "Macrophages: Master Regulators of Inflammation and Fibrosis." Seminars in Liver Disease **30**(3): 245-257.

Wynn, T. A., A. Chawla and J. W. Pollard (2013). "Macrophage biology in development, homeostasis and disease." Nature **496**(7446): 445-455.

Wynn, T. A. and T. R. Ramalingam (2012). "Mechanisms of fibrosis: therapeutic translation for fibrotic disease." Nature Medicine **18**(7): 1028-1040.

Xiantong Zou, A. P., Rebecca Aucott, Prakash Ramachandran, Michelle Clarkson, Scott P Webster, John P Iredale, Brian R Walker, Zoi Michailidou (2013). 11βHSD1 deficiency increases susceptibility to liver fibrosis by activating hepatic stellate cells. Society for Endocrinology BES 2013, Harrogate, UK.

Yamamoto, M., S. Uematsu, T. Okamoto, Y. Matsuura, S. Sato, H. Kumar, T. Satoh, T. Saitoh, K. Takeda, K. J. Ishii, O. Takeuchi, T. Kawai and S. Akira (2007). "Enhanced TLR-mediated NF-IL6 dependent gene expression by Trib1 deficiency." J Exp Med **204**(9): 2233-2239.

Yang, F. (2010). Role and regulation of 11β-hydroxysteroid dehydrogenase in lung inflammation. Ph.D, The University of Edinburgh.

Yau, J. L. W., J. Noble and J. R. Seckl (2011). "11 beta-Hydroxysteroid Dehydrogenase Type 1 Deficiency Prevents Memory Deficits with Aging by Switching from Glucocorticoid Receptor to Mineralocorticoid Receptor-Mediated Cognitive Control." Journal of Neuroscience **31**(11): 4188-4193.

Yoshida, S., H. Amano, I. Hayashi, H. Kitasato, M. Kamata, M. Inukai, H. Yoshimura and M. Majima (2003). "COX-2/VEGF-dependent facilitation of tumor-associated angiagenesis and tumor growth in vivo." Laboratory Investigation **83**(10): 1385-1394.

Youm, J. K., K. Park, Y. Uchida, A. Chan, T. M. Mauro, W. M. Holleran and P. M. Elias (2013). "Local blockade of glucocorticoid activation reverses stress- and glucocorticoid-induced delays in cutaneous wound healing." Wound Repair Regen.

Zhang, J. G., Y. Modi, T. Yarovinsky, J. Yu, M. Collinge, T. Kyriakides, Y. Z. Zhu, W. C. Sessa, R. Pardi and J. R. Bender (2012). "Macrophage beta(2) Integrin-Mediated, HuR-Dependent Stabilization of Angiogenic Factor-Encoding mRNAs in Inflammatory Angiogenesis." American Journal of Pathology **180**(4): 1751-1760.

Zhang, T. Y. and R. A. Daynes (2007). "Macrophages from 11beta-Hydroxysteroid Dehydrogenase Type 1-Deficient Mice Exhibit an Increased Sensitivity to Lipopolysaccharide Stimulation Due to TGF-beta-Mediated Up-Regulation of SHIP1 Expression." J Immunol **179**(9): 6325-6335.

Zhang, T. Y. and R. A. Daynes (2007). "Macrophages from 11beta-hydroxysteroid dehydrogenase type 1-deficient mice exhibit an increased sensitivity to lipopolysaccharide stimulation due to TGF-beta-mediated up-regulation of SHIP1 expression." J Immunol **179**(9): 6325-6335.

Zhang, T. Y. and R. A. Daynes (2007). "Macrophages from 11β-hydroxysteroid dehydrogenase type 1-deficient mice exhibit an increased sensitivity to

lipopolysaccharide stimulation due to TGF-β-mediated up-regulation of SHIP1 expression." J Immunol **179**(9): 6325-6335.
Zhang, T. Y., X. Ding and R. A. Daynes (2005). "The expression of 11 beta-hydroxysteroid dehydrogenase type I by lymphocytes provides a novel means for intracrine regulation of glucocorticoid activities." J Immunol **174**(2): 879-889.
Zhang, Z. (2010). Generation and characterisation of mice with myeloid cell-specific knockout of HSD11b1. Master of Medical Science, University of Edinburgh.
Zhang, Z. G. (2011). Generation and characterisation of mice with myeloid cell-specific knockout of *HSD11b1*. MSc (Medical Science) The University of Edinburgh.
Zhao, L., C. A. Cuff, E. Moss, U. Wille, T. Cyrus, E. A. Klein, D. Pratico, D. J. Rader, C. A. Hunter, E. Pure and C. D. Funk (2002). "Selective interleukin-12 synthesis defect in 12/15-lipoxygenase-deficient macrophages associated with reduced atherosclerosis in a mouse model of familial hypercholesterolemia." J Biol Chem **277**(38): 35350-35356.
Zhou, J., D. F. Liu, C. Liu, Z. M. Kang, X. H. Shen, Y. Z. Chen, T. Xu and C. L. Jiang (2008). "Glucocorticoids inhibit degranulation of mast cells in allergic asthma via nongenomic mechanism." Allergy **63**(9): 1177-1185.
Zizzo, G., B. A. Hilliard, M. Monestier and P. L. Cohen (2012). "Efficient clearance of early apoptotic cells by human macrophages requires M2c polarization and MerTK induction." J Immunol **189**(7): 3508-3520.

Appendix: awards, abstracts and publications

Awards:

2013	Highly recommended Basic Science Oral Presentation of BES
2013	Travel award for BES 2013, British Society of Endocrinology
2013	Early Career Forum Travel Award, The Endocrine Society
2012	Travel award for ECI 2012, British Society of Immunology
2012	Career development Workshop award, British Society of Endocrinology

Abstracts:

Zhang Z, Coutinho AE, Hadoke PW, Salter D, Seckl JR, and Chapman KE. Macrophage-specific 11β-hydroxysteroid dehydrogenase type 1 deficiency promotes angiogenesis but impairs resolution of K/BxN serum induced arthritis. Selected for oral presentation at prize session British Endocrine Societies Meeting, Harrogate 2013

Zhang Z, Coutinho AE, Brownstein DG, Gray M, Salter D, Seckl JR, and Chapman KE. 11β-hydroxysteroid dehydrogenase-1 amplification of glucocorticoid action in myeloid cells promotes resolution of K/BxN arthritis in mice. European Conference of Immunology, Glasgow 2012

Publications:

Chapman KE, Coutinho AE, **Zhang Z**, Kipari T, Savil JS, and Seckl JR. Changing glucocorticoid action: 11β-hydroxysteroid dehydrogenase type 1 in acute and chronic inflammation. *J Steroid Biochem Mol Biol.* http://dx.doi.org/10.1016/j.jsbmb.2013.02.002

Kipari T, Hadoke PW, Iqbal J, Man TY, Miller E, Coutinho AE, **Zhang Z**, Sullivan KM, Mitic T, Livingstone DE, Schrecker C, Samuel K, White CI, Bouhlel MA, Chinetti-Gbaguidi G, Staels B, Andrew R, Walker BR, Savill JS, Chapman KE, Seckl JR. 11β-hydroxysteroid dehydrogenase type 1 deficiency in bone marrow-derived cells reduces atherosclerosis. *FASEB J.* Jan 9, 2013. [Epub ahead of print]

Flow cytometry gating method

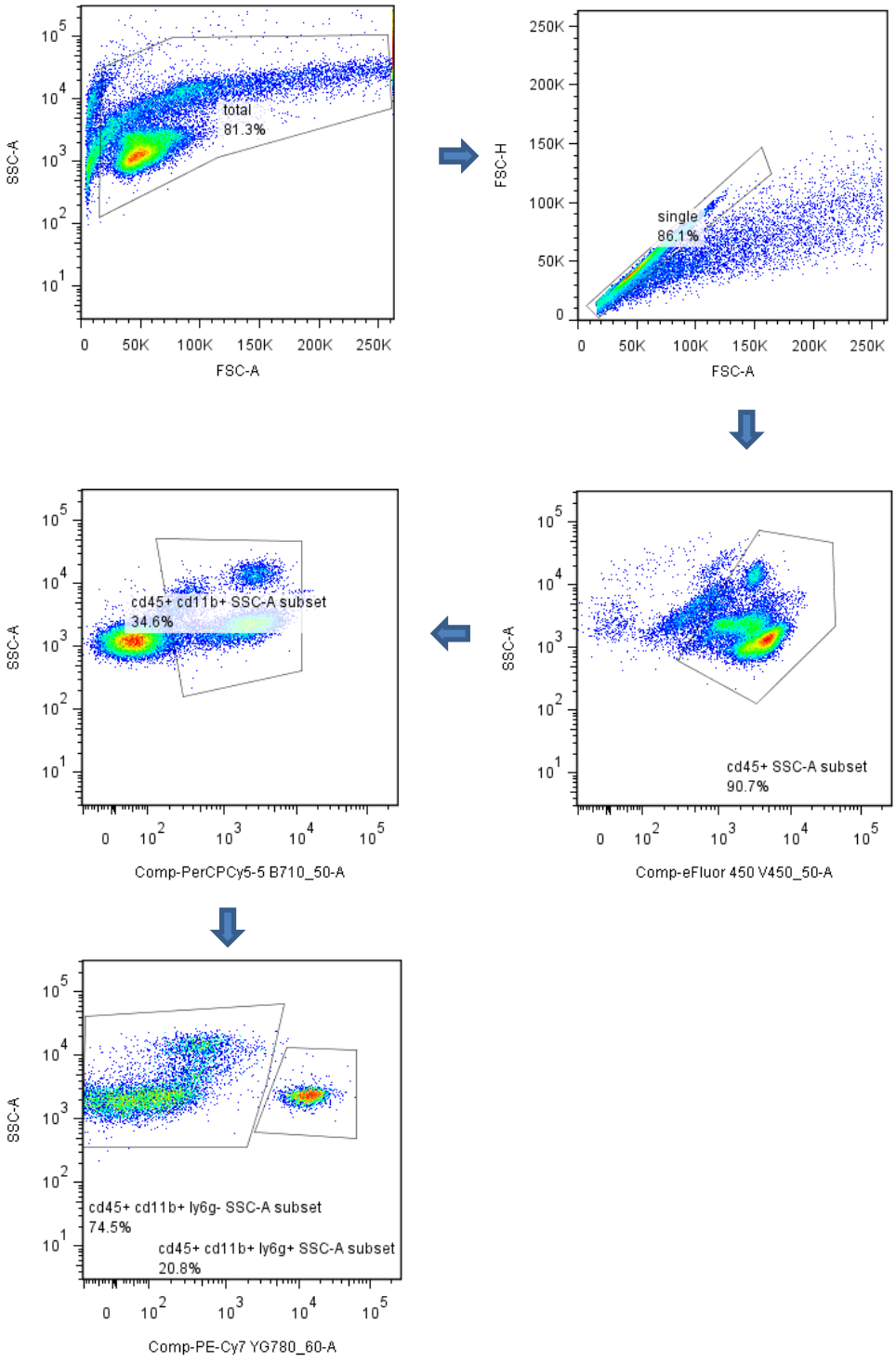

Blood myeloid cell gating method

Singlet cells were gated in the samples before $CD45^+$ population was gated. Myeloid cells then were gated using CD11b antibody, assigned as $CD45^+$ $CD11b^+$. In the myeloid cells, neutrophils were gated using Ly6g, assigned as $CD11b^+$ $Ly6g^+$ and the rest $CD11b^+$ $Ly6g^-$ cells were assigned as monocytes.

Synovial fluid leukocytes gating method

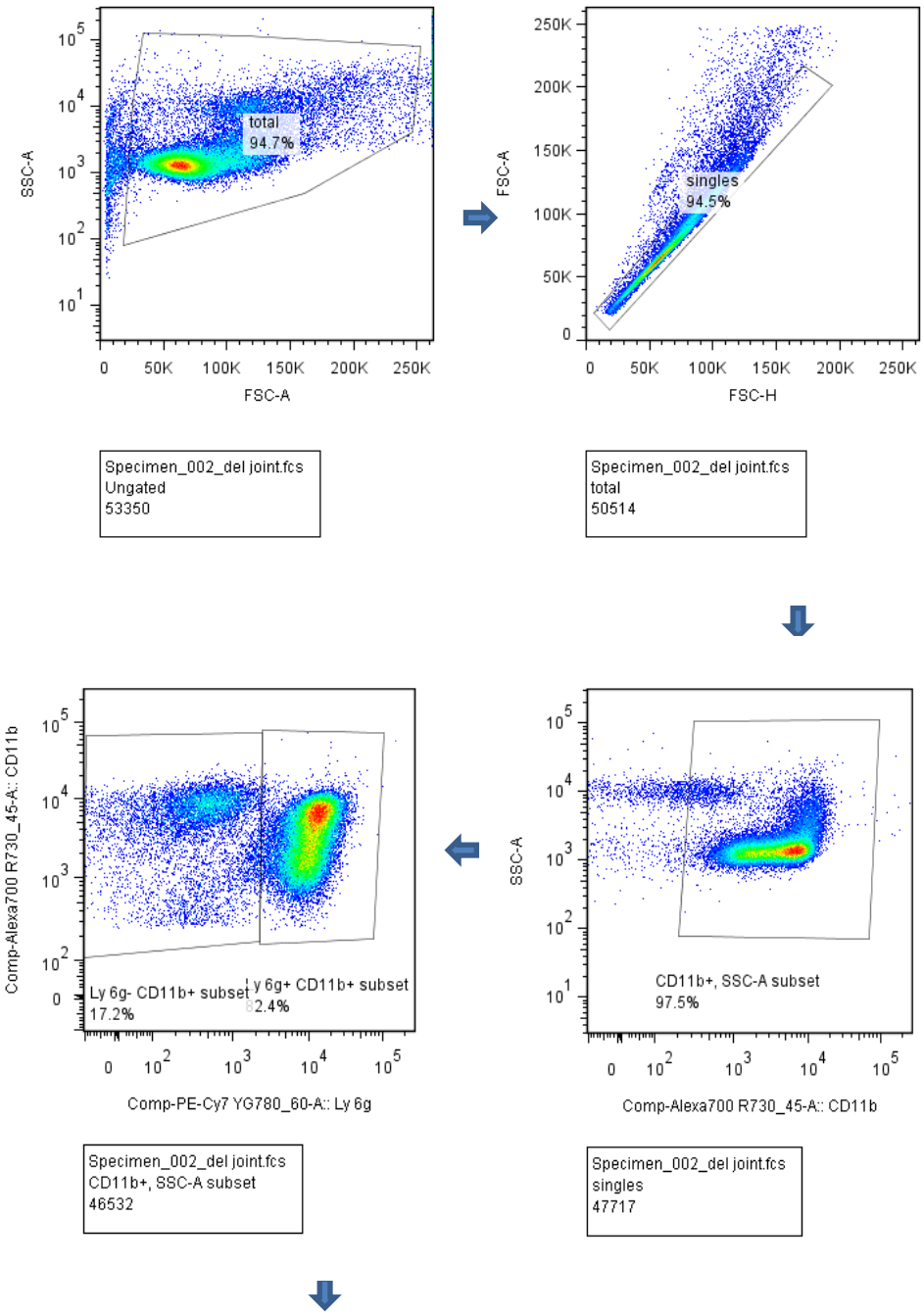

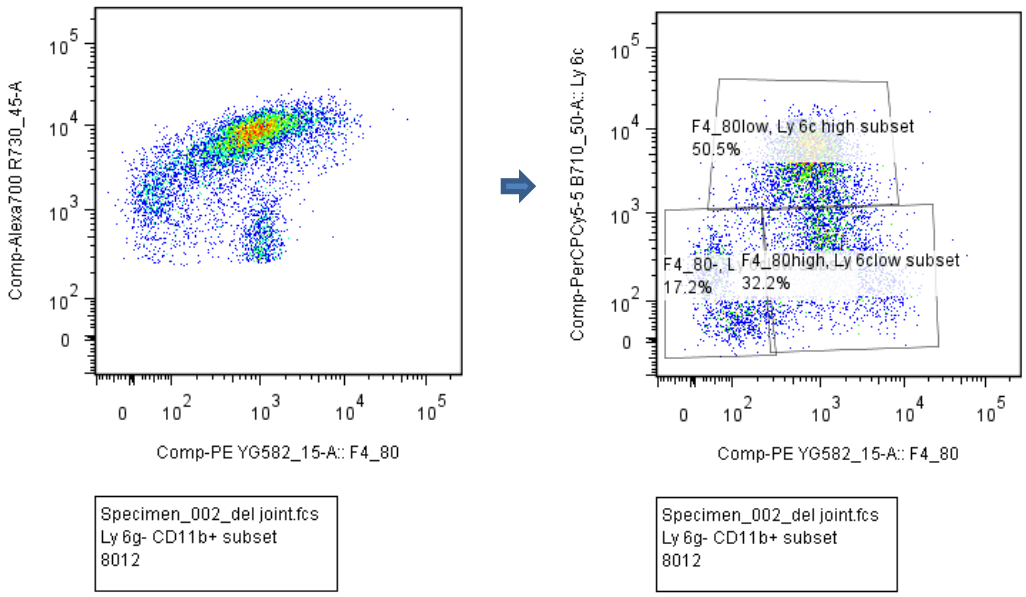

Synovial fluid leukocytes gating method

Singlet cells were first gated from total cells. CD11b antibody was then used to gate myeloid cells. In the $CD11b^+$ myeloid cells, Ly6g antibody was used to gate neutrophils, assigned as $CD11b^+$ $Ly6g^+$ and the rest $CD11b^+$ $Ly6g^-$ cells assigned as monocytes/macrophages. This monocyte/macrophage population is further stained with F4/80 and Ly6c.